Aspects of confinement in Yang-Mills theories

Andréas Tresmontant

THÈSE DE DOCTORAT
DE L'UNIVERSITÉ PIERRE ET MARIE CURIE

Physique

École doctorale : "Physique en Île-de-France"

Laboratoire de physique théorique de la matière condensée
Astroparticules et Cosmologie.

Author

Andréas TRESMONTANT

Aspects of confinement in Yang-Mills theories

Supervisors: Julien Serreau and Matthieu Tissier

27/09/2016

Jury:

M.	Maxim CHERNODUB	Rapporteur
M.	David DUDAL	Rapporteur
M.	François GELIS	Examinateur
M^{me}	Michela PETRINI	Examinatrice
M.	Julien SERREAU	Co-directeur
M.	Matthieu TISSIER	Directeur de thèse

Aspects of confinement in Yang-Mills theories

Abstract: In this thesis, we investigate the infrared regime of Yang-Mills theories. In particular, we follow a recently proposed novel gauge-fixing procedure that aims at dealing with the presence of the so-called Gribov copies. These copies correspond to additional solutions to the gauge equation that are disregarded in the standard Faddeev-Popov procedure. This novel gauge-fixing approach was first implemented in the Landau gauge, where the low momentum regime was investigable by means of simple perturbation theory and the one-loop gluon and ghost propagators were found in good agreement with lattice simulations. In a first part, we extend this proposal to a class of nonlinear covariant gauges (the Curci-Ferrari-Delbourgo-Jarvis gauges). We prove that these gauges are renormalizable in four dimensions and we provide explicit expression of the renormalization constants at one-loop order. Then we compute the various propagators of the theory at one-loop order with and without renormalization group improvement.

The second part of the thesis concerns the finite temperature case and in particular the study of the confinement-deconfinement phase transition. We work in the Landau-DeWitt gauge (a background field extension of the Landau gauge), which allows for an explicit presence of an order parameter of the phase transition. This gauge is implemented following the previous gauge-fixing procedure. In particular it has been shown that the phase transition can be studied in perturbation theory. Here, we compute at one-loop order the gluon and ghost propagators (for SU(2) gauge group) and show that they display clear signals of the phase transition. This is to be put in regards with the results obtained for the Landau gauge propagators.

Keywords : Yang-Mills theories, gauge-fixing, infrared correlation functions, Gribov ambiguities, QFT at finite temperatures, deconfinement phase transition

Contents

Introduction

The strong interaction is one of the four fundamental interactions in Nature (along with the electromagnetic, weak and gravitational ones). It is responsible for the cohesion of atomic nuclei in spite of the presence of the repulsive electromagnetic interaction between charged protons. The particles submitted to the strong interaction are called hadrons, among which, on top of the protons, are for instance the neutrons and the pions. The dynamics of hadrons have been investigated for decades both theoretically and experimentally, leading to the quark model first proposed by Gell-Mann and Zweig in 1964 [1, 2]. The quark model states that hadrons are not the most fundamental particles but are formed of spin 1/2 particles, called the quarks. The existence of quarks was confirmed experimentally and they were found in six different types, called flavors. Later on, Gell-Mann and Fritszch [3, 4] proposed the existence of an underlying SU(3) symmetry group, called the color group, which, accordingly, gives to the quarks extra quantum numbers. Eventually, the color group was taken as a gauge group and the theory was called quantum chromodynamics (QCD). Nowadays, this is the admitted theory to describe the strong interaction at the microscopic level. The gauge bosons, called gluons, are the mediators of the strong interaction and have a similar role to photons in quantum electrodynamic. Although at high energies the colored quarks and gluons are the relevant degrees of freedom, the physical spectrum of QCD is observed to be made only of colorless hadrons and is free from quarks and gluons. This is known as the phenomenon of confinement. In particular, for QCD to be a fundamental theory (as it is believed), the confinement shall naturally emerge from the microscopic action. However, one of the main obstacles one has to face is the fact that the energy regime of QCD that is relevant for confinement is often called nonperturbative and one has to resort to more sophisticated approches than perturbation theory (which is the simplest tool of investigation in quantum field theory (QFT)).

This is a consequence of the pure gauge sector of QCD (part of the QCD action that depends only on the gauge bosons). Indeed, QCD is a non-Abelian gauge theory and, at the difference of quantum electrodynamic, gluons present self-interactions. These self-interactions dramatically change the dynamics of the fundamental degrees of freedom, which, for instance, become more weakly coupled as the energy increases: the so-called asymptotic freedom property discovered by Politzer, Gross and Wilzeck [5, 6]. However, as one goes at lower energies, standard perturbation theory predicts that the coupling constant increases without bound and eventually diverges at a finite energy scale (Landau pole) Λ_{QCD} (which is typically of the order of the proton mass). The divergence of the coupling constant is usually considered as being an artifact of perturbation theory since the latter cannot be trusted at finite but large coupling.

This feature along with the property of asymptotic freedom are believed to be the two sides of the same coin and are consequences of the pure gauge dynamics. Because of this origin, it is believed that most of the features of QCD, and in particular the mechanism of confinement, are generic to non-Abelian gauge theories and can thus be understood by studying their archetype, namely the Yang-Mills theories [7] that consist in the pure gauge sector of QCD.

Nonperturbative numerical (lattice) Monte-Carlo simulations, proposed by Wilson [8] and initiated by Creutz [9], have been extensively used in order to investigate the infrared physics of the strong interactions. The latter is now fairly well described by lattice simulations that are commonly used to determine for instance the spectrum of particles, or important matrix elements entering in the evaluation of scattering amplitudes or decay rates (see e.g. [10]). Although they have provided definite confirmation that confinement does occur [9], there is still no fully satisfactory description nor explanation of the underlying mechanisms starting from first principles, despite the many proposals that have been put forward, see e.g. [11, 12] for a review.

Another lead may lie at finite temperature, which has been the subject of intense studies for the past three decades. QCD is believed to admit a very rich phase diagram whose study is an important theoretical challenge with numerous phenomenological implications for astrophysics, early Universe cosmology or heavy-ion collision experiments. In particular, along the temperature axis, the theory presents a confinement-deconfinement phase transition, where, at high temperatures, hadrons turn into a plasma of quarks and gluons. Thanks to the property of asymptotic freedom, the high temperature regime can be investigated by means of perturbative development supplemented by resummation techniques, the so-called hard thermal loops [13, 14, 15]. Within this approach, the high temperature properties of thermodynamic quantities of the deconfined plasma, such as the entropy, can be reached, though the physics of the phase transition remain inaccessible [16, 17, 18]. Again, the presence of the Landau pole prevents the use of standard perturbation theory in the low temperature confining phase as well as in the vicinity of the transition, which are widely accepted as being nonperturbative. Owing to its achievements in the vacuum, one naturally resorts to lattice simulations, which, after several decades of studies [19, 20, 21], have clearly established the existence of a phase transition in pure SU(N) Yang-Mills theories. The latter is related to the nonvanishing expectation value that the Polyakov loop (the order parameter) [22] develops in the high temperature phase, which, in turn, is associated with the spontaneous breaking of a global symmetry, called the center symmetry of the gauge group. Eventually, these studies were extended to the case of QCD where a crossover was found [23, 24]. On top of its inherent interest, the confinement-deconfinement phase transition can be viewed as a great opportunity for the search of the mechanisms at the origin of confinement. Indeed, the passage from the deconfined to the confined phase shall highlight some important features of the dynamics responsible of the phenomenon.

Nevertheless, the phase diagram along the chemical potential axis is much less understood because, in particular, lattice simulations suffer from a severe sign problem [25, 26]. Although, great efforts are made in order to circumvent the sign problem on the lattice [25, 27, 28], so far one has to resort to analytical/continuum approaches in which the sign problem, though not completely absent, is less severe. More generally,

one of the drawbacks of numerical simulations is their "black-box" character. Indeed, although they provide exact results starting from the microscopic theory, they hardly allow one to access the essential ingredients that actually lead to these results. To tackle this question, one can rely upon analytical approaches, which, although they are approximate in general, are more suited to develop/bring explanations of the observed phenomenon. Among others, the ones that were the most used for the study of the infrared regime of Yang-Mills theories, as well as for the confinement-deconfinement phase transition, are the nonperturbative functional methods based either on truncations of Dyson-Schwinger equations (DSEs), or the functional renormalization group (FRG) [29, 30, 31, 32, 33, 34, 35, 36, 37, 38, 39]. In particular, the FRG has been shown to correctly reproduce the phase diagram of Yang-Mills theories with transition temperatures in agreement with lattice results [33, 35].

Such approaches, as most of the continuum ones, use, as basic building blocks, the Green's functions (correlation functions) of the elementary fields of the theory. These quantities are not gauge invariant and require one to fix the gauge that amounts to choose one gauge field configuration that stands as a representative among each set of physically equivalent configurations. The standard manner to fix the gauge in the continuum is to follow the Faddeev-Popov gauge-fixing procedure [40], which, in particular, introduces auxiliary fields: the so-called Faddeev-Popov ghosts. Working directly on the Green's functions yields an additional difficulty since now the problem becomes specific to the gauge under consideration. In particular, this renders comparisons between different approaches more intricate since it is mandatory to be certain that all the results are derived in the same gauge (which can be a not so trivial task once approximations are made or when comparing numerical to analytical approches). In continuum methods, comparisons with other approaches, and especially with lattice simulations, are of topical importance. Indeed, the nonperturbative DSEs or FRG equations cannot be solved exactly, but require one to make additional approximations. Hence, in order to trust such approaches, it is necessary to quantify the effects of the employed approximation schemes. A general criticism such nonperturbative methods have to face is that, even when well motivated, approximations are hard to check explicitly and it is difficult to compute corrections to the obtained results. Hereby, it is desirable to test them against *ab initio* methods. These are provided by gauge-fixed lattice simulations that aim at the direct calculation of the Green's function both at zero and finite temperature [41, 42, 43, 41, 44, 45, 46]. In the context of correlation functions, lattice simulations are the analogous of the experiments, and provide an important benchmark for continuum approaches. However, the implementation of lattice gauge-fixing procedures is far from being a trivial task. This is particularly true for covariant gauges (which are the most convenient for continuum approaches) because imposing the gauge condition amounts to solve a large set of coupled nonlinear differential equations. More severely, Yang-Mills actions that are gauge-fixed *à la* Faddeev-Popov cannot be directly implemented on the lattice since averages of gauge-invariant quantities are of the indefinite $0/0$ form. This is known as the Neuberger zero problem [47, 48]. In this regard, the Landau gauge stands as a peculiar case. Indeed, the covariant Landau gauge condition can be formulated as an extremization procedure of an auxiliary functional. Thereby, using powerful minimization algorithms one can accordingly fix the gauge on the lattice in a different gauge-fixing procedure than the

Faddeev-Popov one and, in turn, the Neuberger problem is avoided [49, 50, 51, 52].

More generally, beyond the fact that Green's functions are at the basis of continuum approaches, they constitute the basic building blocks of any QFT since they contain all the information of the theory. Hence, the fundamental mechanisms at the origin of confinement shall be encoded into them. Their study in the Landau gauge has received even more attention since the seminal work of Kugo and Ojima [53]. Indeed, in the Landau gauge, Kugo and Ojima were able to derive a consistent confinement scenario based on the deep infrared behavior of the ghost and gluon propagators. This is known as the so-called *scaling* solution, which, in Euclidean space, is characterized by a divergent zero-momentum ghost dressing function (the ghost propagator times its momentum squared). Hereby, their proposal motivated the direct calculation of the correlation functions in the deep infrared regime to see whether or not the system realizes the scaling solution. Although, in the Landau gauge, the scaling solution is found consistent with both the DSEs and the FRG, gauge-fixed lattice simulations have shown that it is actually not realized. Instead, the Landau gauge Yang-Mills correlation functions follow the *decoupling* solution, where, both the ghost dressing function and the gluon propagator remain finite at zero momentum. Although this suggests a massive behavior for the gluons, it has been well established that the associated Källen-Lhemann spectral function is not definite positive and, in turn, gluons cannot be interpreted as stable massive particles, which is consistent with confinement [54, 55]. Later on, the decoupling solution was also proved to be consistent with DSEs and FRG equations, though it is not possible to discard the scaling from the decoupling solution in an internal way within these approaches [56, 57, 58, 59, 60, 43, 61, 62].

All in all, these results tend to show that our understanding of the infrared behavior of the correlation functions, though they constitute the basic building blocks of the theory, is far from being complete. One possible missing ingredient could be nontrivial effects of the gauge-fixing procedure itself that are disregarded by the Fadeev-Popov construction. Indeed, in his seminal work, Gribov showed that, in the case of non-Abelian gauge theories, the solution of the gauge condition is not unique [63]. Instead, there exists an infinite discrete set of solutions, related to one another by gauge transformations, which are called Gribov copies. These copies are not taken into account in the standard Faddeev-Popov procedure. In this case, Gribov copies are shown to give degenerate contributions with alternating signs to the partition function, which eventually cancel out and lead to the Neuberger problem. Although they are believed to be irrelevant at high energies, their presence might dramatically change the infrared behavior of the correlation functions. Gribov copies are consistently dealt with in gauge-fixed lattice simulation, where the algorithms used to fix the gauge actually select a unique copy. However, taking into account these copies in analytical approaches is a fundamental difficulty since it is not known how to build a local gauge-fixed action free of them [64]. This problem was faced by Gribov and later on by Zwanziger in the Landau gauge, where they proposed to restrict the path-integral used in the calculation of the correlation functions to a particular subspace of the gauge field configuration space [63, 65]. In doing so, the number of Gribov copies decreases considerably though several are still present in the gauge-fixed theory. This approach is called the Gribov-Zwanziger scenario and predicts that the gluon and ghost correlation functions follow the scaling solution. The Gribov-Zwanziger scenario has been extended to what is

known as the refined Gribov-Zwanziger scenario [66], where the presence of dimension two condensates is taken into account. In particular, in this last case, one obtains the decoupling solution observed in gauge-fixed lattice simulations. This suggests that, at least in the Landau gauge, Gribov copies are a key ingredient of the infrared dynamics of the correlation functions. Nevertheless, the Landau gauge is only one representative of the covariant gauges and it displays additional symmetries. To gain better insights into the importance of Gribov copies it is therefore desirable to investigate their effects on the correlation functions in other gauges. Only very recently, the covariant linear gauges were studied in lattice simulations [67, 68, 69, 70, 71] and in the (refined) Gribov-Zwanziger proposal (as well as the nonlinear Curci-Ferrari gauges for this latter case) [72, 73].

Recently, a novel gauge-fixing procedure that aims at taking into account the Gribov copies has been put forward by Serreau and Tissier in [74] in the Landau gauge. The central idea consists in dealing with the Gribov copies by averaging over them with a (pseudo) nonuniform statistical weight such that their degeneracy is lifted and the Neuberger problem is avoided. To do so, averages of gauge invariant quantities are defined by a two-step averaging procedure. The first step consists in the (pseudo) nonuniform average over the Gribov copies of a given gauge orbit, while, in the second step, an average over the gauge field configurations with the Yang-Mills action is performed. This results in a genuine gauge-fixing procedure that can be cast under the form of a local field theory by means of the method of replica [75] borrowed from the field of disordered systems in statistical physics. The resulting local action is renormalizable in four space-time dimensions. For what concerns the ghost and gluon sectors, in the Landau gauge, the procedure boils down to have an effective gluon mass. In particular, the gauge-fixed theory is (perturbatively) equivalent to the Landau limit of the Curci-Ferrari model [76, 77]. This has the advantage that, under a suitable choice of renormalization conditions, infrared-safe renormalization group trajectories exist (i.e. without a Landau pole) and the deep infrared regime can be probed perturbatively if the coupling constant remains small enough [78, 79]. In particular, one-loop calculations of the two- and three-point correlation functions show very good agreement with lattice data [79, 80, 81, 82]. This shows that (in the vacuum and in the Landau gauge) most of the nonperturbative dynamics are accurately captured by the presence of such an effective gluon mass. These works constitute the underlying ground of the studies to be presented in this thesis.

The general study of the Landau gauge Yang-Mills correlation functions has been naturally extended at finite temperature in the context of continuum methods [83, 36, 37, 38, 33, 32, 35, 34] as well as in gauge-fixed lattice simulations [84, 85, 86, 87, 88, 89, 90, 91, 46, 92]. As emphasized above, the basic correlation functions are the building blocks of the continuum methods relevant e.g. to the study of the QCD phase diagram. Although the first results obtained from lattice simulations were quite controversial due to the large systematic errors, recent large volume simulations show that, disappointingly, the Landau gauge correlation functions are rather insensitive to the phase transition [90]. Hereby, the Landau gauge does not seem to be the best candidate to study the effects of the deconfinement phase transition by means of approximate methods. In particular, in this gauge, the order parameter of the phase transition does not enter directly into the definition/calculation of the gluon and ghost

propagators, which may explain their poor sensitivity to the phase transition. Recently, it has been put forward in [33, 35, 34] that one can efficiently incorporate the order parameter of the phase transition directly into the microscopic gauge-fixed action by means of background field methods. This eventually amounts to work in a background field extension of the Landau gauge, known as the Landau-DeWitt gauge, where, in particular, the phase transition was correctly described in the framework of the FRG [33, 35, 34]. This background field gauge approach, has been extended in the context of the Serreau-Tissier gauge-fixing proposal in Yang-Mills theories at finite temperature [93, 94, 95, 96] and at finite chemical potential for heavy quarks [97], where, by means of standard perturbation theory, the phase structure was correctly reproduced.

In this thesis, we study various aspects of Yang-Mills theories that are gauge-fixed by the Serreau-Tissier procedure both in the vacuum [98, 99] and at finite temperature [96]. In Chapter I, by starting with the physical problem of confinement in QCD, we review what appears to us to be the main motivations for studying Yang-Mills correlation functions. In particular, in the Landau gauge, we highlight the importance of the effects of Gribov copies on the dynamics of the correlation functions both in lattice simulations and in the continuum through the (refined) Gribov-Zwanziger proposal [63, 65, 66]. As a complementary approach of the latter, we introduce the Serreau-Tissier gauge-fixing proposal and review its main results obtained in the Landau gauge, along the lines of [78, 79, 80, 81, 82]. Then, in Chapter II, we present our works realized in the vacuum. We propose a one-parameter family of nonlinear covariant gauges that can be formulated as an extremization procedure that may be amenable to lattice simulations. When the Gribov ambiguities can be ignored, these gauges reduce to the Curci-Ferrari-Delbourgo-Jarvis gauges [77, 100]. We further propose, following the Serreau-Tissier gauge-fixing procedure, a continuum formulation in terms of a local action which is free of Gribov ambiguities and avoids the Neuberger zero problem of the standard Faddeev-Popov construction. We show that the proposed gauge-fixed action is perturbatively renormalizable in four dimensions and we provide explicit expressions of the renormalization factors at one-loop order. We further compute the various propagators of the theory at one-loop order and we study their momentum dependence down to the deep infrared regime, with and without renormalization-group improvement. In particular, we show that the theory admits infrared-safe renormalization-group trajectories with no Landau pole. Both the gluon and the ghost behave as massive fields at low energy, and the gluon propagator is transverse even away from the Landau gauge limit. We pinpoint the specific effects arising from our treatment of Gribov copies in the gluon and ghost sectors. Finally, in Chapter III, we consider the finite temperature case. After presenting the main features of the confinement-deconfinement phase transition, we review the results obtained in the Landau gauge for the basic gluon and ghost propagators from both lattice simulations [101, 91, 46, 92] and the Curci-Ferrari model [83]. As emphasized above, the poor sensitivity of the correlators to the phase transition leads to consider the Landau-DeWitt gauge where a nontrivial background field value (that stands as an order parameter for the phase transition) explicitly enters in the microscopic action. We expose the main consequences of the presence of a nonvanishing background field and present our works that consist in computing at one-loop order the finite temperature gluon and ghost propagators [96]. We show that, in the Landau-DeWitt gauge, these

display characteristic effects at the phase transition.

Chapter I

Aspects of Yang-Mills correlation functions

The main objective of this thesis consists in studying the infrared (IR) behavior of the correlation functions in Yang-Mills (YM) theories [7]. First of all, in this chapter, we would like to motivate our approach and the interests of our work presented in detail in the following chapters. To do so, we propose to follow step by step what we consider to be a red wire, starting with the physical issue of confinement in Quantum Chromodynamic (QCD) to finish with the study of YM correlation functions in the Serreau-Tissier proposal [74] presented in Sec. I.5.2. Obviously, we do not pretend to present an exhaustive overview of the approaches and the results related to the study of confinement and YM correlation functions, this is way beyond the scope of this thesis. Rather, we choose to present what appears to us as the main ingredients upon which our work relies, how they emerge, and influence, the dynamics of YM theories and how they can be related to the issue of confinement in QCD.

In this spirit, we start in Sec. I.1 by introducing the QCD Lagrangian and YM theories as well as some aspects of confinement. An important result is provided by numerical Monte Carlo simulations [10], which have shown that confinement does occur with the YM Lagrangian as sole input. This motivates to investigate what are the fundamental mechanisms from which confinement originates. To do so, one can resort on continuum methods which, however, are in general not based directly on physical observables but instead rely upon gauge-dependent Green's functions. Hereby, one needs to fix the gauge in order to access such gauge-dependent quantities. This amounts to choose one gauge field configuration that stands as a representative among each set of physically equivalent configurations. We are mostly interested in the covariant gauges, and in particular in the Landau gauge, which can be investigated both numerically and analytically. Thus, in Sec. I.2.1, we review the standard Faddev-Popov gauge-fixing procedure [40] employed in usual perturbative approaches. Then, in Sec. I.2.3, we present possible scenarios that directly connect the behavior of the YM correlation functions to confinement. In particular, we review the key elements of the Kugo-Ojima (KO) scenario [53, 102] based on the so-called Becchi-Rouet-Stora-Tyutin (BRST) symmetry [103, 104, 105]. The KO confinement scenario demands a peculiar behavior of the correlation functions in the deep IR, where the FP gauge-fixed

YM theory cannot be investigated perturbatively and one has to rely upon nonperturbative techniques. Among the continuum ones, the functional renormalization group (FRG) [106] and Dyson-Schwinger equations (DSEs) [107, 108] are briefly introduced in Sec. I.3.1. Their applications to the Landau gauge have shown that two solutions for the YM correlation functions are possible in this gauge. To discard one or another, one is led to proceed to numerical simulations. However, lattice simulations cannot be applied to the FP Lagrangian because of the Neuberger problem [47, 48], discussed in Sec. I.3.2, which is a consequence of the gauge-fixing procedure *a la* FP. Indeed, the FP procedure neglects additional solutions of the gauge equation as first pointed out by Gribov [63]. The existence of Gribov copies and the Gribov-Zwanziger proposal [63, 109, 110, 111] that aims at dealing with them are presented in Sec. I.4. This allows us to stress the effects of Gribov copies on correlation functions, and thus the importance of taking them into account. These results are confirmed in Sec. I.4.3 where we discuss the gauge-fixed lattice simulations which provide a complete way of fixing the gauge. Finally, we are led to present the Serreau-Tissier proposal [74] that consists in a novel approach that consistently deals with the Gribov copies. We emphasize the advantages and the main results of this proposal in Sec. I.5, which stands as the starting point of this thesis.

I.1 Quantum Chromodynamic and the confinement problem

I.1.1 The QCD Lagrangian

Non-Abelian gauge theories are characterized by a non-Abelian gauge group $\mathcal{G}$. In the following we only consider the SU(N) groups. We note by t^a the N^2-1 generators of SU(N) in the fundamental representation, which are $N\times N$ matrices that we choose Hermitians. Our normalization for the generators is such that $\mathrm{tr}\left(t^a t^b\right) = \frac{\delta^{ab}}{2}$, $\left[t^a, t^b\right] = if^{abc}t^c$, with f^{abc} the usual totally antisymmetric SU(N) structure constant. For later convenience we also introduce the totally symmetric SU(N) tensor d^{abc} such that

$$t^a t^b = \frac{\delta^{ab}}{2N}\mathbb{1} + \frac{if^{abc}+d^{abc}}{2}t^c. \tag{I.1.1}$$

Quarks and gluons are represented by local fields in different representations of the gauge group. As in QED, matter fields (here the quarks) are associated with Dirac fields (noted Ψ in the following) in the fundamental representation, while the gauge field A_μ (here the gluons) is in the adjoint representation. Our conventions are such that, fields in the adjoint representation that are written without explicit color index are understood to be contracted with the SU(N) generators: $A_\mu = A_\mu^a t^a$ and are thus $N\times N$ matrices. The QCD Lagrangian is defined in d-dimensional Euclidean spacetime as (we use everywhere the convention that repeated Lorentz and color indices are summed over)

$$\mathcal{L}_{\mathrm{QCD}} = \mathcal{L}_{\mathrm{YM}} + \sum_{f=1}^{N_f}\bar{\Psi}_f\left[\gamma_\mu\left(\partial_\mu - ig_0 A_\mu\right) + m_f\right]\Psi_f, \tag{I.1.2}$$

where $\mathcal{L}_{\rm YM}$ is the pure gauge or YM sector, f, N_f and m_f are respectively the flavor index, the number of flavors, and the associated quark mass, g_0 is the coupling constant and γ_μ are the Dirac matrices (here in Euclidean space). At the difference of QED, in the case of non-Abelian gauge theories, the pure gauge sector is nontrivial due to the presence of nonvanishing structure constant:

$$\begin{aligned} \mathcal{L}_{\rm YM} &= \frac{1}{4} F^a_{\mu\nu} F^a_{\mu\nu} \,, \\ F^a_{\mu\nu} &= \partial_\mu A^a_\nu - \partial_\nu A^a_\mu + g_0 f^{abc} A^b_\mu A^c_\nu . \end{aligned} \tag{I.1.3}$$

We work in Euclidean space throughout this manuscript. This amounts to perform at the very beginning a Wick rotation from the Minkowskian theory. In general, such an analytic continuation is not trivial because of the complex analytic structure of the various quantities present in the theory (e.g. presence of poles and branch cuts). Nevertheless, we shall directly work in the Euclidean version (imaginary time) and wonder about such analytical continuations only when looking for real-time quantities. As we shall see, the underlying motivation is that the nonperturbative lattice simulations are performed in Euclidean space. The QCD Lagrangian, Eq. (I.1.2), with six flavors ($N_f = 6$) and SU(3) gauge group is the case relevant for the physical description of the strong interactions. It is invariant under the gauge transformations, which correspond to (local) transformations of the fields Ψ and A under the action of an element of the gauge group SU(N)

$$\left\{ \begin{array}{rcl} A_\mu(x) & \to & A^U_\mu(x) = U\,(x)\, A_\mu(x) U^\dagger\,(x) + \frac{i}{g_0} U\,(x)\, \partial_\mu U^\dagger\,(x) \,, \\ \Psi(x) & \to & U(x)\Psi(x)\,, \end{array} \right. \tag{I.1.4}$$

with $U(x)$ a local element of SU(N). By Noether theorem, the peculiar case of global transformations (color transformations) induces the existence of a conserved global charge Q_c, namely the color charge.

It is now widely believed that QCD is the correct fundamental description of the strong interaction and is part of the Standard Model of Particles. However, it presents a long-standing unanswered question: why do we only observe hadrons (colorless bound states) while the fundamental degrees of freedom of QCD are the colored quarks and gluons? The confinement mechanism is invoked to cope with this issue.

I.1.2 The phenomenon of confinement

The description of the confinement mechanism should explain how these two asymptotic limits of the strong interactions are related to one another, namely, the ultraviolet (UV) regime accurately described in terms of the colored quarks and gluons, and the infrared (IR) regime where only massive colorless hadrons exist. Loosely speaking, the confinement mechanism can be defined as the fact that free observable particles must be colorless with the (gluonic) massless excitations removed from the physical spectrum (existence of a mass gap). However, a rigorous definition of confinement is still under discussion [11, 12]. For instance, a Higgs-like phase would satisfy the previous definition of a confining theory [11, 112]. A generally accepted sufficient criterion for signaling confinement is the area-law falloff for Wilson loops in the case where the

quarks are statics and of infinitely heavy mass (quenched approximation) [8]. In this case, the Wilson loop is defined as [8]

$$W_{\text{Wilson}}[C] = \text{tr}\ \mathcal{P} \exp\left\{ \oint_C dx_\mu A^a_\mu(x) t^a \right\}, \tag{I.1.5}$$

where $\mathcal{P}$ is the path ordering operator and $C \equiv C(R,T)$ is a rectangular closed contour of extent R and T respectively in the spatial and temporal directions. Note that this is a gauge-invariant observable. It is related to the static quark potential as

$$V_{\text{quark}}(R) = -\lim_{T\to\infty} \frac{\ln \langle W_{\text{Wilson}}[C] \rangle}{T}. \tag{I.1.6}$$

Hereby, the area-law falloff implies that the potential energy of a static quark-antiquark pair grows linearly with the spatial pair separation [12]. According to the definition (I.1.6), for what concerns confinement, one is thus interested to access the large time behavior of the Wilson loop, or more generally, the large distance/low energy properties of the theory. Using the standard perturbative tools of QFT one access easily the UV behavior of the theory thanks to the so-called asymptotic freedom property [113]. On the contrary, perturbation theory predicts that, in the IR, the coupling constant increases without bounds and eventually hits a Landau pole (diverges at finite energy). This may be viewed as a first insight of the confinement phenomenon: the fundamentals degrees of freedom become more and more strongly coupled and eventually cease being the physically relevant ones. It follows that the IR regime is strongly coupled and requires to account for nonperturbative effects, which, in turns, make its investigation a difficult problem that has prevented for more than forty years a fully consistent description of confinement.

UV asymptotic freedom and Landau pole in the IR are thought to be the two sides of the same coin and are consequences of the pure gauge sector. For this reason (among others) it is widely believed that the phenomenon of confinement is generated in the YM sector of QCD. A reliable nonperturbative tool for its investigation is provided by numerical Monte Carlo simulations [9, 114]. They were first proposed by Wilson [8] in order to provide a gauge-invariant, first principle method of computation. One uses a finite space-time discretized into an hyper-cubic lattice of finite lattice spacing noted a in the following. The key idea of Wilson is to introduce the gauge link variables $W_\mu(x)$ defined as [8], [1]

$$W_\mu(x) = \exp\left\{ -i g_0 a A_\mu(x) \right\}, \tag{I.1.7}$$

whose transformation under the action of the gauge group is simpler than that of A_μ. One has

$$W^U_\mu(x) = U(x) W_\mu(x) U^\dagger(x + a\hat{\mu}), \tag{I.1.8}$$

where $\hat{\mu}$ is a unit vector pointing in the space-time direction μ. Accordingly, the discretized YM action writes [8]

$$S_{\text{latt.}}[W] = \frac{2N}{g_0^2} \sum_x \sum_{\mu,\nu} \left(1 - \frac{1}{N} \text{Re}\left[\text{tr}\ W_\mu(x) W_\nu(x + a\hat{\mu}) W^\dagger_\mu(x + a\hat{\nu}) W^\dagger_\nu(x) \right] \right). \tag{I.1.9}$$

[1] More precisely, the gauge link is defined as the parallel transport between two adjacent space-time points: $W_\mu(x) = \mathcal{P} \exp\left\{ ig \int_0^1 dt A_\mu(x + at\hat{\mu}) \right\}$, which is equivalent to the definitions (I.1.7) and (I.1.8) in the continuum limit ($a \to 0$).

In order to compute the expectation value of an observable $\mathcal{O}$, one generates a collection of N_{links} gauge link configurations according to the distribution $\exp(-S_{\text{latt.}}[W])$ and performs a statistical average:

$$\langle \mathcal{O} \rangle \simeq \frac{1}{N_{\text{links}}} \sum_{l=1}^{N_{\text{links}}} \mathcal{O}\left[W_\mu^{(l)}\right], \tag{I.1.10}$$

where the approximate equality becomes exact in the limit of infinite number of gauge links. In particular, this can be done to access the Wilson loop, Eq. (I.1.5), which is found to display the area-law falloff [9].[2] However, although this result proves that confinement occurs in YM theories, it does not explain neither why nor how. Possible confinement mechanisms were proposed and investigated numerically, such as center-vortex dominance [11] and others; see [12] for a review.

To gain more insights into the basic mechanisms underlying the confinement, one possible way is to investigate whether relevant information is encoded in the correlation functions of the basic (gluon) fields.

I.2 Gauge-fixing procedure

In the present manuscript we intend to investigate the YM correlation functions by means of a particular continuum approach. It is well known that correlation functions cannot be directly accessed in gauge theories but require one to fix the gauge first. Moreover, the quadratic part of $\mathcal{L}_{\text{YM}}$ is not invertible, preventing the definition of the tree-level propagators. Equivalently, the conjugate momentum of A_μ, $\Pi_\mu = F_{0\mu}$ is zero for the temporal mode $\mu = 0$ preventing the use of canonical quantization. These are standard features of gauge theories and are consequences of the presence of degenerate field configurations: two field configurations A_μ and A_μ^U that are related by a gauge transformation are physically equivalent. Indeed, in the functional integral formalism, the expectation value of a gauge-invariant observable $\mathcal{O}_{\text{inv}}$ is defined by

$$\langle \mathcal{O}_{\text{inv}}[A] \rangle = \frac{\int \mathcal{D}A\, \mathcal{O}_{\text{inv}}[A]\, e^{-S_{\text{YM}}[A]}}{\int \mathcal{D}A\, e^{-S_{\text{YM}}[A]}}. \tag{I.2.1}$$

Obviously, by gauge invariance, two field configurations A_μ and A_μ^U that are related by a gauge transformation contribute the same to both the numerator and the denominator of the right-hand side of Eq. (I.2.1). We define the gauge orbit $\{A_\mu\}_U = \left\{ A'_\mu \,\middle|\, A'^U_\mu = A_\mu \right\}$ as the set of field configurations that are all related to one another by gauge transformations. One tries to select only one representative per gauge orbit by imposing a gauge condition (an additional constraint), for instance the Landau gauge condition

$$\partial_\mu A_\mu = 0\,. \tag{I.2.2}$$

This is schematically pictured on Fig. I.1, where the gauge condition (blue dashed line) intersects once and only once each gauge orbits (plain black lines). A gauge condition

[2] Let us mention that numerical simulations have also computed (part of) the hadronic spectrum starting with the QCD Lagrangian [115].

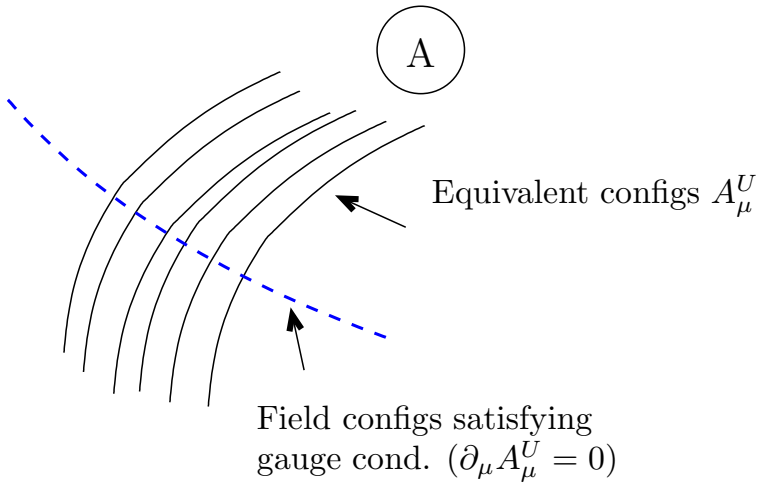

Figure I.1: Gauge-fixing procedure. Black lines represent different gauge orbits. Dashed blue line represents the gauge condition.

that selects a unique representative per gauge orbit is called an ideal gauge condition.

The choice of the gauge is arbitrary since gauge-invariant physical observables are insensitive to this choice. Continuum approaches are more conveniently formulated in covariant gauges, and we shall focus our discussion on this case. The Landau gauge has received a lot of attention, also because it displays additional interesting properties as for instance a purely transverse gluon propagator, or the nonrenormalization of the ghost-gluon vertex [116, 117]. Moreover, as we shall see in Sec. I.4, the Landau gauge can be formulated as an extremization procedure of an external functional. This peculiar property is of utmost importance when discussing its implementation on the lattice [see Sec. I.4.3] or how to deal with the presence of Gribov copies [63]; see Secs. I.4.1, I.4.2 and I.5.

I.2.1 The Faddeev-Popov gauge-fixing procedure

The strategy proposed by Faddeev and Popov (FP) to restrict, in the path-integrals of (I.2.1), the integration over the field configurations that satisfy the gauge equation, is to insert unity written in the form [118]

$$1 = \int \mathcal{D}U \delta\left(f\left[A^U\right]\right) \mathrm{Det}\mathcal{F}\left[A^U\right] , \tag{I.2.3}$$

with $\mathcal{D}U$ the Haar measure on the gauge group, $f[A] = 0$ is the gauge condition, here taken in the Landau gauge $f^a = \partial_\mu A^a_\mu$, and $\mathrm{Det}\mathcal{F}\left[A^U\right]$ is the associated Jacobian. Writing $\lambda^a(x)$ such that $U(x) = \exp(ig_0\lambda^a(x)t^a)$, one defines the so-called FP operator [118]

$$\mathcal{F}^{ab}\left[A\right](x,y) = \left.\frac{\delta f^a[A^\lambda](x)}{\delta\lambda^b(y)}\right|_{\lambda=0} , \tag{I.2.4}$$

where we noted A^λ the gauge-transformed gauge field by the gauge transformation $U(x) = \exp(ig_0\lambda^a(x)t^a)$, that is,

$$\left(A_\mu^\lambda\right)^a = A_\mu^a + \partial_\mu\lambda^a + g_0 f^{abc} A_\mu^b \lambda^c + \mathcal{O}(\lambda^2)\,. \tag{I.2.5}$$

The Jacobian arising in Eq. (I.2.3) is obtained from the FP operator. To be more explicit, we consider the path-integral corresponding to the numerator on the right-hand side of Eq. (I.2.1), where we introduced Eq. (I.2.3):

$$\mathcal{I} = \int \mathcal{D}A\mathcal{D}U\, \mathcal{O}_{\rm inv}[A]\, e^{-S_{\rm YM}[A]} \delta\left(f\left[A^U\right]\right) \mathrm{Det}\mathcal{F}\left[A^U\right]\,. \tag{I.2.6}$$

The case of the denominator of the right-hand side of Eq. (I.2.1) follows trivially by repeating the present discussion for $\mathcal{O}_{\rm inv}[A] = 1$. Using the gauge invariance of $\mathcal{D}A\, e^{-S_{\rm YM}[A]}$ and of $\mathcal{O}_{\rm inv}[A]$, the last equality reduces to

$$\mathcal{I} = \int \mathcal{D}U \int \mathcal{D}A\, \mathcal{O}_{\rm inv}[A]\, e^{-S_{\rm YM}[A]} \delta\left(f\left[A\right]\right) \mathrm{Det}\mathcal{F}\left[A\right]\,, \tag{I.2.7}$$

so that the infinite volume of the gauge group $\int \mathcal{D}U$ can now be factorized out, and only the configurations satisfying the gauge equation $f[A] = 0$ are integrated over. In order to apply the machinery of continuum methods, one needs to recast this last expression under the form of a functional integral with a local action. To do so, one introduces the so-called FP ghost and antighost fields (scalar anticommuting fields) c^a and $\bar{c}^a$ as well as a Nakanishi-Lautrup field ih^a that enforces the gauge condition [119, 120]. Eventually, one obtains that the expectation value of a gauge-invariant quantity $\mathcal{O}_{\rm inv}[A]$ are given by

$$\langle \mathcal{O}_{\rm inv}[A] \rangle = \frac{\int \mathcal{D}\varphi\, \mathcal{O}_{\rm inv}[A]\, e^{-S_{\rm gf}[\varphi]}}{\int \mathcal{D}\varphi\, e^{-S_{\rm gf}[\varphi]}}, \tag{I.2.8}$$

where the brackets $\langle\,\rangle$ correspond to perform the average over the fields $\varphi = A_\mu,\ c,\ \bar{c},\ ih$ with weight $S_{\rm gf}$ which is the Landau gauge FP YM gauge-fixed action. The latter is given by the initial YM action plus a gauge-fixing term

$$\begin{aligned} S_{\rm gf} &= S_{\rm YM} + S_{\rm FP}\,, \\ S_{\rm FP} &= \int_x \left\{ ih^a \partial_\mu A_\mu^a + \partial_\mu \bar{c}^a D_\mu^{ab} c^b \right\}, \end{aligned} \tag{I.2.9}$$

where $\int_x = \int d^dx$ and where in the last equation we used the explicit expression of the FP operator in the Landau gauge, namely $-\partial_\mu D_\mu^{ab}$, with $D_\mu^{ab} = \delta^{ab}\partial_\mu + g_0 f^{acb} A_\mu^c$ the covariant derivative. For simplicity, in the following, we note $D_\mu\varphi^a \equiv D_\mu^{ab}\varphi^b$.

I.2.2 Ghost and BRST symmetries of the FP gauge-fixed action

The gauge-fixed action Eq. (I.2.9) is invariant under the U(1) global transformations

$$c \to e^{i\epsilon} c\,, \quad \bar{c} \to e^{-i\epsilon}\bar{c}, \tag{I.2.10}$$

while all other fields are left untouched. The corresponding conserved charge is the so-called ghost number, defined as follows: ghosts have $+1$ ghost number, antighosts -1 and the other fields have zero charge.

By construction, the (FP) gauge-fixed action Eq. (I.2.9) is no longer gauge invariant. Nevertheless, it was shown by Becchi, Rouet, Stora [105, 104], and, independently, by Tyutin [103] that there exists a remnant of the original gauge symmetry in the gauge-fixed action, namely the so-called BRST symmetry. Its action on the various fields is

$$\delta_{\rm BRST}\ \varphi = \eta s\varphi\,, \qquad \varphi = \{A_\mu, \bar{c}, c, ih\}\ , \tag{I.2.11}$$

with η a constant Grassmannian parameter and s is the BRST operator defined as

$$\begin{aligned} sA^a_\mu &= D_\mu c^a \\ s\bar{c}^a &= ih^a \\ sc^a &= -\frac{1}{2} g_0 f^{abc} c^b c^c \\ sih^a &= 0\,. \end{aligned} \tag{I.2.12}$$

Note in particular that the operator s is of mass dimension 1 and has ghost number 1 according to our convention. Straightforwardly, one can use these relations to prove the nilpotency of the BRST transformation: $s^2 = 0$. Note also that, the BRST transformation of the gauge field A_μ corresponds to a gauge transformation of infinitesimal parameter ηc. In particular, this implies that the BRST transformation is a symmetry of any gauge-invariant functional of the gauge field only.

Alternatively, one can conveniently generalize the FP gauge-fixing procedure by taking as first requirement the existence of the BRST symmetry at the level of the gauge-fixed action [118]. This corresponds to start from a fermionic functional Ψ of mass dimension $d-1$ and ghost number -1 such that $s\Psi$ is the gauge-fixing action. This yields the YM gauge-fixed action

$$S_{\rm gf} = S_{\rm YM}[A] + \int_x s\Psi[\varphi]\,. \tag{I.2.13}$$

Owning to the nilpotent character of the BRST symmetry and to the gauge invariance of $S_{\rm YM}$, one is insured that $S_{\rm gf}$ is BRST symmetric. For instance, in the Landau gauge we have $\Psi = \bar{c}^a \partial_\mu A^a_\mu$. Having a nilpotent BRST symmetry is commonly considered as a necessary requirement for having a consistent theory. Indeed, the proof of renormalizability and unitarity, originally performed respectively by 't Hooft [121, 122] and by Kugo and Ojima [53], strongly rely on it.

I.2.3 Aspects of Green's functions

I.2.3.1 Gluon or ghost infrared dominance

According to its definition, the Wilson loop Eq. (I.1.5) seems directly connected to the behavior of the gluon. It was thus first thought that the gluon sector should display IR singularities in order to enforce an area-law falloff for the Wilson loop. In

this first confinement scenario, known as the IR slavery scenario, the gluon propagator is believed to be IR enhanced, that is, to diverge as $1/p^4$ at low momentum. Assuming an IR ghost suppression, Mandelstam was the first to investigate nonperturbatively (in the context of Dyson-Schwinger equations [107, 108], see also Sec. I.3.1.2 for a brief overview) the Landau gauge gluon propagator that he found to be IR enhanced [123]. This scenario initially received much attention [124, 125] but was eventually discarded since it was proved that the Landau gauge gluon propagator cannot diverge more severely than $1/p^2$ as $p \to 0$ [126].

Another proposal put forward in [30, 127] favors an IR ghost enhancement and an IR gluon suppression. This proposal agrees with the Kugo-Ojima [53] and the Gribov-Zwanziger [63, 109, 110, 111] scenarios. Further studies of the IR regime of the Landau gauge, by means of either nonperturbative functional methods [128, 129, 126, 130, 131, 132, 133] (see Sec. I.3.1), or (gauge-fixed) lattice simulations [134, 135, 136, 137, 138, 139, 140, 44, 141, 142, 143, 144, 43, 42, 145, 146, 147, 148, 149, 45] (see Sec. I.4.3) tend to support an IR ghost dominance, though not necessarily a ghost enhancement. Nevertheless, the hypothesis of an IR enhanced ghost (though not in agreement with the most recent lattice data [137, 134, 138, 139, 140, 44, 141, 142, 143, 144, 43, 42, 145, 146, 147, 148, 149, 45]) has received a lot of attention for years [30, 29, 150, 60, 151] since it allows for many practical advantages in solving the Dyson-Schwinger equations, and perhaps more importantly, since it is believed[3] to satisfy the Kugo-Ojima scenario. This last point is important on the conceptual level because, on top of providing a confinement scenario, it insures the unitarity of the gauge-fixed theory Eq. (I.2.9) (however the proof of Kugo-Ojima should not be taken as fully satisfactory since, the presence of Gribov copies is not faced).

I.2.3.2 The Kugo-Ojima proposal

In their seminal work, Kugo and Ojima (KO) addressed the question of unitarity in YM theories [53, 102]. This issue is general to gauge theories and manifests more explicitly in covariant gauges: part of the excitations described by the fields do not belong to the physical spectrum but are artifacts of the gauge-fixing procedure. This is already the case in QED in the Landau gauge where temporal photon states have negative norms [157], thus ruling out the standard probabilistic interpretation. One encounters alaogous problems in the FP YM gauge-fixed theory Eq. (I.2.9). For instance, ghost fields are zero spin bosonic fields but assume anticommuting commuta-

[3] Here we prefer to take some cautions. If it is true that an IR enhanced ghost is a necessary condition for the Kugo-Ojima proposal, the way the ghost enhancement is implemented into the Dyson-Schwinger equations might be deceitful regarding the realization of the Kugo-Ojima scenario. Indeed, according to Zwanziger [152], in this case the ghost enhancement may signal the realization of the Gribov-Zwanziger scenario. Although both scenarios share close ties [153, 154, 155], the latter breaks the (local) nilpotent BRST symmetry, Eq. (I.2.12), while the former relies on the existence of a conserved nilpotent BRST charge. It shall be mentioned that very recently a nonlocal nilpotent BRST symmetry has been discovered in the context of the Gribov-Zwanziger proposal [156] from which one may succeed in redoing the Kugo-Ojima construction. To our knowledge this has not been performed yet. Thereby, we believe that the interpretation of the ghost enhancement that emerges in the framework of Dyson-Schwinger equations should be taken with care. To our knowledge, this issue has not been fully settled yet.

tion relations which is inconsistent with the spin-statistic theorem [158]. Thereby, such unphysical states must be removed from the physical space of states in order to insure that the physical spectrum contains solely positive norm states which agree with the principles of QFT.

To achieve this, KO proposed the so-called quartet mechanism that relies upon the presence of a nilpotent BRST symmetry. One defines the conserved BRST charge Q_{BRST} associated with the global BRST symmetry. From the total space of states of the theory $\mathcal{V}$ (which presents an indefinite metric) they construct the physical Hilbert space $\mathcal{H}_{\mathrm{phys}}$. A prerequisite for a state $|\Psi\rangle$ to belong to $\mathcal{H}_{\mathrm{phys}}$ is that it is annihilated by the BRST charge

$$Q_{\mathrm{BRST}}\,|\Psi\rangle = 0. \tag{I.2.14}$$

States that belong to the BRST kernel can be categorized into two families: the daughter states $|\Psi_{\mathrm{d}}\rangle \in \mathcal{V}_0$ are BRST exact in the sense that there exists (by definition) a parent state[4] $|\Psi_{\mathrm{p}}\rangle$ such that $|\Psi_{\mathrm{d}}\rangle = Q_{\mathrm{BRST}}\,|\Psi_{\mathrm{p}}\rangle$. The nilpotency of the BRST charge ($Q^2_{\mathrm{BRST}} = 0$) implies that the daughter states do belong to the BRST kernel but are of zero norm. The other family contains genuine physical states which satisfy $|\Psi_{\mathrm{g}}\rangle \in \mathrm{Ker}_{\mathrm{BRST}}$ but are not daughter states. Owing to this last definition, one sees that $\mathcal{V}_0$, which contains the daughter states, is orthogonal to $\mathrm{Ker}_{\mathrm{BRST}}$. Moreover, since daughter states are of zero norm they do not contribute to the norm of the states in $\mathrm{Ker}_{\mathrm{BRST}}$. According to this, KO defined the physical Hilbert space as the so-called BRST cohomology

$$\mathcal{H}_{\mathrm{phys}} = \mathrm{Ker}_{\mathrm{BRST}}/\mathcal{V}_0\,, \tag{I.2.15}$$

which presents a positive definite metric and thus allows for a probabilistic interpretation according to the principles of quantum mechanics. Finally they proved that transition amplitudes between two physical states $\langle\Psi_{\mathrm{g}}|\,\Phi_{\mathrm{g}}\rangle$ are not affected by contributions from the unphysical ones. This is known as the quartet mechanism, which states that all unphysical states are either a parent or a daughter state. Each pair of parent and daughter states defines a BRST doublet that falls into a quartet along with the BRST doublet of conjugated ghost number. Owing to this quartet structure, in transition amplitudes between physical states, each contribution from an unphysical state cancels out with those of the same quartet. Note in particular how the KO proof relies on the existence of an unbroken nilpotent BRST charge.

In the KO confinement scenario, not only auxiliary fields states but also the longitudinal gluon states fall into quartets representation and thus are not part of the physical spectrum. Hence, in the KO's vision, gluon confinement can be understood from an "unitarity issue" picture. However, up to this point nothing insures that genuine physical states carry zero color charge. KO investigated this point and derived criteria for color confinement. Their argument is based on the existence of a conserved color charge associated to color transformations. The color charge is given by [53]

$$Q^a_c = \int d^3x\,\partial_i F^a_{0i} + \{Q_{\mathrm{BRST}}, D_0\bar{c}^a\}\,. \tag{I.2.16}$$

[4]Remark that by the prerequisite of belonging to the BRST kernel, a parent state cannot be a physical state.

For it to be well defined, the first term must not present any (discrete) massless pole[5] (first KO criterion). In such a case, the first contribution vanishes as it consists in a total derivative. The second KO criterion is that the second contribution in Eq. (I.2.16) is also well defined. For the moment, let us assume this to be the case. Since any physical states are annihilated by the BRST charge, color confinement is realized in the sense that $Q_c^a = 0$ in $\mathcal{H}_{\text{phys}}$. On the other hand, the case where Q_c^a cannot be defined would signal a spontaneous breaking of color symmetry and hereby a Higgs-like phase. In the peculiar case of the Landau gauge, in [159], Kugo proved that the second contribution in Eq. (I.2.16) is well defined if the ghost propagator is IR enhanced, which thus appears as a necessary condition for the KO confinement scenario.

The KO relation between the BRST and color charge has attracted a lot of attention to the studies of the Landau gauge Green's functions to see, whether or not, the latter display an IR enhanced ghost[6]. Indeed, as stressed for instance in [151], according to KO, the absence of an IR enhanced ghost leads to a gauge-fixed YM theory that is either not color-confining (global color charge broken) or without nilpotent BRST charge and it is then unclear in general how one can construct the physical space or physical observables out of Green's functions [151].

We would like to end the discussion on the KO proposal by making two remarks. First of all, the KO framework assumes a well defined conserved nilpotent BRST charge, which is motivated by its existence at the perturbative level [Eq. (I.2.12)], however, it could happen that such a charge does not exist at the nonperturbative level[7]. On the other hand, the KO derivation uses as a starting point the FP gauge-fixed action that ignores certain ambiguities in the gauge-fixing procedure called Gribov copies [63]. We come back to the issue of Gribov copies in a later section, see Sec. I.4.1.

I.2.3.3 Positivity violation

Here, we want to briefly mention a way to probe directly from the correlation functions if the excitations produced by the associated fields belong to the physical spectrum or not. Given an Euclidean two-point correlation function of a field Φ in momentum space, that we note here generically $G(p)$, for its poles to be interpreted as stable particles created by the field Φ once the analytical continuation to Minkowski space has been performed, then, $G(p)$ must admit a Källen-Lehman representation [29, 160, 55]

$$G(p) = \int_0^\infty d\mu^2 \, \frac{\rho(\mu^2)}{p^2 + \mu^2} \,, \tag{I.2.17}$$

where the spectral density $\rho(\mu^2)$ is a non-negative function. On the contrary, if the spectral density admits negative values, it implies that the states created by the field Φ cannot be part of the physical spectrum, this is referred to as violation of positivity.

[5] If this is not so, the integral in Eq. (I.2.16) is ill defined.

[6] It has been shown that such a solution is actually unique [129, 133].

[7] Remark that the KO criterion of having an enhanced ghost does not check the existence of such a nonperturbative BRST charge. Rather, it is a consistency condition for having both globally well-defined nilpotent BRST and color charges.

An exhaustive discussion of the confinement scenarios and their relationship with the YM Green's functions is beyond the scope of this manuscript. Rather, by presenting in this section how different IR phenomenologies can lead to very different explanations of the confinement mechanism, we intended to motivate that an accurate knowledge of the YM correlation functions in the IR regime may be important in order to construct possible confinement scenario.

I.3 The infrared regime of Yang-Mills theories

The IR behavior of YM correlation functions is difficult to access because of the presence of a Landau pole at finite energy arising in the FP gauge-fixed theory. Perturbation theory cannot be used to probe the low momentum regime and one has to resort to nonperturbative approaches. Among continuum ones are the functional methods either by truncation of Dyson-Schwinger equations (DSEs) or the functional renormalization group (FRG). Both allow one to derive systems of exact functional equations, which however cannot be solved as such since they involve infinitely many equations. One needs additional truncations in order to put them under a manageable form [130]. However, it is difficult to construct controlled systematic expansion/truncation schemes beside perturbation theory. As a consequence, it is not clear how to estimate the error of a given approximation. One reliable way to cope with this issue is to compare to lattice simulations.

I.3.1 Functional methods

Let us first present the general ideas of some of the main functional methods used in the literature, namely, the FRG [106] and DSEs [107, 108]. We start with some definitions and notations. Given a generic action $S[\phi]$, where ϕ denotes collectively the field content of the theory. One defines the partition function in presence of sources J for all independent fields ϕ of the theory

$$\begin{aligned} Z[J] &= \int \mathcal{D}\phi \, e^{-S[\phi]+\int_x \phi J_\phi} \\ &= e^{W[J]} \,, \end{aligned} \tag{I.3.1}$$

where $W[J]$ is the generating functional for connected Green's functions. Accordingly, one defines the generating functional for the one-particle irreducible (1PI) vertex functions, or quantum effective action (referred to as the effective action for shortness)

$$\Gamma[\phi] = -W[J] + \int_x \phi J_\phi \,. \tag{I.3.2}$$

The various 1PI Green's functions are obtained by differentiation of the generating functionals, for instance, the propagator $G_{\phi\phi}$ of the field ϕ is given by

$$G_{\phi\phi} = \left.\frac{\delta^2 W[J]}{\delta J_\phi \delta J_\phi}\right|_{J=0} = \left.\left(\frac{\delta^2 \Gamma[\phi]}{\delta\phi\delta\phi}\right)^{-1}\right|_{J=0} . \tag{I.3.3}$$

I.3.1.1 The functional renormalization group

The purpose of the FRG [106] is to construct flow equations for the effective action Γ in the spirit of the Wilsonian's renormalization group. One first introduces a UV cutoff scale[8] Λ, at which the bare action S is defined. One also defines the average effective action Γ_k at an IR momentum scale k. It corresponds to the effective action obtained after the system's fluctuations of momentum higher than k have been integrated out. In particular, taking $k \to 0$ corresponds to integrating out all fluctuations so that one recovers the full effective action: $\lim_{k\to 0}\Gamma_k = \Gamma$. Instead, taking $k \to \Lambda$ corresponds to the case where no fluctuations are taken into account and one recovers the bare action: $\lim_{k\to\Lambda}\Gamma_k = S$. Thus, if one is able to derive a flow equation for Γ_k with respect to the cutoff scale k, one can start with the classical action S and progressively integrate the fluctuations down to the IR and access the full effective action Γ. First, it is needed to freeze the degrees of freedom below the scale k, while those of higher momenta are left unaltered. This is achieved by adding a k dependent mass term R_k, called the IR regulator, to the bare action

$$\begin{aligned} S \to & S + \Delta S_k \,, \\ \Delta S_k = & \int_x \frac{1}{2}\phi R_k \phi \,. \end{aligned} \tag{I.3.4}$$

The regulator acts as a large mass that freezes excitations below k while it vanishes for momenta $p \gg k$. Accordingly, the renormalization group (RG) flow of the effective action Γ_k is given by the Wetterich equation [106]

$$k\partial_k \Gamma_k [\phi] = \int_p \frac{1}{2} G^k_{\phi\phi}\, k\partial_k R_k \,, \tag{I.3.5}$$

with $\int_p = \int \frac{d^d p}{(2\pi)^d}$. Here, the propagator appearing in Eq. (I.3.5) is the fully dressed propagator at the scale k and is given by

$$G^k_{\phi\phi}(p) = \frac{1}{\Gamma^{(2)}_k(p) + R_k(p)} \,, \tag{I.3.6}$$

with $\Gamma^{(2)}_k = \delta^2\Gamma_k/\delta\phi^2$. The presence in the propagator $G^k_{\phi\phi}$ of the regulator R_k is inherited from the addition to the initial action of the term ΔS_k, see (I.3.4). In particular, as observed in Eq. (I.3.6), R_k acts as a momentum-dependent mass term which allows to regulate the IR regime. Flow equations for higher 1-PI vertex functions $\Gamma^{(n)}_k = \delta^n\Gamma_k/\delta\phi^n$ are obtained by differentiating further both sides of the Wetterich equation (I.3.5). Although this provides exact equations for the fully dressed vertex functions $\Gamma^{(n)}_k$, the corresponding system cannot be integrated exactly since the flow equation for $\Gamma^{(n)}_k$ depends on $\Gamma^{(n+2)}_k$ with n unbounded. This infinite "tower" of coupled equations needs to be truncated in order to get a closed system. This situation is similar to the one encountered in the case of DSEs, that we now present.

[8] In the context of statistical physics, such a UV cutoff scale is naturally provided by the (inverse) lattice spacing for instance.

I.3.1.2 The Dyson-Schwinger equations

The essence of the DSEs [107, 108] is to provide the exact equations of motion for the full Green's functions of the theory at hand. One way to achieve this, is to remark that, the integral of a total derivative being zero, one has

$$0 = \int \mathcal{D}\phi e^{-S[\phi]+\int_x J_\phi \phi} \left(-\frac{\delta S[\phi]}{\delta \varphi} + J_\varphi \right), \tag{I.3.7}$$

where φ is any of the fields of the theory. This equality immediately yields the DSE

$$\left\langle -\frac{\delta S[\phi]}{\delta \varphi} + J_\varphi \right\rangle_J = 0\,, \tag{I.3.8}$$

where the subscript J means that the average $\langle\ \rangle_J$ is performed in presence of the sources. This equation can be further derived with respect to the sources to obtain a whole set of DSEs.

The DSEs can be derived for the Landau gauge FP action, Eq. (I.2.9). Here, as an example, we display the DSE for the ghost propagator, see also Appendix. A. It is obtained for $\varphi = \bar{c}^a(x)$ in Eq. (I.3.8) and by differentiating once with respect to J_c. It reads

$$\left(G_{\rm gh}^{-1}\right)^{ab}(p) = p^2\delta^{as} - ig_0 p_\mu f^{acd} \int_k G^{ce}_{\mu\nu}(k) G^{dn}_{\rm gh}(k) \Gamma^{nse}_{c\bar{c}A_\nu}(p,-k,k), \tag{I.3.9}$$

where $G_{\rm gh}$ and $G_{\mu\nu}$ are respectively the fully dressed ghost and gluon propagators, and $\Gamma_{c\bar{c}A_\nu}$ is the fully dressed ghost-antighost-gluon (ghost-gluon for short) vertex. In particular, one recognizes a typical one-loop structure for this equation, where $\delta^{ab}p^2$ and $-ip_\mu g_0 f^{scd}$ can be identified to the tree-level inverse ghost propagator and to the tree-level ghost-gluon vertex respectively. Hereby, this equation can conveniently be represented by means of Feynman diagrams as depicted on Fig. I.2. The other DSEs

Figure I.2: Diagrammatic representation of the DSE for the ghost propagator Eq. (I.3.9). Dashed lines represent ghost propagators and wiggly lines gluon propagators. Bold lines and dots are full propagators and full vertices respectively, while normal ones are bare quantities. Original figure taken from [126].

are obtained for the gluon propagator and interaction vertices by performing different derivatives with respect to the sources. For instance, the diagrammatic DSE for the gluon propagator is shown in Fig. I.3.

Although DSEs are exact equations, they cannot be solved exactly in general because, just as the flow equations in the previous section, the $n^{\rm th}$ derivative of Γ is expressed in terms of higher points vertex functions. For instance, solving Eq. (I.3.9) to get the full ghost propagator requires as input the full three-point vertex function $\Gamma_{c\bar{c}A_\nu}$. As emphasized earlier, a model on which one can base truncation schemes is necessary to put the DSEs under a tractable form.

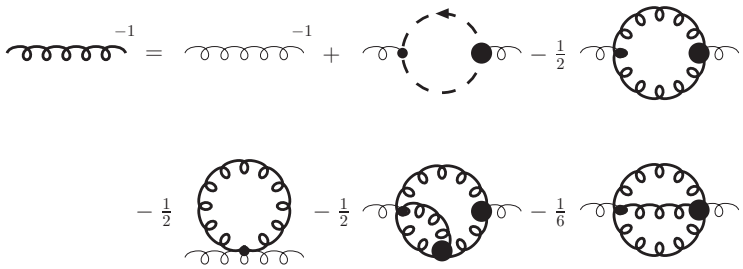

Figure I.3: Diagrammatic representation of the DSE for the gluon propagator. Dashed lines represent ghost propagator and wiggly lines gluon propagators. Bold lines and dots are full propagators and full vertices respectively, while normal ones are bare quantities. Original figure taken from [126].

Mandelstam was the first to use DSEs to reach nonperturbative results on the gluon propagator [123]. Based on the perturbative behavior of the ghost at high energies, which gives the smallest contributions to the gluon sector, Mandelstam assumed an IR gluon dominance. Following this assumption, he proposed to truncate the DSEs by neglecting ghost loops and the full four-gluon vertex (arising only in two-loop diagrams) in the DSE for the gluon propagator depicted in Fig. I.3. As confirmed later on, e.g. in [124], the Mandelstam's truncation scheme is indeed consistent with an IR gluon dominance. However, the very assumption of an IR regime dominated by the gluon sector was actually erroneous. Indeed, further studies of the DSEs [128, 129, 126, 130, 131, 132, 133] revealed that ghost contributions dominate the IR regime of the DSEs. This is also supported by lattice results [134, 135, 136, 137, 138, 139, 140, 44, 141, 142, 143, 144, 43, 42, 145, 146, 147, 148, 149, 45]. In particular, it was eventually shown that an IR enhanced gluon propagator is actually inconsistent with the DSEs [126].

I.3.1.3 The scaling and decoupling solutions

A better understanding of the Landau gauge DSEs led to better truncation schemes. For instance, the effects of three-point functions on the propagators are by now much better understood [131, 161, 61]. In particular, these works have revealed the importance of two-loop diagrams for the gluon propagator [131]. Following these studies, a one-parameter family of solution emerges of the DSEs, and are confirmed by the FRG analysis [162, 163, 164, 165, 166, 31, 151]. The family of solutions is continuously indexed by the renormalization prescription (boundary condition) of the ghost dressing function (see below) at zero momentum. The solutions are given according to the infrared exponent of the gluon and ghost dressing functions, $J(p)$ and $F(p)$, that read (in four dimensional space-time)

$$J(p) \sim (p^2)^{\kappa_A - 1}, \quad \text{and} \quad F(p) \sim (p^2)^{-\kappa_c} \ \text{ as } \ p \to 0\,, \tag{I.3.10}$$

where $J(p) \equiv p^2 G(p)$ and $F(p) \equiv p^2 G_{\rm gh}(p)$, with G and $G_{\rm gh}$ the gluon and the ghost propagator respectively. The solutions can be classified according to two different qualitative behaviors. The first one, called the scaling solution [30], corresponds to the scaling relation $\kappa_A = 2\kappa_c$. It is unique, in the sense that only one boundary

condition, namely a divergent zero momentum ghost dressing function, leads to this solution [30, 127, 151]. In particular it satisfies the KO criterion[9], see above. Hereby, as emphasized earlier, this solution is very appealing from a theoretical point of view and received a lot of attention [30, 29, 150, 60, 151]. In this peculiar case, the full tower of DSEs can be analyzed without truncation schemes [129, 133].

The other type of solutions are called the *decoupling* solutions and do not present the scaling relation $\kappa_A = 2\kappa_c$. In particular the ghost dressing function is IR finite and the gluon propagator does not vanish[10] though the solution still displays an IR ghost dominance as the gluon propagator remains IR suppressed. The decoupling solution is obtained for any boundary condition corresponding to a finite IR ghost dressing function, and hence, this solution is not unique but parametrized by one parameter. It was studied, among others, in [56, 57, 58, 59, 60, 43, 61, 62]. The finiteness of the zero momentum gluon propagator suggests a massive behavior. Nevertheless the decoupling solutions violate positivity, see e.g. [167, 151]. Thereby, the behavior of the gluon propagator cannot be interpreted as the one of a standard massive particle, though, for shortness, we still refer to this as a massive behavior. Finally we mention that both the decoupling and the scaling solutions differ only in the deep IR regime while both agree with the perturbative results in the UV.

In this section we presented two nonperturbative functional approaches. It shall be mentioned that others exist such as the Hamiltonian approach of [168, 169], or two-particle-irreducible (2PI) inspired approaches [170, 35]. We have emphasized the necessity of using (model dependent) truncation schemes. The validity of the latter is challenging to verify as these approaches rely on autoconsistent equations (see for instance the case of IR gluon dominance), and one thus needs to compare with other approaches, e.g., lattice simulations.

Moreover, both the scaling and the decoupling solutions were found consistent with the functional approaches, and additional information is needed in order to know which solution the system realizes. This is a complicated task since they differ only in the nonperturbative regime. Again, the best predictive tool is lattice simulations that provide an exact solution of the dynamics at work.

I.3.2 The Neuberger problem

Another concern of the approaches described above that we have not discussed so far, is the fact that, these nonperturbative approaches are applied to the FP, or more generally, to BRST quantization of the YM action, which may not include all nonper-

[9] It should be stressed that in the KO proposal, a singular ghost dressing function is not a condition that one should impose but rather a consistency criterion that should be investigated/checked through explicit computations/simulations in order to observe whether or not the KO confinement scenario is realized [154]. Moreover, imposing particular boundary conditions might correspond to change the symmetry content of the initial theory [152], and notably the nilpotency of the BRST symmetry [153, 154, 155]. Hence, we believe that one should be cautious in interpreting such a solution in the KO framework. This is further discussed in Sec. I.4.2.

[10] Note that the difference between the scaling and the decoupling solution lies in the IR behavior of the ghost dressing function since an IR nonvanishing gluon propagator is possible with $\kappa_A = 1$ which, in turns, yields an IR enhanced ghost if the scaling relation $\kappa_A = 2\kappa_c$ holds.

turbative effects. At least the presence of multiple solutions of the gauge equations, the so-called Gribov copies [63], are not included. We further present the Gribov copies and review some proposals that intend to deal with them in the next sections. For the moment, in order to motivate the need of taking into account Gribov copies effects, let us proceed in a naive way by assuming that one wants to perform lattice simulations directly from the FP action Eq. (I.2.9). As we now present, this is not possible due to the 0/0 Neuberger problem [47, 48]. In the next section, we link this issue with the fact that the gauge has been fixed according to the FP procedure/BRST quantization.

A crucial point in fixing the gauge (for instance in the FP procedure) is to keep unchanged the expectation value of gauge-invariant operators while the degeneracy, induced by the gauge symmetry, of physically equivalent field configurations is removed. Keeping this in mind, Neuberger proposed to have a closer look at the expectation value of BRST-invariant quantities (among which there are gauge-invariant operators) computed with a BRST gauge-fixed action, that is a gauge-fixed action of the form (see also Eq. (I.2.13))

$$S_{\rm gf} = S_{\rm YM}[A] + \int_x s\Psi[\varphi]\,, \quad \varphi = \{A_\mu, \bar{c}, c, ih\}\,, \tag{I.3.11}$$

with $\Psi = \bar{c}^a \partial_\mu A^a_\mu$ for the peculiar case of the Landau gauge. Let $\mathcal{O}_{\rm BRST} = \mathcal{O}_{\rm inv} + s\mathcal{O}$ be a BRST invariant operator where $\mathcal{O}_{\rm inv}$ is gauge invariant and $\mathcal{O}$ has nothing specific. Neuberger showed that

$$\int \mathcal{D}\varphi e^{-S_{\rm YM}[A] + \int_x s\Psi[\varphi]} \mathcal{O}_{\rm BRST}\,[\varphi] = 0, \tag{I.3.12}$$

assuming that the nilpotent BRST charge is unbroken. Therefore, averages of gauge-invariant quantities are of the indefinite form 0/0. Here, one might hope for cancellation between zeros of the numerator and the denominator to occur. However, the presence of the zeros prevents from a numerical implementation of Eq. (I.3.12). Hereby, the absence of a straightforward nonperturbative method to compute gauge-invariant quantities is uncomfortable as it rises the question whether is it possible to have a well-defined BRST gauge-fixing procedure of the form (I.3.11). This indefinite form is actually a consequence of nonperturbative aspects of the gauge-fixing issue that were neglected in the FP gauge-fixing procedure. The latter fixes the gauge only up to a discrete set of configurations whose contributions in Eq. (I.3.12) exactly cancel out for gauge group of zero Euler character [29].

I.4 Beyond the FP gauge-fixing procedure

I.4.1 Gribov ambiguities and Gribov regions

Let us take a step back in the gauge-fixing procedure. Up to now, we have always assumed that the gauges we were considering (and in particular the Landau gauge) were ideal gauges, that is, the gauge condition admits one and only one solution per gauge orbit. However this is not true in the Landau gauge, as first pointed out by Gribov in his seminal work [63]. The problem is even more sever as Singer showed that in non-Abelian gauge theories it is not possible to find a unique and local gauge

condition that intersects once and only once each gauge orbit [64]. To see this in the Landau gauge, let us consider the following functional

$$\mathcal{H}_{\text{Landau}}[A,U] = \int_x \text{tr}\left[\left(A_\mu^U\right)^2\right]. \tag{I.4.1}$$

We look at its stationary points with respect to the gauge transformation U for fixed gauge field configuration A. This can be done by writing $U \to VU$ with V infinitesimally close to the identity $V \sim e^{ig_0\lambda}$ and making an expansion in λ: $A_\mu^V = A_\mu + D_\mu\lambda + \mathcal{O}(\lambda^2)$. Plugging this expansion into (I.4.1) yields the variation of $\mathcal{H}_{\text{Landau}}$ with respect to an (infinitesimal) gauge transformation

$$\delta_\lambda \mathcal{H}_{\text{Landau}}[A,U] = -2ig_0 \int_x \text{tr}\left[\lambda\left(\partial_\mu A_\mu^U\right) + \mathcal{O}(\lambda^2)\right]. \tag{I.4.2}$$

The condition of being at an extremum requires that the variation of $\delta_\lambda \mathcal{H}_{\text{Landau}}$ be zero for all λ which is realized for

$$\partial_\mu A_\mu^U = 0. \tag{I.4.3}$$

Therefore the extrema (for a given A) of the functional (I.4.1) correspond to different solutions of the Landau gauge condition that belong to the same gauge orbit. The situation is depicted schematically on Fig. I.4. Gribov proved that, indeed, the Landau gauge condition admits multiple solutions known as Gribov copies. For instance, "infinitesimal" copies correspond to the zero modes of the FP operator. Indeed, considering a field configuration A_μ that satisfies the Landau gauge condition and its (infinitesimal) gauge transformation $A_\mu^{'} = A_\mu + D_\mu\lambda$, then $A_\mu^{'}$ is a Gribov copy if $\partial_\mu D_\mu \lambda = 0$, that is, if λ is a zero mode of the FP operator. On top of these "infinitesimal" copies, there also exist copies that are related by finite gauge transformations [171, 172, 173]. The presence of these copies spoils the FP construction presented in

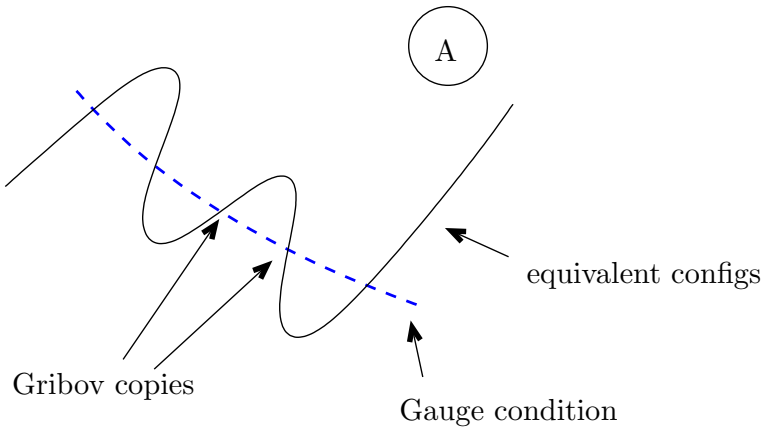

Figure I.4: Gauge-fixing procedure. The black line represents one gauge orbit. Dashed blue line represents the gauge condition.

Sec. I.2.1. Indeed, the writing of the identity *a la* FP, Eq. (I.2.3), is justified under two assumptions, namely that

- the gauge equation $f\left[A^U\right] = 0$ is invertible (i.e. has a unique solution),
- $\mathrm{Det}\mathcal{F}\left[A^U\right]$ is positive definite,

which are not satisfied due to the presence of Gribov copies (see below). Instead, in the presence of Gribov copies, the FP construction amounts to sum over all copies multiplied by the sign of the FP determinant

$$\begin{aligned} Z_{\mathrm{FP}} \equiv \int \mathcal{D}U \delta\left(f\left[A^U\right]\right) \mathrm{Det}\mathcal{F}\left[A^U\right] &= \int \mathcal{D}U \sum_i \frac{\delta\left(U-U_i\right)}{\left|\mathrm{Det}\mathcal{F}\left[A^U\right]\right|} \mathrm{Det}\mathcal{F}\left[A^{U_i}\right] \\ &= \sum_i \frac{\mathrm{Det}\mathcal{F}\left[A^{U_i}\right]}{\left|\mathrm{Det}\mathcal{F}\left[A^{U_i}\right]\right|} \\ &= \sum_i \mathrm{sign}\left[\mathrm{Det}\mathcal{F}\left[A^{U_i}\right]\right] \\ &\equiv \sum_i s(i), \end{aligned} \tag{I.4.4}$$

where here, the sum runs over all Gribov copies A^{U_i} belonging to the gauge orbit of A. It is precisely this type of sum which is responsible for the Neuberger problem [29, 174]. At this point we need to study in more details the structure of Gribov copies, or equivalently the extrema of $\mathcal{H}_{\mathrm{Landau}}$. We go to the next order in (I.4.2)

$$\begin{aligned} \delta_{\lambda^a(x)}\left(\delta_{\lambda^b(y)}\mathcal{H}_{\mathrm{Landau}}\right) &\propto \int_{x,y} \lambda^a(x)\left(-\partial_\mu^x\left(\partial_\mu^x\delta^{ab} + g_0 f^{acb}A_\mu^c(x)\right)\delta(x-y)\lambda^b(y)\right) \\ &= \int_x \lambda^a(x)\mathcal{F}^{ab}(x)\lambda^b(x). \end{aligned} \tag{I.4.5}$$

Hence, the FP operator $\mathcal{F}$ corresponds to the Hessian of the functional $\mathcal{H}_{\mathrm{Landau}}$ along the gauge orbit. Accordingly, Gribov copies that are minima of $\mathcal{H}_{\mathrm{Landau}}$, correspond to a FP operator with only positive eigenvalues (and thus a positive sign in (I.4.4)), while those that are saddle points of $\mathcal{H}_{\mathrm{Landau}}$ with p unstable directions yields a FP operator with p negative eigenvalues (and thus contribute for $(-1)^p$ in (I.4.4)), for a review see [155]. Following the work of Gribov [63], the set of field configurations satisfying the gauge condition can thus be folded into regions according to the number of unstable directions of the FP operator. This is schematically represented on Fig. I.5, where Ω is the set of minima of $\mathcal{H}_{\mathrm{Landau}}$:

$$\Omega = \{A \ : \ \partial_\mu A_\mu = 0, \quad \mathcal{F} > 0\} \ . \tag{I.4.6}$$

Ω is called the first Gribov region, while Ω_2 is the analogous of Ω but for copies that correspond to a FP operator with one unstable direction, Ω_3 those with two unstable directions, and so on. Different regions are separated by the boundaries $\delta\Omega_k$. On the latter, the lowest positive eigenvalue of the FP operator in Ω_{k-1} vanishes.

The first Gribov region Ω presents two important properties: every gauge orbit passes through [175] and it contains $A = 0$, that is, the perturbative region [176]. Other properties of the Gribov region can be found in [176]. Still, Ω contains many different

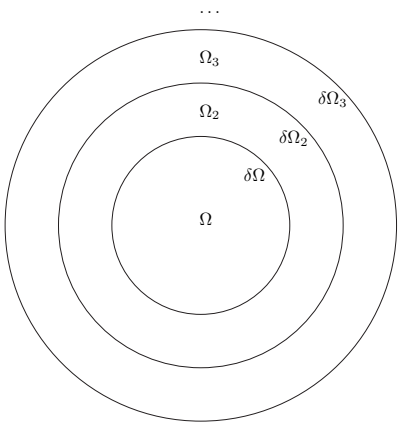

Figure I.5: The different Gribov regions. The k^{th} region Ω_k is the set of Gribov copies with FP operator that admits $k-1$ negative eigenvalues. The boundaries $\delta\Omega_k$ separates the Gribov region Ω_k and Ω_{k+1} while the k^{th} negative eigenvalue of the FP operator on Ω_{k+1} is zero on the boundary. Figure taken from [155].

gauge copies corresponding to different local minima of $\mathcal{H}_{\text{Landau}}$ [171, 172, 173], which is verified by lattice simulations [174]. In order to select a unique representative per gauge orbit, one can look for the absolute minimum of $\mathcal{H}_{\text{Landau}}$. By construction the set of absolute minima (if degenerate) is included in the Gribov region and is commonly referred to as the First Modular Region (FMR) [177].

I.4.2 The Gribov-Zwanziger approach

Gribov copies are ignored in the FP gauge-fixing procedure. Although this is believed to be well justified at high energies (in the perturbative regime), they constitute an important ingredient of the IR domain (at least in the Landau gauge). In order to take this into account, Gribov proposed to revisit the FP procedure by restricting the path-integral over the first Gribov region Ω [63]

$$Z_{\text{GZ}} = \int_{\Omega} \mathcal{D}\phi \, e^{-S_{\text{gf}}}, \tag{I.4.7}$$

with $\phi = \{A_\mu, \bar{c}, c, ih\}$, and S_{gf} is the Landau gauge FP gauge-fixed action Eq. (I.2.9). This insures that the Neuberger problem is avoided since, by construction, the FP operator is positive on Ω. Nevertheless, Ω is plagued by multiple Gribov copies. As emphasized in the previous section, for such a procedure to be fully consistent one should select only one copy per gauge orbit, e.g. by restricting the path-integral to the FMR. However, it is not known so far how to include such a strict restriction. Still, one may hope that the restriction to Ω is sufficient for practical purposes. In order to formulate this restriction into a tractable field theory, Gribov computed in [63] the ghost propagator in a semiclassical approximation (up to second order in perturbation

theory) where the gauge field A is taken as an external background field

$$G^{ab}_{\mathrm{gh}}(p,A) = \frac{\delta^{ab}}{p^2}\frac{1}{1-\sigma(p,A)} = \left(\mathcal{F}^{-1}\right)^{ab}(p,A), \tag{I.4.8}$$

where, on the right-hand side, there is the inverse of the FP operator and σ is found to decrease as the momentum p increases [155]. Following from the relation between the ghost propagator and the FP operator, one sees that the external configuration A lies within Ω as long as $G^{ab}_{\mathrm{gh}}(p,A)$ is strictly positive while the first horizon $\delta\Omega$ is crossed when $G^{ab}_{\mathrm{gh}}(p,A)$ develops a pole more singular than $1/p^2$ (which corresponds to the vanishing of the lowest eigenvalue of the FP operator on the border $\delta\Omega$). This yields the so-called no-pole condition introduced by Gribov in [63]

$$1-\sigma(0,A) \geqslant 0, \tag{I.4.9}$$

where the equality is reached on the boundary $\delta\Omega$. The no-pole condition can be embodied into the functional integral Eq. (I.4.7) by inserting $\theta(1-\sigma(0,A))$, where θ is the Heaviside distribution. Under the functional integral, it was motivated that the Heaviside distribution can be replaced by a Dirac delta [63, 65, 178]. This implies in particular that the leading contributions from Gribov copies are given by those located on the boundary $\delta\Omega$. Later on, Zwanziger generalized the Gribov no-pole condition to all orders [65, 178, 177, 154] and expressed the restriction to Ω through the introduction of a nonlocal "horizon" action S_{h}

$$\begin{aligned} \int_{\Omega} &\to \int e^{-S_h}\,, \\ S_h &= \gamma^4 \int_x h(x)\,, \end{aligned} \tag{I.4.10}$$

where γ is known as the Gribov parameter and has the dimension of a mass, $h(x)$ is the (nonlocal) horizon function

$$h(x) = g_0^2 f^{abc} A^b_\mu(x) \int_y \left(\mathcal{F}^{-1}(x,y)\right)^{ad} f^{dec} A^e_\mu(y)\,. \tag{I.4.11}$$

The Gribov parameter γ is considered as nonperturbative since it encodes the restriction of the path-integral to the first Gribov region Ω. It is determined by a gap equation, the horizon condition [65, 178],

$$\langle h(x)\rangle = 4\left(N^2-1\right)\,, \tag{I.4.12}$$

where here the average is to be computed with FP gauge-fixed YM action supplemented by the additional horizon action Eq. (I.4.10).[11] The horizon function, along with the horizon condition Eqs. (I.4.11)-(I.4.12) are equivalent to a generalization at all orders of the ghost form factor $\sigma(p,A)$ (see Eq. (I.4.8)) and the Gribov no-pole condition Eq. (I.4.9) [180]. The equality in the horizon condition Eq. (I.4.12) (instead of an inequality as in Eq. (I.4.9)) corresponds to take into account only the Gribov copies

[11] As pointed out in [179], the computation of the horizon condition should be performed only once the horizon action S_h has been made local.

located near the boundary $\delta\Omega$ [181]. The nonlocal horizon action Eq. (I.4.10) can be rendered local by the introduction of two pairs of complex conjugate auxiliary fields (see [155] for a review), namely the bosonic $\bar{\varphi}^{ab}_{\mu}$, φ^{ab}_{μ} and Grassmann $\bar{\omega}^{ab}_{\mu}$, ω^{ab}_{μ} fields which form BRST doublets

$$\begin{aligned} s\varphi^{ab}_{\mu} &= \omega^{ab}_{\mu}\,,\; s\omega^{ab}_{\mu} = 0\,, \\ s\bar{\omega}^{ab}_{\mu} &= \bar{\varphi}^{ab}_{\mu}\,,\; s\bar{\varphi}^{ab}_{\mu} = 0\,. \end{aligned} \tag{I.4.13}$$

In terms of these fields, one gets [65, 178, 177] in $d = 4$

$$\begin{aligned} e^{-S_h} &= \int \mathcal{D}\varphi\mathcal{D}\bar{\varphi}\mathcal{D}\omega\mathcal{D}\bar{\omega}\, e^{-S_{\rm loc}}\,, \\ S_{\rm loc} &= \int_x \left\{ \bar{\varphi}^{ac}_{\mu}\mathcal{F}^{ab}\varphi^{bc}_{\mu} - \bar{\omega}^{ac}_{\mu}\mathcal{F}^{ab}\omega^{bc}_{\mu} + \gamma^2 g_0 f^{abc} A^a_{\mu}\left(\varphi^{bc}_{\mu} + \bar{\varphi}^{bc}_{\mu}\right) - 4\gamma^4(N^2-1)\right\}. \end{aligned} \tag{I.4.14}$$

Hereby, a nonperturbative gauge-fixed YM action in the Landau gauge is given by the (local) Gribov-Zwanziger (GZ) action [63, 65, 155]

$$S_{\rm GZ} = S_{\rm YM} + S_{\rm FP} + S_{\rm loc}\,, \tag{I.4.15}$$

where in this expression the Landau gauge expression of the FP operator $\mathcal{F}^{ab}(x) = -\partial_{\mu}D^{ab}_{\mu}(x)$ is used.

An important remark is that the perturbative BRST symmetry, Eq. (I.2.12), is softly broken by the presence of the Gribov parameter γ. Nevertheless, the local action admits a modified (non-nilpotent) BRST symmetry according to which it remains renormalizable [65, 182, 183, 178, 179] though the definition of the physical space (if it exists) is unclear as one cannot repeat the KO treatment.[12] In the GZ theory, the gluon and ghost propagators realize the scaling solution. Indeed, the tree-level gluon propagator is

$$G^{ab}_{\mu\nu}(p) = \delta^{ab}P^{T}_{\mu\nu}(p)\frac{p^2}{p^4 + 2Ng_0^2\gamma^4}\,, \tag{I.4.16}$$

where we introduced the transverse projector $P^{T}_{\mu\nu}(p) = \delta_{\mu\nu} - p_{\mu}p_{\nu}/p^2$. Therefore, already at tree-level, the gluon propagator vanishes at zero momentum. The tree-level ghost propagator behaves as $1/p^2$ at low momenta. The no-pole condition (or equivalently the horizon condition) leads, by construction (see Eq. (I.4.9) and its enforcement with the Dirac delta), to the disparition of the $1/p^2$ behavior at one loop-order. Instead, it turns out that, as p goes to zero, the ghost propagator behaves as $1/p^4$, as first pointed out by Gribov [63] and checked up to two loops later on [185], thus realizing the scaling solution. This prediction has been extended beyond perturbation theory by Zwanziger [181]. Moreover, it was asserted by Zwanziger that, in principle, the restriction of the path-integral to a subdomain should not change the form of functional equations, e.g. DSEs, but is inherited into the boundary conditions that one uses as initial conditions [152]. As we just saw, the restriction to the first Gribov region

[12] We mention again that, recently, it has been discovered that the GZ action is symmetric under a nonlocal but nilpotent BRST-like transformation [184].

is encoded into the horizon condition which, in turns, is transcribed into the IR enhancedment of the ghost propagator, namely that[13] $\lim_{p\to 0}\left[p^2 G_{\rm gh}(p)\right]^{-1} = 0$. Therefore, according to the previous argument of Zwanziger, in the DSEs of the standard Landau gauge FP action, the boundary condition of a divergent ghost dressing function at zero momentum may actually implement the GZ action [152, 155]. Thereby, the interpretation of the scaling solution obtained through the DSEs as the realization of the KO scenario (we recall that the scaling solution was obtained by imposing as initial condition a diverging ghost dressing function, see Sec. I.3.1) seems compromised, as the BRST symmetry (I.2.12) (central in the KO proposal) is broken in the GZ action. Nevertheless, it should be mentioned here that recently it has been discovered that the GZ action admits a nilpotent nonlocal BRST symmetry [184, 156], though to our knowledge, its link to the KO proposal has not been fully settled yet.

As already mentioned, the restriction to the Gribov region Ω implies the presence of the Gribov parameter γ of mass dimension 1 that softly breaks the initial nilpotent BRST symmetry. It turns out, as pointed out in [66], that composite operators can develop nonvanishing expectation values which were previously prevented by the nilpotent BRST symmetry. In particular, it was proposed to take into account the dimension two condensate $\langle 0|\, \bar{\varphi}^{ab}_\mu \varphi^{ab}_\mu - \bar{\omega}^{ab}_\mu \omega^{ab}_\mu \,|0\rangle$ by adding an appropriate source term to the GZ action. This is known as the refined Gribov-Zwanziger (RGZ) action, which was proved to be renormalizable in four dimensions [66]. In particular, due to the effects of the condensate, the gluon propagator does not vanish at zero momentum (even if it stays IR suppressed) and the ghost dressing function remains finite, thus realizing the decoupling solution. The price to pay is the introduction of (at least) one new dimensional parameter related to the nontrivial condensate.

Let us make a few comments on the results presented in this section. First, both the GZ and the RGZ actions are renormalizable despite their breaking of the initial (perturbative) nilpotent BRST symmetry. This is because they admit a modified (non-nilpotent) BRST symmetry which allows one to control the divergences. On the other hand, one cannot do the KO construction of the physical Hilbert space. However, as argued in [66], this might be not such an issue. Gluons are not part of the physical Hilbert space (as can be seen by the violation of positivity in the GZ and RGZ cases [154, 155]) and, therefore, not being able to define the physical space out of them may be not so surprising. Of course, the definition of a physical Hilbert space is mandatory for the consistency of the approach, but the solution might not lie in the gluon and ghost sectors.

With this section we wanted to put forward the striking consequences of the presence of Gribov copies on the IR behavior of the correlation functions and on their interpretation in the Landau gauge. On the one hand, the KO interpretation of the scaling solution is not clear due to the breaking of the initial BRST symmetry and, on the other hand, the RGZ action predicts the decoupling solution. This motivates to better understand the effects of the Gribov copies as there is an increasing belief that they play a crucial role in the IR domain of YM theories and perhaps even for

[13] We drop off the trivial diagonal color structure of the propagators for clarity of the notations.

confinement [186]. We mention that, the Landau gauge is only one representative of the covariant gauges and it displays additional properties, among others for instance the absence of a longitudinal gluon propagator. It would thus be interesting to investigate whether or not the presence of Gribov copies plays such an important role as in the Landau gauge in other covariant gauges. The GZ construction presented here can be applied to gauges that can be defined from the minimization of a functional, akin the Landau gauge with the functional (I.4.1). Accordingly, some of Gribov copies effects have been studied for instance in the (non-covariant) Coulomb gauge [187, 188, 189, 190, 191].[14] However, the Coulomb and Landau gauges are so different that there is no point in making comparisons between the two (though the meaning of comparing gauge dependent quantities in two different gauges is unclear in general). It was thus motivated in [186] that investigations in covariant gauges that are continuously connected to the Landau one are of greater interests. In this line of thoughts, the authors attempted to extend the GZ proposal to the covariant linear gauges. This is not an easy task, the main reason being the fact that the FP operator is not Hermitian and thus has not a real spectrum. Accordingly, one loses the geometrical construction used in the Landau gauge, and, in particular, the identification of a region to restrict the path-integral domain is unclear. Nevertheless, recently, based on the presence of the nonperturbative (and nonlocal) BRST symmetry [184, 156], a BRST-like quantization was employed and the (R)GZ proposal was amended to the linear covariant gauges, see [72] and references herein.

We saw in this section that, in the Landau gauge, taking into account Gribov copies leads to either the scaling or the decoupling solutions depending if condensates are included or not, though both type of solutions were found consistent with the tower of DSEs (and confirmed by the FRG). We shall thus rely on lattice simulations to confirm which solution is chosen by the system, which is the topic of the next section.

I.4.3 Gauge-fixed lattice simulations.

In Sec. I.3.2, we introduced the Gribov ambiguity problem and created the need to take into account Gribov copies through the Neuberger problem that prevents a consistent implementation of the FP gauge-fixed action on the lattice. Gribov copies contribute degenerately with alternating signs in the path-integral yielding the indefinite 0/0 form for expectation value of gauge-invariants quantities. To tackle this issue, one may select a unique Gribov copy. However, this cannot be achieved by means of a local action principle [64], the basis of any continuum formulation. Instead, one has to rely on approximate restriction such as the (R)GZ proposals.[15] On the contrary, this can be done in some case in lattice simulations which, consequently, completely fix the gauge as only one copy is selected.

Recalling that in the Landau gauge the Gribov copies correspond to the extrema

[14] For completeness, we also mention that the maximal Abelian gauge was also investigated in this framework [192, 193, 194, 195].

[15] We recall that the first Gribov region Ω still contains Gribov copies.

of the functional $\mathcal{H}_{\text{Landau}}[A,U]$ (I.4.1), whose discrete version is

$$\mathcal{H}_{\text{Landau latt.}}[W,U] = \text{Re}\,\text{tr}\sum_x \left\{ -\sum_{\mu=1}^{d} W_\mu^U(x) \right\}, \tag{I.4.17}$$

with $W_\mu(x)$ the lattice gauge link (I.1.7) and where we recall that the gauge-transformed link reads $W_\mu^U(x) = U(x)W_\mu(x)U^\dagger(x+a\hat{\mu})$. Fixing the Landau gauge thus boils down to select an extremum (in practice a minimum) of this functional, which can be achieved by using powerful minimization algorithms [49, 50, 51, 52]. Then, the lattice procedure to compute average of a quantity $\mathcal{O}$ can be sketched as follows:

- First, simulate a collection of gauge links $\left\{W_\mu^{(l)}\right\}_{l=1,\dots N_{\text{links}}}$ with the discretized YM weight (I.1.9);
- For each gauge link $W_\mu^{(l)}$, apply repeatedly gauge transformations $W_\mu^{(l)} \to W_\mu^{(l),U}$ according to the minimization algorithms until a minimum of (I.4.17) is reached. The resulting gauge link thus satisfies the gauge equation;
- Perform the statistical average over the the previously obtained gauge-fixed links $\langle\mathcal{O}\rangle \simeq \frac{1}{N_{\text{links}}}\sum_{l=1}^{N_{\text{links}}} \mathcal{O}\left[W_\mu^{(l)}\right]$.

Note that by fixing the gauge according to this procedure, one does not need to include extra auxiliary fields such as ghosts, or the GZ φ, ω fields. Nevertheless, quantities that in the continuum depend on such fields can, in some cases, still be accessed in lattice simulations. For instance, the ghost propagator is obtained through the average of the inverse FP operator $\mathcal{F}^{-1}$. Computing correlation functions according to this procedure thus provides results from a first principle nonperturbative computational method in a gauge-fixed version of YM theories where the gauge has been completely fixed since only one Gribov copy per gauge orbit has been selected. Therefore, a lot of interests were devoted to such numerical simulations and many results were obtained in the Landau gauge, e.g. [137, 134, 138, 139, 140, 44, 141, 142, 143, 144, 43, 42, 145, 146, 147, 148, 149, 45]. In particular, they provide an important benchmark for continuum approaches. For instance, numerical studies of the various vertices confirmed the ghost IR dominance truncation schemes used in DSEs [135, 136]. For our present concerns, we are mostly interested in results for the Landau gauge gluon and ghost propagators. Results from large volume simulations are depicted in Fig. I.6. In particular, one clearly sees a finite ghost dressing function at zero momentum, and a massive gluon propagator. These results go along with the decoupling solution and discard the scaling one. It follows that the RGZ thus agrees (at least qualitatively) with lattice data. Note, however, that both approaches implement the Landau gauge in different ways.

The lattice gauge-fixing procedure presented here relies on the existence of an auxiliary functional to be minimized. Investigation of other covariant gauges connected to the Landau one would be of great interests to infer possible gauge (in)dependent features of the propagators and possible systematic Gribov copies effects, though this would require to define such a family of gauges by means of an extremization procedure.

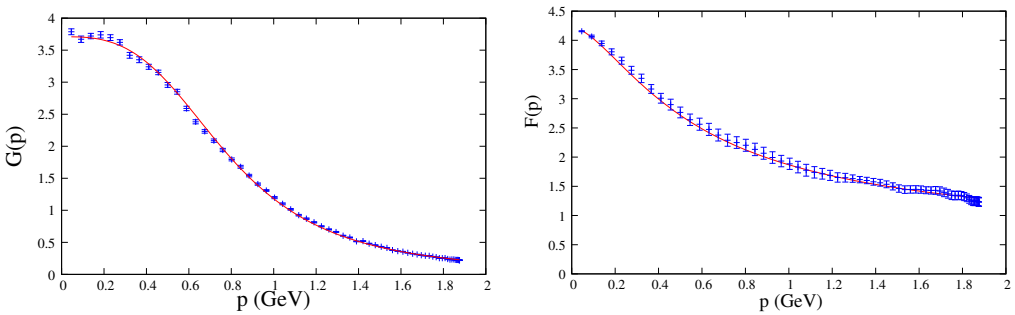

Figure I.6: Lattice results for the gluon propagator $G(p)$ and the ghost dressing function $F(p)$ as function of the momentum p in four dimensions for $SU(2)$ gauge group. Original figure from [79]. Blue crosses are lattice data taken from [196]. Red curves are analytical results obtained in [79], see Sec. I.5.1.

We also mention that, recently, following the proposal put forward in [67] numerical implementations of the covariant linear gauges were achieved [68, 69, 70, 71] but do not actually correspond to the extremization of a local functional. Another related issue is that the FP operator in such gauges is not Hermitian which complicates the discussion of Gribov copies and Gribov regions [186] as well as numerical calculation of the ghost propagator.

I.5 A novel approach to deal with Gribov copies

In the previous sections we intended to motivate that nonperturbative methods, e.g. DSEs, are not completely sufficient to access the IR properties of YM correlation functions. We illustrated this with the Neuberger problem, see Sec. I.3.2, to put forward that one also needs to take into account aspects of the gauge-fixing procedure that are disregarded by the FP procedure in order to tackle the problem of Gribov ambiguities. On the lattice, in certain gauges such as the Landau one, this can be realized completely (only one copy is selected) and reliable results for the correlation functions are obtained. However, the lattice gauge-fixing procedure is purely algorithmic and one does not know the corresponding continuum limit, while selecting a unique copy is not possible in terms of a local QFT. Still, one can cope with the Gribov ambiguity issue through the GZ proposal and obtain good agreement with lattice simulations in the case of the RGZ [197, 198].

In this manuscript, we study an alternative proposal made by Serreau and Tissier (ST) [74] that intends to consistently deal with Gribov copies. Our main work is developed in the next chapters. The ST treatment of Gribov copies has the main advantage that the resulting (Gribov ambiguity free) gauge-fixed action can be studied by simple perturbative tools and presents very good agreement with the available lattice results. We would like to emphasize these points in the next sections. For completeness, it shall be mentioned that one point of the proposal is not fully justified yet. It is related to the technique used to cast under the form of a local QFT the ST procedure: a number n of extra auxiliary fields have to be introduced while averages of physical observable must be evaluated in the limit $n \to 0$. In practice, it is assumed

that one can freely interchange the order the this limit and the path-integral. This will become clear in the next chapter.

I.5.1 The Curci-Ferrari model

Before presenting the ST proposal we first describe the phenomenological Curci-Ferrari (CF) model [76, 77]. Once large volume lattice simulations have well established that it is the decoupling solution which is realized, Tissier, Wschebor, and, later, Peláez reconsidered the CF model. The general model consists in a massive extension of the (FP) gauge-fixed YM action in nonlinear covariant gauges [100]. Tissier Wschebor and Peláez considered the Landau limit of the model

$$S_{\rm CF} = \int_x \left\{ \frac{1}{4} F^a_{\mu\nu} F^a_{\mu\nu} + \partial_\mu \bar{c}^a D_\mu c^a + i h^a \partial_\mu A^a_\mu + \frac{m_0^2}{2} A^a_\mu A^a_\mu \right\}, \tag{I.5.1}$$

with m_0 a (bare) mass parameter. The standard Landau gauge FP action is recovered for $m_0 = 0$. In particular, the mass term does not change the YM one-loop universal beta function for the coupling constant, thereby the model is asymptotically free. Just like in the (R)GZ cases, the mass term softly breaks the nilpotent BRST symmetry Eq. (I.2.12). Nevertheless, the CF model remains renormalizable in four dimension [77] and the renormalization factors were computed up to three loops in a $\overline{\rm MS}$ scheme in [199]. In fact, despite the soft breaking of the BRST symmetry, the CF action Eq. (I.5.1) displays a large set of symmetries. In particular, it admits a modified (non-nilpotent) BRST symmetry, that we note $\hat{s}$, defined by its action on the fundamental fields

$$\hat{s} A^a_\mu = \partial_\mu c^a + g_0 f^{abc} A^b_\mu c^c \,, \quad \hat{s} c^a = -\frac{g_0}{2} f^{abc} c^b c^c \,, \quad \hat{s} \bar{c}^a = i h^a \,, \quad \hat{s} i h^a = m_0^2 c^a \,. \tag{I.5.2}$$

The usual Slavnov-Taylor identities [116, 200] associated with the nilpotent BRST symmetry can be accordingly modified and used to constrain possible UV divergences. We shall make an extensive use of such modified Slavnov-Taylor identities in the next chapter when proving the renormalizability of the ST gauge-fixed action, see Sec. II.3.2. Modified Slavnov-Taylor identities can be derived along standard lines [118]. These identities consist in deriving from the symmetries of the problem various constraints on the Green's functions. For later use, let us proceed to their derivation here. We introduce independent sources for all independent fields and their (modified) BRST variations[16] as

$$S_1 = \int_x \left\{ J^a_\mu A^a_\mu + \bar{\eta}^a c^a + \bar{c}^a \eta^a + i h^a M^a + \bar{K}^a_\mu \hat{s} A^a_\mu + \bar{L}^a \hat{s} c^a \right\}. \tag{I.5.3}$$

According to the definition of the effective action Γ, Eq. (I.3.2), we have that

$$\begin{gathered} \frac{\delta \Gamma}{\delta A^a_\mu} = J^a_\mu \,, \quad \frac{\delta \Gamma}{\delta c^a} = -\bar{\eta}^a \,, \quad \frac{\delta \Gamma}{\delta \bar{c}^a} = \eta^a \,, \\ \frac{\delta \Gamma}{\delta \bar{K}^a_\mu} = -\hat{s} A^a_\mu \,, \quad \frac{\delta \Gamma}{\delta \bar{L}^a} = -\hat{s} c^a \,, \end{gathered} \tag{I.5.4}$$

[16] Since $\hat{s}\bar{c}^a = i h^a$ and $\hat{s} i h^a = m_0^2 c^a$, there is no need to introduce additional sources for the (modified) BRST variations of $\bar{c}$ and ih. Remark also that $\hat{s}^2 (A_\mu, c) = 0$, $\hat{s}^2 \bar{c}^a = m_0^2 c^a$ and $\hat{s}^2 i h^a = m_0^2 \hat{s} c^a$ such that the variations $\hat{s}^2$ do not require additional sources neither.

where $\phi = \{A_\mu, c, \bar{c}, ih\}$ are understood to be the mean value of the corresponding fields in presence of the sources. Performing the transformation $\phi \to \phi + \theta\hat{s}\phi$, with θ an "infinitesimal" Grassmann parameter, in

$$Z = \int \mathcal{D}A\mathcal{D}c\mathcal{D}\bar{c}\mathcal{D}h\, e^{-S_{\rm CF}+S_1}\,, \tag{I.5.5}$$

yields the modified Slavnov-Taylor identity

$$\begin{aligned} 0 &= \int \mathcal{D}\phi\, e^{-S_{\rm CF}+S_1} \int_x \left\{ J^a_\mu \hat{s}A^a_\mu - \bar{\eta}^a \hat{s}c^a + \hat{s}\bar{c}^a \eta^a + M^a \hat{s} i h^a \right\} \\ &= \int_x \left\{ -\frac{\delta\Gamma}{\delta A^a_\mu}\frac{\delta\Gamma}{\delta \bar{K}^a_\mu} - \frac{\delta\Gamma}{\delta c^a}\frac{\delta\Gamma}{\delta \bar{L}^a} + ih^a \frac{\delta\Gamma}{\delta \bar{c}^a} + m_0^2 \frac{\delta\Gamma}{\delta i h^a} c^a \right\}. \end{aligned} \tag{I.5.6}$$

Such an identity, coupled with others derived from the remaining symmetries, e.g., ghost number conservation, allowed Tisser and Wschebor to reduce the number of independent renormalization factors from the five naively suggested by (I.5.1) down to three [201, 202]. In particular, the renormalization factors lead, in a $\overline{\rm MS}$ renormalization scheme, to a UV vanishing mass, and one recovers, at high energies, the standard FP theory.

One of the most important features of the CF model is that it presents IR safe renormalization groups (RG) flows, as first pointed out in [78]. Hereby, one can use standard perturbation theory down to arbitrarily low momentum, which allows one to probe perturbatively the IR regime. Following this observation, Tissier, Wschebor and Peláez computed, at one-loop order in perturbation theory, the various two-point correlation functions as well as the vertices with and without quarks. Remarkably, their one-loop results were found to accurately reproduce the nonperturbative lattice data [79, 80, 81, 82, 203]. For instance, on Fig. I.6, the one-loop gluon propagator and ghost dressing function (red curves) are compared with lattice data (blue crosses). It is remarkable that, at the cost of introducing only one new parameter, such perturbative one-loop calculations accurately describe the IR regime of YM theories. This suggests that most of the nonperturbative dynamics are accurately captured by the effective gluon mass and the residual dynamics can then be treated perturbatively. As we shall see in the next section, the Serrau-Tissier proposal provides a possible origin to such a mass term in relation with the treatment of Gribov copies.

I.5.2 The Serreau-Tissier proposal

The effective approach of Tissier, Wschebor and Peláez can be founded on more solid theoretical grounds according to Serreau and Tissier. Recently, they developed, in the Landau gauge, a new gauge-fixing procedure that consistently deals with the presence of Gribov copies [74]. In the Landau gauge, for what concerns the gluon and ghost sectors, their procedure boils down to the inclusion of an effective gluon mass and the resulting YM gauge-fixed action is perturbatively equivalent to the Landau limit of the CF model Eq. (I.5.1) [74].

The spirit of this proposal is quite different from those of the lattice gauge-fixing procedure and the GZ proposal. In the latter, in order to tackle the presence of Gribov copies, one tries to enforce the initial gauge condition by restricting further the

configuration space and eventually selects a unique Gribov copy as achieved by the lattice. On the contrary, Serreau and Tissier proposed to take into account all Gribov copies, but to provide them with different weights in the path-integral such that their degeneracy is lifted. Applied to the Landau gauge, this legitimate procedure provides another implementation of this gauge in which the resulting gauge-fixed action is free of Gribov ambiguities. The details of the construction are given in the next chapter, see Sec. II.2.1. Let us here draw the main features of the ST gauge-fixing procedure.

In order to cope with the issue of Gribov ambiguities, in the computation of expectation value of an operator $\mathcal{O}$, one first performs a (pseudo) average with a nonuniform statistical weight over the copies belonging to the same gauge orbit.[17] That is, given a field configuration A, along its gauge orbit, one performs the following pseudo average (note the presence of the sign $s(i)$ of the FP operator)

$$\sum_i \mathcal{O}[A^{U_i}] s(i) e^{-\beta_0 \mathcal{H}_{\text{Landau}}[A,U_i]} , \tag{I.5.7}$$

where the sum runs over all extrema of $\mathcal{H}_{\text{Landau}}$, that is, over all Gribov copies[18], $s(i)$ is the sign of the FP operator and $\beta_0 > 0$ is a new gauge parameter, that has the dimension of a square mass. The nonuniform weight $e^{-\beta_0 \mathcal{H}_{\text{Landau}}[A,U_i]}$ thus lifts the degeneracy of the copies according to the landscape of the extrema of $\mathcal{H}_{\text{Landau}}$. Then, one averages over the gauge field configurations A with the YM weight. This gauge-fixing procedure can be put under the form of a local gauge-fixed YM action by introducing auxiliary fields. The resulting (Gribov ambiguity free) gauge-fixed action turns out to be renormalizable in four dimensions [74], see also Sec. II.3.2. Remarkably, in the Landau gauge, most of the auxiliary fields introduced to take into account the presence of Gribov copies essentially decouple from the YM sector and the gluon and ghost sectors are perturbatively equivalent to those of the Landau limit of the CF model presented above. This means that, at least in the Landau gauge, the ST gauge-fixed action can be investigated by means of simple perturbative tools and the results reproduce accurately the lattice data. We believe this is a strong result that such a Gribov ambiguity free implementation of the Landau gauge allows one to access perturbatively the IR regime of YM theories (we recall our previous remark concerning a possible loophole of the present proposal).

Remark that, the ST proposal is, again, another way of implementing the Landau gauge. Hence, as emphasized above, the comparison between different approaches might be unclear. In particular, the lattice selects a unique copy that corresponds to a minimum of $\mathcal{H}_{\text{Landau}}$ while the ST proposal averages over all copies, that is, minima, maxima and saddle points of $\mathcal{H}_{\text{Landau}}$. Hence, depending on the landscape of $\mathcal{H}_{\text{Landau}}$, comparisons between the lattice and the ST results might be meaningful or not. In particular, for both approaches to be compared, $\mathcal{H}_{\text{Landau}}$ shall satisfy

$$\mathcal{H}_{\text{Landau}}\left[A, U_{\text{min.}}\right] < \mathcal{H}_{\text{Landau}}\left[A, U_{\text{sdl.pts./max.}}\right] , \tag{I.5.8}$$

[17] We mention that a similar idea was proposed along the lines of [204, 205] but, there, it was proposed to average with a nonuniform weight over the whole gauge orbit and not solely over the Gribov copies. This proposal was tractable in lattice simulations [206, 207] but it was shown that the corresponding continuum action was nonrenormalizable [205, 208].

[18] Remark that the sum runs over minima, maxima and saddle points, such that all Gribov copies are taken into account.

where $U_{\min}$, $U_{\text{sdl.pts.}}$, $U_{\max}$ are respectively minima, saddle points and maxima. In such a case, for a value of β_0 not too small, the contribution of Gribov copies that are not minima (i.e. outside the first Gribov region Ω) are exponentially suppressed in Eq. (I.5.7). It remains to select a β_0 not too large such that randomly picking one minimum is equivalent to averaging over them with a small lifting. Checking this scenario would require lattice investigations of the landscape of $\mathcal{H}_{\text{Landau}}$. This could be done on small lattices [174] but did not provide any firm answer yet regarding the scenario (I.5.8). Indeed, the number of copies grows exponentially with increasing volume and, so far, lattice procedures are doomed to find only minima of $\mathcal{H}_{\text{Landau}}$ and remain blind to maxima and saddle points. Nevertheless, lattice simulations display small dependences of the correlators with respect to the choice of the copy [43], thus arguing in favor of that scenario (regarding the assumption that selecting one minimum is equivalent to averaging over them). It remains that these are gauge-dependent features, and hereby a priori proper to the Landau gauge as they depend on the peculiar form of $\mathcal{H}_{\text{Landau}}$.

Generalization of the ST proposal to other covariant gauges constitutes one of the main purpose of the work presented in this thesis. In Chapter II, we present a generalization of the Landau functional $\mathcal{H}_{\text{Landau}}$. We show that its extrema define a one-parameter family of nonlinear covariant gauges that are continuously connected to the Landau one. Thus, it opens the way to investigations of covariant gauges for approaches such as the ST proposal or lattice simulations. We briefly study how existing minimization algorithms can be adapted to this case. Then, we implement these gauges within the ST proposal whose details are displayed in Chapter II. In particular, we prove that the resulting local gauge-fixed action is renormalizable in four dimensions for the whole family of gauges (that includes the Landau one). Remarkably, a massive extension the usual FP gauge-fixing procedure applied to these gauges yields a one-parameter family of (massive) nonlinear covariant actions known as the general ξ-gauges CF model. Henceforth, we have at our disposal two actions that differ only by our treatment of Gribov copies and which can be both investigated in perturbation theory. Comparisons of correlation functions between the two thus provide a benchmark to study Gribov copies effects. We perform the calculations in perturbation theory, up to one-loop order. Eventually we show that, in these gauges, both the ST and CF actions present IR safe RG trajectories thus justifying the perturbative approach.

Chapter II

Nonlinear covariant gauges without Gribov ambiguities

In the previous chapter, we motivated that a detailed understanding of the long distance properties of correlation functions in non-Abelian gauge theories is a mandatory step in order to investigate the IR physics of the strong interactions in analytical methods. In particular, the interplay between both lattice and continuum approaches is of key importance, the former providing a benchmark for the latter. Of course, both approaches must be performed in the same gauge in order to do meaningful comparisons. However, as we saw previously, finding gauges which can be investigated in both cases is not an easy task, in part due to the presence of Gribov copies. In this regard, the Landau gauge stands as peculiar since both continuum and lattice studies were performed extensively. In particular, among the former, the revisiting of the (Landau limit of the) Curci-Ferrari (CF) model [77] by Peláez, Tissier and Wschebor has shown recently that most of the nonperturbative gluon dynamics can accurately be accounted for by the presence of an effective mass term [78, 79, 80, 81, 82]. In this massive approach, the absence of a Landau pole allows for perturbative development down to the deep IR and simple perturbative one-loop calculations are found in very good agreement with the lattice data. Moreover, Serreau and Tissier developed a new proposal (hereafter referred to as the ST proposal), which fixes the gauge while the Gribov copies are consistently accounted for, as opposed to the standard FP procedure. The ST proposal was successfully applied to the Landau gauge where it was possible to recast the gauge-fixing procedure under the form of a local field theory [74]. In particular, in the Landau gauge, the resulting gauge-fixed action is perturbatively equivalent to the Landau limit of the CF model for what concerns the gluon and the ghost sectors. Altogether, these two series of works therefore provide a *bona fide* Landau gauge-fixed version of the YM action that can be investigated with simple perturbation theory and whose results agree with those obtained in lattice simulations. This is an exciting result since the common belief is that the IR regime of YM theories is accessible only through nonperturbative techniques. One of the main advantages of this approach is its simplicity at the computational level in comparison to other continuum approaches such as DSEs.

Nevertheless, the Landau gauge is solely one representative of the covariant gauges

and displays additional symmetries and a peculiar geometrical structure of the Gribov copies space. With results only in such a peculiar gauge, it is thus difficult to infer possible gauge-(in)dependent features as well as possible systematic Gribov copies effects on the basic correlators. In this sense, research of other gauges that would allow for both numerical simulations and continuum approaches that handle Gribov ambiguities are interesting. This is the purpose of the present work.

Here, among other works, we describe our studies presented in [209, 99] where we intend to investigate a class of covariant gauges continuously connected to the Landau one. To do so, we define our gauge condition through an extremization procedure of a functional $\mathcal{H}$ that slightly generalizes the one employed for the Landau gauge $\mathcal{H}_{\text{Landau}}$, see (I.4.1). In a first step, in order to gain more insights into these gauges, we neglect the presence of Gribov copies (which is at best valid at high energies) and apply the standard FP procedure. We show in Sec. II.1.1 that the minimization of the functional $\mathcal{H}$ implements the Curci-Ferrari-Delbourgo-Jarvis (CFDJ) gauges [77, 100] that consist in a one-parameter family of nonlinear gauges continuously connected to the Landau one. Although these gauges are known to be both renormalizable and unitary, they are plagued by Gribov ambiguities. In a second time, after discussing the possible lattice implementation of these gauges in Sec. II.1.2, we apply the ST proposal to CFDJ gauges in Sec. II.2. The core of the procedure consists in a (pseudo) average over Gribov copies with a nonuniform weight in order to lift their degeneracy. This provides a continuum formulation of these gauges that consistently deals with Gribov ambiguities. We present in detail the ST approach and show that, eventually, the gauge-fixing procedure can be cast under the form of a local field theory. To achieve this, we introduce the technique of replicas [75], which is commonly used in the context of disordered systems in statistical field theory. As we shall see, replicas are an essential ingredient of the (localized) ST procedure as they insure that the resulting local ST action is a *bona fide* gauge-fixed version of YM theories. Their consequences is exhaustively discussed all along the present manuscript. On top of it, our treatment of Gribov copies introduces also a gauge parameter that controls the lifting of the copies' degeneracy. Eventually, this lifting parameter acts as a mass term for the various fields. Remarkably, the resulting gauge-fixed ST action corresponds to a massive extension of the CFDJ gauges known as the CF action [77], supplemented by a nontrivial replica sector. We show in Sec. II.3.2 that the ST action is multiplicatively renormalizable in four dimensions.

The difference between the bona fide gauge-fixed ST action and the CF model lies in the replica sector. Therefore, Gribov copies effects can be accessed by investigating the possible effects of the replica sector. This is achieved by comparing the gluon and ghost correlators obtained from both the ST procedure and the CF model. In the Landau gauge, where the gluon and ghost sectors are equivalent in both the ST and the CF cases, the theory admits IR safe RG trajectories under suitable choices of renormalization prescriptions. It is therefore natural to adapt such renormalization schemes to the case of the CFDJ gauges, which is done in Sec. II.5. We compute at one-loop order in perturbation theory the gluon and ghost propagators in both the ST procedure and the CF model for the whole family of CFDJ gauges. Apart in the Landau gauge, we observe clear differences between the ST and the CF cases. In particular, even away from the Landau limit, the gluon propagator remains transverse in the ST

case, while a longitudinal gluon propagator develops in the CF model. We investigate in Sec. II.7 the possible presence of IR safe RG trajectories. Although present in both the ST and the CF cases, these are radically different due to the presence of massless modes in the replica sector of the ST action that are absent from the CF model. This highlights another effect of our treatment of Gribov copes. Finally, we end this chapter in Sec. II.7.4 by opening some leads for further investigations that intend to relate more directly the role of Gribov copies with the correlators of the present theory.

II.1 Gauge-fixing procedure

II.1.1 Gauge-fixing functional

We consider the following functional

$$\mathcal{H}[A,\eta,U]=\int_x \mathrm{tr}\left[\left(A_\mu^U\right)^2+\frac{U^\dagger\eta+\eta^\dagger U}{2}\right], \tag{II.1.1}$$

where η is an arbitrary $N\times N$ matrix field, g_0 is the (bare) coupling constant and we recall that

$$A_\mu^U=UA_\mu U^\dagger+\frac{i}{g_0}U\partial_\mu U^\dagger, \tag{II.1.2}$$

with $U(x)\in \mathrm{SU}(N)$.[1] The functional $\mathcal{H}$ is a slight generalization of the functional $\mathcal{H}_{\mathrm{Landau}}$:

$$\mathcal{H}_{\mathrm{Landau}}=\mathcal{H}[A,0,U]. \tag{II.1.3}$$

By analogy with the Landau gauge, we define our gauge condition as (one of) the extrema of $\mathcal{H}$ with respect to U. The gauge equation can be derived along the same lines as for the Landau gauge, see (I.4.2): performing the gauge transformation $U\to VU$, with V infinitesimally close to the identity $V\sim \mathbb{1}+ig_0\lambda$ and making an expansion in λ: $A_\mu^V=A_\mu+D_\mu\lambda+\mathcal{O}(\lambda^2)$, with the usual covariant derivative

$$D_\mu^{ac}=\partial_\mu\delta^{ac}+f^{abc}A_\mu^b\,. \tag{II.1.4}$$

Plugging these expressions into (II.1.1) yields the equation satisfied by the stationary points of $\mathcal{H}$ or, equivalently, to the covariant gauge condition

$$\left(\partial_\mu A_\mu^U\right)^a=\frac{ig_0}{2}\mathrm{tr}\left[t^a\left(U\eta^\dagger-\eta U^\dagger\right)\right]. \tag{II.1.5}$$

For $\eta=0$ we recover the Landau gauge condition as expected from Eq. (II.1.3). The condition Eq. (II.1.5) can be used as a gauge equation for all η. However, this would lead to a field theory that depends on the external η field. Since gauge-invariant quantities are independent of η, one can equivalently average over all realizations of η according to a given probability distribution $\mathcal{P}[\eta]$. In principle, the choice for $\mathcal{P}[\eta]$

[1] We recall our conventions for the $\mathrm{SU}(N)$ group: the $\{t^a\}_{a=1,\dots,N^2-1}$ form a basis of the $\mathrm{su}(N)$ Lie algebra and our convention is that $\mathrm{tr}\,t^at^b=\delta^{ab}/2$, $\left[t^a,t^b\right]=if^{abc}t^c$, with f^{abc} the totally antisimmetric structure constant. The totally symmetric structure constant d^{abc} is defined by: $t^at^b=\mathbb{1}\delta^{ab}/2N+t^c(if^{abc}+d^{abc})/2$.

is arbitrary but might lead to additional technical difficulties or even worse, to a non-renormalizable field theory if $\mathcal{P}[\eta]$ contains derivative terms for instance. In practice we choose a gaussian weight that introduces a (bare) gauge parameter ξ_0:

$$\mathcal{P}[\eta] = \mathcal{N} \exp\left(-\frac{g_0^2}{4\xi_0}\int_x \mathrm{tr}\ \eta^\dagger\eta\right), \tag{II.1.6}$$

with $\mathcal{N}$ a normalization factor. Note that, the Landau gauge ($\eta = 0$) is recovered by taking $\xi_0 \to 0$ in $\mathcal{P}[\eta]$.

Just like in the Landau gauge, for a given A and η, the functional $\mathcal{H}$ admits many extrema U_i corresponding to Gribov copies. In order to gain better insights into the field theory that describes the gauges (II.1.5), we first neglect these copies (which is at best justified in the UV regime) and apply the standard FP gauge-fixing procedure. Setting again $U \to (\mathbb{1} + ig_0\lambda)U$ in (II.1.5) and expanding in λ, we obtain the FP operator

$$\mathcal{F}^{ac}(x,y) = \left\{\partial_\mu\left(D_\mu^U\right)^{ac} + \frac{g_0^2}{2}\mathrm{tr}\left(t^a t^c U\eta^\dagger + \eta U^\dagger t^c t^a\right)\right\}\delta(x-y), \tag{II.1.7}$$

with $D_\mu^U\varphi \equiv D_\mu[A^U]\varphi = \partial_\mu\varphi - ig_0[A_\mu^U,\varphi]$. The corresponding FP gauge-fixed action, for fixed η, is

$$\begin{aligned} S_{\mathrm{gf}}^\eta[A,c,\bar c,h,U] &= S_{\mathrm{YM}}[A] + S_{\mathrm{FP}}^\eta[A,c,\bar c,h,U],\\ S_{\mathrm{FP}}^\eta[A,c,\bar c,h,U] &= \int_x\left\{\partial_\mu\bar c^a D_\mu^U c^a + ih^a\left(\partial_\mu A_\mu^U\right)^a + \frac{g_0}{2}\mathrm{tr}\left[\eta^\dagger R + R^\dagger\eta\right]\right\}, \end{aligned} \tag{II.1.8}$$

with $R = (h - g_0\bar c c)U$. Note in particular that U appears on its own through R and not only through the gauge transformed gauge field A^U. Thus the standard FP trick, that aims at factorizing out the volume of the gauge group, cannot be applied here. This is where the choice of the weight $\mathcal{P}[\eta]$ used to average over the external η field becomes crucial as R (and so the "problematic" U) appears always along η in Eq. (II.1.8). Indeed, for the gaussian choice of $\mathcal{P}[\eta]$, Eq. (II.1.6), we have

$$\int \mathcal{D}\eta\mathcal{P}[\eta]\, e^{-\frac{g_0}{2}\int_x \mathrm{tr}[\eta^\dagger R + R^\dagger\eta]} \propto e^{\xi_0\int_x \mathrm{tr}[R^\dagger R]}, \tag{II.1.9}$$

which is independent of U, and hence the FP trick can be applied to factorize out the volume of the gauge group. The resulting effective FP gauge-fixed action is

$$\begin{aligned} S_{\mathrm{gf}}[A,c,\bar c,h] =& S_{\mathrm{YM}}[A] + S_{\mathrm{CFDJ}}[A,c,\bar c,h],\\ S_{\mathrm{CFDJ}}[A,c,\bar c,h] =& \int_x\left\{\partial_\mu\bar c^a D_\mu c^a + ih^a\partial_\mu A_\mu^a + \xi_0\left[-\frac{(ih^a)^2}{2} - \frac{g_0}{2}f^{abc}ih^a\bar c^b c^c - \frac{g_0^2}{4}\left(f^{abc}\bar c^b c^c\right)^2\right]\right\}. \end{aligned} \tag{II.1.10}$$

The gauge-fixing term S_{CFDJ} corresponds to the Curci-Ferrari-Delbourgo-Jarvis gauges, which were extensively studied in the literature [77, 100, 210, 201, 211]. They correspond to covariant nonlinear gauges (note the difference with the covariant linear gauges by the presence of the four-ghost term in Eq. (II.1.10)). In particular they were shown to be renormalizable in four dimensions, and unitary as they possess a nilpotent

BRST symmetry. However, these gauges are plagued by the presence of Gribov copies which correspond to the different extrema of the functional (II.1.1). Thus, akin for the Landau gauge, in order to completely fix the gauge, one may select a unique extremum of $\mathcal{H}$. As emphasized earlier, up to now, this is not possible in the continuum. In the next section we discuss the possible implementation of the CFDJ gauges on the lattice.

II.1.2 Lattice implementation of the CFDJ gauges

Covariant gauges are very difficult to implement in lattice simulations because solving the gauge condition amounts to solve a large set of coupled nonlinear partial differential equations. The Landau gauge stands as a peculiar case because it can be formulated as an extremization procedure, which is much easier to implement on the lattice, provided that the extremization algorithms converge. As presented in Sec. I.4.3 of the previous chapter, the Landau gauge was successfully implemented on the lattice by minimization of the functional $\mathcal{H}_{\text{Landau}}$ and, in turn, was extensively studied [41, 42, 139, 140, 44, 147, 148, 149, 45]. We saw in the previous section that the CFDJ gauges also correspond to the extrema of an external functional, namely $\mathcal{H}$ [see (II.1.1)], which slightly generalizes the one used in the Landau gauge. This thus keeps open the possibility that the CFDJ gauges might be implemented on the lattice by extrimizing the functional $\mathcal{H}$ following the minimization algorithms routinely employed for the implementation of the Landau gauge. Of course, this would require to generalize/adapt all the latter to the present case. These consist in algorithms that minimize $\mathcal{H}_{\text{Landau}}$ both globally and locally, whose detailed discussion is beyond the scope of the present thesis. Here, instead, as an illustration, we propose a possible generalization of the Los Alamos algorithm [51], which is routinely employed to locally minimize $\mathcal{H}_{\text{Landau}}$ in lattice gauge-fixing procedure.

Many numerical minimization techniques, such as the Los Alamos algorithm, require, as a necessary (but not sufficient) condition, that the (discretized) functional to be minimized be linear in the gauge transformation U at each space-time point. It is the case for the Landau gauge part of $\mathcal{H}$ (left term on the right hand side of Eq. (II.1.1)) [41], and it is obviously so for the η part. We believe that this is an encouraging point regarding the feasibility of the algorithm to be presented below. In the following, we propose a simple and straightforward generalization to the CFDJ gauges of the Los Alamos (locally minimizing) algorithm.

We restrain ourselves to the SU(2) case. For SU(3), the general strategy consists in applying successively the minimization algorithm on the three (non-independent) SU(2) subgroups of SU(3). Introducing the rescaled matrix $M(x) = a^2 g_0^2 \eta(x)/2$, the discrete version of the minimizing functional (II.1.1) in terms of the gauge link $W_\mu^U(x) = U(x)W_\mu(x)U^\dagger(x + a\hat{\mu})$ is, up to an irrelevant constant [41, 51, 209],

$$\mathcal{H}_{\text{latt.}}[W, M, U] = \text{Re}\,\text{tr}\sum_x \left\{ M^\dagger(x)U(x) - \sum_{\mu=1}^{d} W_\mu^U(x) \right\}. \tag{II.1.11}$$

The Landau gauge functional is recovered for $\eta = 0$, i.e. $M = 0$ [41]. Owing to the linearity of $\mathcal{H}_{\text{latt.}}$ in U at each lattice point, we can use the Los Alamos algorithm by generalizing it from the Landau gauge case. This algorithm aims at minimizing the

functional site by site by successive gauge transformations. We first define

$$B(x) = -M^\dagger(x) + \sum_{\mu=-d}^{d} W_\mu(x) U^\dagger(x + a\hat{\mu}), \tag{II.1.12}$$

and

$$C(x) = \frac{\mathbb{1}}{4}\mathrm{tr}(B(x) + B^\dagger(x)) + \frac{\sigma_a}{4}\mathrm{tr}[\sigma_a(B(x) - B^\dagger(x))]\,, \tag{II.1.13}$$

where $\sigma_{a=1,2,3}$ are the Pauli matrices. The Los Alamos algorithm states that applying iteratively on each lattice site the gauge transformation

$$U_{\min}(x) = \frac{C^\dagger(x)}{\sqrt{\det C(x)}}, \tag{II.1.14}$$

systematically decreases the functional $\mathcal{H}_{\text{latt.}}$ [212, 98]. In the present case, the only difference with the Landau gauge is the presence of the M term in the definition of B, see Eq. (II.1.12). Therefore, the minimization is done for a given η, while we showed in the last section that the CFDJ gauges are obtained after averaging over the η field with the gaussian weight (II.1.6). In the lattice version, this yields an average over the M matrix field with the discretized gaussian weight

$$\mathcal{P}_{\text{latt.}}[M] = \exp\left\{-\frac{1}{\xi_0 g_0^2}\mathrm{tr}\sum_x \left[M^\dagger(x)M(x)\right]\right\}. \tag{II.1.15}$$

In conclusion, to compute the averages of an operator $\mathcal{O}$ in the CFDJ gauges on the lattice, one should first simulate a collection of gauge links $\left\{W_\mu^{(l)}\right\}_{l=1,\dots N_{\text{links}}}$ with the discretized YM weight, and a collection $\left\{M^{(k)}\right\}_{k=1,\dots N_\eta}$ of matrix fields M with weight (II.1.15). Then, apply iteratively the gauge transformation (II.1.14) until a minimum is reached[2]. For the same gauge link configuration, repeat the operation for the N_η configurations of M and average over them. Finally, repeat the whole process for all simulated link configurations and perform the average over them.

We stress that the previous discussion is far from being an actual proof of the feasibility of the lattice implementation of the CFDJ gauges. Rather, we aimed at illustrating how algorithms employed in the Landau gauge could be extended to the CFDJ gauges with an explicit example. In particular, a definite proof of the feasibility of the previous procedure would require an actual implementation in lattice simulations. More generally, the Landau gauge implementation requires, on top of local minimization procedures (akin the one presented above), global ones. We did not perform the generalization of the global procedures to the present case.

II.2 The CFDJ gauges in the Serreau-Tissier proposal

In this section, we apply the ST proposal to the gauges defined by the extrema of the functional (II.1.1) in order to formulate a continuum version of the CFDJ gauges

[2] In practice the lattice is split into odd and even lattice sites. The first step is to apply the transformation (II.1.14) on all even sites while the odd ones are left untouched. Then a second gauge transformation is performed that consists in (II.1.14) on odd sites while even ones are left untouched. This procedure is repeated until a minimum is reached.

free of Gribov ambiguities. We then prove that the resulting gauge-fixed action is renormalizable in dimension $d = 4$.

II.2.1 The Serreau-Tissier gauge-fixing procedure

The functional (II.1.1) admits many extrema (indexed by i in the following) $U_i \equiv U_i[A, \eta]$ for given A and η. The extrema U_i correspond to the Gribov copies. As emphasized earlier, the ST proposal consistently deals with these copies by defining averages through a two-step procedure. First, we perform a pseudo average over the Gribov copies of a given gauge orbit and we simultaneously average over the η field with the gaussian weight (II.1.6). The degeneracy of the copies is lifted by using a nonuniform weight to perform the average over the Gribov copies. More precisely, we define the first step of the procedure as

$$\langle \mathcal{O}[A] \rangle = \frac{\int \mathcal{D}\eta \mathcal{P}[\eta] \sum_i \mathcal{O}[A^{U_i}] s(i) e^{-\beta_0 \mathcal{H}[A,\eta,U_i]}}{\int \mathcal{D}\eta \mathcal{P}[\eta] \sum_i s(i) e^{-\beta_0 \mathcal{H}[A,\eta,U_i]}}, \tag{II.2.1}$$

where the sum runs over all Gribov copies U_i (i.e. all extrema of $\mathcal{H}$), $s(i)$ is the sign of the determinant of the FP operator (II.1.7) evaluated at the i^{th} copy, and $\beta_0 > 0$ is a (bare) gauge parameter that controls the lifting over the copies. We shall assume that the sets of copies that present the same value of $\mathcal{H}$ are of zero measure such that none of the copies contribute degenerately in the sum Eq. (II.2.1) and the Neuberger problem is thus avoided. The presence of the integration over η with the weight (II.1.6) introduces another (bare) gauge parameter ξ_0 for which the Landau gauge is recovered when $\xi_0 = 0$. Remark the crucial property that gauge-invariant quantities are blind to this first-step average

$$\langle \mathcal{O}_{\text{inv}}[A] \rangle = \mathcal{O}_{\text{inv}}[A], \tag{II.2.2}$$

as it should be since it corresponds to the average over a given gauge orbit (the one that supports the fixed field configuration A in Eq. (II.2.2)). Note in particular that, for this property to hold, the presence of the denominator in the definition (II.2.1) is mandatory. On the one hand, the peculiar case of $\beta_0 = 0$ corresponds to a flat weight over the copies so that their degeneracy is not lifted. According to the property (II.2.2), due to the cancellation among the FP signs, the case $\beta_0 = 0$ leads to the indefinite Neuberger 0/0 form of Eq. (II.2.1) when considering gauge invariant quantities. On the other hand, the limit $\beta_0 \to \infty$ corresponds to select only the absolute minimum of $\mathcal{H}$ and thus generalizes the absolute Landau gauge.

Notice that the way to average over η is not unique. For instance, one could have performed the η integration *after* having averaged over the copies, that is

$$\langle \mathcal{O}[A] \rangle' = \int \mathcal{D}\eta \mathcal{P}[\eta] \frac{\sum_i \mathcal{O}[A^{U_i}] s(i) e^{-\beta_0 \mathcal{H}[A,\eta,U_i]}}{\sum_i s(i) e^{-\beta_0 \mathcal{H}[A,\eta,U_i]}}. \tag{II.2.3}$$

As we describe below, once the replicas are introduced, this way of performing the η integration leads to a more complicated effective gauge-fixed action, and this is not pursued further in this thesis.

Once the contribution of the Gribov copies has been taken into account in Eq. (II.2.1), the second step of the ST procedure consists in averaging over the gauge field A with

the YM weight, that we note hereafter with an overall bar

$$\overline{\mathcal{O}[A]} = \frac{\int \mathcal{D}A\, \mathcal{O}[A] e^{-S_{\rm YM}[A]}}{\int \mathcal{D}A\, e^{-S_{\rm YM}[A]}}. \tag{II.2.4}$$

All in all, the procedure

$$\overline{\langle \mathcal{O}[A] \rangle} \tag{II.2.5}$$

defines average values of quantities in the CFDJ gauges implemented in a Gribov ambiguity free manner as long as the lifting parameter β_0 is strictly positive. In particular, owing to the denominator in Eq. (II.2.1), the procedure (II.2.5) corresponds to a genuine gauge-fixing procedure as gauge-invariant quantities are sensible only to the second step average Eq. (II.2.4), that is, the average performed with the gauge invariant YM weight.

II.2.2 Field theoretical formulation

Although mandatory for having a bona fide gauge-fixing procedure, the presence of the denominator in Eq. (II.2.1) makes (II.2.5) nonlocal, and thus requires additional work to be cast under the form of a local field theory. This is the purpose of this section following the steps of [74].

Owing to the standard FP procedure, by introducing the auxiliary fields c, $\bar{c}$, ih (ghost, antighost and Nakanishi-Lautrup fields), we have the following identity

$$\sum_i \mathcal{X}[A,\eta,U_i] s(i) = \int \mathcal{D}U \mathcal{D}c \mathcal{D}\bar{c} \mathcal{D}h\, \mathcal{X}[A,\eta,U]\, e^{-S^\eta_{\rm FP}[A^U,c,\bar{c},h]}\,, \tag{II.2.6}$$

whereby the sum on the left-hand side runs over all Gribov copies, $S^\eta_{\rm FP}$ has been defined in Eq. (II.1.8), $\mathcal{D}U$ is the Haar measure over the gauge group and $\mathcal{X}[A,\eta,U]$ is any functional of A, U and η. The sign $s(i)$ was introduced for the purpose of (II.2.6). In the following, we collect the set of fields U, c, $\bar{c}$ and h in a single symbol $\mathcal{V}$ for reasons that will soon become clear. Using the identity (II.2.6) for $\mathcal{X}[A,\eta,U] = \mathcal{O}[A^U] \exp\{-\beta_0 \mathcal{H}[A,\eta,U]\}$ or $\mathcal{X}[U] = \exp\{-\beta_0 \mathcal{H}[A,\eta,U]\}$, the first step of the procedure, Eq. (II.2.1), rewrites

$$\langle \mathcal{O}[A] \rangle = \frac{\int \mathcal{D}\mathcal{V} \mathcal{D}\eta\, \mathcal{P}[\eta]\, O[A^U]\, e^{-S^\eta_{\rm FP}[A,\mathcal{V}] - \beta_0 \mathcal{H}[A,\eta,U]}}{\int \mathcal{D}\mathcal{V} \mathcal{D}\eta\, \mathcal{P}[\eta]\, e^{-S^\eta_{\rm FP}[A,\mathcal{V}] - \beta_0 \mathcal{H}[A,\eta,U]}}\,. \tag{II.2.7}$$

We get, using (II.1.9) with $R = (h - g_0 \bar{c} c + \beta_0/g_0) U$,

$$\langle \mathcal{O}[A] \rangle = \frac{\int \mathcal{D}\mathcal{V} \mathcal{O}[A^U]\, e^{-S_{\rm CF}[A,\mathcal{V}]}}{\int \mathcal{D}\mathcal{V}\, e^{-S_{\rm CF}[A,\mathcal{V}]}}, \tag{II.2.8}$$

with

$$S_{\rm CF}[A,\mathcal{V}] \equiv S_{\rm CF}[A^U, c, \bar{c}, h], \tag{II.2.9}$$

and where the CF action $S_{\rm CF}$ is given by

$$\begin{aligned} S_{\rm CF}[A,c,\bar{c},h] =& S_{\rm CFDJ}[A,c,\bar{c},h] + S_{\beta_0}[A,c,\bar{c}] \\ =& \int_x \Big\{ \partial_\mu \bar{c}^a D_\mu c^a + i h^a \partial_\mu A^a_\mu + \beta_0 \left[\frac{1}{2}(A^a_\mu)^2 + \xi_0 \bar{c}^a c^a \right] \\ & + \xi_0 \Big[-\frac{(ih^a)^2}{2} - \frac{g_0}{2} f^{abc} i h^a \bar{c}^b c^c - \frac{g_0^2}{4} \left(f^{abc} \bar{c}^b c^c \right)^2 \Big] \Big\}. \end{aligned} \tag{II.2.10}$$

It corresponds to the CFDJ action (II.1.10) supplemented by a mass term for the gluon and ghost fields. Notice that Eq. (II.2.8) involves A^U instead of A. Let us stress the difference between the pure CF model, Eq. (II.2.10), and the CFDJ gauges implemented through the ST proposal. Averages in the CF model are obtained as

$$\langle \mathcal{O}[A] \rangle_{\rm CF} = \frac{\int \mathcal{D}A \mathcal{D}c \mathcal{D}\bar{c} \mathcal{D}h \, \mathcal{O}[A] \, e^{-S_{\rm YM} - S_{\rm CF}[A,c,\bar{c},ih]}}{\int \mathcal{D}A \mathcal{D}c \mathcal{D}\bar{c} \mathcal{D}h \, e^{-S_{\rm YM} - S_{\rm CF}[A,c,\bar{c},ih]}}, \tag{II.2.11}$$

while for the ST proposal

$$\overline{\langle \mathcal{O}[A] \rangle} = \frac{\int \mathcal{D}A \, \frac{\int \mathcal{D}\mathcal{V} \, \mathcal{O}[A^U] \, e^{-S_{\rm CF}[A,\mathcal{V}]}}{\int \mathcal{D}\mathcal{V} \, e^{-S_{\rm CF}[A,\mathcal{V}]}} \, e^{-S_{\rm YM}}}{\int \mathcal{D}A \, e^{-S_{\rm YM}}}. \tag{II.2.12}$$

Again, the presence of the denominator $1/\int \mathcal{D}\mathcal{V} \, e^{-S_{\rm CF}[A,\mathcal{V}]}$ in the ST proposal insures that Eq. (II.2.12) is a genuine gauge-fixed theory as opposed to the CF case, Eq. (II.2.11). However, as noticed earlier, this renders the right hand side of Eq. (II.2.12) nonlocal in A. In order to bypass this issue, we use the method of replicas [75] that is commonly used in the context of disordered systems. It consists in rewriting formally a denominator as

$$\begin{aligned} \frac{1}{X} &= \lim_{n \to 0} X^{n-1} \\ &= \lim_{n \to 0} \prod_{k=1}^{n-1} X_k, \end{aligned} \tag{II.2.13}$$

where $n-1$ independent copies of X, indexed by the replica index k, are introduced. We use this technique to put the expression (II.2.12) under the form of a local field theory. We begin by rewriting the denominator $1/\int \mathcal{D}\mathcal{V} \, e^{-S_{\rm CF}[A,\mathcal{V}]}$ as

$$\frac{1}{\int \mathcal{D}\mathcal{V} \, e^{-S_{\rm CF}[A,\mathcal{V}]}} = \lim_{n \to 0} \left(\int \mathcal{D}\mathcal{V} \, e^{-S_{\rm CF}[A,\mathcal{V}]} \right)^{n-1}. \tag{II.2.14}$$

Introducing $n-1$ independent replicas $\mathcal{V}_k$, indexed hereafter by the replica index k, we get

$$\frac{1}{\int \mathcal{D}\mathcal{V} \, e^{-S_{\rm CF}[A,\mathcal{V}]}} = \lim_{n \to 0} \int \prod_{k=1}^{n-1} \left(\mathcal{D}\mathcal{V}_k \, e^{-S_{\rm CF}[A,\mathcal{V}_k]} \right). \tag{II.2.15}$$

Here, the $n \to 0$ limit is to be understood as the limit of the right-hand side analytically continued to continuous values of n. We thus finally obtain the first step average,

Eq. (II.2.8), in the replica formalism

$$\begin{aligned}\langle \mathcal{O}[A] \rangle &= \lim_{n\to 0} \int \mathcal{D}\mathcal{V}\, \mathcal{O}[A^U]\, e^{-S_{\rm CF}[A,\mathcal{V}]} \int \prod_{k=1}^{n-1} \left(\mathcal{D}\mathcal{V}_k\, e^{-S_{\rm CF}[A,\mathcal{V}_k]} \right) \\ &= \lim_{n\to 0} \int \prod_{k=1}^{n} \mathcal{D}\mathcal{V}_k\, \mathcal{O}[A^{U_1}]\, e^{-S_{\rm CF}[A,\mathcal{V}_k]},\end{aligned} \tag{II.2.16}$$

where the choice of the replica 1 is totally arbitrary because of the obvious permutation symmetry among the replicas. In the following of this manuscript, we shall assume everywhere that the $n \to 0$ limit and the path-integral over A commute. Accordingly, the ST procedure (II.2.5) is formally written as

$$\overline{\langle \mathcal{O}[A] \rangle} = \lim_{n\to 0} \frac{\int \mathcal{D}A \prod_{k=1}^{n} \mathcal{D}\mathcal{V}_k\, \mathcal{O}[A^{U_1}] e^{-S[A,\{\mathcal{V}\}]}}{\int \mathcal{D}A\, e^{-S_{\rm YM}[A]}}, \tag{II.2.17}$$

with the action $S[A,\{\mathcal{V}\}]$

$$S[A,\{\mathcal{V}\}] = S_{\rm YM}[A] + \sum_{k=1}^{n} S_{\rm CF}[A,\mathcal{V}_k]\,. \tag{II.2.18}$$

This action satisfies the identity

$$\int \mathcal{D}A\, e^{-S_{\rm YM}[A]} \underset{n\to 0}{\sim} \int \mathcal{D}A \prod_{k=1}^{n} \mathcal{D}\mathcal{V}_k\, e^{-S[A,\{\mathcal{V}\}]}, \tag{II.2.19}$$

as seen by taking $\mathcal{O} = 1$ in (II.2.17). Using this last property, the ST procedure is put under the form of a local field theory, with action S, Eq. (II.2.18),

$$\overline{\langle \mathcal{O}[A] \rangle} = \lim_{n\to 0} \frac{\int \mathcal{D}A \left(\prod_{k=1}^{n} \mathcal{D}\mathcal{V}_k\right)\, \mathcal{O}[A^{U_1}]\, e^{-S[A,\{\mathcal{V}\}]}}{\int \mathcal{D}A \left(\prod_{k=1}^{n} \mathcal{D}\mathcal{V}_k\right)\, e^{-S[A,\{\mathcal{V}\}]}}\,. \tag{II.2.20}$$

Finally, the volume of the gauge group, $\int \mathcal{D}U$, still needs to be factorized out for perturbative calculations (in order to being able to invert the quadratic part of the gauge-fixed action and access the free propagators). This is achieved by singularizing one of the replicas, say the replica 1, by performing the change of variables $A \to A^{U_1}$ and $U_k \to U_k U_1^{-1}$, $\forall\, k > 1$. Renaming $(c_1, \bar{c}_1, h_1) \to (c, \bar{c}, h)$ for later convenience, Eq. (II.2.20) reduces to

$$\overline{\langle \mathcal{O}[A] \rangle} = \lim_{n\to 0} \frac{\int \mathcal{D}(A,c,\bar{c},h,\{\mathcal{V}\})\, \mathcal{O}[A]\, e^{-S[A,c,\bar{c},h,\{\mathcal{V}\}]}}{\int \mathcal{D}(A,c,\bar{c},h,\{\mathcal{V}\})\, e^{-S[A,c,\bar{c},h,\{\mathcal{V}\}]}}\,, \tag{II.2.21}$$

with $\mathcal{D}(A,c,\bar{c},h,\{\mathcal{V}\}) \equiv \mathcal{D}(A,c,\bar{c},h) \left(\prod_{k=2}^{n} \mathcal{D}\mathcal{V}_k\right)$ and the ST action $S[A,c,\bar{c},h,\{\mathcal{V}\}]$ is given by

$$S[A,c,\bar{c},h,\{\mathcal{V}\}] = S_{\rm YM}[A] + S_{\rm CF}[A,c,\bar{c},h] + \sum_{k=2}^{n} S_{\rm CF}[A,\mathcal{V}_k]\,. \tag{II.2.22}$$

To summarize, Eq. (II.2.21) provides a continuum implementation of the CFDJ gauges, which is free of Gribov ambiguities. In particular, the procedure consists in a

bona fide gauge-fixing procedure as averages of gauge-invariant observables are equals to those computed with the YM weight only. For such property to hold, the $n \to 0$ limit is crucial as it accounts for the presence of the denominator in Eq. (II.2.1). The only assumption made so far was the interchange of the $n \to 0$ limit with the path-integral over A. Although the writing Eq. (II.2.21) remains somewhat formal, the ST procedure can be understood as follow: compute averages for fixed n with the ST action (II.2.22), noted hereafter with square brackets [.]. In perturbative calculations these result in analytic functions of n, to which we then take the $n \to 0$ limit such as

$$\overline{\langle \mathcal{O}[A] \rangle} = \lim_{n \to 0} \left[\mathcal{O}\left[A\right](n) \right]. \tag{II.2.23}$$

Let us briefly comment the ST action S, (II.2.22). Obviously, the usual CF model is recovered for $n = 1$ so that

$$\langle \mathcal{O}[A] \rangle_{\mathrm{CF}} = \left[\mathcal{O}\left[A\right](n=1) \right]. \tag{II.2.24}$$

This shows that the CF model cannot correspond to a gauge-fixed version of YM theories where the Gribov copies were taken into account according to the ST proposal. Indeed, independence of gauge-invariant quantities w.r.t. the gauge-fixing part requires to take the limit $n \to 0$. Nevertheless, comparisons of quantities in the $n \to 0$ limit with $n = 1$ allow one to conveniently access the effects of our treatment of Gribov copies.

Note that the replica sector of the ST action (the part $\sum_{k=2}^{n} S_{\mathrm{CF}}[A, \mathcal{V}_k]$) does not involve any mixing between different replicas. This is a consequence of our way of averaging over the η field, Eq. (II.2.1). The study would be different if we would average over η as

$$\langle \mathcal{O}[A] \rangle' = \int \mathcal{D}\eta \mathcal{P}[\eta] \frac{\sum_i \mathcal{O}[A^{U_i}] s(i) e^{-\beta_0 \mathcal{H}[A,\eta,U_i]}}{\sum_i s(i) e^{-\beta_0 \mathcal{H}[A,\eta,U_i]}}. \tag{II.2.25}$$

Following the same techniques as earlier, see (II.2.6), we get

$$\langle \mathcal{O}[A] \rangle' = \int \mathcal{D}\eta\, \mathcal{P}[\eta]\, \frac{\int \mathcal{D}\mathcal{V}\, \mathcal{O}[A^U]\, e^{-S^{\eta}_{\mathrm{FP}}[A,\mathcal{V}] - \beta_0 \mathcal{H}[A,\eta,U]}}{\int \mathcal{D}\mathcal{V}\, e^{-S^{\eta}_{\mathrm{FP}}[A,\mathcal{V}] - \beta_0 \mathcal{H}[A,\eta,U]}}. \tag{II.2.26}$$

In order to perform the η integral, we first need to introduce the replicas yielding

$$\langle \mathcal{O}[A] \rangle' = \lim_{n \to 0} \int \mathcal{D}\eta\, \mathcal{P}[\eta] \int \left(\prod_{k=1}^{n} \mathcal{D}\mathcal{V}_k \right) \mathcal{O}[A^{U_1}]\, e^{-\sum_{k=1}^{n} S^{\eta}_{\mathrm{FP}}[A,\mathcal{V}_k] - \beta_0 \mathcal{H}[A,\eta,U_k]}. \tag{II.2.27}$$

Using again (II.1.9), now with $R = \sum_{k=1}^{n} (\beta_0/g_0 + h_k - g_0 \bar{c}_k c_k) U_k$, eventually leads to

$$\langle \mathcal{O}[A] \rangle' = \lim_{n \to 0} \int \left(\prod_{k=1}^{n} \mathcal{D}\mathcal{V}_k \right) \mathcal{O}[A^{U_1}]\, e^{-\sum_{k=1}^{n} S_{\mathrm{CF}}[A,\mathcal{V}_k] - \sum_{k \neq l} S_{k,l}}, \tag{II.2.28}$$

with

$$S_{k,l} = \xi_0 \mathrm{tr} \left\{ U_k^{-1} \left[\beta_0 \left(c_k \bar{c}_k + \bar{c}_l c_l - \frac{h_k + h_l}{g_0} - \frac{\beta_0}{g_0^2} \right) - h_k h_l - g_0^2 c_k \bar{c}_k \bar{c}_l c_l + g_0 \left(h_k \bar{c}_l c_l + c_k \bar{c}_k h_l \right) \right] U_l \right\}. \tag{II.2.29}$$

In particular, this introduces couplings between different replicas in the bare action. This is a common feature in disordered systems (e.g. spin glasses) [75]. Here this yields a much more complicated theory and this way of performing the integration over η was not pursued further.

II.3 The ST action

In the last section we applied the ST proposal to the CFDJ gauges. Eventually, by introducing the replicas, we recast the procedure into a form suited for the use of local quantum field theory techniques. In particular, accessing averages in the ST gauge-fixed theory amounts to: first compute them with the ST action (II.2.22), and then perform the limit of vanishing replica number. This implies that the computations are to be performed for fixed n. In this section, we are thus lead to investigate further the ST which, here and in the following, is always considered for finite n. We first rewrite the ST action under an equivalent and elegant supersymmetric (SUSY) form. This allows one to exhibit nontrivial symmetries of the theory. Exploiting the latter, we prove that it is renormalizable in four dimensions.

II.3.1 Supersymmetric formulation of the CF action

It is known that the CF action (II.2.10) can be recast into a SUSY form [202]. It is therefore not surprising that the ST action (II.2.22) also admits such a formulation [74, 98], that we now review. We start from the CF action evaluated at A^U (that is for the replica sector of the ST action, see (II.2.22)) and we recast it under a more symmetric form by introducing $\hat{h}^a = ih^a + \frac{g_0}{2} f^{abc}\bar{c}^b c^c$

$$\begin{aligned} S_{\rm CF} = \int_x \Big\{ & \frac{\beta_0}{2}(A^{U,a}_\mu)^2 + \frac{1}{2}\Big(\partial_\mu \bar{c}^a D^U_\mu c^a + D^U_\mu \bar{c}^a \partial_\mu c^a\Big) \\ & + \hat{h}^a \partial_\mu A^{U,a}_\mu + \xi_0 \Big[\beta_0 \bar{c}^a c^a - \frac{(\hat{h}^a)^2}{2} - \frac{g_0^2}{8}\left(f^{abc}\bar{c}^b c^c\right)^2\Big]\Big\}, \end{aligned} \tag{II.3.1}$$

where $A^{U,a} = (A^U)^a$ and we recall that $D^U_\mu \varphi = \partial_\mu \varphi - i g_0 \left[A^U_\mu, \varphi\right]$. We then introduce a couple of Grassmannian coordinates $(\theta, \bar{\theta}) = \underline{\theta}$ that satisfy $\theta^2 = \bar{\theta}^2 = \theta\bar{\theta} + \bar{\theta}\theta = 0$. The Grassmann space spanned by $\underline{\theta}$ is taken to be curved and its geometry is defined by its line element $ds^2 = g_{MN} dN dM = 2 g_{\theta\bar{\theta}} d\bar{\theta} d\theta$, where the Grassmann metric g_{MN} is given by [202]

$$\begin{aligned} g_{\bar{\theta}\theta} &= -g_{\theta\bar{\theta}} = \beta_0 \bar{\theta}\theta + 1\,, \\ g^{\bar{\theta}\theta} &= -g^{\theta\bar{\theta}} = \beta_0 \bar{\theta}\theta - 1\,. \end{aligned} \tag{II.3.2}$$

Accordingly, one defines the invariant integration measure

$$\int_{\underline{\theta}} = \int d\theta d\bar{\theta}\, g^{1/2}(\theta, \bar{\theta})\,, \tag{II.3.3}$$

with

$$g^{1/2}(\theta, \bar{\theta}) = \beta_0 \bar{\theta}\theta - 1, \tag{II.3.4}$$

such that

$$\int_{\underline{\theta}} 1 = \beta_0. \tag{II.3.5}$$

On the superspace $(x, \theta, \bar{\theta})$, made of the d-dimensional Euclidean space supplemented by the Grasmmann space, one defines the SU(N) supermatrix field

$$\mathcal{V}(x, \underline{\theta}) = \exp\left\{ ig_0 \left(\bar{\theta} c + \bar{c}\theta + \bar{\theta}\theta \hat{h} \right) \right\} U. \tag{II.3.6}$$

Let us consider now the following SUSY nonlinear (NL) sigma model defined on the superspace $(x, \underline{\theta})$

$$S_{\rm SUSY}[A, \mathcal{V}] = \frac{1}{g_0^2} \int_{x,\underline{\theta}} {\rm tr} \left\{ D_\mu \mathcal{V}^\dagger D_\mu \mathcal{V} + \frac{\xi_0}{2} g^{MN} \partial_N \mathcal{V}^\dagger \partial_M \mathcal{V} \right\}, \tag{II.3.7}$$

where $D_\mu \mathcal{V} = \partial_\mu \mathcal{V} + i g_0 \mathcal{V} A_\mu$. Plugging the definition (II.3.6) into (II.3.7) and performing the Grassmann integration, one gets that [98]

$$S_{\rm SUSY}[A, \mathcal{V}] = S_{\rm CF}[A^U, c, \bar{c}, h]. \tag{II.3.8}$$

This relation makes obvious the interest of introducing $\mathcal{V}$ (II.3.6). Finally, for later purposes, it is useful to rewrite, again, Eq. (II.3.7) as

$$S_{\rm CF}[A, \mathcal{V}] = \int_{x,\underline{\theta}} \left\{ \frac{1}{2} \left(L_\mu^a - A_\mu^a \right)^2 + \frac{\xi_0}{4} g^{MN} L_N^a L_M^a \right\}, \tag{II.3.9}$$

where we introduced the vector fields

$$L_\mu = \frac{i}{g_0} \mathcal{V}^\dagger \partial_\mu \mathcal{V} \quad \text{and} \quad L_M = \frac{i}{g_0} \mathcal{V}^\dagger \partial_M \mathcal{V} \tag{II.3.10}$$

which belong to the adjoint representation of SU(N). Aspects of this SUSY formulation for the CF model were discussed in great details in [202]. In particular, it is worth mentioning the geometrical interpretation of the ST lifting parameter β_0 that appears here as the curvature of the Grassmann space.

The action (II.3.7) inherits the Grasmann subspace isometries given by the invariance under the transformations according to the five independent Killing vectors χ^M

$$\begin{aligned} \chi^\theta &= a_s(1 + \beta_0 \bar{\theta}\theta) + \bar{\theta} a_t - \theta a_c \\ \chi^{\bar{\theta}} &= a_{\bar{s}}(1 + \beta_0 \bar{\theta}\theta) + a_{\bar{t}} \theta + \bar{\theta} a_c, \end{aligned} \tag{II.3.11}$$

where a_s, $a_{\bar{s}}$, a_t, $a_{\bar{t}}$, a_c are free parameters, see [202] for details. The SUSY action (II.3.7) is invariant under the linear transformations $\mathcal{V}_k \to \mathcal{V}_k + \chi^M \partial_M \mathcal{V}_k$ and so is the associated quantum effective action $\Gamma_{\rm SUSY}$ [118]. Eventually, these isometries insure that $\Gamma_{\rm SUSY}$ is covariant in Grassmann coordinates, that is, covariant derivatives[3] are contracted with the metric[4] $g_{\rm MN}$ and integrals over the Grassmann subspace come with the proper measure Eq. (II.3.3).

[3] In the present case under consideration, covariant derivatives reduce to standard derivatives ∂_M.

[4] In principle, contractions with the Riemann tensor R_{MN} should also be considered. However, this situation is not encountered in the present case.

In conclusion, the ST action can be expressed according to the SUSY form of the CF action as

$$\begin{aligned} S[A,c,\bar{c},h,\{\mathcal{V}\}] =& S_{\rm YM}[A] + S_{\rm CF}[A,c,\bar{c},h] + \sum_{k=2}^{n} S_{\rm SUSY}[A,\mathcal{V}_k], \\ =& \int_x \Big\{ \frac{1}{4}(F^a_{\mu\nu})^2 + \frac{\beta_0}{2}(A^{U,a}_\mu)^2 + \xi_0\beta_0\bar{c}^a c^a + \partial_\mu\bar{c}^a D_\mu c^a + ih^a\partial_\mu A^a_\mu \\ &+ \xi_0\Big[-\frac{(ih^a)^2}{2} - \frac{g_0}{2} f^{abc} ih^a\bar{c}^b c^c - \frac{g_0^2}{4}\left(f^{abc}\bar{c}^b c^c\right)^2 \Big]\Big\} \\ &+ \sum_{k=2}^{n} \frac{1}{g_0^2}\int_{x,\underline{\theta}} {\rm tr}\Big\{ D_\mu\mathcal{V}^\dagger D_\mu\mathcal{V} + \frac{\xi_0}{2} g^{MN}\partial_N\mathcal{V}^\dagger\partial_M\mathcal{V}\Big\}, \end{aligned} \tag{II.3.12}$$

The ST action thus corresponds to a set of $n-1$ replicated gauged SUSY NL-sigma models coupled to a gauge-fixed YM field with gauge-fixing action $S_{\rm CF}[A,c,\bar{c},h]$. Each replica k of NL-sigma model comes with its own set of Grassmann variables $(\underline{\theta}_k)$ and its corresponding isometries.

II.3.2 Renormalizability of the ST action

II.3.2.1 Symmetries

We now list the symmetries of the ST action. This will allow us to constrain the UV divergences of the theory and eventually to prove its multiplicative renormalizability. We begin by enumerating the linear symmetries. There are the global SU(N) color symmetries and the isometries of the Euclidean space R^4. The ghost symmetry corresponds to the invariance of the ST action under

$$c \to e^{i\epsilon}c, \quad \bar{c} \to e^{-i\epsilon}\bar{c}, \tag{II.3.13}$$

yielding the ghost number conservation. There are the isometries associated to each curved Grassmann space replica that were described above. As emphasized earlier, they insure that the effective action is covariant on each Grassmann subspace. There is also a discrete symmetry under the permutation of the replicas: $\mathcal{V}_k \leftrightarrow \mathcal{V}_l$ for $k,l = 2,\ldots,n$.

The ST action (II.3.12) also admits nonlinear symmetries which yield Slavnov-Taylor identities. One, inherited from the initial gauge symmetry, is the modified BRST symmetry $\hat{s}$ of the CF model presented in the previous chapter, see (I.5.2), that can be enlarged to the SUSY sector. For simplicity, from now on, we refer to this enlarged modified BRST symmetry as the BRST symmetry and denote it s. The fields of the ST action transform under s as

$$\begin{aligned} sA^a_\mu &= \partial_\mu c^a + g_0 f^{abc} A^b_\mu c^c, \\ sc^a &= -\frac{g_0}{2} f^{abc} c^b c^c, \\ s\bar{c}^a &= ih^a, \\ sih^a &= \beta_0 c^a \end{aligned} \tag{II.3.14}$$

and

$$s\mathcal{V}_k = -ig_0\mathcal{V}_k c\,, \quad k = 2, \dots, n\,. \tag{II.3.15}$$

In the sector $(A, c, \mathcal{V}_k)$ this simply corresponds to a gauge transformation with Grassmann parameter c^a. In particular, $s^2 = 0$ when restricted to this sector while its nilpotency is softly broken by the mass term β_0 on the sector $(\bar{c}, ih)$. Accordingly, we define the t transformation such that $s^2 = \beta_0 t$, whose explicit action on the primary fields is given by

$$\begin{aligned} t\bar{c}^a &= c^a, \\ tih^a &= -\frac{g_0}{2} f^{abc} c^b c^c \end{aligned} \tag{II.3.16}$$

and $tA^a_\mu = tc^a = t\mathcal{V}_k = 0$.

There is a last family of symmetries that concern only the SUSY sector. They consist in global left color rotations of the NL-sigma model fields $\mathcal{V}_k \to V_{L,k}\mathcal{V}_k$ with $V_{L,k} \in \mathrm{SU}(N)$, whose generators δ^a_k are defined by [98]

$$\delta^a_k \mathcal{V}_l = i\delta_{kl} t^a \mathcal{V}_l, \tag{II.3.17}$$

so that each replica superfield can be transformed independently from the others. This last family of symmetries thus contains $(N^2-1)\times(n-1)$ independent generators. Note that, these symmetries are actually nonlinear since the $\mathcal{V}_k$ are superfields constrained to belong to the $\mathrm{SU}(N)$ group. To make this more explicit, it turns out to be more convenient to use the following linear parametrization for the $\mathrm{SU}(N)$ superfields given in terms of $2N^2$ superfields $(a^0_k, b^0_k, a^a_k, b^a_k)$:

$$\mathcal{V}_k = (a^0_k + ib^0_k)\mathbb{1} + i(a^a_k + ib^a_k)t^a. \tag{II.3.18}$$

The constraint that $\mathcal{V}_k \in \mathrm{SU}(N)$ implies that there are only $N^2 - 1$ unconstrained superfields among the $2N^2$ ones appearing in Eq. (II.3.18). We choose the a^a_k as the $N^2 - 1$ unconstrained superfields while a^0_k, b^0_k, and b^a_k are functions of a^a_k such that $\mathcal{V}_k$ in Eq. (II.3.18) belongs to the $\mathrm{SU}(N)$ group. In practice we will not need their explicit expressions. In this representation, the generators of the $(N^2-1)\times(n-1)$ global left color rotations act on the superfields a^a_k as [98]

$$\delta^a_k a^b_l = \delta_{kl}\left(\delta^{ab} a^0_k + \frac{1}{2} f^{abc} a^c_k - \frac{1}{2} d^{abc} b^c_k\right) \tag{II.3.19}$$

and on the constrained ones as

$$\begin{aligned} \delta^a_k a^0_l &= -\delta_{kl}\frac{a^a_k}{2N}\,, \qquad \delta^a_k b^0_l = -\delta_{kl}\frac{b^a_k}{2N}, \\ \delta^a_k b^b_l &= \delta_{kl}\left(\delta^{ab} b^0_k + \frac{1}{2} f^{abc} b^c_k + \frac{1}{2} d^{abc} a^c_k\right). \end{aligned} \tag{II.3.20}$$

For later use, we also write down the BRST action on those superfields

$$\begin{aligned} sa^a_k &= g_0\left(-a^0_k c^a + \frac{1}{2} f^{abc} a^b_k c^c + \frac{1}{2} d^{abc} b^b_k c^c\right), \\ sa^0_k &= \frac{g_0}{2N} a^b_k c^b\,, \qquad sb^0_k = \frac{g_0}{2N} b^b_k c^b\,, \\ sb^a_k &= g_0\left(-b^0_k c^a + \frac{1}{2} f^{abc} b^b_k c^c - \frac{1}{2} d^{abc} a^b_k c^c\right). \end{aligned} \tag{II.3.21}$$

We mention that the generators of the nonlinear symmetries considered above induce a closed (super)algebra:

$$\begin{aligned} &\{s, s\} = 2\beta_0 t\,, \\ &[\delta_k^a, \delta_l^b] = i\delta_{kl} f^{abc} \delta_k^c\,, \\ &[\delta_k^a, s] = [\delta_k^a, t] = [s, t] = [t, t] = 0\,. \end{aligned} \tag{II.3.22}$$

We are now in position to prove the perturbative renormalizability in $d = 4$ of the ST action. Our proof relies on standard arguments where, using the symmetries listed above, we constrain the possible divergent terms $\Gamma^{\rm div}$ appearing in the quantum effective action Γ [118]. First, we introduce sources for all independent fields and their variations under the symmetries

$$\begin{aligned} S_1 \;=\; & \int_x \Big\{ J_\mu^a A_\mu^a + \bar\eta^a c^a + \bar c^a \eta^a + i h^a M^a + \bar K_\mu^a s A_\mu^a + \bar L^a s c^a \Big\} \\ +\; & \sum_{k=2}^{n} \int_{x,\underline\theta} \Big\{ P_k^0 a_k^0 + P_k^a a_k^a + R_k^0 b_k^0 + R_k^a b_k^a \\ & \qquad + \bar Q_k^0 s a_k^0 + \bar Q_k^a s a_k^a + \bar T_k^0 s b_k^0 + \bar T_k^a s b_k^a \Big\}. \end{aligned} \tag{II.3.23}$$

Since $t\bar c^a = c^a$, $tih^a = -\frac{g_0}{2} f^{abc} c^b c^c = sc^a$ there is no need to introduce associated independent sources for the t variations. The same is true on the SUSY sector for s^2, $s\delta_k^a = \delta_k^a s$, and $\delta_k^a \delta_l^b$ which can be fully expressed in terms of either the (super)fields themselves or their variations under s or δ_k^a, see Eq. (II.3.22). From Eq. (II.3.23) and the ST action, we define the connected generating functional $W = \ln \int \mathcal{D}(A, c, \bar c, h, \{\mathcal{V}\})\, e^{-S+S_1}$. By performing a Legendre transform of W with respect to the sources J_μ^a, $\bar\eta^a$, η^a, M^a, P_k^a, we get the 1-PI vertex generating functional or quantum effective action Γ in presence of sources for the composite fields a_k^0, b_k^0, b_k^a, sA_μ^a, sc^a, sa_k^0, sa_k^a, sb_k^0, sb_k^a associated to the ST action.

Γ inherits all the linear symmetries of the ST action [118]. In particular, ghost number conservation insures that all terms belonging to Γ have zero ghost number. We recall that each replica superspace comes with its own set of Grassmann variables and so its own set of isometries. The constraints induced by the nonlinear symmetries are more complicated. To handle them we follow the standard procedure of [118] and introduce the renormalized transformations $\tilde s, \tilde t, \tilde\delta_k^a$ defined by their action on the primary fields

$$\begin{aligned} &\tilde s A_\mu^a = -\frac{\delta\Gamma}{\delta \bar K_\mu^a}\,, \quad \tilde s c^a = -\frac{\delta\Gamma}{\delta \bar L^a}\,, \quad \tilde s a_k^a = -\frac{\delta_\theta \Gamma}{\delta \bar Q_k^a} \\ &\tilde s \bar c^a = i h^a\,, \quad \tilde s i h^a = \beta_0 c^a, \end{aligned} \tag{II.3.24}$$

where we have defined the covariant functional derivative $\delta_\theta\Gamma/\delta\phi = (g^{-1/2})\delta\Gamma/\delta\phi$ with any superfield ϕ, and g is the determinant of the Grassmann metric defined in (II.3.3). This accounts for the curved Grassmann directions. We also define

$$\tilde t \bar c^a = c^a\,, \quad \tilde t i h^a = -\frac{\delta\Gamma}{\delta \bar L^a} \tag{II.3.25}$$

and

$$\tilde{\delta}^a_k a^b_l = \delta_{kl}\left(-\delta^{ab}\frac{\delta_\theta\Gamma}{\delta P^0_k} + \frac{1}{2}f^{abc}a^c_k + \frac{1}{2}d^{abc}\frac{\delta_\theta\Gamma}{\delta R^a_k}\right) \tag{II.3.26}$$

with all other variations being zero.

The original symmetries $sS = tS = \delta^a_k S = 0$ imply the following Zinn-Justin equations

$$\tilde{s}\Gamma = \sum_{k=2}^{n}\int_{x,\underline{\theta}}\left\{P^0_k\frac{\delta_\theta\Gamma}{\delta\bar{Q}^0_k} + R^0_k\frac{\delta_\theta\Gamma}{\delta\bar{T}^0_k} + R^a_k\frac{\delta_\theta\Gamma}{\delta\bar{T}^a_k}\right\}, \tag{II.3.27}$$

$$\tilde{t}\Gamma = 0\,, \tag{II.3.28}$$

and

$$\begin{aligned}\tilde{\delta}^a_k\Gamma = \int_{x,\underline{\theta}}\Bigg\{&\frac{1}{2N}\left(P^0_k a^a_k - R^0_k\frac{\delta_\theta\Gamma}{\delta R^a_k} - \bar{Q}^0_k\frac{\delta_\theta\Gamma}{\delta\bar{Q}^a_k} - \bar{T}^0_k\frac{\delta_\theta\Gamma}{\delta\bar{T}^a_k}\right) + \left(R^a_k\frac{\delta_\theta\Gamma}{\delta R^0_k} + \bar{Q}^a_k\frac{\delta_\theta\Gamma}{\delta\bar{Q}^0_k} + \bar{T}^a_k\frac{\delta_\theta\Gamma}{\delta\bar{T}^0_k}\right)\\ &+ \frac{f^{abc}}{2}\left(R^b_k\frac{\delta_\theta\Gamma}{\delta R^c_k} + \bar{Q}^b_k\frac{\delta_\theta\Gamma}{\delta\bar{Q}^c_k} + \bar{T}^b_k\frac{\delta_\theta\Gamma}{\delta\bar{T}^c_k}\right) - \frac{d^{abc}}{2}\left(R^b_k a^c_k + \bar{Q}^b_k\frac{\delta_\theta\Gamma}{\delta\bar{T}^c_k} - \bar{T}^b_k\frac{\delta_\theta\Gamma}{\delta\bar{Q}^c_k}\right)\Bigg\}.\end{aligned} \tag{II.3.29}$$

We now use these equations in order to constrain the possible divergent terms arising in Γ.

II.3.2.2 Constraining the UV divergences

We note $\Gamma^{\rm div} = \int d^4x\,\mathcal{L}^{\rm div}(x)$ the divergent part of the effective action and define $\mathcal{L}^{\rm div}(x)$ the most general local Lagrangian density which, by power counting, includes operators of mass dimension lower than or equal to 4 compatible with the symmetries of the problem. Moreover, we shall assume that $\Gamma^{\rm div}$ can be written under the form of a (local) series in the various fields.

$\Gamma^{\rm div}$ must satisfy the symmetry identities Eqs. (II.3.27)–(II.3.29) that we use as constraints on the possible terms that appear in $\mathcal{L}^{\rm div}(x)$. Listing all the possible terms appearing in $\mathcal{L}^{\rm div}(x)$ is straightforward but lengthy and not illuminating, so we present the key arguments. First, note that Grassmann variables have mass dimension -1. Indeed, the Grassmann metric g must be dimensionless which implies that $[\bar{\theta}] = [\theta] = -1$. The identities $\int d\theta\,\theta = \int d\bar{\theta}\,\bar{\theta} = 1$ further imply that $[d\theta] = [d\bar{\theta}] = 1$. Hereby, for the terms of the form $\int_{\underline{\theta}}\mathcal{L}_2(x,\underline{\theta})$, $\int_{\underline{\theta},\underline{\theta}'}\mathcal{L}_3(x,\underline{\theta},\underline{\theta}')$ be of mass dimension lower than or equal to 4, the Lagrangian densities $\mathcal{L}_2$ and $\mathcal{L}_3$ must be respectively of mass dimension lower than or equal to 2 and 0. Recalling that s is of mass dimension 1 and of ghost number 1, with the same kind of reasoning we deduce the mass dimension and ghost number of the fields, sources, and Grassmann coordinates that we resume in Table II.1. Let us present an example in order to illustrate the strategy. We list the possible terms appearing in $\Gamma^{\rm div}$ that involve the source $\bar{K}^a_\mu$ and which are of mass dimension lower than or equal to 4. A first possibility is $\tilde{g}\bar{K}^a_\mu f^{abc}A^b_\mu c^c$, where $\tilde{g}$ is an unknown renormalization constant. Another possibility is $\kappa_1\bar{K}^a_\mu\partial_\mu c^a$ with κ_1 another unknown renormalization constant. By inspection of Table II.1, using power counting, ghost number conservation, Euclidean covariance and the isometries of the

	A	c	$\bar{c}$	ih	a	$\bar{K}$	$\bar{L}$	P	R	$\bar{Q}$	$\bar{T}$	θ	∂_θ	$d\theta$	$\bar{\theta}$	$\partial_{\bar{\theta}}$	$d\bar{\theta}$
dim.	1	1	1	2	0	2	2	2	2	1	1	-1	1	1	-1	1	1
ghost nb.	0	1	-1	0	0	-1	-2	0	0	-1	-1	1	-1	-1	-1	1	1

Table II.1: Mass dimension and ghost number of the fields, sources, and Grassmann coordinates.

replica Grassmann spaces, these are the only possible couplings of $\bar{K}$ with the fields A, $\bar{c}$, c, ih, a. For instance, power counting tells us that the only possibility to couple $\bar{K}_\mu$ to ih is through the combination $ih\bar{K}_\mu$ without additional derivatives, though it breaks covariance and ghost number conservation. One might have though to include Grassmann coordinates: $\theta\bar{\theta}ih\partial_\mu\bar{K}_\mu c$ which is of mass dimension 4, ghost number 0 and satisfies the Euclidean covariance. However Grassmann isometries implies that such an operator must appear in Γ with proper integration measure, that is, of the form $\int_{\underline{\theta}}\mathcal{L}_2(x,\underline{\theta})$. In $\mathcal{L}_2(x,\underline{\theta})$, only the terms of mass dimension lower than and equal to 2 contribute to $\Gamma^{\rm div}$. Hence, $\bar{K}_\mu$ cannot be coupled to ih in $\Gamma^{\rm div}$. Similarly, covariance requires that possible couplings to the superfields a are of the form $\bar{K}_\mu\partial_\mu a$, which is of mass dimension 3, while Grassmann isometries require that such a term appear in Γ under the form of $\int_{\underline{\theta}}\mathcal{L}_2(x,\underline{\theta})$. Accordingly, there is no term in $\Gamma^{\rm div}$ that couples $\bar{K}$ to the superfields a. Along the same lines, one deduces that it is not possible to couple $\bar{K}$ to $\bar{c}$ nor to any sources of Table II.1.

Eventually, the inspection of Table II.1 shows that terms in $\Gamma^{\rm div}$ are at most linear in the (super)sources and we can thus write

$$\Gamma_{\rm div}=\Gamma_0-\Gamma_1, \tag{II.3.30}$$

where Γ_0 and Γ_1 are respectively independent of and linear in the sources. According to the definitions (II.3.24), we define

$$\begin{aligned}\Gamma_1=&\int_x\left\{\bar{K}^a_\mu\tilde{s}A^a_\mu+\bar{L}^a\tilde{s}c^a\right\}\\&+\sum_{k=2}^n\int_{x,\underline{\theta}}\left\{P^0_k\tilde{a}^0_k+R^0_k\tilde{b}^0_k+R^a_k\tilde{b}^a_k+\bar{Q}^0_kX^0_k+\bar{Q}^a_k\tilde{s}a^a_k+\bar{T}^0_kY^0_k+\bar{T}^a_kY^a_k\right\}.\end{aligned} \tag{II.3.31}$$

Note however that, the unknown functions $\tilde{s}A^a_\mu$, $\tilde{s}c^a$, and $\tilde{s}a^a_k$ are formally defined in Eq. (II.3.24) but here with $\Gamma\to\Gamma_{\rm div}$. $\tilde{a}^0_k$, $\tilde{b}^0_k$, $\tilde{b}^a_k$ are unknown functions of the unconstrained a^a_k fields and stand as the renormalized versions of the functions a^0_k, b^0_k and b^a_k. Note that a^0_k, b^0_k and b^a_k are of mass-dimension zero, null ghost number, and depend only on the unconstrained a^a_k superfields.[5] Along the same lines, we have introduced X^0_k, Y^0_k and Y^a_k to account for the renormalized versions of sa^0_k, sb^0_k, sb^a_k. *A priori*, since $\tilde{s}$ is unknown apart from its formal definition Eq. (II.3.24), akin for the renormalized functions $\tilde{a}^0_k$, $\tilde{b}^0_k$, $\tilde{b}^a_k$, nothing guaranties at this stage that the renormalized functions X^0_k, Y^0_k, Y_k are given by $\tilde{s}\tilde{a}^0_k$, $\tilde{s}\tilde{b}^0_k$, $\tilde{s}\tilde{b}^a_k$.

[5]Indeed, any term that depends on the other fields would require to come along with some combination of θ, $\bar{\theta}$ to insure a zero mass-dimension. Such combination will violate either ghost number conservation or the Grassmannian isometries. For instance a term of the form $A^2_\mu\theta\bar{\theta}$ is consistent with zero mass dimension and ghost number, but violates the isometry under the Killing vector $\chi=\left(-\theta,\bar{\theta}\right)$.

We are now looking for the expressions of the unknown transformations $\tilde{s}, \tilde{t}, \tilde{\delta}^a_k$ in terms of the primary fields. Let us first consider the case of $\tilde{\delta}^a_k$. Applying its formal definition (II.3.26) to $\Gamma_{\rm div}$ with Γ_1 given by Eq. (II.3.31), we immediately get from the source terms

$$\tilde{\delta}^a_k a^b_l = \delta_{kl}\left(\delta^{ab}\tilde{a}^0_k + \frac{1}{2}f^{abc}a^c_k - \frac{1}{2}d^{abc}\tilde{b}^c_k\right). \tag{II.3.32}$$

Since $\tilde{a}^0_k$, $\tilde{b}^0_k$, $\tilde{b}^a_k$ are functions of only the a^a_k, this last equality does consist in a (implicit) definition of the transformation $\tilde{\delta}^a_k$ in terms of the fundamental fields a^a_k. Inserting Eq. (II.3.31) in the symmetry identity (II.3.29) and extracting the terms linear in P^0_k, R^0_k, and R^a_k, we find that

$$\begin{aligned}
&\tilde{\delta}^a_k\tilde{a}^0_l = -\delta_{kl}\frac{a^a_k}{2N}\,, \qquad \tilde{\delta}^a_k\tilde{b}^0_l = -\delta_{kl}\frac{\tilde{b}^a_k}{2N},\\
&\tilde{\delta}^a_k\tilde{b}^b_l = \delta_{kl}\left(\delta^{ab}\tilde{b}^0_k + \frac{1}{2}f^{abc}\tilde{b}^c_k + \frac{1}{2}d^{abc}a^c_k\right).
\end{aligned} \tag{II.3.33}$$

The superfield a^a_k along with the unknown functions $\tilde{a}^0_k$, $\tilde{b}^0_k$, $\tilde{b}^a_k$ can be grouped altogether into a matrix superfield

$$\tilde{\mathcal{V}}_k = (\tilde{a}^0_k + i\tilde{b}^0_k)\mathbb{1} + i(a^a_k + i\tilde{b}^a_k)t^a. \tag{II.3.34}$$

From (II.3.32) and (II.3.33), we get that

$$\tilde{\delta}^a_k\tilde{\mathcal{V}}_l = i\delta_{kl}t^a\tilde{\mathcal{V}}_l\,, \tag{II.3.35}$$

which shows that $\tilde{\mathcal{V}}_k$ transforms linearly under a transformation of SU(N). It follows that

$$\tilde{\mathcal{V}}^\dagger_k\tilde{\mathcal{V}}_k = Z\mathbb{1}, \tag{II.3.36}$$

with Z a constant.

We now move to the case of the renormalized BRST transformation $\tilde{s}$. We already saw above that the most general terms that can be coupled to the source $\bar{K}_\mu$ in $\Gamma^{\rm div}$ are given by $\kappa_1\bar{K}^a_\mu\partial_\mu c^a$ and $\tilde{g}\bar{K}^a_\mu f^{abc}A^b_\mu c^c$, so that using (II.3.24)

$$\tilde{s}A^a_\mu = \kappa_1\partial_\mu c^a + \tilde{g}f^{abc}A^b_\mu c^c. \tag{II.3.37}$$

Similar considerations lead to[6]

$$\tilde{s}c^a = -\frac{\tilde{g}}{2}f^{abc}c^b c^c. \tag{II.3.38}$$

Along the same lines, one eventually gets the most general form of the renormalized BRST symmetry acting on the matrix superfield $\tilde{\mathcal{V}}_k$ [98]

$$\tilde{s}\tilde{\mathcal{V}}_k = -i\tilde{g}\tilde{\mathcal{V}}_k c\,, \quad k = 2,\ldots,n\,. \tag{II.3.39}$$

[6] More precisely, by the same kind of considerations one arrives at the conclusion that $\tilde{s}c^a$ is of the form $\tilde{s}c^a = -\frac{\tilde{g}'}{2}f^{abc}c^b c^c$, where $\tilde{g}'$ is a priori a new renormalization constant, independent of $\tilde{g}$. Then, by investigating the constraint Eq. (II.3.27), particularly the $\bar{K}$ dependent part, one realizes that this constraint reduces in this sector to $\tilde{s}\tilde{s}A^a_\mu = 0$. Applying twice the transformation $\tilde{s}$ to A^a_μ and isolating the $\partial_\mu c$ part, one immediately gets $0 = \kappa_1 f^{abc}\left(\tilde{g} - \tilde{g}'\right)\partial_\mu c^b c^c$, yielding $\tilde{g}' = \tilde{g}$.

From the action of the renormalized symmetries on the elementary fields Eqs. (II.3.37), (II.3.38), (II.3.39) and Eq. (II.3.35), we are now able to determine the form of Γ_0, which satisfies

$$\tilde{s}\Gamma_0 = \tilde{t}\Gamma_0 = \tilde{\delta}^a_k\Gamma_0 = 0. \tag{II.3.40}$$

Using the fact that, by power counting, there can be at most two sets of Grassmann variables, we parametrize the solution as

$$\Gamma_0 = \int_x \mathcal{L}_1(A,c,\bar{c},h) + \sum_{k=2}^{n}\int_{x,\underline{\theta}} \mathcal{L}_2(A,c,\bar{c},h,a_k(\underline{\theta})) + \sum_{k,k'=2}^{n}\int_{x,\underline{\theta},\underline{\theta}'} \mathcal{L}_3(a_k(\underline{\theta}),a_{k'}(\underline{\theta}')). \tag{II.3.41}$$

Power counting implies that $\mathcal{L}_3$ is of mass dimension zero. Therefore, it cannot involve the fields A, c, $\bar{c}$, or h. Similarly, it cannot involve any derivatives ∂_μ or ∂_M. It is thus a potential term for the superfields a_k and $a_{k'}$ (or equivalently $\tilde{\mathcal{V}}_k$ and $\tilde{\mathcal{V}}_{k'}$). The only possible such term compatible with the symmetry (II.3.35) is a function of $\tilde{\mathcal{V}}_k^\dagger\tilde{\mathcal{V}}_k$ and $\tilde{\mathcal{V}}_{k'}^\dagger\tilde{\mathcal{V}}_{k'}$, which is trivial due to (II.3.36) so that $\mathcal{L}_3 = 0$. Notice that, in the sector $(A,c,\tilde{\mathcal{V}}_k)$, the transformation $\tilde{s}$ is, up to a multiplicative factor κ_1, a (left) gauge transformation with Grassmannian gauge parameter c^a and effective coupling constant $\tilde{g}/\kappa_1$. A solution to $\tilde{s}\mathcal{L}_1 = 0$ is thus a YM-like term with an appropriate field-strength tensor, see below. Apart from this term, the combinations

$$X = \frac{\beta_0}{2\kappa_1}\left(A^a_\mu\right)^2 - \tilde{s}\left(A^a_\mu\partial_\mu\bar{c}^a\right), \tag{II.3.42}$$

$$Y = \beta_0\bar{c}^a c^a - \tilde{s}\left[\bar{c}^a\left(ih^a + \frac{\tilde{g}}{2}f^{abc}\bar{c}^b c^c\right)\right] \tag{II.3.43}$$

are the only independent solutions to $\tilde{s}\mathcal{L}_1 = 0$ with the correct dimension, symmetries, and ghost number. Thus

$$\mathcal{L}_1 = \frac{Z_1}{4}(\tilde{F}^a_{\mu\nu})^2 + \kappa_2 X + \frac{\kappa_3}{2}Y, \tag{II.3.44}$$

with

$$\tilde{F}^a_{\mu\nu} = \partial_\mu A^a_\nu - \partial_\nu A^a_\mu + \frac{\tilde{g}}{\kappa_1}f^{abc}A^b_\mu A^c_\nu. \tag{II.3.45}$$

Explicitly, one has

$$\begin{aligned}\mathcal{L}_1 = &\frac{Z_1}{4}(\tilde{F}^a_{\mu\nu})^2 + \kappa_2\left\{\frac{\beta_0}{2\kappa_1}(A^a_\mu)^2 - iA^a_\mu\partial_\mu h^a + \partial_\mu\bar{c}^a\tilde{s}A^a_\mu\right\}\\ &+\kappa_3\left\{\beta_0\bar{c}^a c^a + \frac{(h^a)^2}{2} - \frac{\tilde{g}}{2}f^{abc}ih^a\bar{c}^b c^c - \frac{\tilde{g}^2}{4}(f^{abc}\bar{c}^b c^c)^2\right\},\end{aligned} \tag{II.3.46}$$

with $\tilde{s}A^a_\mu$ given in (II.3.37). This is trivially invariant under $\tilde{t}$ and $\tilde{\delta}^a_k$.

Let us now consider the NL-sigma model sector $\mathcal{L}_2$. The constraint $\tilde{\delta}^a_k\mathcal{L}_2 = 0$ is accounted for by using the $\mathrm{SU}_R(N)$ invariants $\tilde{\mathcal{V}}_k^\dagger\partial\ldots\partial\tilde{\mathcal{V}}_k$, with an arbitrary number of bosonic and Grassmannian derivatives, as building blocks. The term with no derivatives is trivial due to (II.3.36). The isometries of the embedding superspace and the

fact that $\mathcal{L}_2$ can only contain local terms of mass dimension lower than 2 restricts the set of possible invariants to ($M = \theta, \bar{\theta}$)

$$\tilde{L}_{k,\mu} = \frac{i}{\tilde{g}}\tilde{\mathcal{V}}_k^\dagger \partial_\mu \tilde{\mathcal{V}}_k \quad \text{and} \quad \tilde{L}_{k,M} = \frac{i}{\tilde{g}}\tilde{\mathcal{V}}_k^\dagger \partial_M \tilde{\mathcal{V}}_k\,. \tag{II.3.47}$$

Both $\tilde{L}_{k,\mu}$ and $\tilde{L}_{k,M}$ have mass dimension one. Their ghost numbers are 0 for $\tilde{L}_{k,\mu}$, 1 for $\tilde{L}_{k,\bar{\theta}}$ and -1 for $\tilde{L}_{k,\theta}$. The variation of $\tilde{L}_{k,\mu}$ under $\tilde{s}$ is

$$\tilde{s}\tilde{L}^a_{k,\mu} = Z\partial_\mu c^a + \tilde{g} f^{abc}\tilde{L}^b_{k,\mu}c^c \tag{II.3.48}$$

It follows that $\tilde{L}_{k,\mu}/Z - A_\mu/\kappa_1$ transforms covariantly

$$\tilde{s}\left(\tilde{L}^a_{k,\mu} - \frac{Z}{\kappa_1}A^a_\mu\right) = \tilde{g} f^{abc}\left(\tilde{L}^b_{k,\mu} - \frac{Z}{\kappa_1}A^b_\mu\right)c^c. \tag{II.3.49}$$

Similarly, $\tilde{L}_{k,M}$ transforms covariantly:

$$\tilde{s}\tilde{L}^a_{k,M} = -\tilde{g} f^{abc}\tilde{L}^b_{k,M}c^c. \tag{II.3.50}$$

The most general dimension-two Lagrangian $\mathcal{L}_2$ satisfying $\tilde{s}\mathcal{L}_2 = 0$ is thus

$$\mathcal{L}_2 = \frac{Z_2}{2}\left(\tilde{L}^a_{k,\mu} - \frac{Z}{\kappa_1}A^a_\mu\right)^2 + \frac{Z_3}{4}g^{MN}\tilde{L}^a_{k,N}\tilde{L}^a_{k,M} \tag{II.3.51}$$

We see that the most general divergent part compatible with the symmetries eventually reads

$$\begin{aligned}\mathcal{L} = \frac{Z_1}{4}(\tilde{F}^a_{\mu\nu})^2 + \kappa_2\Big\{&\frac{\beta_0}{2\kappa_1}(A^a_\mu)^2 - iA^a_\mu\partial_\mu h^a + \partial_\mu\bar{c}^a\tilde{s}A^a_\mu\Big\}\\ &+ \kappa_3\left\{\beta_0\bar{c}^a c^a + \frac{(h^a)^2}{2} - \frac{\tilde{g}}{2}f^{abc}ih^a\bar{c}^b c^c - \frac{\tilde{g}^2}{4}(f^{abc}\bar{c}^b c^c)^2\right\}\\ &+ \sum_{k=2}^n\int_{x,\underline{\theta}}\left\{\frac{Z_2}{2}\left(\tilde{L}^a_{k,\mu} - \frac{Z}{\kappa_1}A^a_\mu\right)^2 + \frac{Z_3}{4}g^{MN}\tilde{L}^a_{k,N}\tilde{L}^a_{k,M}\right\},\end{aligned} \tag{II.3.52}$$

which has the same form as the bare Lagrangian (II.3.12) (see also (II.3.9)). This demonstrates the (multiplicative) renormalizability of the present theory. So far we have eight independent renormalization constants $\kappa_{1,2,3}$, $Z_{1,2,3}$, Z, and $\tilde{g}$. As described in Appendix B.1, the original symmetry between the replicas $k = 1$ and $k \geq 2$ leads to the relations

$$Z_2Z^2 = \kappa_1\kappa_2 \quad \text{and} \quad Z_3Z^2 = \kappa_3 \tag{II.3.53}$$

which reduce the number of independent renormalization constants to six. In particular, it follows that all replicas contribute a mass term for the gauge field

$$\frac{Z_2Z^2}{2\kappa_1^2}\int_{\underline{\theta}}(A^a_\mu)^2 = \frac{\beta_0\kappa_2}{2\kappa_1}(A^a_\mu)^2, \tag{II.3.54}$$

identical to the one in (II.3.46). The total A^2 contribution is thus proportional to n, as expected from the replica symmetry.

Notice that the proof is valid for arbitrary n and does not rely on taking the limit $n \to 0$ (though the renormalization factors might depend on n and actually does, see below). It is a crucial point for the consistency of the present approach. Indeed, one may have though that, since the ST proposal corresponds to a gauge-fixing procedure only for $n \to 0$, it would be sufficient to have proved the renormalizability only in this limit. However, as emphasized above, in computing averages, we should first work in the finite n theory and eventually take the limit $n \to 0$ (and in particular, the perturbative series is constructed for finite n).

II.4 Perturbation theory

We now intend to compute the basic correlation functions of the CFDJ gauges in perturbation theory. As we saw earlier, the ST proposal requires to first compute these correlation functions for finite n with the ST action (II.3.12) and ultimately to perform the limit $n \to 0$. In the last section, we have proved that the ST action is multiplicatively renormalizable for finite n allowing us to construct a meaningful perturbative series. In this section, we compute the various one-loop contributions to the two-point vertex functions of the present theory. To do so, we first derive the Feynman rules corresponding to the SUSY formulation of the ST action and go through actual calculations. As a check of our proof of renormalizability we extract the various divergent parts arising in the loop contributions to the two-point vertex functions and show how they can be absorbed in the renormalization constants introduced in the previous section. Finally, we present also the calculations performed in the non-SUSY formalism, see Eq. (II.2.22), that we used to check our computations.

II.4.1 Feynman rules

We are primarily interested in computing at one-loop order the various two-point vertex functions defined as the second derivatives of the effective action Γ at fixed n:

$$\Gamma_{XY}(p,\underline{\theta},\underline{\theta}') = \left.\frac{\delta^{(2)}_{\theta}\Gamma}{\delta X(p,\underline{\theta})\delta Y(-p,\underline{\theta}')}\right|_0 , \tag{II.4.1}$$

where X and Y denote any of the (super)fields, the subscript 0 means that the derivative is evaluated at vanishing fields, and $\delta_\theta/\delta X$ is the covariant functional derivative defined in the previous section if X is a superfield, and reduces to a standard functional derivative otherwise.

We use the exponential representation of SU(N) matrix superfield. Accordingly, we introduce the superfield Λ^a_k for each replica, such that

$$\mathcal{V}_k(x,\underline{\theta}_k) = \exp\left[ig_0 t^a \Lambda^a_k(x,\underline{\theta}_k)\right]. \tag{II.4.2}$$

In the SUSY formulation that we are considering here, the superfields Λ^a_k stand as the basic fields in terms of which we want to derive the Feynman rules. To access the relevant ones for one-loop order calculations, we need to expand $\mathcal{V}_k(x,\underline{\theta}_k)$ in powers of $g_0\Lambda_k$ up to order g_0^2 in the SUSY part of the ST action, Eq. (II.3.12). In practice, we work in momentum Euclidean space with the Fourier convention $\partial_\mu \to -ip_\mu$. Since

the Grassmann spaces are curved, it is not useful to introduce the associated Fourier variables. The first step is to access the various free or tree-level propagators obtained by inversion of the two-point vertex functions. For instance, in the ghost sector of the ST action (II.3.12), we obtain the bare tree-level two-point ghost vertex function

$$\Gamma_{c\bar{c}}(p) = p^2 + \beta_0 \xi_0, \tag{II.4.3}$$

which can be trivially inverted to get the free (bare) ghost propagator

$$\Big[c^a(-p)\,\bar{c}^b(p)\Big]_0 = \frac{\delta^{ab}}{p^2 + \beta_0 \xi_0}, \tag{II.4.4}$$

where the square brackets mean that we are working at finite n and the subscript 0 denotes an average with the quadratic part of the action (II.3.12). On the other hand, the quadratic part of the action (II.3.12) couples the different fields in the sector (A, ih, Λ_k) and therefore its inversion is not trivial. Nevertheless, spacetime and Grassmann isommetries imply the following decomposition of the one-loop two-point vertex functions in the (A, ih, Λ_k) sector[7]

$$\Gamma_{A_\mu A_\nu}(p) = P^T_{\mu\nu}(p)\Gamma_T(p) + P^L_{\mu\nu}(p)\Gamma_L(p) \tag{II.4.5}$$

and

$$\Gamma_{ihA_\mu}(p) = -\Gamma_{A_\mu ih}(p) = ip_\mu \Gamma_{ihA}(p), \tag{II.4.6}$$

where we introduced the longitudinal and transverse projectors $P^L_{\mu\nu}(p) = p_\mu p_\nu/p^2$, $P^T_{\mu\nu}(p) = \delta_{\mu\nu} - p_\mu p_\nu/p^2$. We define the covariant Dirac delta function on the curved Grassmann space that satisfies $\int_{\underline{\theta}} \delta(\underline{\theta}, \underline{\theta}') f(\underline{\theta}) = f(\underline{\theta}')$.[8] In particular, one has $\delta_\theta X(\underline{\theta})/\delta X(\underline{\theta}') = \delta(\underline{\theta}, \underline{\theta}')$ for a given superfield X. We also define the Laplace operator on the curved Grassmann space $\Box_{\underline{\theta}} = \frac{1}{\sqrt{g(\underline{\theta})}} \partial_M \sqrt{g(\underline{\theta})} g^{MN} \partial_N$ that satisfies the identity $\Box_{\underline{\theta}} \delta(\underline{\theta}, \underline{\theta}') = -2 + 2\beta_0 \delta(\underline{\theta}, \underline{\theta}')$.[9] This definition of the Laplace operator corresponds to a natural extension to the case of a curved superspace of the formulas usually used when considering curved space-time, e.g. in General Relativity, [213]. With these definitions, and using further the replica symmetry, the two-point vertex functions involving the superfields read

$$\begin{aligned}\Gamma_{\Lambda_k \Lambda_l}(p, \underline{\theta}, \underline{\theta}') = \delta_{kl} \big[\Gamma_1(p) \delta(\underline{\theta}, \underline{\theta}') + \Gamma_2(p) \Box_{\underline{\theta}} \delta(\underline{\theta}, \underline{\theta}')\big] \\ + (\delta_{kl} - 1)\Gamma_3(p)\end{aligned} \tag{II.4.7}$$

and

$$\Gamma_{\Lambda_k A_\mu}(p, \underline{\theta}) = -ip_\mu \Gamma_4(p), \tag{II.4.8}$$

Note that we have extracted everywhere a unit matrix in color space. These two-point vertex functions can be grouped altogether in a matrix representation

[7] Possible non zero $\Gamma_{\Lambda_k ih}$ term can only appear at least at two-loop order.
[8] Explicitly it is defined as $\delta(\underline{\theta}, \underline{\theta}') = g^{-1/2}(\underline{\theta})\,(\bar{\theta} - \bar{\theta}')(\theta - \theta')$.
[9] Explicitly, $\Box_{\underline{\theta}} = 2\beta_0(\theta\partial_\theta + \bar{\theta}\partial_{\bar{\theta}}) + 2(1 - \beta_0 \bar{\theta}\theta)\partial_\theta \partial_{\bar{\theta}}$.

$$\Gamma^{(2)} = \begin{pmatrix} \Gamma_T P^T_{\mu\nu} + \Gamma_L P^L_{\mu\nu} & -ip_\mu \Gamma_{ihA} & ip_\mu \Gamma_4 \\ ip_\nu \Gamma_{ihA} & \Gamma_{ihih} & 0 \\ -ip_\nu \Gamma_4 & 0 & \delta_{kl}\Big[\Gamma_1 \delta(\underline{\theta}_k, \underline{\theta}'_l) + \Gamma_2 \Box_{\underline{\theta}_k} \delta(\underline{\theta}_k, \underline{\theta}'_l)\Big] + (\delta_{kl} - 1)\Gamma_3 \end{pmatrix}. \tag{II.4.9}$$

This matrix representation makes sense only for $n > 0$ due to the presence of the $n-1$ replicas. On the other hand, for $n = 1$, which corresponds to the usual CF model, all the SUSY sector is absent.

At tree-level, the scalar functions Γ_T, Γ_L, Γ_{ihA} and $\Gamma_{1,\dots,4}$ are trivially extracted from the quadratic part of the action Eq. (II.3.12) and we find

$$\begin{aligned} \Gamma_T(p) &= p^2 + n\beta_0 \\ \Gamma_L(p) &= n\beta_0 \\ \Gamma_{ihA}(p) &= 1 \\ \Gamma_{ihih}(p) &= -\xi_0 \\ \Gamma_1(p) &= p^2 \\ \Gamma_2(p) &= \xi_0/2 \\ \Gamma_3(p) &= 0 \\ \Gamma_4(p) &= 1. \end{aligned} \tag{II.4.10}$$

Details of the inversion of the two-point vertex matrix $\Gamma^{(2)}$ is postponed to Appendix D. After inversion, we obtain the remaining (bare) tree-level propagators of the ST action:

$$\Big[A^a_\mu(-p)\, A^b_\nu(p)\Big]_0 = \delta^{ab}\left(\frac{P^T_{\mu\nu}(p)}{p^2 + n\beta_0} + \frac{\xi_0 P^L_{\mu\nu}(p)}{p^2 + \beta_0\xi_0}\right), \tag{II.4.11}$$

$$\Big[ih^a(-p) ih^b(p)\Big]_0 = \frac{-\beta_0 \delta^{ab}}{p^2 + \beta_0\xi_0}, \tag{II.4.12}$$

$$\Big[ih^a(-p) A^b_\mu(p)\Big]_0 = \frac{i\delta^{ab} p_\mu}{p^2 + \beta_0\xi_0}. \tag{II.4.13}$$

We observe that, in the (A, ih) sector, the only consequence of the replicas is through the n factor in the square mass $n\beta_0$ of the transverse gluon propagator. The correlator of the superfields Λ_k reads

$$\Big[\Lambda^a_k(-p, \underline{\theta})\, \Lambda^b_l(p, \underline{\theta}')\Big]_0 = \delta^{ab}\left[\frac{\delta_{kl}\delta(\underline{\theta}, \underline{\theta}')}{p^2 + \beta_0\xi_0} + \frac{\xi_0(1 + \delta_{kl})}{p^2(p^2 + \beta_0\xi_0)}\right]. \tag{II.4.14}$$

Note in particular that nontrivial correlations between different replicas can only appear for $\xi_0 \neq 0$. Finally, there are nontrivial mixed correlators

$$\Big[ih^a(-p)\Lambda^b_k(p, \underline{\theta})\Big]_0 = \frac{\delta^{ab}}{p^2 + \beta_0\xi_0} \tag{II.4.15}$$

and

$$\Big[\Lambda^a_k(-p, \underline{\theta}) A^b_\mu(p)\Big]_0 = \frac{i\xi_0\delta^{ab} p_\mu}{p^2(p^2 + \beta_0\xi_0)}. \tag{II.4.16}$$

We can already observe how the Landau gauge ($\xi_0 = 0$) and the $\xi_0 \neq 0$ cases differ by inspection of the different masses of the tree-level propagators. Indeed, for $\xi_0 = 0$ all modes are massless apart from the transverse gluons. The latter are purely transverse while in the general ξ-gauges they also display a longitudinal propagator. For what concerns the SUSY sector, the mixed correlator $\left[\Lambda_k^a(-p,\underline{\theta})A_\mu^b(p)\right]_0$ vanishes in the Landau gauge. Moreover, as already noticed, the correlator $\left[\Lambda_k^a(-p,\underline{\theta})\,\Lambda_l^b(p,\underline{\theta}')\right]_0$ becomes diagonal in replica but also ultra-local ($\propto \delta(\underline{\theta},\underline{\theta}')$) in Grasmann space.

We now proceed to the derivation of the interaction vertices relevant for one-loop calculations. As usual they are obtained from terms in Eq. (II.3.12) with more than two powers in the fields. In the non-supersymmetric $(A, c, \bar{c}, ih)$ sector, the vertices are identical to those of the CF model. These include the usual YM ones, namely the three and four gluon interactions as well as the standard ghost-antighost-gluon vertex. For $\xi_0 \neq 0$ there are also a four-ghost vertex as well as an $ihc\bar{c}$ interaction [see Eq. (C.1.1)]. To get the vertices of the SUSY NL-sigma models, we again have to expand the exponential parametrization $\mathcal{V}_k(x,\underline{\theta}_k) = \exp\left[ig_0 t^a \Lambda_k^a(x,\underline{\theta}_k)\right]$ in powers of $g_0\Lambda_k$. There is thus an infinite number of SUSY vertices. They involve an arbitrary number of Λ_k legs and either one or zero gluon leg. An important remark is to note that all these vertices always involve the same replica. Among this infinity of SUSY vertices, only those that contribute up to order g_0^2 are relevant for one-loop calculations. For instance, there is an $A\Lambda_k\Lambda_k$ vertex that reads

$$\frac{\delta_\theta}{\delta\Lambda_k^a(p_1,\underline{\theta})}\frac{\delta_{\theta'}}{\delta\Lambda_l^b(p_2,\underline{\theta}')}\frac{\delta}{\delta A_\mu^c(p_3)}S = i\frac{g_0}{4}f^{abc}\delta_{kl}(2\pi)^d\delta^{(d)}(p_1+p_2+p_3)\delta(\underline{\theta},\underline{\theta}')(p_1-p_2)_\mu \tag{II.4.17}$$

Note that this vertex is also present in the Landau gauge. There is no cubic Λ^3 interaction. This is easily understood as follow. Vertices involving the superfields, but no gluon leg, come along with two derivatives (normal or Grassmannian ones). Cubic vertices only involve the antisymmetric structure constant $f^{abc}\partial_\mu\Lambda_k^a\partial_\mu\Lambda_k^b\Lambda_k^c = f^{abc}g^{MN}\partial_N\Lambda_k^a\partial_M\Lambda_k^b\Lambda_k^c = 0$. Finally, at this order of approximation there are the two quartic vertices $A\Lambda_k^3$ and Λ_k^4 [see Eqs.(C.1.3), (C.1.4)].

Before applying this set of rules to perform actual computations, let us make few comments on the Landau gauge ($\xi_0 = 0$) case. We recover the Landau gauge Feynman rules of [74] for $\xi_0 = 0$. In this case, drastic simplifications occur. The part of the SUSY sector, (II.3.7), that involves Grassmann derivatives vanishes for $\xi_0 = 0$ and Eq. (II.3.7) becomes local in Grassmann variables. Consequently, the propagators and vertices do not involve Grassmann derivatives. Therefore, closed loops of superfields that involve p SUSY vertices show the following Grassmann structure:

$$\int_{\underline{\theta}_1,\ldots,\underline{\theta}_p}\delta(\underline{\theta}_1,\underline{\theta}_2)\ldots\delta(\underline{\theta}_p,\underline{\theta}_1) = 0. \tag{II.4.18}$$

Hence, in the Landau gauge, neither the gluon nor the ghost sectors receive any loop contribution from the replica superfields. The replica sector only gives contribution to the bare tree-level gluon mass $n\beta_0$. Henceforth, for what concerns the gluon and ghost sectors, the Landau gauge ST action is perturbatively equivalent to the Landau limit of the CF model.

II.4.2 One-loop two-point vertex functions

We now proceed to the one-loop computations of the two-point vertex functions of the ST action in the CFDJ gauges, that is the one-loop contributions to the scalar functions (II.4.3) and (II.4.10). As emphasized before, we keep n finite untill the end of the calculations. We apply the Feynman rules derived in the previous section. Calculations are straightforward but lengthy and not particularly enlightening. We thus only display the one-loop Feynman diagrams in Figs. II.1 – II.5 and illustrate their computations with a couple of examples, in particular in order to present how the dependences in Grassmann parameters are treated. Most of these diagrams are UV divergent in $d \geq 4$ and we regularize them by using dimensional regularization setting $d = 4 - \epsilon$.

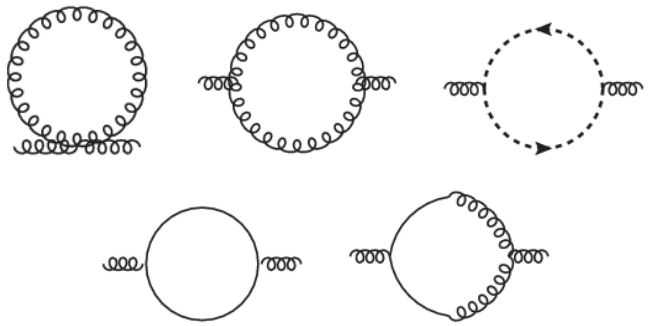

Figure II.1: One-loop diagrams for the vertex Γ_{AA}. We use the standard graphical conventions for the gluon (wiggly) and ghost (dashed) lines. The plain line represents the superfield correlator (II.4.14). The second diagram on the second line involves a mixed A-Λ correlator (II.4.16). The diagrams of the first line are present in the Landau gauge and *a fortiori* in the CF model. The diagrams of the second line involve the superfield sector and are thus specific of the present gauge fixing (they are proportional to $n-1$ and thus vanish in the CF model). The first one is proportional to $\beta_0\xi_0$ and the second one to $\beta_0\xi_0^2$.

We treat explicitly the contribution to the gluon two-point vertex function of the first diagram on the second line of Fig. II.1, which involves the vertex Eq. (II.4.17) and a loop of superfields. Its contribution to the gluon self-energy is given by

$$\begin{aligned}\Gamma^{\Lambda-\text{loop}}_{A^a_\mu A^b_\nu}(p) =& \frac{g_0^2}{8}\sum_{i,j=2}^{n}\int_k\int_{\underline{\theta}_i,\underline{\theta}_j} f^{acd}(k_\nu+\ell_\nu)\left\{\frac{\delta_{ij}\delta(\underline{\theta}_i,\underline{\theta}_j)}{k^2+\beta_0\xi_0}+\frac{(1+\delta_{ij})\xi_0}{k^2(k^2+\beta_0\xi_0)}\right\}\\ &\times f^{bdc}(k_\mu+\ell_\mu)\left\{\frac{\delta_{ij}\delta(\underline{\theta}_i,\underline{\theta}_j)}{\ell^2+\beta_0\xi_0}+\frac{(1+\delta_{ij})\xi_0}{\ell^2(\ell^2+\beta_0\xi_0)}\right\},\end{aligned} \tag{II.4.19}$$

where a, b and μ, ν are respectively the color and Lorentz indices of the external gluon legs carrying momentum p and where $\ell_\mu = k_\mu - p_\mu$. We use the notation $\int_k = \mu^\epsilon \int \frac{d^dk}{(2\pi)^d}$, with $d = 4-\epsilon$ in dimensional regularization. The arbitrary scale μ is introduced for dimensional reasons. The replica indices i, j are associated with the internal superfield

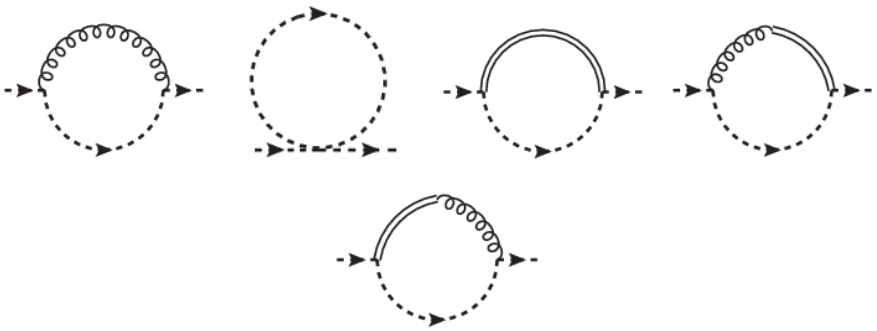

Figure II.2: One-loop diagrams for the vertex $\Gamma_{c\bar{c}}$. We use the standard graphical conventions for the gluon (wiggly) and ghost (dashed) lines. The double plain line represents the $ih - ih$ correlator (II.4.12). The fourth and fifth diagrams involve a mixed ih-A correlator (II.4.13). Only the first diagram on the first line is present in the Landau gauge. All the others are present in the CF model. There is no diagram involving the superfields.

lines. The Grassmannian integrals are trivially performed using the identities

$$\int_{\underline{\theta}} \delta(\underline{\theta},\underline{\theta}')f(\underline{\theta}) = f(\underline{\theta}')\,, \quad \delta\,(\underline{\theta},\underline{\theta}) = 0 \quad \text{and} \quad \int_{\underline{\theta}} 1 = \beta_0. \tag{II.4.20}$$

After summing over the replica indices, we obtain the following momentum integral:

$$\Gamma^{\Lambda-\text{loop}}_{A^a_\mu A^d_\nu}(p) = -\delta^{ad}(n-1)\frac{g_0^2 N\beta_0\xi_0}{8} \times \int_k \frac{(k_\mu+\ell_\mu)\,(k_\nu+\ell_\nu)}{(k^2+\beta_0\xi_0)\,(\ell^2+\beta_0\xi_0)} \left(\frac{2}{k^2}+\frac{2}{\ell^2}+\frac{(n+2)\beta_0\xi_0}{k^2\ell^2}\right), \tag{II.4.21}$$

which is logarithmically divergent in the UV.

For later use, let us show the result obtained for the second diagram on the second line of Fig. II.1, which also involves the replica sector. A similar calculation yields

$$\Gamma^{\text{mixed}}_{A^a_\mu A^d_\nu}(p) = -\delta^{ad}(n-1)\frac{g_0^2 N\beta_0\xi_0^2}{d-1} P^T_{\mu\nu}(p) \times \int_k \frac{k^2p^2-(k\cdot p)^2}{k^2\ell^2\,(k^2+\beta_0\xi_0)\,(\ell^2+\beta_0\xi_0)}. \tag{II.4.22}$$

It is transverse and UV finite. As expected, both replica contributions are $\propto n-1$ and vanish identically in the CF model ($n = 1$).

We remark that the two sunset diagrams contributing to the superfield two-point vertex function, namely the last two ones in Fig. II.4, present non-diagonal terms in replicas so that $\Gamma_{\Lambda_k\Lambda_l}$ develops nontrivial correlations between different replicas at one-loop order as compared to the tree-level case (see Eq. (II.4.9) and (II.4.10)). However the off-diagonal divergent part of diagram three and four of Fig. II.4 are respectively $g^2N\xi_0^2/32\pi^2\epsilon$ and $-g^2N\xi_0^2/32\pi^2\epsilon$. Therefore correlations between different replicas are UV finite as required by renormalizability.

We mention that in the inversion of the two-point vertex function matrix (II.4.9) we considered a possible nonzero value for correlations between different replicas ($\Gamma_3 \neq 0$) but no correlation between ih and the superfields. Indeed, such correlations are absent at one-loop order, but we stress that they might appear at two-loop.

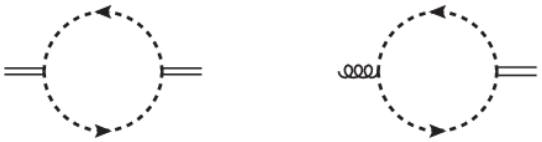

Figure II.3: One-loop diagrams for the vertices Γ_{ihih} (left) and Γ_{ihA} (right). We use the standard graphical conventions for the gluon (wiggly) and ghost (dashed) lines. The double plain lines represent the ih legs. Both diagrams are present in the CF model. There is no diagram involving the superfields.

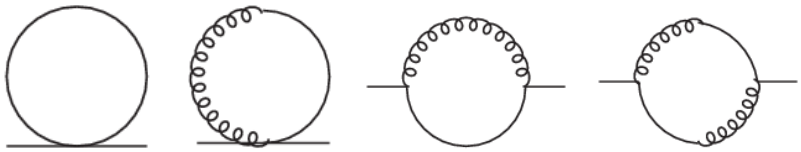

Figure II.4: One-loop diagrams for the vertex $\Gamma_{\Lambda\Lambda}$. We use the standard graphical conventions for the gluon (wiggly) and ghost (dashed) lines. The plain line represents the superfield correlator (II.4.14). The second and fourth diagrams involve a mixed A-Λ correlator (II.4.16).

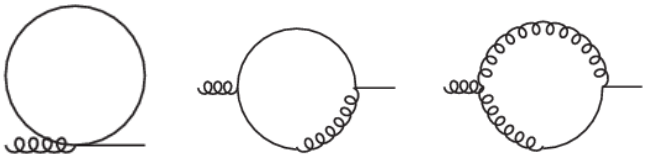

Figure II.5: One-loop diagrams for the vertex $\Gamma_{A\Lambda}$. We use the standard graphical conventions for the gluon (wiggly) and ghost (dashed) lines. The plain line represents the superfield correlator (II.4.14). The two last diagrams involve a mixed A-Λ correlator (II.4.16).

II.4.3 One-loop renormalization

II.4.3.1 UV divergences

The calculation of the other diagrams of Figs. II.1 – II.5 goes along the same lines and consists in standard one-loop momentum integrals once the Grassmannian integrations are performed. Although their expressions are pretty cumbersome and therefore given in Appendix C, the divergent parts can easily be evaluated. Altogether, the one-loop Feynman diagrams, Figs. II.1 – II.5, yield nine divergent structures

$$\begin{aligned}
&\Gamma^{\rm div}_{A_\mu A_\nu}(p) = n\beta_0\delta_{\mu\nu}\left\{1+\kappa\frac{3+\xi_0}{4}\right\} + p^2 P^T_{\mu\nu}(p)\left\{1-\kappa\left(\frac{13}{6}-\frac{\xi_0}{2}\right)\right\},\\
&\Gamma^{\rm div}_{ih\,ih}(p) = -\xi_0\left(1+\kappa\frac{\xi_0}{4}\right),\\
&\Gamma^{\rm div}_{ihA_\mu}(p) = ip_\mu\left(1+\kappa\frac{\xi_0}{4}\right),\\
&\Gamma^{\rm div}_{c\bar c}(p) = p^2\left(1-\kappa\frac{3-\xi_0}{4}\right) + \beta_0\xi_0\left(1+\kappa\frac{\xi_0}{4}\right),\\
&\Gamma^{\rm div}_{\Lambda_k A_\mu}(p,\underline{\theta}) = -ip_\mu\left(1+\kappa\frac{\xi_0}{6}\right),\\
&\Gamma^{\rm div}_{\Lambda_k\Lambda_l}(p,\underline{\theta},\underline{\theta}') = p^2\delta_{kl}\delta(\underline{\theta},\underline{\theta}')\left\{1-\kappa\left(\frac{3}{4}-\frac{\xi_0}{12}\right)\right\} + \frac{\xi_0}{2}\delta_{kl}\Box_{\underline{\theta}}\delta(\underline{\theta},\underline{\theta}')\left\{1+\kappa\frac{\xi_0}{12}\right\}.
\end{aligned} \tag{II.4.23}$$

where $\kappa = g_0^2 N/8\pi^2\varepsilon$. Note that the proof of renormalizability states that only six independent renormalization factors are necessary to eliminate the UV divergences while nine different divergent structures are found at one-loop order for the two-point vertex functions.

II.4.3.2 Renormalization of the divergent parts

We define renormalized fields and constants in the standard way

$$A^{a\mu} = \sqrt{Z_A}\,A^{a\mu}_r\,,\quad c^a = \sqrt{Z_c}\,c^a_r\,,\quad \bar c^a = \sqrt{Z_c}\,\bar c^a_r\,,\quad h^a = \sqrt{Z_h}h^a_r\,, \tag{II.4.24}$$

and

$$\beta_0 = Z_\beta\beta\,,\quad \xi_0 = Z_\xi\xi\,,\quad g_0 = Z_g g. \tag{II.4.25}$$

It is useful to also introduce rescaled Grassmann variables θ_r and $\bar\theta_r$ such that the measure (II.3.4) reads $\beta_0\bar\theta\theta - 1 = \beta\bar\theta_r\theta_r - 1$. We thus define

$$\begin{aligned}
&\theta = Z_\beta^{-1/2}\theta_r\,,\quad \partial_\theta = Z_\beta^{1/2}\partial_{\theta_r}\,,\quad d\theta = Z_\beta^{1/2}d\theta_r\,,\\
&\bar\theta = Z_\beta^{-1/2}\bar\theta_r\,,\quad \partial_{\bar\theta} = Z_\beta^{1/2}\partial_{\bar\theta_r}\,,\quad d\bar\theta = Z_\beta^{1/2}d\bar\theta_r\,.
\end{aligned} \tag{II.4.26}$$

Accordingly, we introduce a renormalized metric as

$$g_r^{M_r N_r}(\underline{\theta_r}) = g^{MN}(\underline{\theta}), \tag{II.4.27}$$

with $M_r, N_r \in \left\{\theta_r, \bar{\theta}_r\right\}$. In particular, this implies

$$\int_{\underline{\theta}} = Z_\beta \int_{\underline{\theta_r}}, \tag{II.4.28}$$

where $\int_{\underline{\theta_r}} = \int d\theta_r d\bar{\theta}_r(\beta\bar{\theta}_r\theta_r - 1)$. Finally, we define the corresponding renormalized superfields as

$$\Lambda_k = \sqrt{\frac{Z_\Lambda}{Z_\beta}}\,\Lambda_{r,k}. \tag{II.4.29}$$

such that the kinetic term of the fields $\Lambda^a_{r,k}$ is normalized as

$$\frac{1}{2}\int_{\underline{\theta}} (\partial_\mu \Lambda^a_k)^2 = \frac{Z_\Lambda}{2}\int_{\underline{\theta_r}} \left(\partial_\mu \Lambda^a_{r,k}\right)^2. \tag{II.4.30}$$

These definitions of the renormalized constants are convenient for actual perturbative calculations but are different from the constants $\kappa_{1,2,3}$, $Z_{1,2,3}$, Z, and $\tilde{g}$ used in the proof of renormalizability, see Sec. II.3.2. The dictionary between these two sets can easily be done by rewriting Eqs. (II.3.46), (II.3.51) in terms of renormalized quantities (according to the definitions (II.4.24), (II.4.25) and (II.4.29)) and by demanding that the effective action be finite. For instance, let us have a look to the gluon mass term appearing in $\mathcal{L}_1$ [Eq. (II.3.46)]:

$$\kappa_2 \frac{\beta_0}{2\kappa_1}(A^{a\mu})^2 = \kappa_2 \frac{\beta}{2\kappa_1} Z_A Z_\beta (A^{a\mu}_r)^2. \tag{II.4.31}$$

Demanding that the renormalized effective action be finite leads to

$$\frac{\kappa_2}{\kappa_1} = \frac{1}{Z_A Z_\beta}\,. \tag{II.4.32}$$

Following the same argument, and using the identities (II.3.53), eventually yields

$$\begin{aligned} Z_1 &= 1/Z_A\,, \\ \kappa_2\kappa_1 &= 1/Z_c\,, \\ \kappa_3 &= \xi_0/(Z_\beta Z_\xi Z_c)\,, \\ \tilde{g}/\kappa_1 &= g_0/(Z_g\sqrt{Z_A})\,, \\ Z &= Z_\Lambda Z_g^2/Z_\beta\,. \end{aligned} \tag{II.4.33}$$

Furthermore, inspection of the term $\kappa_2 A^a_\mu \partial_\mu i h^a$ in (II.3.46) with the above identities leads to the constraint

$$Z_h = Z_\beta Z_c\,. \tag{II.4.34}$$

Although in practice we do not need explicitly this dictionary, we remark that, owing to the constraint (II.4.34), there are only six independent renormalization factors among the seven defined in (II.4.24), (II.4.25) and (II.4.29), in agreement with our proof of renormalizability. Notice that the relations (II.4.32), (II.4.33) and (II.4.34) are valid only for the divergent parts. Let us also mention that in the case of the Landau gauge ($\xi_0 = 0$), the number of independent renormalization constants is even further reduced

down to three owing to three additional constraints, namely $Z_A Z_c Z_\beta = Z_g\sqrt{Z_A}Z_c = Z_\Lambda/Z_c = 1$, see Appendix B.1.

In the following, we only refer to renormalized fields and correlators and we suppress the index r for simplicity. The explicit one-loop expressions of the (divergent parts of) the renormalization constants can be straightforwardly read off Eq. (II.4.23). For instance the divergent parts of the renormalized $\Lambda-\Lambda$ two-point vertex function reads

$$\Gamma^{\rm div}_{\Lambda_k\Lambda_l}(p,\underline{\theta},\underline{\theta}') = p^2\delta_{kl}\delta(\underline{\theta},\underline{\theta}')Z_\Lambda\left\{1-\kappa\left(\frac{3}{4}-\frac{\xi}{12}\right)\right\}+\frac{\xi}{2}\delta_{kl}\Box_{\underline{\theta}}\delta(\underline{\theta},\underline{\theta}')Z_\Lambda Z_\xi Z_\beta\left\{1+\kappa\frac{\xi}{12}\right\}, \tag{II.4.35}$$

yielding

$$\begin{aligned}\delta Z^{\rm div}_\Lambda &= 1+\kappa\left(\frac{3}{4}-\frac{\xi}{12}\right),\\ \delta Z^{\rm div}_\Lambda+\delta Z^{\rm div}_\xi+\delta Z^{\rm div}_\beta &= 1-\kappa\frac{\xi}{12},\end{aligned} \tag{II.4.36}$$

where we defined $\delta Z_\alpha = Z_\alpha - 1$ and div denotes the divergent part.

Eventually, the nine divergent structures of Eq. (II.4.23) are renormalized by the five independent counterterms

$$\delta Z^{\rm div}_A = \left(\frac{13}{6}-\frac{\xi}{2}\right)\kappa, \tag{II.4.37}$$

$$\delta Z^{\rm div}_c = \left(\frac{3}{4}-\frac{\xi}{4}\right)\kappa, \tag{II.4.38}$$

$$\delta Z^{\rm div}_\beta = \left(-\frac{35}{12}+\frac{\xi}{4}\right)\kappa, \tag{II.4.39}$$

$$\delta Z^{\rm div}_\xi = \left(\frac{13}{6}-\frac{\xi}{4}\right)\kappa, \tag{II.4.40}$$

$$\delta Z^{\rm div}_\Lambda = \left(\frac{3}{4}-\frac{\xi}{12}\right)\kappa, \tag{II.4.41}$$

We also verify the constraint Eq. (II.4.34) at one-loop order:

$$Z_h = Z_\beta Z_c = 1-\kappa\frac{13}{6}. \tag{II.4.42}$$

The sixth constant required to fully renormalize the theory is the renormalization of the bare coupling constant g_0 but we do not need it at the present order of approximation. We notice that the divergent parts of the renormalization factors are independent of n at one loop. We thus recover the expressions of the independent factors Z_A, Z_c, Z_β, Z_ξ of the CF model (which, we recall, corresponds to $n=1$), where Z_β is identified to the square mass renormalization factor, see [199]. We do not see any reason for this trivial n dependence to hold beyond one loop and we expect explicit differences with the CF model to arise at higher loop orders.

II.4.4 Non-supersymmetric formalism

We recall that, the ST action admits another formulation than the SUSY one, see Eq. (II.2.22), where the auxiliary fields $c_k,\ \bar{c}_k,\ ih_k,\ U_k$ of the replica sector are not merged into a supermatrix field. In this formalism the ST action reads

$$S[A,c,\bar{c},h,\{\mathcal{V}\}] = S_{\rm YM}[A] + S_{\rm CF}[A,c,\bar{c},h] + \sum_{k=2}^{n} S_{\rm CF}[A^{U_k},c_k,\bar{c}_k,h_k], \tag{II.4.43}$$

with

$$\begin{aligned} S_{\rm CF}[A^U,c,\bar{c},h], = \int_x \Big\{ \partial_\mu \bar{c}^a D^U_\mu c^a + ih^a \partial_\mu (A^U_\mu)^a + \beta_0 \Big[\frac{1}{2}(A^U_\mu)^a (A^U_\mu)^a + \xi_0 \bar{c}^a c^a \Big] \Big\} \\ + \xi_0 \int_x \Big\{ -\frac{(ih^a)^2}{2} - \frac{g_0}{2} f^{abc} ih^a \bar{c}^b c^c - \frac{g_0^2}{4} \Big(f^{abc} \bar{c}^b c^c \Big)^2 \Big\}. \end{aligned} \tag{II.4.44}$$

In order to use a perturbative development, we introduce the fields λ_k (one for each replica k) to parametrize the matrix fields $U_k = \exp[ig_0 \lambda_k^a t^a]$. In the same way as we did previously, we expend the U_k in powers of $g_0\lambda_k$ to get the relevant one-loop Feynman rules. It is interesting to have a look at the tree-level bare propagators in the sector $(A_\mu, ih, ih_k, \lambda_k)$. As in the SUSY case, the quadratic part of the ST action is not diagonal in the fields, leading to mixed correlators. The (A, ih) sector is the same as in the SUSY case Eqs. (II.4.11)–(II.4.13). However, mixed correlators in the (ih, ih_k, λ_k) read

$$\Big[ih^a(-p) A^b_\mu(p) \Big]_0 = \frac{i\delta^{ab} p_\mu}{p^2 + \beta_0 \xi_0}, \tag{II.4.45}$$

$$\Big[ih^a_k(-p) A^b_\mu(p) \Big]_0 = 0, \tag{II.4.46}$$

$$\Big[ih^a(-p) \lambda^b_k(p) \Big]_0 = -\Big[ih^a_k(-p) \lambda^b_k(p) \Big]_0 = \frac{\delta^{ab}}{p^2 + \beta_0 \xi_0}. \tag{II.4.47}$$

Note the sign difference between the correlators involving ih and ih_k. It turns out to be more convenient to rewrite the action in a more symmetric form by performing the following shifts: $\hat{h}^a \to \hat{h}^a + \partial_\mu A^a_\mu / \xi_0$, where we recall that $\hat{h}^a = ih^a + \frac{g_0}{2} f^{abc} \bar{c}^b c^c$, and similarly for $\hat{h}_k$. In doing so the $\hat{h}^a$, $\hat{h}^a_k$ decouple and can be integrated out. Note that this is also advantageous for practical calculations as the number of different fields reduces. The ST action (II.4.43) becomes

$$S = S_{\rm YM}[A] + S_{\rm CF}[A,c,\bar{c}] + \sum_{k=2}^{n} S_{\rm CF}[A^{U_k},c_k,\bar{c}_k], \tag{II.4.48}$$

where

$$\begin{aligned} S_{\rm CF}[A,c,\bar{c}] = \int_x \Big\{ \frac{\beta_0}{2}(A^a_\mu)^2 + \frac{(\partial_\mu A^a_\mu)^2}{2\xi_0} + \frac{1}{2}\Big(\partial_\mu \bar{c}^a D_\mu c^a + D_\mu \bar{c}^a \partial_\mu c^a \Big) \\ + \beta_0 \xi_0 \bar{c}^a c^a - \frac{g_0^2 \xi_0}{8} (f^{abc} \bar{c}^b c^c)^2 \Big\}. \end{aligned} \tag{II.4.49}$$

Again, parametrizing $U_k = \exp[ig_0\lambda_k^a t^a]$ we get the Feynman rules relevant for one-loop computations. In particular, note the obvious symmetry between replicas on the tree-level propagators

$$\left[c_k^a(-p)\bar{c}_l^b(p)\right]_0 = \delta_{kl}\left[c^a(-p)\bar{c}^b(p)\right] = \delta^{ab}\frac{\delta_{kl}}{p^2+\beta_0\xi_0}, \tag{II.4.50}$$

$$\left[\lambda_k^a(-p)\lambda_l^b(p)\right]_0 = \delta^{ab}\frac{\xi_0(1+\delta_{kl})}{p^2(p^2+\beta_0\xi_0)}, \tag{II.4.51}$$

$$\left[\lambda_k^a(-p)A_\mu^b(p)\right]_0 = \delta^{ab}\frac{i\xi_0 p_\mu}{p^2(p^2+\beta_0\xi_0)}. \tag{II.4.52}$$

The vertices are obtained in a straightforward manner.

II.4.4.1 One-loop calculations

Our point here, is to compute the one-loop divergent parts of the various two-point vertex functions in the non-SUSY formalism as a crosscheck of our one-loop SUSY calculations performed previously. In this formalism, beside the presence of the mixed correlator $\left[\lambda_k^a(-p)A_\mu^b(p)\right]$, calculations are very standard since there is neither Grassmannian nor SUSY terms. Although the loss of the explicit SUSY character leads to more standard calculations, they are more numerous (forty four one-loop Feynman diagrams for the two-point vertex functions). Let us mention that our calculations satisfied several nontrivial checks. For instance, replica symmetry requires that $\Gamma_{c_k\bar{c}_l}(p) = \delta_{kl}\Gamma_{c\bar{c}}(p)$. However, at one-loop order, $\Gamma_{c_k\bar{c}_l}(p)$ involves the same Feynman diagrams as those in $\Gamma_{c\bar{c}}(p)$, plus diagrams that involve the λ_k fields. It is therefore a very nontrivial check of our calculations to verify that the contributions of the diagrams involving the fields λ_k exactly cancel out (not only the divergent parts, but also the finite ones).

Eventually, we extract the one-loop divergent parts of the various two-point vertex functions

$$\begin{aligned}\Gamma^{\rm div}_{A_\mu A_\nu}(p) = {} & n\beta_0\delta_{\mu\nu}\left\{1+\kappa\frac{3+\xi_0}{4}\right\} + p^2 P^T_{\mu\nu}(p)\left\{1-\kappa\left(\frac{13}{6}-\frac{\xi_0}{2}\right)\right\} \\ & - \frac{n}{\xi_0}p^2 P^L_{\mu\nu}(p)\left\{1+\kappa\frac{\xi_0}{4}\right\}.\end{aligned} \tag{II.4.53}$$

The first two lines are identical to those of Eq. (II.4.23) and the last line is the renormalization of the $(\partial_\mu A_\mu^a)^2/\xi$ term in the formalism with the ih, ih_k fields integrated out. For the ghost sector, we get

$$\Gamma^{\rm div}_{c_k\bar{c}_l}(p) = \delta_{kl}\,\Gamma^{\rm div}_{c\bar{c}}(p) = \delta_{kl}\left\{p^2\left(1-\kappa\frac{3-\xi_0}{4}\right)+\beta_0\xi_0\left(1+\kappa\frac{\xi_0}{4}\right)\right\}, \tag{II.4.54}$$

which is unchanged as compared to the previous calculation in Eq. (II.4.23). Finally, in the replicated sigma model sector, we have

$$\Gamma^{\rm div}_{\lambda_k A_\mu}(p) = -ip_\mu\beta_0\left(1+\kappa\frac{\xi_0}{6}\right) - ip_\mu\frac{p^2}{\xi_0}\left\{1-\kappa\left(\frac{3}{4}-\frac{\xi_0}{6}\right)\right\} \tag{II.4.55}$$

and

$$\Gamma^{\rm div}_{\lambda_k\lambda_l}(p) = \delta_{kl}\beta_0 p^2\left\{1-\kappa\left(\frac{3}{4}-\frac{\xi_0}{12}\right)\right\} + \delta_{kl}\frac{p^4}{\xi_0}\left\{1-\kappa\left(\frac{3}{2}-\frac{\xi_0}{12}\right)\right\}. \tag{II.4.56}$$

II.4.4.2 Relation to superfield formalism

The relation with the SUSY formalism is not trivial. According to the representation (II.3.6) and (II.4.2), we can identify the relation (for each replica) between the superfield Λ_k and the basic fields $c_k, \bar{c}_k, h_k, \lambda_k$. We get

$$\Lambda_k = \lambda_k + \bar{\theta}c'_k + \bar{c}'_k\theta + \bar{\theta}\theta\hat{h}'_k \tag{II.4.57}$$

with

$$c'_k = c_k + \frac{ig_0}{2}[c_k,\lambda_k] - \frac{g_0^2}{12}[[c_k,\lambda_k],\lambda_k] + \dots, \tag{II.4.58}$$

$$\bar{c}'_k = \bar{c}_k + \frac{ig_0}{2}[\bar{c}_k,\lambda_k] - \frac{g_0^2}{12}[[\bar{c}_k,\lambda_k],\lambda_k] + \dots \tag{II.4.59}$$

and

$$\hat{h}'_k = \hat{h}_k + \frac{ig_0}{2}[\hat{h}_k,\lambda_k] - \frac{g_0^2}{12}\left\{[[\hat{h}_k,\lambda_k],\lambda_k] - [[\bar{c}_k,c_k],\lambda_k]\right\} + \dots, \tag{II.4.60}$$

where the dots denote higher order (nonlinear terms). The above relations highlight the fact that the superfield Λ_k is a nonlinear composite of the fields λ_k, c_k , $\bar{c}_k$, and h_k. These relations concern the basic fields that are integrated over in the path-integral. However, although written with the same notations, the variables of the effective action Γ correspond to averages of these fields variables in the presence of nontrivial sources, e.g., as in Eq. (II.3.23). At the level of the effective action, we thus need to take into account the nontrivial renormalization of the nonlinear composite fields (II.4.58)-(II.4.60). In particular, one has, at linear order,

$$c'_k = \sqrt{Z'_c}c_k + \dots, \tag{II.4.61}$$

$$\bar{c}'_k = \sqrt{Z'_c}\bar{c}_k + \dots, \tag{II.4.62}$$

$$\hat{h}'_k = \sqrt{Z'_h}ih_k + \dots, \tag{II.4.63}$$

where the dots stand for nonlinear and/or nonlocal contributions and where the composite field renormalization factors Z'_c and Z'_h do not depend on the replica index due to the replica symmetry. At linear order, we write

$$\Lambda_k = \lambda_k + \sqrt{Z'_c}\bar{\theta}c_k + \sqrt{Z'_c}\bar{c}_k\theta + \sqrt{Z'_h}\bar{\theta}\theta ih_k + \dots \tag{II.4.64}$$

This shows that both λ_k and Λ_k renormalize in the same way. For instance, defining $\lambda^a_k = \sqrt{Z_\lambda}\lambda^a_{r,k}$, in terms of renormalized quantities, Eq. (II.4.64) reads (where for clarity we reintroduced the index r) according to (II.4.24), (II.4.25) and (II.4.29)

$$\sqrt{\frac{Z_\Lambda}{Z_\beta}}\Lambda_{r,k} = \sqrt{Z_\lambda}\lambda_{r,k} + \sqrt{\frac{Z_c Z'_c}{Z_\beta}}\left(\bar\theta_r c_{r,k} + \bar c_{r,k}\theta_r + \sqrt{\frac{Z'_h}{Z'_c}}\bar\theta_r\theta_r i h_{r,k}\right) + \dots , \tag{II.4.65}$$

where we used $Z_h = Z_\beta Z_c$, see Eq. (II.4.34). For the quadratic part of the effective action to have the desired expressions in terms of either the renormalized superfields $\Lambda_{r,k}$ or the renormalized fields $\lambda_{r,k}$, $c_{r,k}$, $\bar c_{r,k}$, and $h_{r,k}$, we must have

$$\Lambda_{r,k} = \lambda_{r,k} + \bar\theta_r c_{r,k} + \bar c_{r,k}\theta_r + \bar\theta_r\theta_r i h_{r,k} + \dots \tag{II.4.66}$$

This leads to relations among the renormalization factors of the two formalisms. We conclude that

$$Z'_h = Z'_c \tag{II.4.67}$$

and that

$$Z_\lambda = \frac{Z_\Lambda}{Z_\beta} = \frac{Z_c Z'_c}{Z_\beta}. \tag{II.4.68}$$

In particular, the first equality in Eq. (II.4.68) is satisfied at one loop, see Eqs. (II.4.37)–(II.4.41). Accordingly, the composite field renormalization factor Z'_c appearing in the second equality in Eq. (II.4.68) can be obtained from the first equality, we find,

$$Z'_c = 1 + \kappa\frac{\xi}{6}. \tag{II.4.69}$$

We now conclude Sec. II.4. Here we have investigated the two-point vertex functions of the ST action at one-loop order in perturbation theory. In particular, we have explicitly checked at one-loop order our proof of renormalizability by eliminating all the UV divergences by means of five independent renormalization constants. These computations were performed in two equivalent formalisms as a nontrivial crosscheck. An important remark to be made is that, so far, we remained at finite n while the $n \to 0$ limit is yet to be performed. Although elimination of the divergences can be done at finite n, the renormalization of the finite parts display a nontrivial interplay with the $n \to 0$ limit, which is discussed in the next sections.

II.5 One-loop propagators.

Now that we have computed the one-loop contributions and have explicitly shown how to eliminate their UV divergences we can move forward and investigate the various (one-loop) propagators of the ST action. This demands in particular to invert the renormalized two-point vertex function matrix, the analogous of (II.4.9) but where all the Γ_α functions are renormalized vertex functions. Let us stress again that the inversion, has to be performed prior to the $n \to 0$ limit, see Appendix D. For instance,

the one-loop ghost and gluon propagators are given in terms of the various one-loop renormalized vertex functions Γ_α as

$$G_{\rm gh}(p) = \lim_{n\to 0} \Gamma^{-1}_{c\bar{c}}(p) \tag{II.5.1}$$

and

$$G_T(p) = \lim_{n\to 0} \Gamma^{-1}_T(p), \tag{II.5.2}$$

$$G_L(p) = \lim_{n\to 0} \frac{\Gamma_{ihih}\left(\Gamma_1 + \beta_0\,(n-2)\,\Gamma_3\right)}{\left(\Gamma_L\Gamma_{ihih} - (\Gamma_{ihA})^2 p^2\right)\left(\Gamma_1 + \beta_0\,(n-2)\,\Gamma_3\right) - \Gamma_{ihih} p^2 \beta_0 (\Gamma_4)^2 (n-1)}, \tag{II.5.3}$$

where we have decomposed the gluon propagator $G_{\mu\nu}(p)$ into transverse and longitudinal parts as in Eq. (II.4.5). Here, $G_L(p)$ is obtained through the inversion of the two-point vertex functions matrix Eq. (II.4.9). Details of the inversion and definition of the other propagators are provided in Appendix D.

II.5.1 Renormalization of the finite parts

II.5.1.1 n-dependent renormalization schemes

Before that we define a set of renormalization prescriptions for the two-point vertex functions, let us come back for a moment to the Landau gauge ($\xi_0 = 0$). We saw in the previous section that, in this case, the ST proposal is perturbatively equivalent to the (Landau limit of the) CF model if the bare gluon square masses of both models are identified, namely $n\beta_0$ for the ST case and m_0^2 for the CF model. We recall that a very important feature of the CF model is that, under suitable renormalization prescriptions, it displays IR safe renormalization group (RG) flows and can thus be investigated perturbatively down to (deep) infrared momenta [78]. This motivates to consider renormalization schemes where such an equivalence is preserved at the level of the renormalized theory. It was therefore proposed in [74] to consider renormalization schemes for the ST action where, instead of renormalizing the gauge-fixing parameter β_0 as $\beta_0 = Z_\beta \beta$ (which yields the usual FP theory in the limit $n \to 0$), it is $n\beta_0$ which is renormalized as $n\beta_0 = Z_{m^2} m^2$. Consequently, part of the n dependence is absorbed into the bare parameter and the $n \to 0$ limit is performed at fixed renormalized (transverse) gluon mass. In doing so, the equivalence with the CF model holds for the renormalized theory. The consequence is that the renormalized ST action displays the same IR safe RG trajectories as those of the CF model. We thus have a genuine gauge-fixed version of YM theories that can be investigated perturbatively at all momentum scales.

For $\xi_0 \neq 0$, we shall adopt similar renormalization schemes (with $n\beta_0 = Z_{m^2} m^2$).[10] Consequently, the difference between the renormalized ST gauge-fixed action and the CF action (for arbitrary ξ_0) lies in the SUSY replica sector, which is absent from the latter. The replica sector therefore encodes the effects of our treatment of Gribov copies and differentiates the CF model ($n = 1$) from the genuine gauge-fixed YM theory (ST

[10] Although the discussion of possible IR safe RG trajectories will appear later on, we mention here that we investigated renormalization schemes where $\beta_0 = Z_\beta \beta$ also for $\xi_0 \neq 0$. In the $n \to 0$ limit we have always found a Landau pole thus preventing a perturbative investigation of the IR regime.

proposal $n \to 0$). On the one hand, these effects are not conveniently accessed through a direct investigation of the correlators of the SUSY sector since this sector is proper to the present proposal and has no equivalent to be compared with. This is further discussed in Sec. II.7.4. Moreover, it is not clear what is the meaning of the replica sector once the limit $n \to 0$ has been performed. On the other hand, comparisons between the correlators of the gluon and ghost sectors, which are shared by both the ST and the CF actions, highlight the effects of our treatment of Gribov copies.

Nevertheless, for $\xi_0 \neq 0$, the SUSY sector does not decouple and "auxiliary" modes (others than the transverse gluons) are massive already at tree-level, with bare square mass $\beta_0\xi_0$, see Eqs. (II.4.11)-(II.4.16). Defining the renormalized gauge parameter ξ as $\xi_0 = Z_\xi \xi$ would lead to a renormalized auxiliary square mass of $m^2 \xi Z_{m^2} Z_\xi / n$ that eventually blows up in the limit $n \to 0$. Alternatively, we can absorb some of the n dependence into the bare gauge parameter ξ_0 such that the $n \to 0$ limit is performed at fixed renormalized auxiliary square mass, namely $\xi_0/n = Z_\xi\, \xi$ leading to $\beta_0\xi_0 = Z_\xi Z_{m^2} m^2 \xi$.[11] We thus define

$$n\beta_0 = Z_{m^2} m^2 \quad \text{and} \quad \frac{\xi_0}{n} = Z_\xi\, \xi, \tag{II.5.4}$$

and Z_g, Z_A, Z_c, Z_Λ, and Z_h are defined as in (II.4.24), (II.4.25).[12] We note that these definitions can be equally used to renormalize the CF model ($n = 1$) since the proof of renormalizability and the one-loop results obtained in Eqs. (II.4.37)-(II.4.41) are valid for arbitrary n.

The absorption of partial n dependence into the bare parameters (II.5.4) leads to drastic simplifications of the perturbative series in the $n \to 0$ limit as we now show.

II.5.1.2 Consequences of the $n \to 0$ limit

Important consequences follow directly from the choice (II.5.4), which enables us to make firm predictions that could compared with possible future lattice simulations. First, not only transverse gluons are massive, but also the auxiliary fields and in particular the ghosts which acquire a renormalized tree-level square mass $Z_{m^2} Z_\xi \xi m^2$. Moreover, various correlators which are proportional to ξ_0 now vanish in the limit $n \to 0$. For instance, the renormalized tree-level longitudinal gluon propagator (see Eq. (II.4.11)) vanishes in this limit and the gluon propagator is exactly transverse as in the Landau gauge. We expect this property to remain valid to all orders of perturbation theory. We can easily convince ourselves of it at one-loop order by counting powers of n as follow: any combination of $n\beta_0$, $\xi_0\beta_0$ counts to zero power of n while any ξ_0 alone counts to one power of n and β_0 to n^{-1}. For instance, inspection of the ST action

[11] Note that such choices are arbitrary and one could have also chosen a renormalization of the kind $\xi_0/n^2 = Z_\xi\, \xi$, in such a way that auxiliary masses still vanish outside the Landau gauge. All these renormalizations schemes are acceptable with the proof of renormalizability but lead to different phenomenologies. Comparisons with lattice data would be needed to discard different scenarios. Here, we choose to consider $\xi_0/n = Z_\xi\, \xi$ because it corresponds to a "minimal" n dependence, in the sense that the limit $\xi \to 0$ is smooth and yields the Landau limit of the CF model studied in [79].

[12] We note that in the present scheme, $Z_{m^2} = Z_\beta \left[\beta \to m^2/n, \xi \to n\xi\right]$. In particular we have $\Lambda_k = \sqrt{Z_\Lambda / Z_{m^2}}\, \Lambda_{r,k}$. For a more detailed discussion on the renormalization of the Grassmann parameters see Appendix E.

(II.3.12) tells us that the $ihc\bar{c}$ vertex counts for $\xi_0 \propto n$, while the tree-level expression of the bare ghost propagator, Eq. (II.4.4), tells us that the ghost propagator counts to 0 power of n. Accordingly, we easily see that $\Gamma_{ihih}(p)$, which is given by the left diagram of Fig. II.3, is proportional to ξ_0 up to functions of $\xi_0\beta_0$ and $n\beta_0$. Following our power counting rule, the renormalized one-loop vertex $\Gamma_{ihih}(p)$ thus scales as n and hence vanishes in the limit $n \to 0$. The same argument leads to conclude that $\Gamma_{ihA}(p)$ is finite in this limit, see (II.4.10). According to Eq. (II.5.3), we see that the one-loop longitudinal gluon propagator vanishes in the $n \to 0$ limit:

$$G_L(p) = 0. \tag{II.5.5}$$

This is a remarkable nontrivial effect of our treatment of Gribov copies since Eq. (II.5.5) is a pure consequence of the $n \to 0$ limit and therefore of our average over the copies. For instance, in the CF model, with the definitions Eq. (II.5.4), one gets (see Appendix B.2)

$$G_L^{\mathrm{CF}}(p) = -\left.\frac{m^2\Gamma_{ihih}(p)}{\Gamma_L(p)\Gamma_{c\bar{c}}(p)}\right|_{n=1}. \tag{II.5.6}$$

Eq. (II.5.6) is only valid for $n = 1$ since it uses Slavnov-Taylor identities that are proper to the CF model, see Appendix. B.2. This consists in a strong prediction of the present theory as the transversality of the gluon propagator is believed to be a Landau gauge feature. Note that this is a consequence of the present class of renormalization schemes (II.5.4), and is independent of the peculiar renormalization prescriptions that we use below to fix the finite parts of the renormalization constants.

Gribov copies effects influence also other sectors of the theory, though in a less dramatic manner than for the longitudinal gluons. For instance, the transverse gluon sector receives contributions from the superfields (and so from Gribov copies) in the $n \to 0$ limit through the diagram involving a superfield loop (first diagram of the second line of Fig. II.1). According to Eq. (II.4.21), this contribution reads, in the limit $n \to 0$, as

$$\lim_{n\to 0}\Gamma_T^{\Lambda-\mathrm{loop}}(p) = \frac{g^2N\xi m^2}{(d-1)}P_{\mu\nu}^T(p)\int_k \frac{k_\mu k_\nu}{(k^2+\xi m^2)\,(\ell^2+\xi m^2)}\left(\frac{1}{k^2}+\frac{1}{\ell^2}+\frac{\xi m^2}{k^2\ell^2}\right). \tag{II.5.7}$$

On the contrary, the superfield contribution (II.4.22) is proportional to $\beta_0\xi_0^2 \propto nm^2\xi^2$ and vanishes in the limit $n \to 0$. We stress again that the contribution (II.5.7) is absent in the CF model (remark the $(n-1)$ prefactor in Eq. (II.4.21)). As an illustration, from Eq. (II.5.7), we observe that this superfield loop diagram contributes to the transverse gluon two-point vertex function at zero momentum

$$\begin{aligned}\lim_{n\to 0}\Gamma_T^{\Lambda-\mathrm{loop}}(p=0) &= \frac{g^2N\xi m^2}{d}\int_k \frac{2k^2+\xi m^2}{k^2(k^2+\xi m^2)^2}\\ &= \frac{g^2N\xi m^2}{32\pi^2}\left\{\frac{2}{\epsilon}+1+\ln\left(\frac{\bar{\mu}^2}{\xi m^2}\right)\right\},\end{aligned} \tag{II.5.8}$$

where we neglected terms $\mathcal{O}(\epsilon)$ in the last equality and $\bar{\mu}^2 = 4\pi e^{-\gamma}\mu^2$ with γ the Euler constant. It thus renormalizes the one-loop transverse gluon mass at the difference of the CF model where such contribution is absent.

It is interesting to note that the finite ξ case displays many features similar to the Landau gauge due to the $n \to 0$ limit. A first one is that, as already mentioned, the gluon propagator is purely transverse. Moreover, many diagrams are proportional to ξ_0 and hence vanish in the $n \to 0$ limit just like the superfield contribution (II.4.22) to the gluon two-point vertex as we discussed above. For instance a typical feature of the Landau gauge is that the h sector does not receive any contribution from the loops (to any order), see (B.1.7) of Appendix B.1. In the present case, as emphasized above, the contributions of the one-loop diagrams of Fig. II.3 are respectively proportional to ξ_0^2 and to ξ_0 (see also (C.2.18) and (C.2.20)), so that the h sector of the theory is not renormalized in the limit $n \to 0$. We thus have

$$\lim_{n\to 0} \Gamma_{ihA}(p) = \lim_{n\to 0} \sqrt{Z_A Z_h} \tag{II.5.9}$$

and

$$\lim_{n\to 0} \frac{\Gamma_{ihih}(p)}{n\xi} = -\lim_{n\to 0} Z_h Z_\xi. \tag{II.5.10}$$

Remark however that, so far, we have only checked this to be true at one-loop order, while this is true to any order in the Landau gauge. However, we expect the general argument developed here to be valid at any loop order.

Let us also mention that the ghosts receive small loop corrections in the IR regime. One can easily see this in the present case even for finite ξ by inspection of the diagrams contributing to the ghost two-point vertex depicted in Fig. II.2 (see also Appendix C.2.2). The diagrams which are not present in the Landau gauge vanish when n is taken to zero. These include, the tadpole diagram (second diagram of Fig. II.2, see (C.2.12)) and the diagrams involving the ih correlators (third, fourth and fifth diagrams of Fig. II.2, see (C.2.14) and (C.2.16)) which are all proportional to ξ_0 up to powers of $\beta_0\xi_0$ and thus vanish for $n \to 0$. The gluon sunset (first diagram of Fig. II.2) is already present in the Landau gauge. Here, the difference is that both the internal ghost and the internal gluon propagators are massive. Finally it can be shown that this last diagram is proportional to p^2. We conclude that, in the limit $n \to 0$, the ghost two-point vertex function at vanishing momentum does not receive corrections at one-loop order, that is,

$$\lim_{n\to 0} \Gamma_{c\bar{c}}(p=0) = \left(\lim_{n\to 0} Z_c Z_\xi Z_{m^2}\right) \xi m^2. \tag{II.5.11}$$

Finally, we employ the same definitions of the renormalized square masses as described above for the CF model. In that case $n = 1$ and there is no issue with the n dependence of the renormalized parameters. Note also that the nonrenormalization relations (II.5.9)–(II.5.11) do not hold in that case. Instead a relation which is known to hold at all orders in perturbation theory in the CF model is that the combination $(Z_\xi^2 Z_c Z_{m^2}/Z_A)_{n=1}$ is finite [214, 201, 202].

In what follows, we consider additional renormalization prescriptions in order to fix the finite parts of the various renormalization constants. We explicitly show that, indeed, this scheme is consistent with renormalizability and we compute the renormalized

two-point vertex functions. Finally, we obtain the renormalized one-loop propagators of the ST proposal and of the CF model.

II.5.2 Infrared-safe scheme

This set of renormalization prescriptions is inspired from the infrared-safe scheme put forward in [79, 78, 74], that we adapt to the case $\xi \neq 0$. In the Landau gauge, this renormalization scheme leads to IR safe RG trajectories [78, 74]. That is, RG trajectories without a Landau pole. As we shall see below, this is also true in the present case for $\xi \neq 0$. In order to adapt the prescription used in [79, 78], we consider the following relation

$$Z_\xi^2 Z_c Z_{m^2} = Z_A. \tag{II.5.12}$$

In the CF model ($n = 1$), Eq. (II.5.12) is shown to be true to all order of perturbation theory for the divergent parts [214, 201, 202]. The infrared-safe scheme is defined by imposing this equality also at the level of the finite parts of the renormalization constants. We remark from Eqs. (II.4.37)–(II.4.41) that the relation Eq. (II.5.12) is also satisfied by the divergent parts at one-loop order for arbitrary n. We thus use this relation for the ST case as a renormalization prescription by imposing it also for the finite parts.[13] In order to fix the remaining renormalization factors, we impose that the following renormalized vertex functions assume their tree-level expressions at a renormalization scale μ:

$$\Gamma_T(\mu) = m^2 + \mu^2, \tag{II.5.13}$$
$$\Gamma_{c\bar{c}}(\mu) = \xi m^2 + \mu^2, \tag{II.5.14}$$
$$\Gamma_1(\mu) = \mu^2, \tag{II.5.15}$$
$$\Gamma_{ihih}(\mu) = -n\xi \tag{II.5.16}$$
$$\Gamma_{ihA}(\mu) = 1. \tag{II.5.17}$$

Defining $\Pi_\alpha(p)$ as the loop diagrams contributions to the corresponding (renormalized) two-point vertex with the same index, such that for instance $\Gamma_T(p) = Z_A(p^2 + Z_{m^2}m^2) + \Pi_T(p)$, this set of renormalization prescriptions along with Eq. (II.5.12) are used to get the expressions of the renormalization constants in terms of the (renormalized)

[13] However, here, we are not able to prove that the divergent part will satisfy it beyond one-loop order. We can still use it to fix the finite parts at all orders of perturbation theory. Indeed, one can always replace Eq. (II.5.12) by $Z_\xi^2 Z_c Z_{m^2} = Z_A \hat{Z}$, with $\hat{Z} = 1 + \mathcal{O}(g^4)$ chosen such that Z_{m^2}, Z_A, Z_c, and Z_ξ have the correct divergent parts required by renormalizability, but in such a way that $\hat{Z}$ does not affect the finite parts.

one-loop contributions. Their divergent parts are

$$\delta Z_A^{\rm div} = \left(\frac{13}{6} - \frac{n\xi}{2}\right)\kappa \;\to\; \frac{13}{6}\kappa, \tag{II.5.18}$$

$$\delta Z_c^{\rm div} = \left(\frac{3}{4} - \frac{n\xi}{4}\right)\kappa \;\to\; \frac{3}{4}\kappa, \tag{II.5.19}$$

$$\delta Z_{m^2}^{\rm div} = \left(-\frac{35}{12} + \frac{n\xi}{4}\right)\kappa \;\to\; -\frac{35}{12}\kappa, \tag{II.5.20}$$

$$\delta Z_\xi^{\rm div} = \left(\frac{13}{6} - \frac{n\xi}{4}\right)\kappa \;\to\; \frac{13}{6}\kappa, \tag{II.5.21}$$

$$\delta Z_\Lambda^{\rm div} = \left(\frac{3}{4} - \frac{n\xi}{12}\right)\kappa \;\to\; \frac{3}{4}\kappa, \tag{II.5.22}$$

$$\delta Z_h^{\rm div} = -\frac{13}{6}\kappa, \tag{II.5.23}$$

where we indicated the various $n \to 0$ limits, and correspond to those required by renormalibility, see Eqs. (II.4.37)–(II.4.41). In particular we verify that we can use this renormalization scheme for $n = 1$ in which case we recover the divergent parts of the CF model [210, 199, 98] except, of course, for Z_Λ. One can check explicitly that in the $n \to 0$ limit we do verify the relations (II.5.9) and (II.5.10). Note also that, due to our definition of ξ (II.5.4), we trivially recover the divergent parts of the Landau gauge [74] in this limit.

An important remark to be made is that in this renormalization scheme, the parameters m^2 and ξm^2 do not correspond to the square masses of the (transverse) gluons and ghosts respectively. Instead, the transverse gluon square mass is given by the value of the inverse gluon propagator at zero momentum[14]

$$\begin{aligned} m^2_{\rm gluon} &= G_T^{-1}(0) \\ &= \lim_{n\to 0} \left\{ m^2 + \Pi_T(0) \right\}, \end{aligned} \tag{II.5.24}$$

and likewise for the ghost square mass.

Remark that, the infrared-safe renormalization prescriptions, Eqs. (II.5.12)-(II.5.17), lead to several identities among the renormalization factors in the $n \to 0$ limit. For instance, the renormalization prescription (II.5.16) combined with the identity (II.5.10) yields

$$\lim_{n\to 0} Z_h Z_\xi = 1\,. \tag{II.5.25}$$

Similarly, the relation (II.5.9) with the prescription Eq. (II.5.17) implies that

$$\lim_{n\to 0} Z_h Z_A = 1\,. \tag{II.5.26}$$

Combining this with Eq. (II.5.25), we obtain that

$$\lim_{n\to 0} \frac{Z_A}{Z_\xi} = 1\,. \tag{II.5.27}$$

[14] Notice that we did not define it as the the value at zero momentum of the corresponding renormalized two-point vertex function because of a possible non trivial $n \to 0$ limit.

Finally, this last relation along with the prescription Eq. (II.5.12) leads to

$$\lim_{n\to 0} Z_c Z_\xi Z_{m^2} = 1\,. \tag{II.5.28}$$

II.5.3 Zero-momentum renormalization scheme

We have also investigated other renormalization schemes. In particular, we have studied the zero-momentum scheme put forward in the Landau gauge in [78]. This scheme was adapted to the $\xi \neq 0$ case and we investigated it in great details in [99]. In the present thesis, we only detail the infrared-safe scheme and make a few comments on the one at zero-momentum. In the latter, both m^2 and ξm^2 correspond respectively to the gluon and ghost square masses by replacing the renormalization prescriptions Eqs. (II.5.12), and (II.5.17) by

$$\Gamma_T(0) = m^2 \quad \text{and} \quad \Gamma_{c\bar{c}}(0) = \xi m^2. \tag{II.5.29}$$

This renormalization scheme is consistent with renormalizability. However, once RG improvement is taken into account a Landau pole develops thus spoiling the perturbative approach for low momentum scales. It was argued, first in the peculiar case of the Landau gauge [78] and then for finite ξ [99], that such a Landau pole is an artifact due to inconsistent renormalization prescriptions. Indeed, in this scheme, for small momenta, the one-loop gluon propagator is found to be a nonmonotonous function of the momentum while the two renormalization conditions Eq. (II.5.13) and Eq. (II.5.29), when imposed simultaneously, require that $G_T^{-1}(0) < G_T^{-1}(\mu)$. When RG improvement is turned on and a renormalized sliding scale $\mu = p$ is used, where p is the momentum scale at which we evaluate the correlators, the last inequality becomes inconsistent for small p with the one-loop behavior of the gluon propagator. Consequently, as the IR is probed deeper, larger RG corrections arise and, eventually, a Landau pole develops. In order to cope with this issue, it was proposed, in the Landau gauge, to use a renormalization scale of the form $\mu^2 = M^2 + p^2$, where M is a "freezing" scale. Performing such a running for the renormalization scale μ leads to RG corrections for momenta higher than M while these are frozen below and strict perturbation theory is then used, see [79]. Such a procedure is, in general, legitimate in massive theories where we expect the RG flow to freeze below the mass scale of the problem. However, as we shall see in the next section, due to the presence of massless excitations in the SUSY sector, see Eqs. (II.4.14), (II.4.16), the RG flow never freezes out in this case. This is to be put in contrast with the CF model ($n = 1$) where all modes are effectively massive for $\xi \neq 0$. Hence, such a freezing put by hand appears not justified in the ST case ($n \to 0$). We therefore do not present in details the zero-momentum scheme and refer the reader to [99].

II.5.4 Renormalization of the coupling constant

There remains to renormalize the coupling constant. We adopt the so-called Taylor scheme [116] which consists in fixing the value of Z_g, Eq. (II.4.25), from the ghost-antighost-gluon vertex at vanishing ghost momentum

$$\Gamma_{Ac\bar{c}}(p, 0, -p) = g \tag{II.5.30}$$

The Feynman diagrams contributing to $\Gamma_{Ac\bar{c}}$ at one-loop order are shown in Fig. II.6.

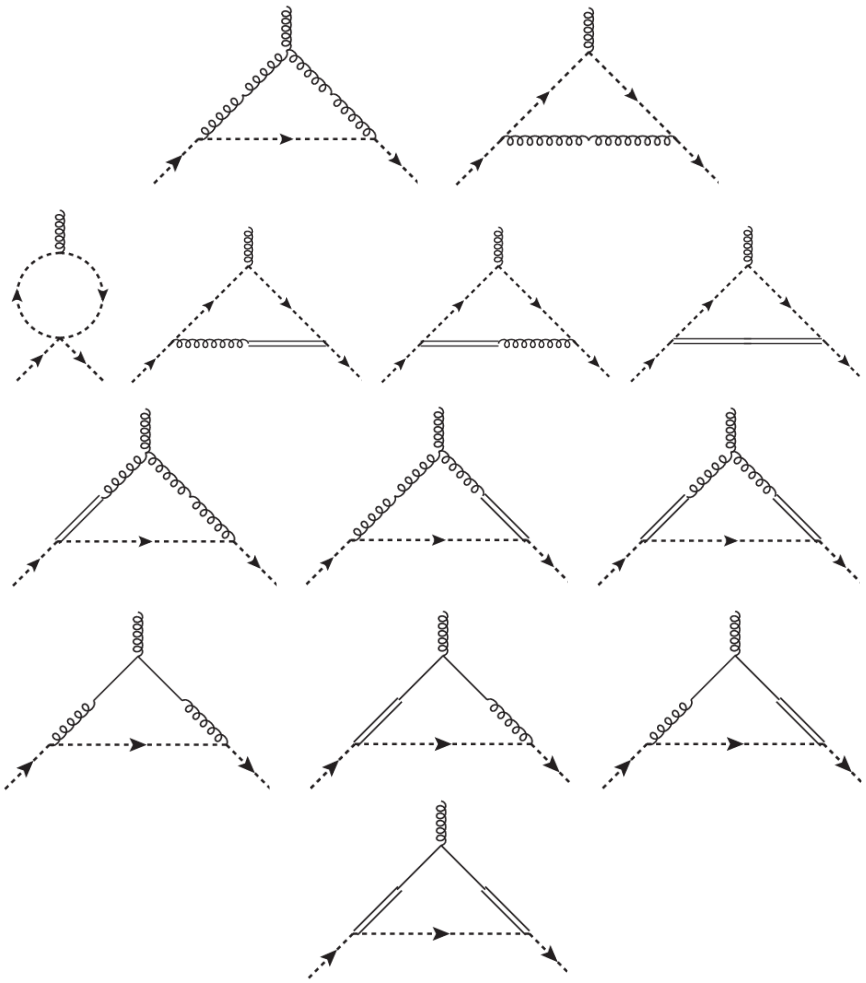

Figure II.6: One-loop contributions to the ghost-antighost-gluon vertex function $\Gamma_{Ac\bar{c}}$. The diagrams on the first line are present in the standard Landau gauge (but here with massive gluon and ghost propagators) and are proportional to the antighost external momentum. The topologies on the second and third lines are present in the standard CFDJ gauges and give contributions proportional to ξ_0. The replicated superfield sector only contributes in the diagrams of the last two lines.

The two usual YM diagrams (first line of Fig. II.6) involve, at the vertex where the external ghost leg is attached, a Lorentz contraction between a gluon propagator and the (internal) antighost momentum. For vanishing external ghost momentum, both the antighost and the gluon propagators in the loop carry the same momentum (up to a sign). It follows that only the longitudinal gluon propagator contributes to these diagrams, which are thus proportional to $\xi_0 \propto n\xi$ and vanish in the limit $n \to 0$. One can use the n power counting argument developed previously for the remaining diagrams. Inspection of the ST action (II.3.12) and of the tree-level bare propagators, Eq. (II.4.4) and Eqs. (II.4.11)-(II.4.16) yields that

- the $c\bar{c}c\bar{c}$ vertex counts for $\xi_0 \propto n$
- the $ihc\bar{c}$ vertex counts for $\xi_0 \propto n$
- the mixed correlator $\Lambda - A$ counts for $\xi_0 \propto n$
- the $ih - ih$ correlator counts for $\beta_0 \propto n^{-1}$

all other vertices or correlators involved in Fig. II.6 count for 0 power of n. Accordingly, the digram involving the $ih - ih$ correlator (last diagram of the second line of Fig. II.6) counts for $\xi_0^2 \beta_0 \propto n$. All the remaining diagrams count for either $\xi_0 \propto n$ or $\xi_0^2 \propto n^2$. Hereby, they all vanish in the $n \to 0$ limit. We conclude that the vertex $\Gamma_{Ac\bar{c}}(p, 0, -p)$ does not receive any radiative corrections at one-loop order in the limit $n \to 0$. The renormalization factors Z_g, Z_A and Z_c thus satisfy the relation

$$\lim_{n\to 0} Z_g Z_c \sqrt{Z_A} = 1, \tag{II.5.31}$$

which completely fixes the factor Z_g. In particular one has

$$\delta Z_g^{\text{div}} = -\frac{11}{6}\kappa. \tag{II.5.32}$$

It is worth mentioning that in the Landau gauge, the relation (II.5.31) holds for the divergent parts to all orders of perturbation theory [116]. We have only checked that this is so at one-loop order in the present case ($\xi \neq 0$). In particular, we do not know whether or not it is compatible with the renormalizability of the theory at higher orders. But, as in the case of the renormalization prescription (II.5.12), we can always impose the prescription Eq. (II.5.31) for the finite parts only.

The identity (II.5.31) is valid only in the limit $n \to 0$ with the definitions (II.5.4). It does not hold in the CF case ($n = 1$), where the contributions to the ghost-antighost-gluon vertex proportional to ξ_0 do not vanish. For the purpose of comparing the $n \to 0$ and $n = 1$ results, we employ a renormalization scheme for $n = 1$ as close as possible to that used for $n \to 0$, namely

$$Z_g Z_c Z_\xi^2 = Z_A^{3/2}, \tag{II.5.33}$$

valid for the divergent parts of the CF model [202].[15] As discussed above, we extend this equality to the finite parts, which gives us a definition of the renormalization coefficient Z_g in the CF model. It can be checked that this definition coincides with Eq. (II.5.31) in the limit $\xi \to 0$.

II.6 One-loop results

We present our results for the gluon and the ghost propagators at one-loop order in the SU(3) theory.[16] In the following, in strict perturbation theory where there is no running, we set the renormalization scale $\mu = 1$ GeV and we use the values of the

[15] The definition of the renormalization factor Z_ξ used here differs from that of [202].
[16] Results for SU(2) are qualitatively similar.

parameters m and g that provide the best fits to the lattice results in the Landau gauge in [79], that is, $m = 0.39$ GeV and $g = 3.7$ in the infrared-safe scheme. Notice that the relevant expansion parameter is $3g^2/(16\pi^2) \lesssim 1$. We have no reason, *a priori*, to exclude a dependence of the parameters m and g at a certain scale with the value of ξ at the same scale. Such dependences would have to be inferred from fits to lattice data. In the absence of such data, we assume fixed values of m and g adjusted from lattice data at $\xi = 0$.

II.6.1 Gluon and ghost sectors

The ghost and the transverse gluon propagators in the infrared-safe scheme are shown in Fig. II.7.

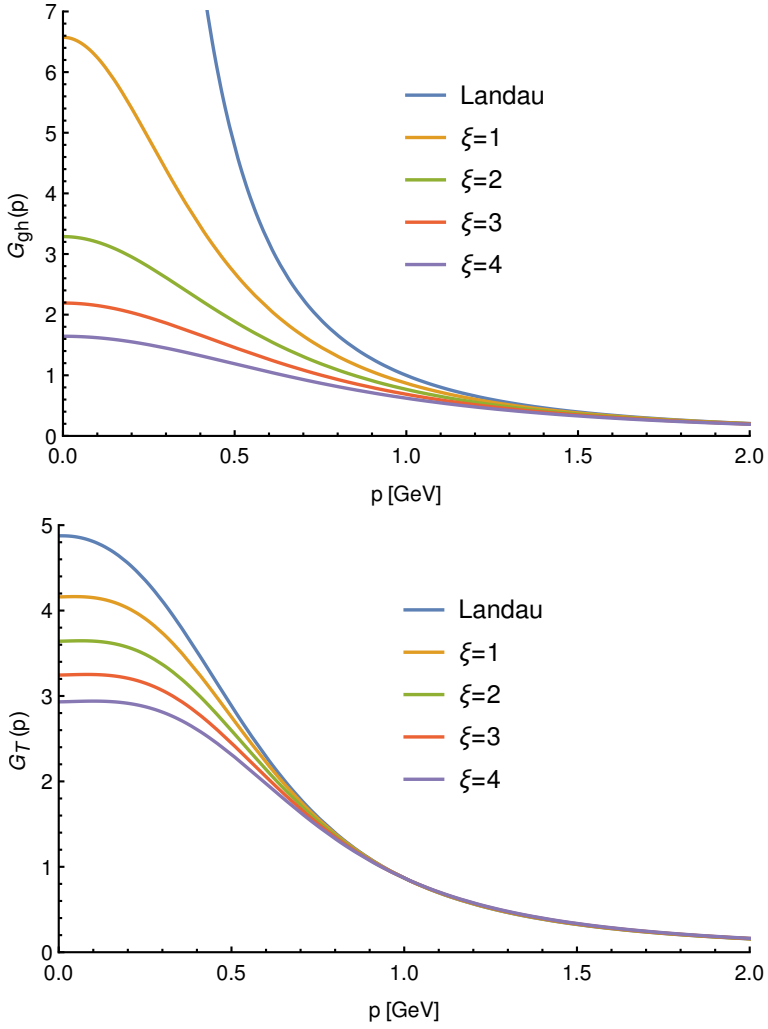

Figure II.7: The ghost (top) and the transverse gluon (bottom) propagator as a function of momentum for various values of ξ in the infrared-safe renormalization scheme with $m = 0.39$ GeV and $g = 3.7$.

We check that we recover the results of [79] (in the appropriate renormalization scheme) for $\xi = 0$. In particular, we observe that the ghost propagator develops a zero-momentum pole as $\xi \to 0$. For higher values of ξ, the ghost propagator is very similar to the one obtained in the CF model ($n = 1$); see Fig. II.8. This is expected for one-loop order results. Indeed all the diagrams contributing to the one-loop ghost propagator (see Fig. II.2) are present in the CF model. In particular there is no contribution from the replica sector at this order. Moreover, one can easily show that the three diagrams involving the ih fields (last three diagrams of Fig. II.2) cancel each other. The ghost tadpole is the same in both $n \to 0$ and $n = 1$ cases. So that eventually the only difference comes from the absence ($n \to 0$) or presence ($n = 1$) of the internal longitudinal gluon propagator in the sunset diagram of Fig. II.2.

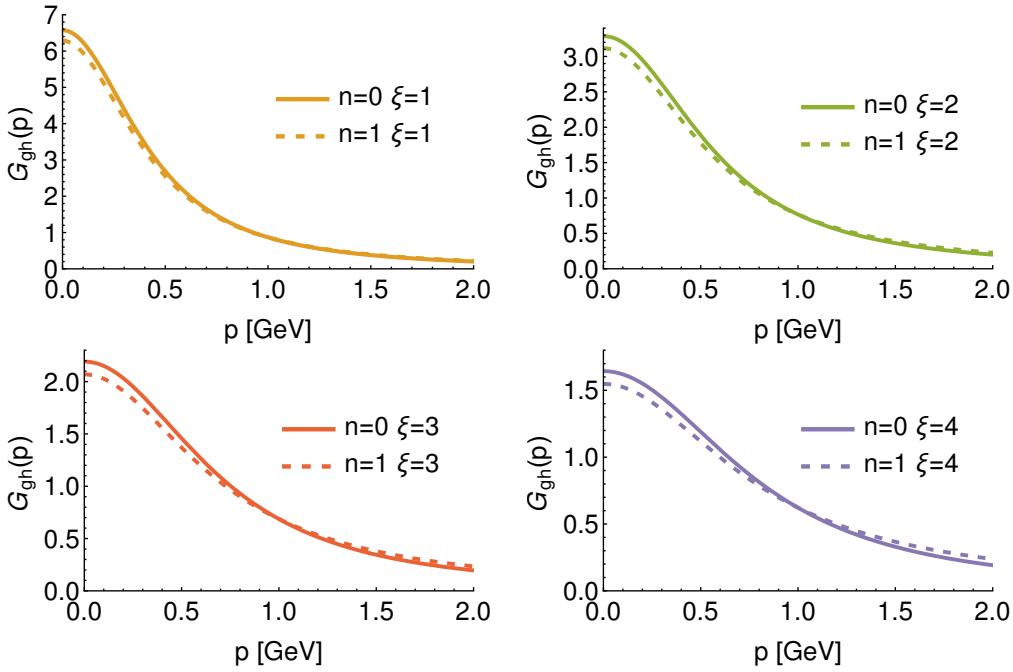

Figure II.8: The ghost propagator computed in either the present gauge fixing ($n \to 0$) or the CF model ($n = 1$) in the infrared-safe scheme with $m = 0.39$ GeV and $g = 3.7$ for various values of ξ.

The value of the gluon propagator at vanishing momentum is not fixed and varies strongly with ξ. This can be traced to the fact that the zero-momentum value of the gluon propagator is not fixed by the renormalization prescriptions Eqs.(II.5.13)-(II.5.17), but instead admit an implicit ξ-dependence through the second equation in Eq. (II.5.12). This has to be put in regards with our previous comment at the end of Sec. II.5.2, see (II.5.24). We observe that the approach to the $p = 0$ value flattens as ξ is increased. This appears to be a consequence of our treatment of the Gribov copies, see e.g. the discussion above (II.5.8). Indeed, a comparison of the transverse gluon propagator computed in the present gauge-fixed theory ($n \to 0$) and in the CF model ($n = 1$) is shown in Fig. II.9. The CF model does not display the flattening as p approaches zero. This effect is more important for increasing ξ, which is consistent with

the fact the cases $n \to 0$ and $n = 1$ are equivalent in the Landau gauge. Equivalently, in the gluon sector, the difference between both cases comes from the superfield sector which decouples for $\xi = 0$.

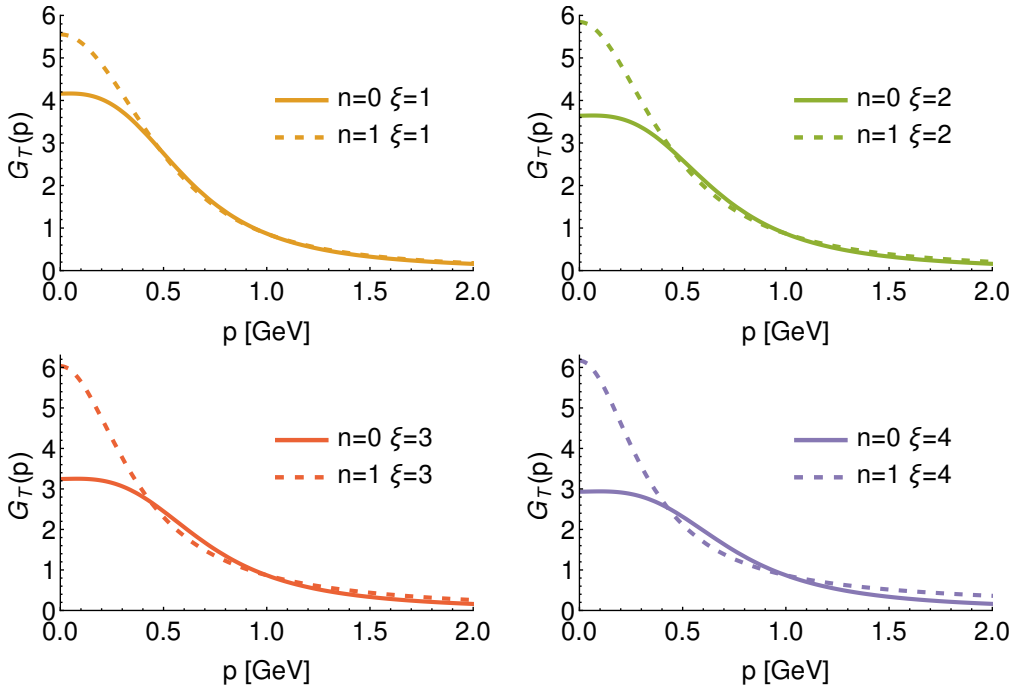

Figure II.9: The transverse gluon propagator computed in either the present gauge fixing ($n \to 0$) or the CF model ($n = 1$) in the infrared-safe scheme with $m = 0.39$ GeV and $g = 3.7$ for various values of ξ.

We notice also that in the CF case, the gluon propagator also presents a longitudinal part, which for completeness is displayed in Fig. II.10 (while it is identically null for $n \to 0$).

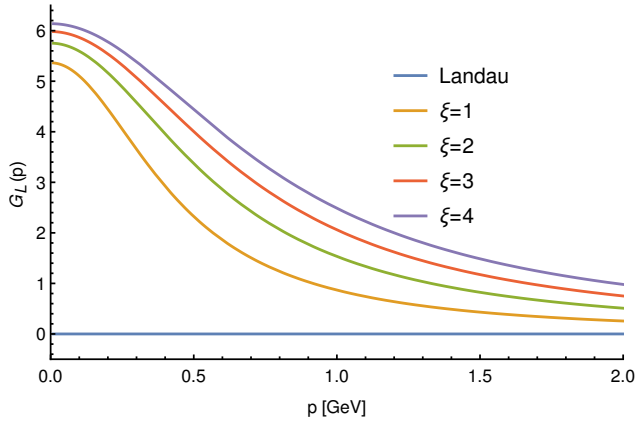

Figure II.10: The longitudinal gluon propagator in the CF model ($n = 1$) as a function of momentum for various values of ξ in the infrared-safe scheme.

It is worth mentioning that the transverse gluon propagator presents a nonmonotonous behavior at small momenta (though the effect is too small to be observed on Fig. II.7 with the scale used) and hence displays a violation of positivity, see Sec. I.2.3. The same analysis was performed in the zero-momentum renormalization scheme and can be found in [99].

II.6.2 Replica sector

We now move to the the replica sector. Notice that, the meaning of this sector in the limit $n \to 0$ is somewhat unclear. Nevertheless, we present here our results for completeness. As emphasized earlier, there are massless excitations in the replica sector even for $\xi \neq 0$. They correspond to the λ_k fields present in the SUSY representation Eq. (II.4.57) that we recall here for simplicity:

$$\Lambda_k = \lambda_k + \bar{\theta} c'_k + \bar{c}'_k \theta + \bar{\theta}\theta \hat{h}'_k \,. \tag{II.6.1}$$

Notice that the mass dimension of λ_k is zero. It turns out convenient to rescale it prior to the $n \to 0$ limit

$$\tilde{\lambda}_k = \sqrt{\frac{m^2}{n}} \lambda_k, \tag{II.6.2}$$

in such a way that $\tilde{\lambda}_k$ has canonical mass dimension. This is discussed in details in Appendix E. We define the $\tilde{\lambda} - \tilde{\lambda}$ propagator[17] as

$$\begin{aligned} G^{\tilde{\lambda}}_{kl}(p) &= \lim_{n\to 0} \left[\tilde{\lambda}_k(-p)\tilde{\lambda}_l(p)\right]_0 \\ &= \delta_{kl} G_{\text{diag}}(p) + (1-\delta_{kl}) G_{\text{non diag}}(p). \end{aligned} \tag{II.6.3}$$

At tree-level, Eq. (II.4.51), we have that

$$G_{\text{diag}}(p) = 2G_{\text{non diag}}(p) = \frac{2m^2\xi}{p^2\,(p^2+m^2\xi)} \,. \tag{II.6.4}$$

Since there are massless excitations, we accordingly define the $\tilde{\lambda} - \tilde{\lambda}$ dressing function

$$\begin{aligned} F_{\text{diag}}(p) &= \frac{p^2}{2m^2\xi} G_{\text{diag}}(p), \\ F_{\text{non diag}}(p) &= \frac{p^2}{m^2\xi} G_{\text{non diag}}(p). \end{aligned} \tag{II.6.5}$$

On Fig. II.11 we display the (diagonal) one-loop $\tilde{\lambda} - \tilde{\lambda}$ dressing function. Remark that the correlator $\tilde{\lambda}_k - \tilde{\lambda}_l$ is identically null[18] for $\xi = 0$ (see also Eq. (II.4.51)), though its dressing function, seen as a continuous function of the parameter ξ, admits a nontrivial limit for $\xi \to 0$. In particular, in this limit, the $\tilde{\lambda} - \tilde{\lambda}$ dressing function develops a zero-momentum pole. Notice that the tree-level property (II.6.4), namely

[17] We extract everywhere a trivial unit color matrix.

[18] Indeed, the correlator $\tilde{\lambda} - \tilde{\lambda}$ is given by the $\underline{\theta}_k$, $\underline{\theta}_l$ independent part of the correlator $[\Lambda_k \Lambda_l]$ (see Appendix E and Eq. (E.0.2) for instance) while the SUSY sector becomes ultra-local ($\propto \delta\left(\underline{\tilde{\theta}}_k, \underline{\tilde{\theta}}_l\right)$) in the Landau gauge.

that $F_{\rm diag}(p)/F_{\rm non\,diag}(p) = 1$ is observed to remain true at one-loop order. The zero momentum value is quite sensitive to the value of ξ. This is due to the presence in $F_{\rm diag}$ of the tree-level square mass $m^2\xi$. In order to get rid of this somehow artificial ξ dependence, it is interesting to compare $F_{\rm diag}$ to its tree-level value in order to focus on loop effects. On Fig. II.12 is shown the difference $F^{-1}_{\rm diag}(p)-(p^2+m^2\xi)$. The apparently crossing point between the various curves is actually an artifact of our choices of ξ that are close to one another, while for higher or lower values they do not cross all at the same point. As we see on Fig. II.12, the loop contributions are actually negatives for small momenta and increase with ξ. Hereby, there is a competition between loop

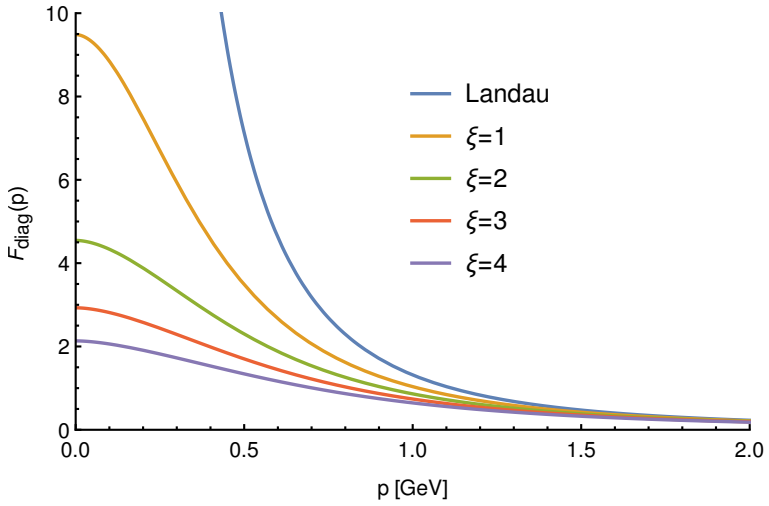

Figure II.11: The diagonal $\tilde{\lambda}-\tilde{\lambda}$ dressing function $F_{\rm diag}$ as a function of momentum for various values of ξ in the infrared-safe scheme. It is divergent at zero-momentum in the Landau gauge.

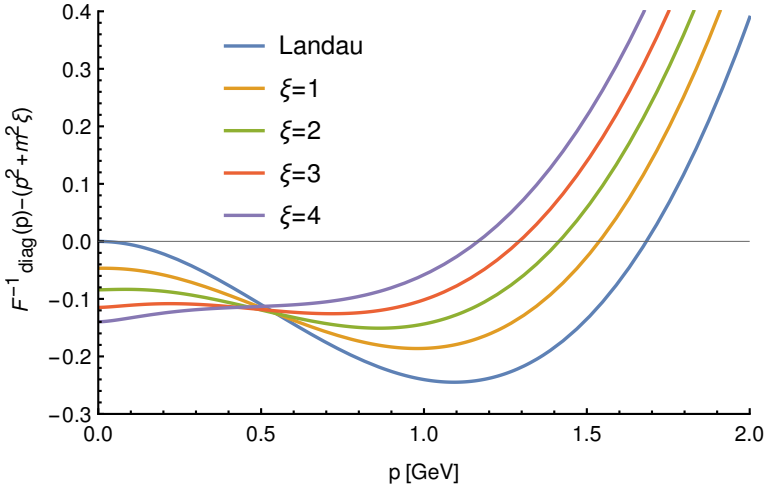

Figure II.12: Comparison of $F^{-1}_{\rm diag}$ with its tree-level value as a function of momentum for various values of ξ in the infrared-safe scheme.

and tree-level effects. In general, this is a dangerous situation for the perturbative approach since it might result in a pole if loop effects become too large. However, for the range of parameters considered here we do not encounter such a pole at finite momenta. The zero momentum pole in the Landau gauge is already present at tree-level, see Eq. (II.4.51), as confirmed in Fig. II.12 where the Landau gauge $\tilde{\lambda}-\tilde{\lambda}$ dressing function does not receive loop corrections at zero momentum.

Notice also that the SUSY sector contains replicated ghost and antighost fields c'_k and $\bar{c}'_k$, see Eq. (II.6.1). Ghost correlators of two different replicas k and l are obviously equal due to the replica permutation symmetry, while the relation between the correlators of replicated and non-replicated ghosts is less obvious. On Fig. II.13 is shown the ratio $G_{\rm gh}(p)/G^k_{\rm gh}(p)$ where $G^k_{\rm gh}(p)$ is the propagator of the replicated ghosts. Both coincide in the Landau gauge while this is not so for $\xi \neq 0$. Remark already that, the replicated ghost correlator is not null in the Landau gauge. This stresses that, although in the Landau gauge the replica sector decouples from the ghost and gluon sectors, it remains nontrivial. The difference mentioned above is due to the fact that the non-replicated ghost fields correspond to the replica that was singled out in the gauge-fixing procedure. Moreover, let us recall that the replicated c'_k and $\bar{c}'_k$ fields that appear in the decomposition Eq. (II.6.1) differ from the c_k and $\bar{c}_k$ fields appearing in the non-SUSY version of the ST action, see Sec. II.4.4. Both sets are related in perturbation theory by the relations Eq. (II.4.58) that we recall here

$$c'_k = c_k + \frac{ig_0}{2}[c_k,\lambda_k] - \frac{g_0^2}{12}[[c_k,\lambda_k],\lambda_k] + \dots , \tag{II.6.6}$$

$$\bar{c}'_k = \bar{c}_k + \frac{ig_0}{2}[\bar{c}_k,\lambda_k] - \frac{g_0^2}{12}[[\bar{c}_k,\lambda_k],\lambda_k] + \dots . \tag{II.6.7}$$

One-loop calculations in the non-SUSY version of the theory showed that $[c(-p)\,\bar{c}(p)]_0 = [c_k(-p)\,\bar{c}_k(p)]_0$ for arbitrary ξ as expected from the replica symmetry which simply reduces to the relabeling $c \leftrightarrow c_k$, $\bar{c} \leftrightarrow \bar{c}_k$ in the ghost sector. Turning back to the c'_k, $\bar{c}'_k$ case, using the relations (II.6.6), (II.6.7) and Wick theorem, we get at one-loop order (for simplicity we work in direct space)

$$\begin{aligned}\left[c'^a_k(x)\,\bar{c}'^b_k(y)\right]_0 = \left[c^a(x)\,\bar{c}^b(y)\right]_0 - \frac{g^2}{2}\frac{m^2}{n}\Big\{ & f^{acd}f^{buv}\,[c^u(x)\bar{c}^c(y)]_0\left[\tilde{\lambda}^v_k(x)\tilde{\lambda}^d_k(y)\right]_0 \\ & + \frac{1}{6}f^{bce}f^{edu}\,[c^a(x)\bar{c}^u(y)]_0\left[\tilde{\lambda}^c_k(y)\tilde{\lambda}^d_k(y)\right]_0 \\ & + \frac{1}{6}f^{ace}f^{edu}\left[c^u(x)\bar{c}^b(y)\right]_0\left[\tilde{\lambda}^c_k(x)\tilde{\lambda}^d_k(x)\right]_0\Big\} ,\end{aligned} \tag{II.6.8}$$

where we used that $[c(x)\,\bar{c}(y)]_0 = [c_k(x)\,\bar{c}_k(y)]_0$. The first line corresponds to a sunset diagram with one ghost and one $\tilde{\lambda}-\tilde{\lambda}$ propagators. The two last lines of Eq. (II.6.8) correspond to one ghost propagator to which is attached at one edge a $\tilde{\lambda}-\tilde{\lambda}$ tadpole. We saw previously, in discussing the $\tilde{\lambda}-\tilde{\lambda}$ correlator, that it actually vanishes identically in the Landau gauge so that for $\xi = 0$ we have $\left[c'^a_k(-p)\,\bar{c}'^b_k(p)\right]_0 = \left[c^a(-p)\,\bar{c}^b(p)\right]_0$ as observed on Fig. II.13.

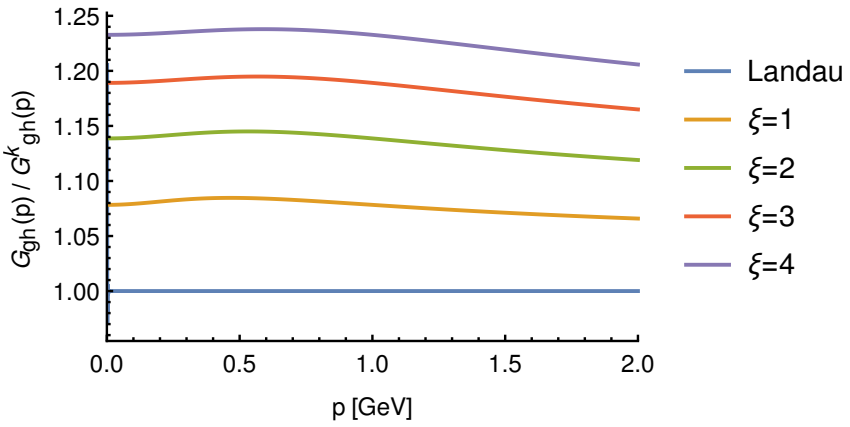

Figure II.13: Comparison of the replicated ghost propagator $G^k_{\rm gh}(p)$ to the non-replicated one $G_{\rm gh}(p)$ a function of momentum for various values of ξ in the infrared-safe scheme. Both coincide in the Landau gauge.

II.7 Renormalization-group analysis

We now perform the RG analysis. One of the main strength of the ST approach in the Landau gauge, is that, perturbation theory is justified down to zero momentum thanks to IR safe RG trajectories as opposed to the standard FP case. Therefore, investigation of such possible RG flows also at $\xi \neq 0$ seems crucial to us and necessary to justify the previous perturbative calculations. Moreover, the ST approach relies on taking into account the Gribov copies. Henceforth, it is interesting to investigate whether the copies affect the UV sector or not as it is the common belief.

In the following, we define the RG beta functions β_α for the parameters $\alpha = m^2, g, \xi$ as

$$\beta_\alpha = \left.\frac{d\,\alpha}{d\ln\mu}\right|_0 = -\alpha \left.\frac{d\ln Z_\alpha}{d\ln\mu}\right|_0 , \tag{II.7.1}$$

as well as the anomalous dimension for the various fields Φ

$$\gamma_\Phi = \left.\frac{d\ln Z_\Phi}{d\ln\mu}\right|_0 , \tag{II.7.2}$$

where the subscript 0 means that the right-hand side is evaluated at fixed bare quantities.

II.7.1 UV behavior

Let us first briefly consider the high energy limit. In this regime, we can simply use the $\overline{\rm MS}$ scheme in which the beta functions are straightforwardly obtained from the divergent parts of the renormalization constants Z_g, Z_{m^2} and Z_ξ. We note that, this UV behavior is insensitive to the details of the renormalization prescriptions used since it depends only on the divergent parts. In particular, we recover the universal

one-loop beta function for the coupling constant

$$\beta_g^{\mathrm{UV}} = -g\frac{11}{6}\frac{g^2N}{8\pi^2}, \tag{II.7.3}$$

so that asymptotic freedom is preserved (as it should). Remark that for our (perturbative) proof of renormanilazability to be meaningful, an asymptotically UV free theory is necessary. According to Eq. (II.5.20) the beta function of the mass parameter m^2 is

$$\beta_{m^2}^{\mathrm{UV}} = -m^2\frac{35}{12}\frac{g^2N}{8\pi^2}, \tag{II.7.4}$$

and, therefore, m vanishes at high energies. We remark also that UV flows of both g and m are identical to those of the Landau gauge. The beta function for ξ reads

$$\beta_\xi^{\mathrm{UV}} = \xi\frac{13}{6}\frac{g^2N}{8\pi^2}, \tag{II.7.5}$$

hence, the Landau gauge is an unstable UV fixed point. We also define the ghost (or auxiliary) square mass parameter m_{gh}^2 as

$$m_{\mathrm{gh}}^2(\mu) = m^2(\mu)\xi(\mu). \tag{II.7.6}$$

Its beta function is straightforwardly obtained from those of ξ and m^2 and reads, in the UV, as

$$\beta_{m_{\mathrm{gh}}^2}^{\mathrm{UV}} = -m_{\mathrm{gh}}^2\frac{3}{4}\frac{g^2N}{8\pi^2}, \tag{II.7.7}$$

so that m_{gh}^2 also vanishes at high energies. We thus finally recover a massless theory in the high energy regime. Moreover, in this regime, the ghost and gluon propagators follow the standard one-loop behavior [99]

$$G_{\mathrm{gh}}^{\mathrm{UV}}(p) \propto \frac{1}{p^2}\left[1+\frac{11Ng^2(\mu_*)}{48\pi^2}\ln\left(\frac{p^2}{\mu_*^2}\right)\right]^{-\frac{9}{44}} \tag{II.7.8}$$

$$G_T^{\mathrm{UV}}(p) \propto \frac{1}{p^2}\left[1+\frac{11Ng^2(\mu_*)}{48\pi^2}\ln\left(\frac{p^2}{\mu_*^2}\right)\right]^{-\frac{13}{22}}, \tag{II.7.9}$$

where μ_* and p are UV scales, that is, $\mu_*, p \gg m, m_{\mathrm{gh}}$. Remark, however, that these results are independent of ξ, and hence we do not recover exactly the FP case (in particular there is no longitudinal gluon propagator in the present case). Note that this is a consequence of the n-dependent renormalization scheme (II.5.4) employed here. Indeed, following a renormalization scheme as in (II.4.25), we then recover the standard FP theory in the UV from a $\overline{\mathrm{MS}}$ scheme, see Eqs (II.4.39), (II.4.40).

II.7.2 Renormalization group flows

We now investigate the RG flows down to the deep IR regime in the infrared-safe renormalization scheme. Explicit expressions of the beta functions and anomalous dimensions are gathered in the supplemental material (Mathematica file) of [99], see

Ref. [51] of it. Note that, the prescription (II.5.31) implies at one-loop order that the ghost anomalous dimension is given by

$$\gamma_c = \left.\frac{d\ln Z_c}{d\ln\mu}\right|_0 = -\frac{1}{2}\gamma_A + \frac{\beta_g}{g}. \tag{II.7.10}$$

For later use, we also mention that Eq. (II.5.27) yields

$$\gamma_A = -\frac{\beta_\xi}{\xi}, \tag{II.7.11}$$

We integrate numerically the flow equations Eqs. (II.7.1), (II.7.2) with initial conditions at the scale $\mu_0 = 1$ GeV. We use as initial conditions the values of the mass and coupling parameters of the previous section, namely $m(\mu_0) = 0.39$ GeV and $g(\mu_0) = 3.7$, and we vary the gauge-fixing parameter $\xi(\mu_0)$. We find that the infrared-safe RG flows can be integrated down to arbitrarily small scales μ without encountering a Landau pole, depending on the choice of initial conditions[19], as it was first pointed out in [79, 74] in the case $\xi = 0$.

Figure II.14 and II.15 show the RG flows of the parameters g, m and ξ for various values of $\xi(\mu_0)$. We observe that both the coupling and the mass first increase for decreasing μ and then are attracted towards zero in the IR. We also see that the maximal values of both parameters decrease with increasing $\xi(\mu_0)$ and are, therefore, maximal in the Landau gauge. In all cases we have considered, the coupling remains small enough for perturbation theory to be (qualitatively) meaningful: we recall that the relevant expansion parameter is $3g^2/(16\pi^2)$. We thus expect that our perturbative calculations would provide even more agreements with lattice data (if lattice implementation is possible) in the present case than in the Landau gauge. Finally, we observe that the gauge-fixing parameter ξ is first attracted towards zero as μ decreases but eventually diverges in the limit $\mu \to 0$. In particular, we find that the Landau gauge fixed point ($\xi = 0$) is unstable in the IR.

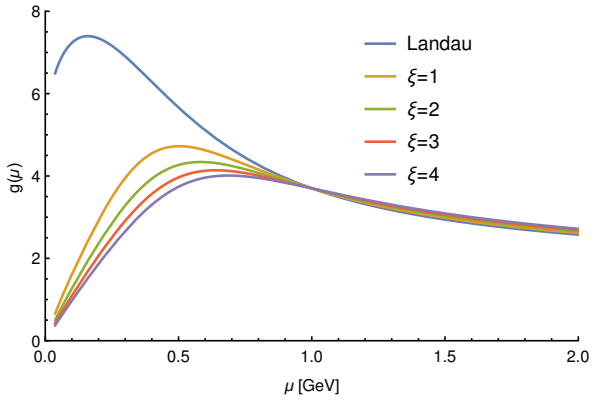

Figure II.14: Running of the parameter $g(\mu)$ in the infrared-safe scheme, for various values of $\xi(\mu_0) \equiv \xi$.

[19] For instance, it is clear that in the case $m(\mu_0) = \xi(\mu_0) = 0$ (which implies $m(\mu) = \xi(\mu) = 0$ for all μ and thus corresponds to the standard FP Landau gauge) one gets a Landau pole.

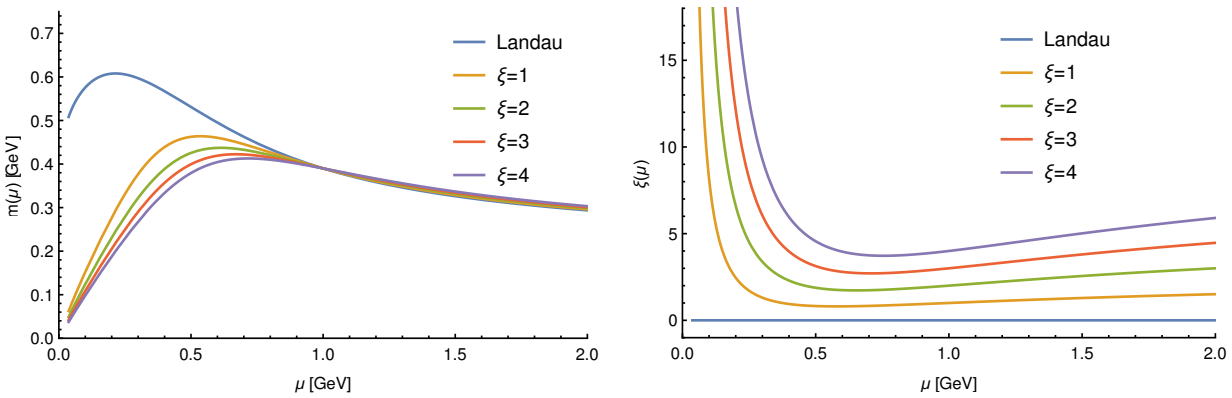

Figure II.15: Running of the parameters $m(\mu)$ and $\xi(\mu)$ in the infrared-safe scheme, for various values of $\xi(\mu_0) \equiv \xi$.

It is interesting to check the running of the ghost mass parameter $m_{\rm gh}(\mu)$ shown in Fig. II.16, which is attracted towards a nontrivial fixed point in the IR so that $\xi(\mu) \sim 1/m^2(\mu)$ when $\mu \to 0$. The product $\xi(\mu)g^2(\mu)$ (right panel of Fig. II.16) is also attracted toward a nontrivial fixed point as $\mu \to 0$ such that $\xi(\mu) \sim 1/m^2(\mu) \sim 1/g^2(\mu)$ in this regime. This illustrates a key difference between the Landau gauge and the present case. Indeed, according to the flows of Fig. II.15 (see also [79]), in the Landau gauge, the gluon effective IR action corresponds to the (trivial) massless free Gaussian theory while, for $\xi \neq 0$, gluons remain coupled to the replica sector through the effective coupling constant $\xi(\mu)g^2(\mu)$. In the latter case, the IR effective theory thus remains nontrivial.

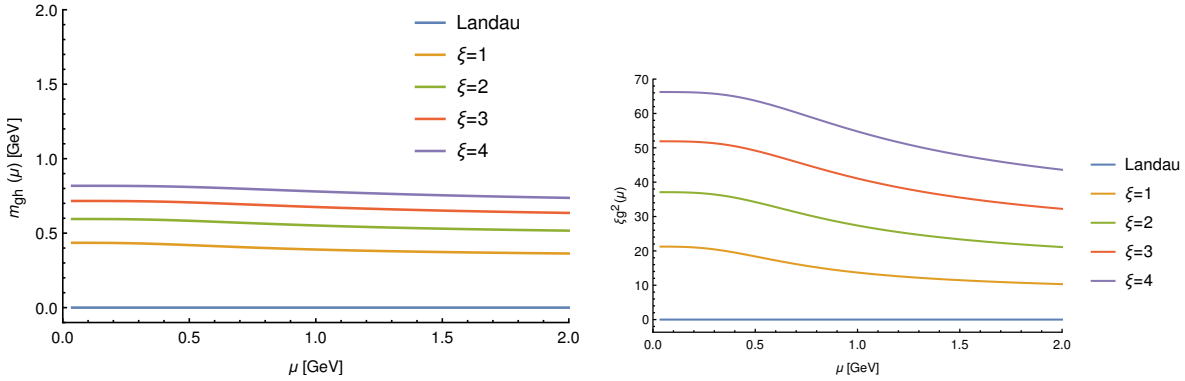

Figure II.16: Left panel: Running of the ghost mass parameter $m_{\rm gh}(\mu) = m(\mu)\sqrt{\xi(\mu)}$ in the infrared-safe scheme, for various values of $\xi(\mu_0) \equiv \xi$. Right panel: Running of the product $\xi(\mu)g^2(\mu)$ in the infrared-safe scheme, for various values of $\xi(\mu_0) \equiv \xi$. Remark that we have $3\xi(\mu)g^2(\mu)/16\pi^2 \lesssim 1$.

We remark that, as emphasized in Sec. II.5.3, the RG flows of the independent parameters g and m never freeze out because of the presence of massless excitations. Therefore, a possible freezing of the RG flow put by hand (as proposed for the zero-momentum scheme) does not seem justified for $\xi(\mu_0) \neq 0$. This is a peculiar feature of

the present theory and, more precisely, of the way Gribov copies are handled since the remaining massless modes are present only in the superfield sector as seen in Fig. II.11. Indeed, things are different in the CF model ($n = 1$) in which the SUSY sector is absent. We observe that the RG flow freezes below a certain scale, see Fig. II.17. This is to be

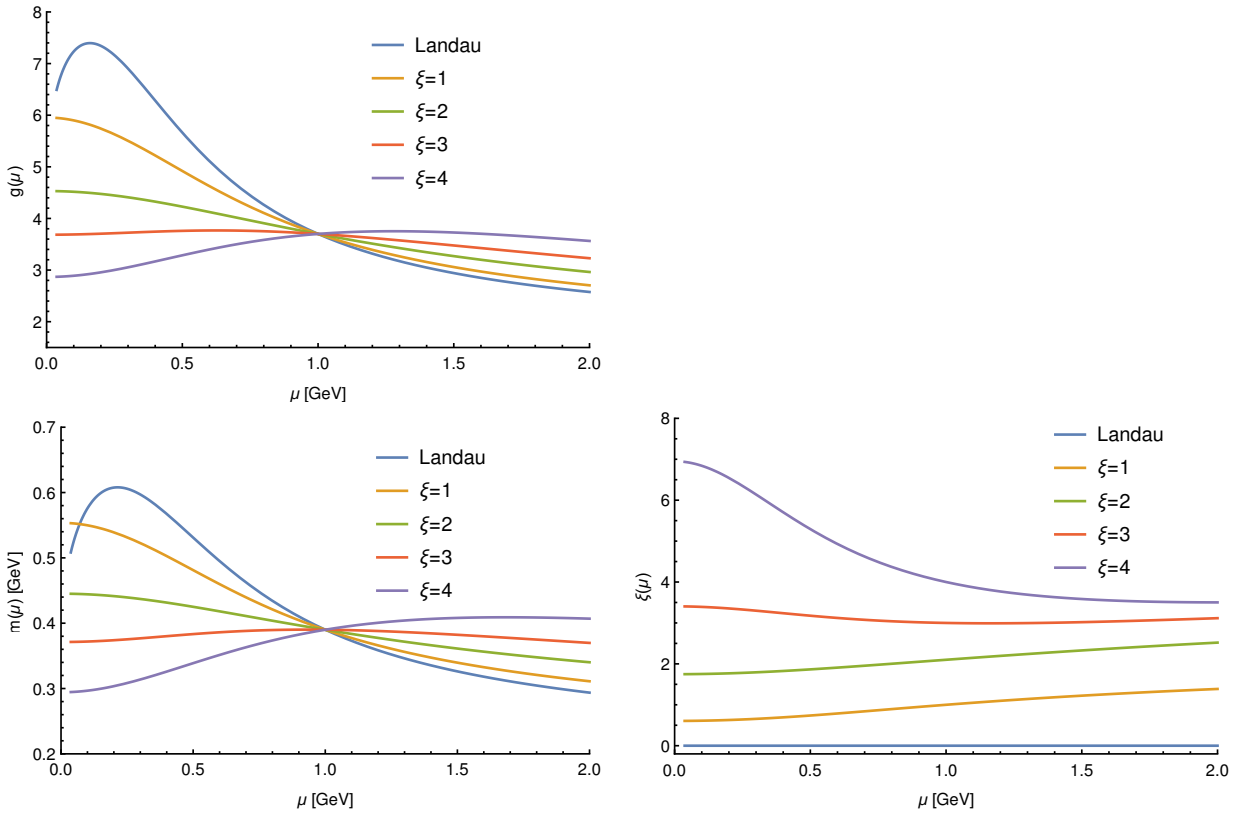

Figure II.17: The RG flow of the parameters $g(\mu)$, $m(\mu)$, and $\xi(\mu)$ in the CF model ($n = 1$) with the infrared-safe scheme.

expected since, for $\xi(\mu_0) \neq 0$, the CF model only contains massive degrees of freedom that decouple in the deep IR. On the contrary, in the Landau gauge where the ghosts are massless, the CF model is equivalent to the case $n \to 0$, as already discussed, and we see that the RG flow does not freeze. As a consequence of the RG freezing for $\xi(\mu_0) \neq 0$, the coupling and mass parameters g and m do not vanish in the IR and the gauge-fixing parameter ξ does not diverge. All the parameters reach constant values. We mention that the renormalized coupling constant is defined differently in both cases. For $n \to 0$ we used Eq. (II.5.31), which is not valid for $n = 1$ and was replaced by Eq. (II.5.33). This difference might influence the RG flows. Nevertheless, the infrared-safety of this renormalization scheme in the CF model is also verified, and the flows can be integrated down to zero momentum.

II.7.3 RG-improved ghost and gluon propagators

Notice that, although for $n \to 0$ the mass parameter $m(\mu)$ is attracted towards zero, it does not imply that gluons become effectively massless in the IR. Indeed, in the infrared-safe scheme, the renormalized mass parameter m is defined through Eq. (II.5.13) and does not correspond to the actual gluon mass. The latter is, instead, given by Eq. (II.5.24). The same remark can be made for the ghosts (apart from the Landau gauge). Indeed, these propagators do not diverge as $p \to 0$ (exect for the ghost propagator in the Landau gauge), as observed on Fig. II.18 where it is displayed the RG-improved ghost and (transverse) gluon propagators for the $n \to 0$ case. We used for the RG scale $\mu = p$. We explicitly verify on Fig. II.18 that the ghost propagator at

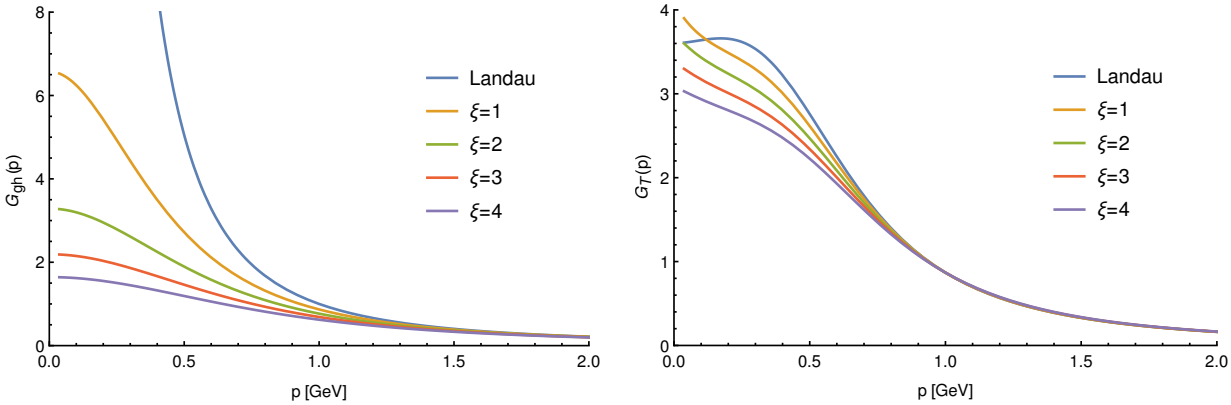

Figure II.18: RG-improved ghost (left) and transverse gluon (right) propagators as functions of momentum in the infrared-safe scheme with $\mu = p$, for various values of $\xi(\mu_0) \equiv \xi$.

zero momentum does not receive any RG correction, namely

$$G_{\rm gh}(0) = \frac{1}{m^2_{\rm gh}(\mu_0)}, \tag{II.7.12}$$

as expected from the nonrenormalization relation (II.5.11).

In the gluon sector, however, we observe strong differences between the RG-improved propagator and the one obtained in strict perturbation theory, see Fig. II.7. In particular, for $\xi \neq 0$ the flattening near $p = 0$ observed earlier is turned into a linear behavior. This is a consequence of the equality (II.7.11) which yields, for $\mu = p$

$$G_T(p) = \frac{\xi(\mu_0)}{\xi(p)} \frac{1}{p^2 + m^2(p)}, \tag{II.7.13}$$

which rewrites as

$$G_T(p) = \frac{\xi(\mu_0)}{m^2_{\rm gh}(p)} \frac{\tilde{m}^2(p)}{1 + \tilde{m}^2(p)}, \tag{II.7.14}$$

where we have defined the dimensionless mass parameter $\tilde{m}(\mu) = m(\mu)/\mu$. The fact that the ghost mass parameter (II.7.6) reaches a plateau for sufficiently small μ and not too small $\xi(\mu_0)$ implies that the $p \to 0$ behavior of the gluon propagator is governed

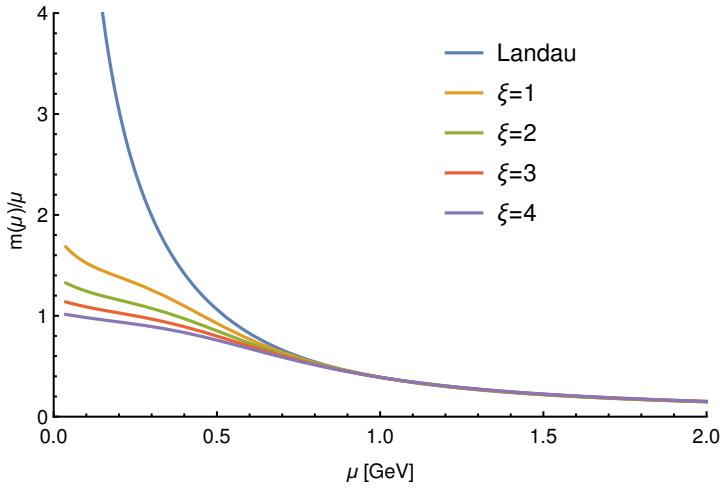

Figure II.19: Running of the dimensionless mass parameter $\tilde{m}(\mu) = m(\mu)/\mu$ in the infrared-safe scheme, for various values of $\xi(\mu_0) \equiv \xi$.

by the function $\tilde{m}^2(p)/[1+\tilde{m}^2(p)]$, a monotonously increasing function of $\tilde{m}^2(p)$. The running of the latter is shown in Fig. II.19, where we observe that it is a monotonously decreasing function of p and that, for $\xi(\mu_0)$ not too small, it reaches an IR fixed point, which is approached linearly. We conclude that, for $\xi(\mu_0)$ not too small,

$$G_T(p \to 0) = \frac{\xi(\mu_0)}{m_{\rm gh}^2(0)} \frac{\tilde{m}^2(0)}{1+\tilde{m}^2(0)} \left[1 + \mathcal{O}(p)\right], \tag{II.7.15}$$

where the linear term in p is negative.

This peculiar behavior for $\xi(\mu_0) \neq 0$ in the $n \to 0$ case is to be put in regard with the one observed in the case of the CF model[20] ($n = 1$) displayed on Fig. II.20. The RG-improved ghost and gluon propagators for the CF model present little change as compared to the results from strict perturbation theory (Figs. II.8 – II.10), for ξ not too small, despite the relatively important change of the running parameters in the range of momenta considered here. RG corrections seem more important for small ξ. This is to be expected since as ξ gets smaller the CF results come closer (and eventually coincide) with those of the $n \to 0$ case where RG corrections are important. Alternatively, as ξ decreases, the masses of the auxiliary modes get smaller so that the scale below which the RG is frozen is reduced. Nevertheless, the RG-improved results in the CF model are dramatically different from those of the theory considered here ($n \to 0$), in particular for the gluon sector. Although these qualitative differences might have diverse origins, such as, for instance, the difference in the definition of the coupling constant, altogether they illustrate the important role played by the replica sector of the theory and, in turn, by the Gribov copies, particularly in the IR.

[20] We recall that, in the CF model, our prescription for the renormalized coupling constant is given by Eq. (II.5.33).

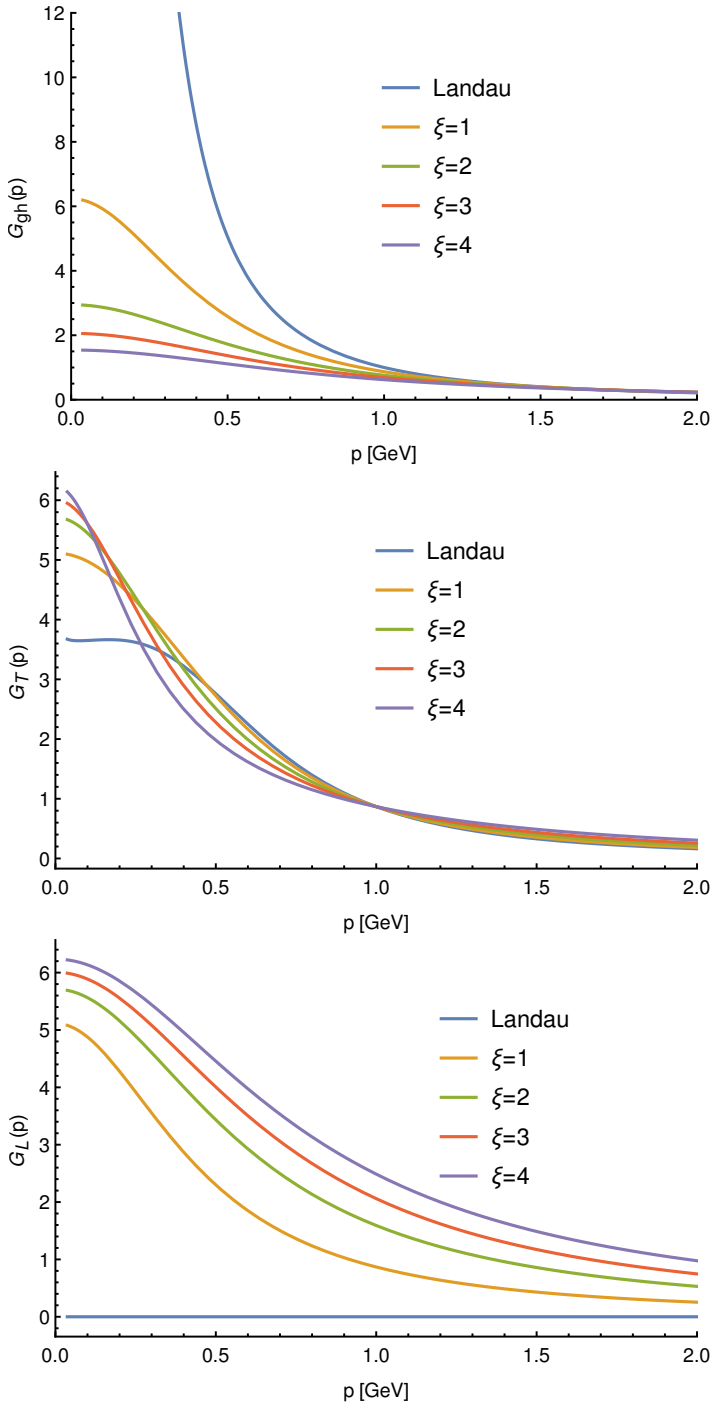

Figure II.20: The RG-improved ghost and gluon propagators in the CF model ($n = 1$) with the infrared-safe scheme.

II.7.4 Correlation among Gribov copies

So far, we were mainly interested in the ghost and gluon sectors while the SUSY sector encodes our treatment of Gribov copies. However, the computation of this sector was mandatory in order to perform the $n \to 0$ limit since the two-point vertex functions Γ_1, Γ_3, Γ_4 (see (II.4.9)) appear in the definition of the longitudinal gluon propagator (see Eq. (II.5.3)), or for the computation of the renormalization factor Z_Λ needed to compute the RG flows for instance. Still, the relationship between the superfields Λ, or more precisely the scalar λ fields, with the Gribov copies remains somewhat unclear. This makes possible interpretations of the λ sector uneasy. In particular, once the limit $n \to 0$ has been performed, it is not clear what meaning should be granted to the replica sector.[21] Moreover, this sector is, *a priori*, not accessible in (would be) lattice simulations.[22] All in all, this suggests that attempting to get information on Gribov copies directly from the replica sector is probably not the wisest choice. Again, studying nontrivial effects of this sector onto the gluon and/or ghost correlation functions seems the most suited.

One way of realizing this program would consist in computing the variance associated with the $\langle\ \rangle$ average of the ST procedure, see (II.2.1). For instance $\overline{\langle A\rangle\langle A\rangle}$ corresponds to correlation among different gauge orbits at the difference of $\overline{\langle AA\rangle}$ (for a moment, we drop off the Lorentz and color indices for clarity) and can be accessed in lattice simulations (assuming such simulations are feasible and will be perform according to II.1.2). More precisely, let us consider $C := \langle A\rangle\langle A\rangle - \langle AA\rangle$, which, according to Eq. (II.2.1), is given by

$$C = \frac{\int \mathcal{D}\eta_1\mathcal{D}\eta_2\mathcal{P}[\eta_1]\mathcal{P}[\eta_2]\sum_{i,j} s(i)s(j)e^{-\beta_0\mathcal{H}[A,\eta_1,U_i]-\beta_0\mathcal{H}[A,\eta_2,U_j]}\left(A^{U_i}A^{U_j} - A^{U_i}A^{U_i}\right)}{\int \mathcal{D}\eta_1\mathcal{D}\eta_2\mathcal{P}[\eta_1]\mathcal{P}[\eta_2]\sum_{i,j} s(i)s(j)e^{-\beta_0\mathcal{H}[A,\eta,U_i]-\beta_0\mathcal{H}[A,\eta,U_j]}}, \tag{II.7.16}$$

where i, j index Gribov copies and we choose the same gauge parameter β_0. C thus represents correlations between different Gribov copies $i \neq j$. Using the identities (II.2.6), (II.1.9) and (II.2.8) yields

$$C = \frac{\int \mathcal{D}\mathcal{V}_1\mathcal{D}\mathcal{V}_2\ \left(A^{U_1}A^{U_2} - A^{U_1}A^{U_1}\right)\ e^{-S_{\rm CF}[A,\mathcal{V}_1,\xi_0^1]-S_{\rm CF}[A,\mathcal{V}_2,\xi_0^2]}}{\int \mathcal{D}\mathcal{V}_1\mathcal{D}\mathcal{V}_2\, e^{-S_{\rm CF}[A,\mathcal{V}_1,\xi_0^1]-S_{\rm CF}[A,\mathcal{V}_2,\xi_0^2]}}, \tag{II.7.17}$$

where ξ_0^1 and ξ_0^2 are two free (bare) gauge parameters appearing once the integrations over η_1, η_2 have been performed. According to general ST procedure presented in II.2.1, by taking $\xi_0^1 = \xi_0^2 \equiv \xi_0$ and introducing the replicas, we thus have, after

[21] We recall that, in the initial ST gauge-fixing procedure, see Eq. (II.2.12), there is no replica sector. The latter is introduced in order to formulate the ST procedure as a local field theory, but it is merely a matter of convenience for the continuum methods.

[22] Indeed, auxiliary fields are introduced in order to have a local field theory. This is for convenience (if not mandatory) for continuum methods though they are not necessary for lattice simulations. For instance, the lattice action does not involve ghost fields. Nevertheless, the propagator of the latter can be obtained through the FP operator which is present in the lattice procedure. However, in the present case, there is no such equivalent of the FP operator for the λ fields and hence, the possibility that their correlator be measured on the lattice is not guaranteed.

factorization of the volume of the gauge group,

$$\overline{C} = \lim_{n\to 0} \frac{\int \mathcal{D}A \left(\prod_{k=2}^{2n} \mathcal{D}\mathcal{V}_k\right) \left(AA^{U_2} - AA\right) e^{-S[A,\{\mathcal{V}\}]}}{\int \mathcal{D}A \left(\prod_{k=2}^{2n} \mathcal{D}\mathcal{V}_k\right) e^{-S[A,\{\mathcal{V}\}]}}\,, \tag{II.7.18}$$

where we explicitly let $2n$ replicas in order to stress that the previous derivation simply amounts to introduce $2n$ replicas instead of n. This is obviously equivalent to redefining $n = 2n$ in the limit $n \to 0$. Eventually, we have that $\overline{C}$ is given through the following correlator

$$\overline{C} = \lim_{n\to 0} \left\{ \left[AA^{U_k}\right] - [AA] \right\}, \tag{II.7.19}$$

that can be computed in perturbation theory. For instance, putting back Lorentz and color indices, $\overline{C}^{ab}_{\mu\nu}(x,y)$ is given at lowest order in perturbation theory by

$$\overline{C}^{ab}_{\mu\nu}(x,y) = \lim_{n\to 0} \partial^y_\nu \left[A^a_\mu(x)\lambda^b_k(y)\right]_0 . \tag{II.7.20}$$

Higher order terms will involve composite operators of the kind $[A(x)\lambda(y)\dots\lambda(y)]$ and $[A(x)A(y)\lambda(y)\dots\lambda(y)]$, and were not computed. Note however that, they always involve either $\lambda-\lambda$ or $\lambda-A$ correlators, which are null in the Landau gauge ($\xi_0 = 0$), see Eqs. (II.4.51), (II.4.52). Hereby, in the peculiar case of the Landau gauge, we have that $\overline{C}^{ab}_{\mu\nu}(x,y) = 0$. Hence we interpret this result as the fact that there is no cross contribution from two different Gribov copies to the gluon sector. This turns out to be a peculiar feature of the Landau gauge.

II.8 Summary and discussions

We now conclude this chapter. We have proposed a formulation of a class of nonlinear covariant gauges as an extremization procedure. Ignoring Gribov ambiguities this class of gauges is equivalent to the CFDJ gauges. We have applied the ST gauge-fixing procedure proposed in [74] to deal with Gribov ambiguities in an analytical way. This procedure amounts to averaging over the Gribov copies along each gauge orbit with a suitable weight. This lifts the degeneracy between the different copies and avoids the usual Neuberger zero problem. We have shown that our averaging procedure can be formulated as a local field theory which is perturbatively renormalizable in $d = 4$. This requires a set of six independent renormalization factors. We have provided explicit expressions of the latter at one-loop order in perturbation theory. The presence of a modified (non-nilpotent) BRST symmetry (see (II.3.14) and (II.3.15)) insures the renormalizability of the present theory though we do not know how to construct the physical space since one cannot redo the Kugo-Ojima construction.

The resulting gauge-fixed theory has the form of the CF model augmented by a nontrivial sector of replicated scalar, ghost, and antighost fields, which can be written as SUSY nonlinear sigma models coupled to the gauge field, see Eq. (II.3.12). This extends the proposal of [74] away from the particular case of the Landau gauge and provides a more generic framework. For instance, unlike in the Landau gauge, the nonlinear sigma model fields do not decouple in the perturbative calculation of ghost

and gluon correlators and the present gauge-fixed version of the YM theory exhibits explicit differences with the standard CF model.

A key ingredient of the continuum formulation is the replica technique and the interplay between the limit $n \to 0$ and renormalization. Indeed, part of the n dependence of the theory can be absorbed in the definition of the renormalized parameters [74, 98, 99]. In the present work, we have employed a minimal scheme which, first, allows one to reproduce the results of [79] in the Landau gauge ($\xi = 0$) and, second, has a smooth $\xi \to 0$ limit. In the present manuscript, we have studied the infrared-safe renormalization scheme and have presented results for the ghost and gluon propagators at one-loop order with and without RG improvement. For completeness we have also presented our results for the replica sector. Finally, we have compared our results to those of the CF model, obtained by simply setting the number of replicas to $n = 1$. This allows one to pinpoint the peculiar effects of the superfield sector of our theory, which is related to our particular treatment of Gribov ambiguities. As emphasized above, more information on the effects of Gribov copies might be captured by studying nontrivial averages of the kind $\overline{\langle A\rangle \langle A\rangle}$.

The first important aspect of the present treatment of Gribov copies is the fact that the basic fields of the theory acquire effective masses, related to the gauge-fixing parameters β_0 and ξ_0. In contrast to the Landau gauge ($\xi_0 = 0$), not only the transverse gluons, but also the FP ghosts are massive. A striking difference between the CF model ($n = 1$) and the gauge-fixed theory ($n \to 0$) is the fact that, in the latter case, the gluon propagator remains transverse in momentum space even away from the Landau gauge. This is already visible at tree level. At one-loop order in a strict perturbative expansion—i.e., without RG improvement—we also observe important differences between the $n = 1$ and the $n \to 0$ cases, mainly in the transverse gluon propagator, which receives direct contributions from the replica sector. It is important to note that these contain massless degrees of freedom, which lead to nonanalyticities at small momentum. These are absent in the case $n = 1$. The role of massless excitations in the gauge-fixed theory is further illustrated by implementing RG improvement where it is found that the RG flows never freeze out. These results of the gauge-fixed theory are to be compared to the corresponding ones in the CF model, where all degrees of freedom are massive and the RG flow freezes in the IR, resulting in quantitative but not qualitative changes as compared to the strict perturbative results.

One drawback of the present approach is that (up to now) we do not know how fix the mass parameter in an internal way. This has to be put in regard with the Gribov-Zwanziger approach where the Gribov parameter is fixed by a self-consistent equation while here we have to resort to fit the lattice data when available. The fact that, the present class of gauges is formulated as an extremization procedure, keeps open the possibility that these gauges be amenable in lattice simulations by generalization of the lattice gauge-fixing procedures employed in the Landau gauge. This amounts to generalize the minimization algorithms used on the Landau functional $\mathcal{H}_{\text{Landau}}$. We have proposed a possible generalization to the present case of the Los Alamos algorithm that aims at locally minimizing the functional $\mathcal{H}$ (see Eq. (II.1.1)), though an actual procedure would require also the generalization of global minimization algorithms. However (assuming for a moment that such simulations are possible and will be performed), beside the systematic difficulties of interpretation between numerical

and continuum results for what concerns gauge-dependent quantities[23] several reasons might lead to a disagreement of the present previous results with lattice data. As we already mentioned, our choice of renormalization, Sec. II.5, might have been chosen differently and we need actual lattice data to discriminate one or another. This can be inferred from the strong predictions of the present proposal as, for instance, the transversallity of the gluon propagator for $\xi \neq 0$. Also, it is possible that we did illegitimate operations such as the interchange of the $n \to 0$ limit with the path-integral (see Eq. (II.2.14)). Nevertheless, if disagreement of the present results with lattice data is observed one may wonder first about the spectrum of Gribov copies with respect to the value of the functional $\mathcal{H}$. Indeed, in the ST procedure, we average over all of them while the lattice gauge-fixing procedure pinpoints a unique copy which is, in particular, a minimum of $\mathcal{H}$ (we recall that the copies correspond to any extrema, not only minima). For both approaches to be comparable therefore, it shall be equivalent to either randomly pick one minimum (as the lattice does) or to average over the whole set of Gribov copies with a suitable weight (as the ST proposal does). This assumes the following inequality to be true

$$\mathcal{H}\left[A, U_{\text{min.}}\right] < \mathcal{H}\left[A, U_{\text{sdl.pts./max.}}\right]. \tag{II.8.1}$$

In the Landau gauge, indications suggest that this is not exactly the case but that the value of $\mathcal{H}_{\text{Landau}}$ admits overlaps between minima and saddle points [174]. Nevertheless, due to the good agreement between perturbative calculations and lattice results, it is reasonable to assume in this case that these overlaps do not compromise the comparison of the perturbative calculation with the lattice data. However, we have no clue of what happens for $\xi \neq 0$. If these inequalities are violated too strongly, it would probably result in a disagreement between our present results and the lattice ones. Remark however that (II.8.1) being violated does not imply a strong dependence of the lattice results in the choice of the Gribov copy selected, though it is most likely. Hereby, in order to clarify these issues, it would be desirable to perform a numerical investigation of the gauges presented in this chapter.

[23] Comparisons of gauge-dependent quantities between numerical and continuum approaches are never easy. Indeed, both gauge-fixed theories are not equivalent. One can easily convinced of that by inspection of the lattice gauge-fixing procedure that selects exactly one Gribov copy. The continuum equivalent (if it exists at all) is hence a highly nonlocal action. Otherwise said, strictly speaking, the gauge-fixed action used in continuum approaches is actually never the continuum version of the associated gauge-fixed lattice simulations that one intends to compare with. Note this is a very general issue one cannot cope with, and is also present in the Landau gauge. Since we are comparing gauge-dependent quantities, it might result from it differences which are hardly quantifiable.

Chapter III

Yang-Mills theories at finite temperature

In the last chapter, we discussed in detail the studies of YM theories in the vacuum realized in [98, 99, 209]. They are to be included in a larger series of works, along with [79, 78, 74, 81, 80, 82]. For our present purpose, the main conclusion of these studies is that, in the vacuum and in the Landau gauge, the most relevant IR aspects of the YM correlation functions are accurately captured by an effective gluon mass (which might be related to a peculiar treatment of the Gribov copies) and the deep IR regime can be accessed perturbatively.

As emphasized earlier, a great challenge is the study of the complete QCD phase diagram. On the one hand, lattice simulations undergo a severe sign problem [25, 26] and calculations with realistic quark masses are limited to small values of the chemical potential in units of temperature. On the other hand, continuum approaches have to face the nonperturbative character of the theory for not too large temperatures. Although a lot of efforts are dedicated at circumventing the sign problem on the lattice [25, 27, 28], we shall focus here on an alternative strategy. In general, continuum methods are not submitted to such a severe sign problem, and hence, a possible path-way consists in generalizing at finite temperature/chemical potential the continuum approaches used to investigate the (vacuum) IR regime of YM theories. As emphasized earlier, these approaches rely upon approximation schemes, which, for being trustable, should be checked, e.g., by confrontation against lattice simulations when they are available. The latter, now, describe well the phase diagram at vanishing chemical potential along the temperature axis. Indeed, lattice simulations have now firmly established that there exists a confinement-deconfinement phase transition in YM theories [19, 215], whose mains aspects are reviewed in Sec. III.2. In particular, it is now understood that the order of the phase transition depends on the color symmetry group under consideration and is found of first order for SU(3) and second order for SU(2).[1] A relevant order parameter for the phase transition is provided by the Polyakov loop [22] whose nonvanishing expectation value signals the spontaneous breaking of the center symmetry [216] associated to the phase transition. Thereby, in

[1] We also mention that lattice simulations have also established that, in the presence of light dynamical quarks with realistic masses, the phase transition becomes a crossover [24].

this regime, lattice simulations provide a benchmark for continuum methods. Hence, on top of its inherent interest, the detailed description by means of continuum methods of the confinement-deconfinement phase transition in YM theories also provides a laboratory for continuum approaches where they can be checked against lattice data. If successful, this would consist in a good starting point to extend the former also at finite chemical potential.

In this spirit, nonperturbative continuum methods were amended to the finite temperature case such as the FRG [33, 32, 34, 35], truncations of DSEs [36, 37, 38], the Hamiltonian approach of [168], two-particle-irreducible techniques [35, 170], or the GZ proposal [217, 218]. It is therefore natural to extend at finite temperature the perturbative approach of the CF model presented previously. This has been done in a series of works [83, 93, 94, 95] and recently also for QCD at finite chemical potential [97] in the presence of heavy quark masses. However, although the phase transition is a physical phenomenon, its effects on the YM correlators might depend on the gauge under consideration. Therefore, for gauge-dependent approximate methods, such as the continuum ones, it might be to choose a gauge in which the Green's functions on which the approach is based be sensitive to the phase transition in order to consistently keep tracks of its effects.

Owing to the numerous studies performed in the vacuum, the Landau gauge appears as a natural candidate and, accordingly, has received a lot of attention also at finite temperature. In this gauge, and in the vicinity of the phase transition, the YM correlators have been investigated by means of both numerical [101, 91, 46, 92] and continuum methods, e.g., with the FRG [33, 219, 35], the GZ proposal [218], truncations of DSEs [220, 89, 221], two-particle-irreducible inspired approximations [170, 35], the Hamiltonian approach [222, 223], or perturbative calculations in the CF model [83], see [45] for a review. The main results for the Landau gauge gluon and ghost propagators are presented in Sec. III.3. On the one hand, lattice calculations in the Landau gauge found no sign of the phase transition, neither in the ghost propagator (which is in fact essentially independent of the temperature) nor in the magnetic gluon propagator, which is roughly speaking associated with the correlation function for the space-components of the gluons, see below for more details. The situation is less clear for the electric sector, which involves the time-component of the gluon field, more directly connected to the Polyakov loop, see Sec. III.2. Early results in the SU(2) theory, where the phase transition is second order, seemed to show a clear singularity of the electric susceptibility (i.e., the electric propagator at vanishing frequency and momentum) [46] at the critical temperature. However, these data present an extreme sensitivity to both the lattice size and the lattice spacing for temperatures slightly below the transition temperature [101, 224], for reasons that are not fully understood yet, see however [225]. Nevertheless, more recent lattice simulations indicate that this signal disappears at larger volumes [90]. On the other hand, all the continuum approaches typically find a slight nonmonotonous behavior of the electric susceptibility below the transition, but no clear sign of the transition, in qualitative agreement with the latest lattice results of, e.g., [90].

The disappointing conclusion was that, in the Landau gauge, the basic correlators show few, if any, signals of the phase transition. It has been argued that this is a consequence of some drawbacks of the Landau gauge. Indeed, this gauge breaks explicitly

the center symmetry of the finite temperature problem. Moreover, the correlators do not present an explicit dependence in the order parameter of the phase transition (the Polyakov loop), which might explain their small response to the phase transition [93]. Although the Polyakov loop is a complicated object, it has been argued in [33, 34, 35] that one can alternatively incorporate to the YM action a nontrivial background value for the gauge field that acts as an equivalent order parameter; see also [94, 226]. A definite proof has been given in [95]. More precisely, this corresponds to work in the Landau-DeWitt (LDW) gauge, which is a straightforward generalization of the Landau gauge in presence of a nontrivial background field. This gauge has the main advantage that the center symmetry is explicit [33]. In fact, one can show that certain background field configurations obtained by minimizing a particular potential to be defined below, provide alternative order parameters for the center symmetry, that are equivalent to the (gauge-invariant but more difficult to access) Polyakov loop [95]. Within this framework, the FRG predicts the correct order of the phase transition, as well as convincing transition temperatures [33, 35, 34]. It is worth mentioning that, the GZ proposal has also been implemented within such a background field formalism, where it was found that the Gribov mass directly feels the confinement-deconfinement phase transition [217].

The LDW gauge has been implemented in the massive perturbative approach [93, 94, 95, 96, 97], where, in particular, the phase transition was accessed perturbatively as we review in Sec. III.4. This general set-up consists in our starting point for the calculations of the YM correlators and the investigation of their possible response to the phase transition. This study corresponds to our work of [96] and is presented in detail in Sec. III.5 along with our results.

III.1 Yang-Mills theories at finite temperature: the framework

For later convenience, let us proceed by introducing the massive extension of the Landau gauge FP action at finite temperature in d-dimensional Euclidean space-time.[2] It reads

$$S_0 = \int_x \left\{ \frac{1}{4} F^a_{\mu\nu} F^a_{\mu\nu} + \frac{m_0^2}{2} A^2_\mu + \partial_\mu \bar{c}^a D_\mu c^a + i h^a \partial_\mu A^a_\mu \right\}, \tag{III.1.1}$$

where the field strength tensor $F^a_{\mu\nu}$, the covariant derivative D_μ and the auxiliary fields, namely the FP ghost and antighost c and $\bar{c}$, and Nakanishi-Lautrup field ih, were introduced in Chapter. I. The standard Landau gauge FP action is recovered for $m_0 = 0$. At finite temperature, the Euclidean time, that we note τ, is bounded such that

$$\int_x = \int_0^\beta d\tau \int d^{d-1}x \,, \tag{III.1.2}$$

where $\beta = 1/T$ is the inverse temperature. Despite their commuting or anticommuting character, both type of fields present in Eq. (III.1.1) are periodic in time

$$\varphi(\tau, \mathbf{x}) = \varphi(\tau + \beta, \mathbf{x}). \tag{III.1.3}$$

[2] Details and pedagogical lecture notes can be found in [227].

In the following we note with capital letters, e.g. K, the momenta with the Fourier convention that $\partial_\mu \to -iK_\mu$. The periodic boundary condition (III.1.3), implies that their time component, K_0, is discrete and given by the so-called Matsubara frequencies $\omega_n = 2\pi n T\,,\ n \in \mathbb{Z}$, such that $K = (\omega_n, \mathbf{k})$. In the following, we drop the suffix n and simply note ω the Matsubara frequencies, except when summing over in loop calculations where we explicitly reintroduce the suffix.

Since the time direction is singularized with respect to the spatial ones, the general "Lorentz" decomposition is more complicated at finite temperature than in the vacuum. For a generic symmetric rank-two tensor $T_{\mu\nu}(K)$, that depends on the four momentum K, one has

$$T_{\mu\nu}(K) = \delta_{\mu\nu} T_\delta(K) + K_\mu K_\nu T_{\rm K}(K) + (n_\mu K_\nu + n_\nu K_\mu)\, T_{\rm nK}(K) + n_\mu n_\nu T_{\rm n}(K)\,, \quad \text{(III.1.4)}$$

where n_μ characterizes the thermal bath frame. Everywhere in the following, we work in the frame where the thermal bath is at rest, that is, $n = (1, \mathbf{0})$. One also defines in this context the transverse $P^T_{\mu\nu}(K)$ and longitudinal $P^L_{\mu\nu}(K)$ projectors

$$P^T_{\mu\nu}(K) = (1 - \delta_{\mu 0})\,(1 - \delta_{\nu 0}) \left(\delta_{\mu\nu} - \frac{K_\mu K_\nu}{k^2} \right) \quad \text{(III.1.5)}$$

and

$$P^L_{\mu\nu}(K) + P^T_{\mu\nu}(K) = P^\perp_{\mu\nu}(K) = \delta_{\mu\nu} - \frac{K_\mu K_\nu}{K^2}\,, \quad \text{(III.1.6)}$$

where we noted $k^2 = \mathbf{k}^2$ and $K^2 = \omega^2 + k^2$.

In the (massive) Landau gauge, the gluon propagator $\mathcal{G}^{ab}_{\mu\nu}(K) = \delta^{ab}\mathcal{G}_{\mu\nu}(K)$ is diagonal in color space and transverse with respect to K: $K_\mu \mathcal{G}_{\mu\nu}(K) = 0$. Hereby, it admits the decomposition

$$\mathcal{G}_{\mu\nu}(K) = P^T_{\mu\nu}(K)\mathcal{G}_T(K) + P^L_{\mu\nu}(K)\mathcal{G}_L(K). \quad \text{(III.1.7)}$$

In the following, we refer in an equivalent way to $\mathcal{G}_T$ as the transverse or magnetic (gluon) sector and $\mathcal{G}_L$ as the longitudinal or electric (gluon) sector. They can be accessed from the gluon polarization tensor $\Pi^{ab}_{\mu\nu}(K)$ and, for later convenience, we use a perturbative-like writing: $\Pi^{ab}_{\mu\nu}(K) = g_0^2 N \delta^{ab} \Pi_{\mu\nu}(K)$, with N the number of color of the fundamental representation of the SU(N) group. The expressions of the magnetic and electric gluon propagators are

$$\mathcal{G}_{T/L}(K) = \frac{1}{K^2 + m_0^2 + g_0^2 N\, \Pi_{T/L}(K)}\,, \quad \text{(III.1.8)}$$

where

$$\Pi_T(K) = \frac{P^T_{\mu\nu}(K)\Pi_{\mu\nu}(K)}{d-2}\,, \quad \text{(III.1.9)}$$

$$\Pi_L(K) = P^L_{\mu\nu}(K)\Pi_{\mu\nu}(K). \quad \text{(III.1.10)}$$

Similarly, we define the ghost self-energy $\Sigma^{ab}(K) = g_0^2 N \delta^{ab} \Sigma(K)$ as well as the ghost propagator $\mathcal{G}^{ab}(K) = \delta^{ab}\mathcal{G}(K)$, which reads

$$\mathcal{G}(K) = \frac{1}{K^2 + g_0^2 N\, \Sigma(K)}. \quad \text{(III.1.11)}$$

For later convenience, we also define the ghost dressing function at zero Matsubara frequency

$$F(k) = k^2 \mathcal{G}(\omega = 0, k). \tag{III.1.12}$$

III.2 The confinement-deconfinement phase transition

In the previous section we introduced the basic ingredients of YM theories at finite temperature and we chose deliberately to present the massive Landau gauge. This turns convenient for the discussions to come in Sec. III.5, but first, we would like to introduce some aspects of the confinement-deconfinement phase transition, which, as emphasized earlier, occurs in YM theories at finite temperature.

III.2.1 The Polyakov loop as an order parameter

We consider the case where the quarks are statics and of infinitely heavy masses (quenched approximation). Within this approximation, starting at zero temperature (vacuum) where quarks and gluons are confined, by increasing the temperature one eventually ends in a phase where the free energy of an isolated static quark becomes finite and, in turn, is interpreted as the deconfined phase. The traced Polyakov loop [228] (referred as the Polyakov loop for shortness) provides a relevant order parameter for the confinement-deconfinement phase transition [22]. It is defined as

$$\ell = \frac{1}{N}\mathrm{tr}\left\langle P \exp\left\{ ig_0 \int_0^\beta d\tau\, A_0(\tau, \mathbf{x}) \right\} \right\rangle , \tag{III.2.1}$$

where P is the path ordering operator (matrices are ordered from left to right according to the decreasing value of their time argument). The free energy F_q of an isolated static (of infinitely heavy mass) quark in the thermal gluon bath is related to the expectation value of the Polyakov loop as [216, 229, 11]

$$\exp\{-\beta F_q\} = \ell\,. \tag{III.2.2}$$

Hereby, a vanishing Polyakov loop (as found in the low temperature phase) corresponds to $F_q \to \infty$, that is, an infinite static quark free energy signaling the confined phase. On the contrary, a finite value of ℓ yields a deconfined static quark state.

III.2.2 Spontaneous breaking of the center symmetry

The Polyakov loop (III.2.1) transforms under the action of a local group element $U(\tau, \mathbf{x}) \in SU(N)$ as [216, 229, 11]

$$\ell \to \frac{1}{N}\mathrm{tr}\left[U(0, \mathbf{x}) \left\langle P \exp\left\{ ig_0 \int_0^\beta d\tau\, A_0(\tau, \mathbf{x}) \right\} \right\rangle U^\dagger(\beta, \mathbf{x}) \right] , \tag{III.2.3}$$

and hence, is invariant under the transformations that admit periodic boundary conditions: $U(\tau+\beta, \mathbf{x}) = U(\tau, \mathbf{x})$. These correspond to the standard gauge transformations. Nevertheless, the gauge-invariant YM action admits a larger group of symmetries than

the above periodic transformations [230]. These consist in gauge transformations with twisted periodic boundary conditions:

$$U(\tau+\beta,\mathbf{x}) = U(\tau,\mathbf{x})Z, \tag{III.2.4}$$

where Z is an element of a global and discrete group, namely the center of SU(N). One recovers the standard gauge transformations for $Z = \mathbb{1}$. The center is defined as the quotient group of the group of generalized gauge transformations (III.2.4) by the subgroup of standard gauge transformations. In the case of SU(N), the center is isomorphic to $\mathbb{Z}_N = \left\{ z_k \mathbb{1} : \, z_k = e^{i2\pi k/N}, \, k = 0, \dots N-1 \right\}$.

According to Eq. (III.2.3), the Polyakov loop gets multiplied by the phase z_k under the generalized gauge transformations (III.2.4)

$$\ell = z_k \ell \,, \tag{III.2.5}$$

so that the deconfined phase, signaled by a nonvanishing Polyakov loop, corresponds to a phase where the center symmetry is spontaneously broken. Note that, one could imagine (although this situation is not expected) that the Polyakov loop vanishes in the phase where the center is broken. In such a case, the corresponding phase would still be a confined phase since the static quark free energy would be infinite. Thence, it is really the zero or nonzero value of the Polyakov loop which signals the confined or deconfined phase rather than the spontaneous breaking of the Z_N symmetry.[3]

III.3 Landau gauge correlation functions and the phase transition

Lattice studies performed in the pure gauge case have confirmed the occurrence of the confinement-deconfinement phase transition. The order of the phase transition depends on the gauge group under consideration and on the dimensionality (in $d = 4$ it is second order phase transition for SU(2), first order for SU(3)) [231, 23, 215, 24]. After such a confirmation, some attention was dedicated to investigate the possible signals of the phase transition on the basic gluon and ghost correlators. Although the high-temperature regime can be accessed in perturbation theory (supplemented by resummation techniques, the so-called Hard Thermal Loops [14, 13, 15]), one cannot access the domain of temperature lower than a few times the transition temperature [16, 18, 17]. in turn, as emphasized above, various nonperturbative techniques, as well as the perturbative study of the CF model, were extended at finite temperature in order to calculate the Landau gauge correlation functions.

III.3.1 The lattice results

Gauge-fixed lattice simulations were performed for thermal YM theories in the Landau gauge in $d = 4$ for gauge groups SU(2) and SU(3), see e.g. [84, 85, 86, 87, 88,

[3] Remark that here we restrain the discussion to the case where all the static matter sources are in the fundamental representation. For an enlarged discussion in the case where different representations are considered see e.g. [12, 95].

89, 90, 91, 46, 92]. However, they display strong systematic uncertainties in particular near the transition temperature [101, 224]. Nevertheless, some general qualitative features have emerged:

- The ghost propagator displays very small temperature dependence [88]. This feature is also captured in the framework of DSEs [220] and FRG [219].
- The magnetic mass, defined as the square root of the inverse correlator at zero Matsubara frequency and momentum, remains finite and increases monotonously with the temperature. In the extreme infrared, the magnetic correlator is found to increase linearly with momentum, a behavior characteristic of the zero temperature gluon propagator in the Landau gauge in $d = 3$ [88].
- Finally, the electric gluon sector represents the correlation of the temporal gluon field, see Eq. (III.1.6). Owing to the definition of the Polyakov loop Eq. (III.2.1), the electric sector is widely believed to be the most sensitive to the phase transition. Unfortunately, this correlator presents the largest uncertainties due to lattice artifacts, particularly near the phase transition, see Fig. III.1 and [101, 224]. In particular, the electric (Debye) mass is nonmonotonous with respect to the temperature [89]. Although early lattice simulations in SU(2) suggested that the Debye mass is minimum (even vanishing) at the transition temperature [46], larger volume simulations now favor a finite minimum (with a rather small mass ratio of $1.1 - 1.5$ with respect to the vacuum value) at a temperature T such that $T \simeq 0.86\, T_c$, with T_c the critical temperature [101]. This is summarized in Fig. III.2 where, as the lattice volume increases, the minimum value of the Debye mass increases and the position of the minimum is shifted to lower temperatures.

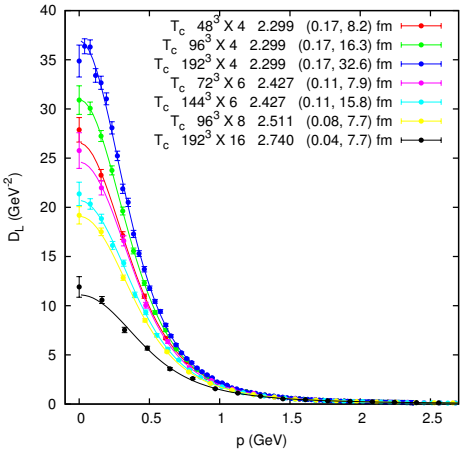

Figure III.1: The longitudinal gluon propagator at zero Matsubara frequency and at the transition temperature T_c as a function of the momentum p in $d = 4$ for SU(2). Results are given for different lattice spacing a and lattice sizes L (both in fm) labeled in parentheses (a, L), and for different discretization $N_s^3 \times N_t$. The most reliable data are obtained for the largest value of N_t (black curve). Original figure taken from [90].

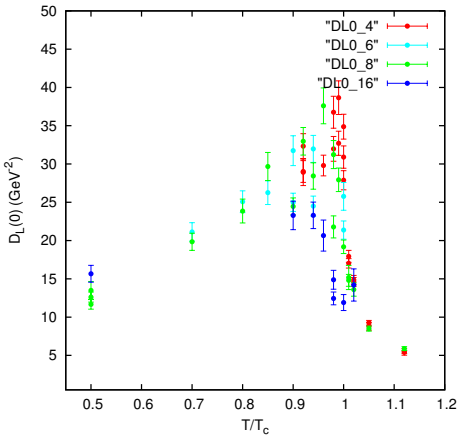

Figure III.2: The longitudinal gluon propagator at zero frequency and zero momentum as a function of the temperature, in $d = 4$ for SU(2). Results are given for different discretization of the temporal direction N_t and labeled as "$DL0\_N_t$". The most reliable data are obtained for the largest value of N_t (blue points). Original figure taken from [90].

All in all, as the lattice results become more reliable, they tend to suggest that the basic correlators are little sensitive to the phase transition, and in particular no dramatic signal is observed in the electric sector at T_c, see Figs. III.1-III.2. These results are now fairly well described by continuum methods. For instance, in Fig. III.3 is displayed the FRG results of [219] for the magnetic (transverse) and electric (longitudinal) gluon propagators which are compared with the corresponding lattice results. As we present in the next section, the perturbative calculations performed in the CF model also reproduce these results.

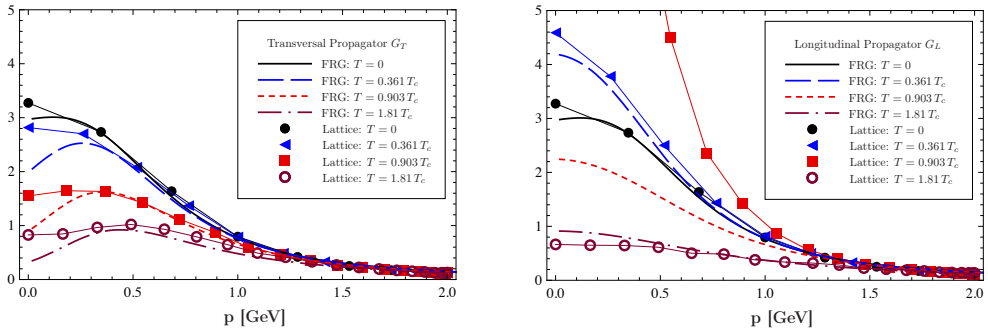

Figure III.3: Left panel: Transversal gluon propagator in comparison with lattice results [46, 89]. Right panel: Longitudinal gluon propagator in comparison with lattice results [39]. The lattice data have been rescaled such that the $T = 0$ propagators match at intermediate momenta $p \gtrsim 1$GeV. Original figure taken from [219].

III.3.2 Perturbative results in the massive Landau gauge

The massive approach of the series of works of [79, 78, 74, 81, 80, 82, 98, 209] has been extended at finite temperature in the Landau gauge [83]. It consists in considering the action Eq. (III.1.1) introduced in Sec. III.1 that corresponds to a gauge-fixed version of the YM action where the Landau gauge is implemented according to the ST gauge-fixing procedure [74], see Sec. I.5 and Sec. II.2.

We recall that, in the Landau gauge, the SUSY sector appearing in the gauge-fixing procedure decouples (in perturbation theory) from the ghost and gluon sectors. This remains true at finite temperature because all fields (SUSY and non-SUSY ones) have the same periodic boundary conditions. Therefore, there is no need to introduce the SUSY sector explicitly here; see Eq. (II.4.18) of Sec. II.4.1. The mass term[4] m_0 appearing in the action Eq. (III.1.1) accounts for the presence of Gribov copies. We remark that, *a priori*, it should present a temperature dependence since the distribution of Gribov copies depends on the temperature. We again mention that, in principle, it should be possible to fix this mass in an *ab initio* way (akin the Gribov parameter through the horizon condition, see Eq. (I.4.12) of Sec. I.4.2). However, so far, such analogous condition has not been derived and m_0 thus appears as an external parameter, which is to be fixed by comparisons with lattice simulations for instance.

In [83], the authors computed the finite temperature gluon and ghost propagators from the massive action (III.1.1) at one-loop order in perturbation theory. The thermal contributions do not yield divergences so that only the vacuum contributions need to be renormalized. The one-loop transverse gluon propagator reproduces the same behavior as the one found in lattice simulations and FRG [see Fig. III.3], namely a $3d$-behavior for small momenta and a monotonously increasing magnetic mass with respect to the temperature. This is depicted in Fig. III.4. The monotonous increase of the magnetic mass yields a dramatic consequence, namely a pole in the ghost sector. This is a consequence of a nonrenormalization theorem (see [232, 201, 79, 78] for the case $T = 0$, see also Appendix F)

$$\mathcal{G}_{T,0}^{-1}(K)F_0^{-1}(K)\Big|_{\omega=0,k\to 0} = m_0^2, \tag{III.3.1}$$

where we explicitly added a suffix 0 to stress that these are bare quantities, and F_0 is the (bare) ghost dressing function defined in Eq. (III.1.12). In particular, it is understood in (III.3.1) that one has to take $\omega = 0$ prior to perform the limit $k \to 0$. After renormalization (in the zero-momentum renormalization scheme [see Eq. (II.5.29) of Sec. II.5.3] used in [83]), this identity implies the following one-loop IR behavior of

[4] Remark that according to the ST gauge-fixing procedure, the mass term is proportional to the number of replica n which eventually has to be taken to zero, see Sec. II.2 of Chapter. II. Nevertheless, as we saw, the n dependence of the mass term can be reabsorbed into the bare parameters of the theory under a suitable choice of renormalization scheme, see Sec. II.5.1 of Chapter. II. Here and in the following, we only consider such kind of renormalization schemes, so that, in a short-hand notation, we do not write explicitly the n dependence of the bare mass that will be trivially absorbed in the renormalization. Accordingly, the gluon and ghost sectors are effectively equivalent to those of the CF model.

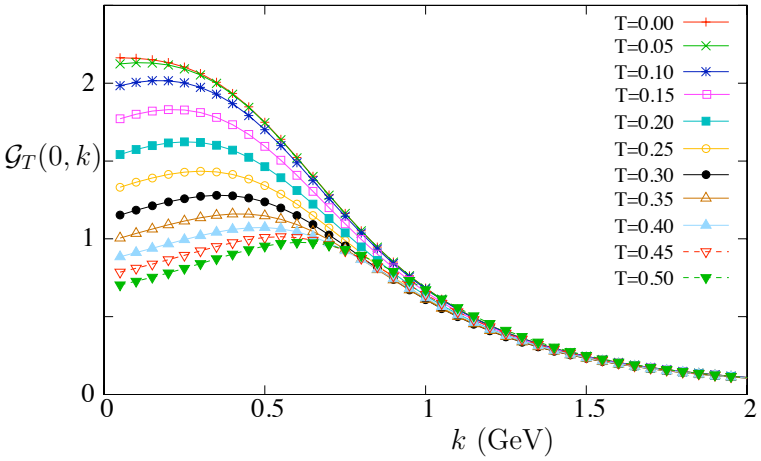

Figure III.4: One-loop transverse gluon propagator as a function of the momentum for different temperatures. Computations performed in the massive action Eq. (III.1.1). Original figure taken from [83].

the thermal part of the ghost self-energy

$$\begin{aligned} g^2 N\, \Sigma_{\text{th}}(0,k\to 0) &\sim -\frac{k^2}{m^2} g^2 N\, \Pi_{T,\text{th}}(0,k\to 0) \\ &\sim k^2 \left(1 - \frac{M^2_{\text{mag}}(T)}{m^2}\right) . \end{aligned} \tag{III.3.2}$$

The last line eventually turns negative because of the (linearly increasing) behavior of the magnetic mass at large temperatures. In particular, this leads to the appearance of a pole in the ghost dressing function at sufficiently high temperatures [83], see Fig. III.5. This pole can be overcome by allowing the (renormalized) parameters to depend on the temperature. In practice, the temperature dependence was fixed by finding, for each temperature, the value of the parameters for which the perturbative results agree the best with lattice data. Similar treatment was needed in other approaches, as for instance in [218]. In the present case, it results in a slightly decreasing (renormalized) coupling constant with respect to the temperature that ranges from $g = 7$ for $T = 0$ to $g = 5$ at $T = T_c$. With these temperature-dependent parameters, the previous pole is avoided and both the magnetic gluon propagator and the ghost dressing function are found in good agreement with lattice results. On the other hand, in the electric sector, although the Debye mass shows the nonmonotonous behavior observed in lattice data, it initially does not reproduce well the latter at the quantitative level, with a too small mass ratio and a lower temperature at which the Debye mass is minimum. Let us mention though that, as lattice simulations are performed on larger volumes, their results get closer to the perturbative ones [233].

In this section, the main point we wanted to stress is that, in the Landau gauge, YM correlators display poor signals of the confinement-deconfinement phase transition. In this regard, the Landau gauge seems to be not the best choice of gauge to study the phase transition by means of approximate continuum methods. In particular, the

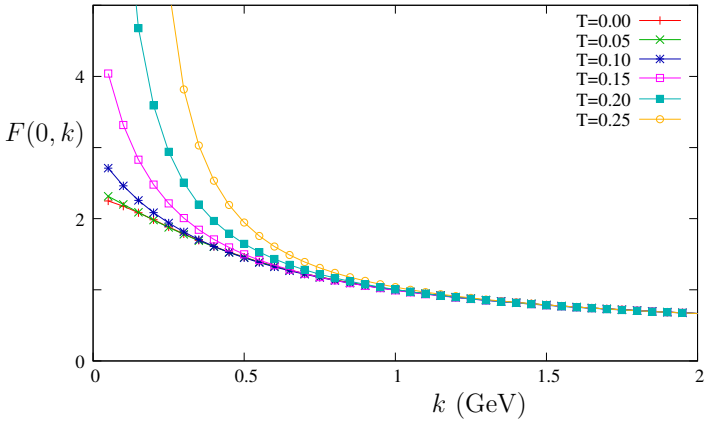

Figure III.5: Ghost dressing function as a function of the momentum, for different temperatures, ranging from 0 to 0.25 GeV. The infrared dressing function is strongly enhanced as the temperature is increased. It even shows a pole for temperatures larger than 0.25 GeV. Original figure taken from [83].

Polyakov loop (the order parameter of the phase transition) does not enter at any level in the definition nor in the calculation of the correlators. On top of it, we presented in Sec. III.2 that the phase transition displays tight links with the Z_N symmetry, which, in turn, is explicitly broken in the Landau gauge [95] (see Sec.III.4.2).

Moreover, for what concerns the perturbative approach, although the results of [83] provide fairly good agreement with the lattice, in general, near a phase transition, one expects the critical fluctuations of some order parameter to play an important role. The latter are usually not captured by a perturbative calculation as presented above and require another ingredient related to the presence of a nontrivial order parameter. For instance, one can think to the Ising model where one attempts to study the phase transition in a perturbative approach. Of course, as it is well known, one would add to the initial Hamiltonian an external small magnetic field in order to account for a possible nonzero value of the magnetization. In this case, the phase transition can be accessed for instance in the mean-field approximation. In the case of the confinement-deconfinement phase transition, this motivates further the inclusion of an order parameter into the action for the perturbative approach.

III.4 The (massive) Landau-DeWitt gauge

As emphasized above, it would be desirable to have an approach where the order parameter and the Z_N symmetry are explicitly accounted for, and which can be investigated by means of both lattice simulations and continuum methods. Such a proposal has been put forward in [33, 35, 34] where the authors used background field methods that allow to maintain explicitly the Z_N-center symmetry at the level of the effective action Γ. Accordingly, in the framework of the FRG, they studied the confinement-deconfinement phase transition for $N = 2$ and $N = 3$ in a background field extension of the Landau gauge (the Landau-DeWitt gauge, see below). Their results predict the

correct order of the phase transition as well as transition temperatures in agreement with the lattice. These background field methods were implemented in the framework of the massive approach of [79, 78, 74, 81, 80, 82, 98, 209, 83] first in [93, 94, 95] which we now review.

III.4.1 The general set-up

The theory is quantized by means of background field methods [234, 235, 236, 118]. One introduces an *a priori* arbitrary background field configuration $\bar{A}_\mu$ and accordingly defines the fluctuating field $a_\mu = A_\mu - \bar{A}_\mu$. The Landau-DeWitt (LDW) gauge is defined by the condition

$$\bar{D}_\mu a_\mu = 0, \tag{III.4.1}$$

where $\bar{D}_\mu$ is the background covariant derivative defined as

$$\bar{D}_\mu \varphi = \partial_\mu \varphi - i g_0 [\bar{A}_\mu, \varphi]\,. \tag{III.4.2}$$

Note in particular that, for vanishing background field the Landau gauge is recovered. The gauge transformation of the gauge field $A_\mu = \bar{A}_\mu + a_\mu$ can be decomposed in two ways: either

$$\begin{aligned} &\bar{A}_\mu \to \bar{A}_\mu \\ &a_\mu \to a_\mu^U = U a_\mu U^{-1} + \frac{i}{g_0} U \bar{D}_\mu U^{-1}\,, \end{aligned} \tag{III.4.3}$$

or

$$\begin{aligned} &\bar{A}_\mu \to \bar{A}_\mu^U = U \bar{A}_\mu U^\dagger + \frac{i}{g_0} U \partial_\mu U^\dagger \\ &a_\mu \to U a_\mu U^{-1}\,. \end{aligned} \tag{III.4.4}$$

The condition (III.4.1) fixes the symmetry (III.4.3), but (III.4.4) remains a symmetry of the family of gauge-fixed actions labeled by $\bar{A}$, namely $S_{\bar{A}}[\varphi] = S_{\bar{A}^U}[U\varphi U^{-1}]$ with $\varphi = (a, c, \bar{c}, h)$. Observe that the transformation $a \to a^U$ is very similar to the usual gauge transformation (see (I.1.4)) except that the partial derivative is replaced by the background covariant derivative: $\partial_\mu \to \bar{D}_\mu$.

Similarly to Landau, the LDW gauge can be obtained by extremizing the functional

$$\mathcal{H}_{\rm LDW}[a, U] = \int_x \mathrm{tr}\left\{ a_\mu^U a_\mu^U \right\}\,, \tag{III.4.5}$$

which is a simple generalization of the Landau functional $\mathcal{H}_{\rm Landau}[A, U]$, see (I.4.1) of Sec. I.4. Hereby, it is expected (and confirmed in [237]) that the methods routinely employed to implement the Landau gauge in lattice simulations can be adapted to the LDW gauge.

Here, we apply the ST procedure to the LDW gauge, all the same as in Landau with $A_\mu \to a_\mu$ and $D_\mu \to \bar{D}_\mu$. We arrive at the following effective gauge-fixed action [93]

$$S_{\bar{A}} = \int_x \mathrm{tr}\left\{ \frac{1}{2} F_{\mu\nu} F_{\mu\nu} + m_0^2 a_\mu a_\mu + 2\bar{D}_\mu \bar{c} D_\mu c + 2ih\bar{D}_\mu a_\mu \right\}. \tag{III.4.6}$$

In terms of the field a_μ, we have

$$F_{\mu\nu} = \bar{F}_{\mu\nu} + \bar{D}_\mu a_\nu - \bar{D}_\nu a_\mu - ig_0[a_\mu, a_\nu], \tag{III.4.7}$$

with $\bar{F}^a_{\mu\nu} = F^a_{\mu\nu}[\bar{A}]$ the field strength tensor evaluated at $A = \bar{A}$, and

$$D_\mu\varphi = \partial_\mu\varphi - ig_0[A_\mu, \varphi] = \bar{D}_\mu\varphi - ig_0[a_\mu, \varphi]. \tag{III.4.8}$$

Remark the important point that, it is the fluctuating field a_μ which appears with a mass term in (III.4.6) and not A_μ. In the context of the ST proposal, this comes from the form of the minimization functional (III.4.5) (see Sec.II.2.1). This property is crucial in order to insure that the action Eq. (III.4.6) admits the following symmetry [118]

$$S_{\bar{A}}[\varphi] = S_{\bar{A}^U}[U\varphi U^{-1}], \quad \varphi = (a, c, \bar{c}, h), \tag{III.4.9}$$

where U is a local SU(N) matrix, and $\bar{A}^U$ was defined in (III.4.4). Due to its close resemblance with a gauge transformation, the symmetry (III.4.9) is often called background gauge symmetry. Introducing sources J_φ for the fields $\varphi = (a, c, \bar{c}, h)$, one defines [118]

$$e^{W_{\bar{A}}[J_\varphi]} = \int \mathcal{D}\varphi \, \exp\left[-S_{\bar{A}}[\varphi] + \int_x J_\varphi\varphi(x)\right], \tag{III.4.10}$$

and the Legendre transformation of $W_{\bar{A}}[J_\varphi]$ with respect to the sources J_φ leads to the effective action $\Gamma_{\bar{A}}[\varphi]$. Here, the fields φ are now to be understood as average values in the presence of sources. Moreover, since the background gauge transformations, Eq. (III.4.4), are linear, one has

$$\Gamma_{\bar{A}}[\varphi] = \Gamma_{\bar{A}^U}[U\varphi U^{-1}]. \tag{III.4.11}$$

In particular, by taking $U(x)$ as a local element of SU(N) with twisted periodic boundary conditions (Eq. (III.2.4) with $Z \neq \mathbb{1}$), one sees that the center symmetry is encoded into the background gauge symmetry at the level of the effective action.

To evaluate physical observables at zero sources, one should minimize $\Gamma_{\bar{A}}[\varphi]$ with respect to φ at a given background field configuration $\bar{A}$. Still, according to the LDW gauge condition, Eq. (III.4.1), the choice of the background $\bar{A}$ is merely a choice of gauge, which should thus be chosen for convenience. In particular, in presence of the background, the Polyakov loop, Eq. (III.2.1), reads

$$\ell = \frac{1}{N}\mathrm{tr}\left\langle P\exp\left\{ig_0\int_0^\beta d\tau\,\left(\bar{A}_0(\tau,\mathbf{x}) + a_0(\tau,\mathbf{x})\right)\right\}\right\rangle_{\min}, \tag{III.4.12}$$

where the brackets stand for an average with the gauge-fixed theory (III.4.6), and the suffix min means that the right-hand side of Eq. (III.4.12) is evaluated at an absolute minimum $\varphi_{\min}[\bar{A}]$ of $\Gamma_{\bar{A}}[\varphi]$. Hereby, it turns out convenient to choose (if it exists) a background $\bar{A} = \bar{A}_s$ such that $\varphi_{\min}[\bar{A}_s] = 0$. Henceforth, we shall refer to such background field configurations as self-consistent backgrounds since they correspond to $\langle a\rangle_{\min} = 0$ or equivalently to $\langle A\rangle_{\min} = \bar{A}_s$. One should consider the following functional of the background field

$$\tilde{\Gamma}[\bar{A}] = \Gamma_{\bar{A}}[0], \tag{III.4.13}$$

which is invariant under the background gauge transformations Eq. (III.4.4) owing to Eq. (III.4.11). An important remark is to note that $\tilde{\Gamma}[\bar{A}]$ is not a Legendre transform but, according to its definition Eq. (III.4.13), it corresponds to the effective action $\Gamma_{\bar{A}}$ evaluated for vanishing φ in presence of the background configuration $\bar{A}$. Thus, in the definition Eq. (III.4.13), $\bar{A}$ is in general not a self-consistent background field and $\Gamma_{\bar{A}}[0]$ is not the minimum of $\Gamma_{\bar{A}}[\varphi]$. Nevertheless, it has been argued that self-consistent background fields are absolute minima of $\tilde{\Gamma}[\bar{A}]$ [93, 94, 95] (see also Appendix G). Therefore, for the evaluation of physical observables, one can either minimize $\Gamma_{\bar{A}}[\varphi]$ with respect to φ for a given $\bar{A}$, or, alternatively, minimize $\tilde{\Gamma}[\bar{A}]$ with respect to $\bar{A}$. The main lines of the proof goes as follow:[5] consider the functional $\tilde{\Gamma}[\bar{A}]$ evaluated for a self-consistent background $\bar{A}_s$. By construction, one has that[6]

$$\tilde{\Gamma}[\bar{A}_{\rm s}] = \Gamma_{\bar{A}_{\rm s}}[0] = \Gamma_{\bar{A}_{\rm s}}[a_{\rm min}[\bar{A}_{\rm s}]]\,. \tag{III.4.14}$$

The right-hand side is related to the free energy of the system according to $-\ln Z = \Gamma_{\bar{A}}[a_{\rm min}[\bar{A}]]$ and thus does not depend on the "gauge choice" $\bar{A}$.[7]Therefore, the background independence of the partition function yields $\Gamma_{\bar{A}_{\rm s}}[a_{\rm min}[\bar{A}_{\rm s}]] = \Gamma_{\bar{A}}[a_{\rm min}[\bar{A}]]\ \forall \bar{A}$. Since the right-hand side of this last equality is evaluated at the minimum, one has that $\Gamma_{\bar{A}}[a_{\rm min}[\bar{A}]] \leq \Gamma_{\bar{A}}[a]\ \forall a$. In particular, this is true by taking $a = 0$ on the right-hand side. Eventually, this leads to

$$\tilde{\Gamma}[\bar{A}_{\rm s}] \leq \Gamma_{\bar{A}}[0] = \tilde{\Gamma}[\bar{A}] \quad \forall\ \bar{A}\,, \tag{III.4.15}$$

that is, a self-consistent background is necessarily an absolute minimum of the functional $\tilde{\Gamma}[\bar{A}]$. The rest of the proof follows the same lines and one shows that either the absolute minima of $\tilde{\Gamma}[\bar{A}]$ correspond exactly to the self-consistent backgrounds or there is no self-consistent background at all [95]. This finally shows the equivalence for the evaluation of gauge-invariant quantities either by minimizing $\Gamma_{\bar{A}}[a]$ with respect to a for fixed background $\bar{A}$ or by minimizing the functional of the background $\tilde{\Gamma}[\bar{A}]$ with respect to $\bar{A}$.

III.4.2 The background potential in SU(2)

In the following, we consider only self-consistent background fields. Moreover, since by definition a self-consistent background satisfies $\bar{A}_s(\tau, \mathbf{x}) = \langle A \rangle_{\rm min}$, it is sufficient to consider homogeneous background fields in the temporal direction, that is

$$\bar{A}_\mu(\tau, \mathbf{x}) = \bar{A}_0 \delta_{\mu 0}\,. \tag{III.4.16}$$

With no loss of generality, the (Hermitian) matrix $\bar{A}_0$ can be restricted to belong to the Cartan subalgebra[8] of the color group [34]. Here, for simplicity, we consider

[5] We shall assume for the sake of clarity that $\varphi_{\rm min} = 0$ for all fields $\varphi = \bar{c},\ c,\ ih$.

[6] It is important to note here that $\bar{A}_{\rm s}$ is *not* assumed to be a minimum of $\tilde{\Gamma}[\bar{A}]$. On the contrary, by definition of a self-consistent background, $a = 0$ *is* the minimum of $\Gamma_{\bar{A}_{\rm s}}[a]$.

[7] This property can be shown in the $m_0 = 0$ case, though, it is not clear how to enforce it in the present $m_0 \neq 0$ case. See discussion in Appendix. G.

[8] We recall that the Cartan subalgebra of a group is defined by the generators of the Lie algebra t^a_C that satisfy $[t^a_C, t^b_C] = 0$.

only the case of SU(2). For a generalization to SU(3) and other groups see [95] and Appendix H. Among the three SU(2) generators (in the Cartesian basis) (t^1, t^2, t^3) defined in Sec. I.1 of Chapter. I, we choose $t^3 = \sigma^3/2$, where $\sigma^3 = \mathrm{diag}(1, -1)$ is the third Pauli matrice, as the generator of the one-dimensional SU(2) Cartan subalgebra. Hereby, we set $\bar{A}_0 = \bar{A}_0^3 t^3$. We also define

$$r = g_0 \beta \bar{A}_0^3 \,, \tag{III.4.17}$$

as well as the background field potential [93, 33, 35]

$$V(r) = \frac{1}{\beta\Omega} \tilde{\Gamma}[\bar{A}] \,, \tag{III.4.18}$$

where Ω is the spatial volume. Accordingly, one tries to find $r_{\min}$ that minimizes $V(r)$, which can be computed by means of continuum methods, e.g. in perturbation theory as done in [93, 94].

As emphasized earlier, the center symmetry is encoded into the background gauge symmetry Eq. (III.4.9). To see this, consider gauge transformations of the peculiar form

$$U(\tau, \mathbf{x}) = \exp\{i\tau\phi/\beta\} \,, \tag{III.4.19}$$

where $\phi = \phi^3 t^3$ is a constant element of the SU(2) Cartan subalgebra. For $U(\tau, \mathbf{x})$ of the form (III.4.19), the background field is changed under a background gauge transformation (III.4.4) as

$$\bar{A}_0^3 \to \bar{A}_0^3 + \frac{\phi^3}{\beta g_0} \Rightarrow r \to r + \phi^3 \,. \tag{III.4.20}$$

Moreover, for $U(\tau, \mathbf{x})$ of the form (III.4.19), we have that

$$\begin{aligned} U(\tau + \beta, \mathbf{x})^\dagger U(\tau, \mathbf{x}) &= \exp\left[i\phi^3 t^3\right] \\ &= \mathbb{1} \cos\left[\frac{\phi^3}{2}\right] + \sigma^3 i \sin\left[\frac{\phi^3}{2}\right] . \end{aligned} \tag{III.4.21}$$

Thus, standard periodic boundary conditions require that $\phi^3 = 0 \mod[4\pi]$, while periodic boundary conditions up to a center element (for SU(2) the center is given by $\mathbb{Z}_2 = \{+1, -1\}$) necessitate $\phi^3 = 2\pi \mod[4\pi]$. Therefore, owing to the background gauge symmetry, Eq. (III.4.11), the $\mathbb{Z}_2$-center symmetry implies that the background potential $V(r)$ is 2π-periodic in r. Moreover, the gauge-fixed action is invariant under the charge-conjugation transformation[9] [93] $\bar{A}_\mu \to -\bar{A}_\mu$, $\varphi \to -\varphi^\dagger$ that yields the parity symmetry of the potential (III.4.18) under $r \to -r$. Hereby, it is sufficient to study the background potential $V(r)$ on the interval $r \in [0, \pi]$ [93, 94, 95]. In particular, the above properties of parity and 2π-periodicity imply that $r = 0$ and $r = \pi$ are always extrema of $V(r)$, where $r = \pi$ is the $\mathbb{Z}_2$-center symmetric point [95] (see also Eq. (III.4.22) below).

We recall that, physical observables have to be evaluated at the physical point $r = r_{\min}$ (or equivalently, $\bar{A} = \bar{A}_{\min}$). Following the discussion above, the value $r_{\min}$

[9] In SU(2), this corresponds to a global color rotation.

(or equivalently, $\bar{A}_{\min}$) constitutes an order parameter for the realization of the center symmetry [95, 226]. In the present case, for gauge group SU(2), $r_{\min} = \pi$ corresponds to the phase where the center symmetry is realized, while it is spontaneously broken for $r_{\min} \in [0, \pi[$. Note that, in particular, the Landau gauge corresponds to $\bar{A} = 0$. The general discussion presented here has been generalized for SU(3) and other gauge groups in [95], see also [34].

III.4.3 The background potential at two-loop order and the phase transition

In the previous sections, we saw that the inclusion of a background field configuration $\bar{A}_\mu$ eventually leads to the calculation of the background field potential $V(r)$ that needs to be minimized in order to evaluate physical observables. In particular, it is interesting to investigate the behavior of the Polyakov loop. At tree-level, it is given by, see Eq. (III.4.12),

$$\ell = \frac{1}{2}\mathrm{tr}\exp[ir_{\min}t^3] = \cos\frac{r_{\min}}{2}\,. \tag{III.4.22}$$

Hence, as expected, the center symmetric point $r_{\min} = \pi$ yields a vanishing Polyakov loop, which signals the confined phase. In contrast, for $r_{\min} \in [0, \pi[$ the $\mathbb{Z}_2$-center symmetry is spontaneously broken and a nonzero Polyakov loop develops, signaling the deconfined phase.

In practice, the background field potential has been computed up to two-loop order in [94] for SU(2) and in [95] for SU(3) and other gauge groups. A second-order phase transition was found, as expected, for SU(2), see Fig. III.6, with a critical temperature of $T_c = 0.285$ GeV for $m \simeq 0.68$ GeV and $g \simeq 7.5$. These values of the parameter were inferred from lattice calculations of ghost and gluon propagators in the Landau gauge at vanishing temperature. The second order character of the phase transition can directly be observed at the level of the order parameter $r_{\min}(T)$, which is a continuous function of T but presents a cusp at the critical temperature, as depicted in Fig. III.7.

It is worth mentioning that, at asymptotically high temperatures, the background reaches a finite value r_∞ given by [94]

$$\frac{r_\infty}{\pi} = 1 - \sqrt{\frac{8\pi^2 + g^2}{8\pi^2 + 7g^2}}\,. \tag{III.4.23}$$

This is a two-loop feature, while at one-loop order one has $r_\infty = 0$ [93]. Notice that, the limit (III.4.23) ignores possible high temperature RG or resummation effects. In particular, with the development (III.4.23), one has that $r_\infty \to 0$ as $g \to 0$. Remark that, after the critical temperature, $r_{\min}(T)$ displays a slight nonmonotonous behavior before reaching its asymptotic value r_∞.

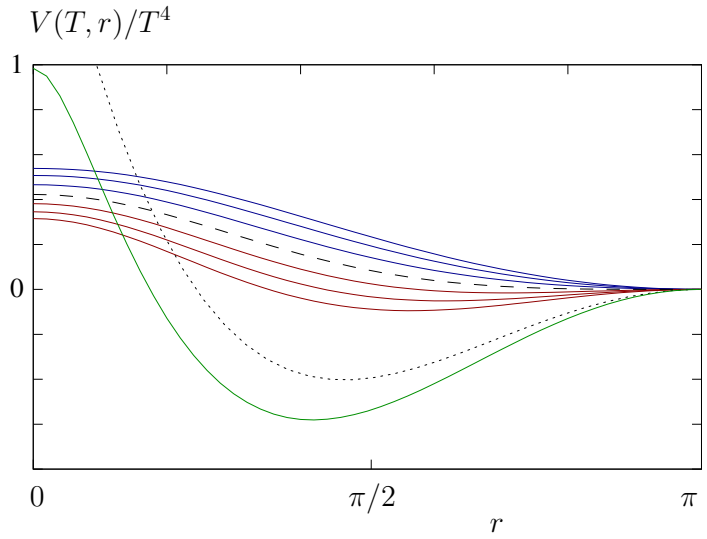

Figure III.6: Rescaled two-loop background field potential $V(T,r)/T^4$ for various temperatures, below (blue) and above (red) the critical temperature (dashed black). The green curve corresponds to a higher temperature and shows the approach to the asymptotic infinite temperature limit (dotted line). All curves have been shifted by their respective values at $r = \pi$ for clarity. Original figure taken from [94].

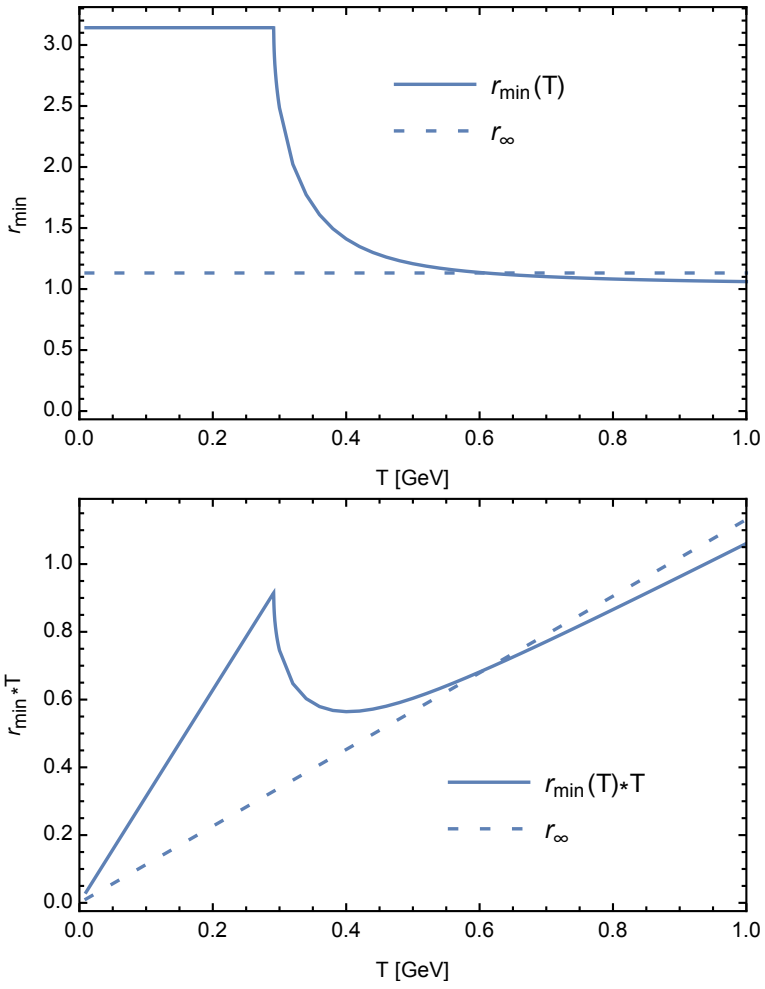

Figure III.7: The physical background $r_{\min}(T)$ and its asymptotic value r_∞, Eq. (III.4.23), for the SU(2) theory as a function of the temperature, obtained from the minimization of the potential (III.4.18) at two-loop order (top panel). For $T < T_c$, the minimum sits at the Z_2-symmetric point $r = \pi$. The symmetry is spontaneously broken for $T > T_c$ and the transition is continuous. The bottom plot shows the dimensionful background $= r_{\min}(T)T \propto \bar{A}_{\min}(T)$.

III.5 Propagators at one-loop order in the LDW gauge

In this section we present in detail our work realized in [96]. It consists in the computation of the YM propagators at one-loop order (that is next-to-leading order) in the massive LDW gauge for the SU(2) theory. We are mostly interested in investigating the possible signals of the phase transition that the correlators might display. Here and in the following, we note the background r but it is implicitly understood that eventually all the quantities computed shall be evaluated for $r = r_{\min}$. For practical aspects, we use $r_{\min}$ that minimizes the two-loop (i.e. next-to-leading order) background potential computed in [94]. The obtained $r_{\min}(T)$ is depicted in Fig. III.7. First, in Sec. III.5.1, we review some implications of the presence of the background field and in particular we give the Feynman rules of the theory [94]. Then, we proceed to the one-loop calculations of the various correlators in Sec. III.5.2 and finally present our results in Sec. III.5.4.

III.5.1 Canonical basis and Feynman rules

The background field $\bar{A}_\mu = \bar{A}_0^3 t^3 \delta_{\mu 0}$ introduces a preferred direction in color space. For instance, let us consider the action of the background covariant derivative $\bar{D}_\mu$ on a field φ. It reads in color component

$$\left(\bar{D}_\mu \varphi\right)^a = \partial_\mu \varphi^a + g_0 \delta_{\mu 0} f^{a3c} \bar{A}_0^3 \varphi^c \,. \tag{III.5.1}$$

Hereby, the different color modes couple differently to the background that lifts their degeneracy and induces a nontrivial color structure of the various correlators (in particular the color mode 3 does not receive any contribution from the background in Eq. (III.5.1)). Thus, one sees that the standard Cartesian basis t^a is not the most appropriate to derive the Feynman rules. Instead, we work in the so-called canonical (or Cartan-Weyl) bases [94, 95], which diagonalize the background covariant derivative $\bar{D}_\mu$. In the following, we work with the same choice of SU(2) Cartan subalgebra as previously, with generator $t^3 = \sigma^3/2$. A canonical basis is given by

$$t^0 = t^3 \,, \quad t^\pm = \frac{t^1 \pm i t^2}{\sqrt{2}}, \tag{III.5.2}$$

which satisfies

$$[t^\kappa, t^\lambda] = \varepsilon^{\kappa\lambda\tau} t^{-\tau} \quad \text{and} \quad \mathrm{tr}\{t^\kappa t^{-\lambda}\} = \frac{\delta^{\kappa\lambda}}{2} \,, \tag{III.5.3}$$

with $\kappa, \lambda, \tau \in \{0, +, -\}$ and where $\varepsilon^{\kappa\lambda\tau}$ is the completely antisymmetric tensor, with $\varepsilon^{0+-} = 1$. Nevertheless, for the sake of keeping notations as closed as possible to the standard ones, in the following we note the structure constant $f^{\kappa\lambda\tau}$. In particular, the structure constant satisfies

$$(f^{\kappa\lambda\tau})^* = -f^{(-\kappa)(-\lambda)(-\tau)} = f^{\kappa\lambda\tau}. \tag{III.5.4}$$

Fields that are in the adjoint representation can accordingly be decomposed as $\varphi = \varphi^\kappa t^\kappa$. From now on, we shall always assume that we are in the canonical basis. In

Fourier space, with the convention $\partial_\mu \to -iK_\mu$, the action of the background covariant derivative reduces to

$$(\bar{D}_\mu\varphi)^\kappa \to -iK_\mu^\kappa\varphi^\kappa(K), \tag{III.5.5}$$

where $K_\mu^\kappa = K_\mu + \kappa r T\delta_{\mu 0}$ defines a generalized momentum.[10] As explained in [94], the latter is conserved by virtue of the invariance under translations in Euclidean space and under the residual global SO(2) symmetry corresponding to those color rotations that leave the background invariant. The index $\kappa = 0, \pm$ labels the corresponding Noether charges and we see that the covariant derivative simply shifts the Matsubara frequencies of the charged color modes by $\pm rT$. Hereby, we shall sometimes use a short-hand notation for the background covariant derivative in the canonical basis as (no sum over κ)

$$(\bar{D}_\mu\varphi)^\kappa \equiv \partial_\mu^\kappa\varphi^\kappa\,. \tag{III.5.6}$$

We now present the Feynman rules in the canonical basis. We use the same notations and conventions as those introduced in Sec. III.1. The tree-level propagators, see Fig. III.8, read

$$\langle c^{-\kappa}(-K)\bar{c}^\kappa(K)\rangle = G_0(K^\kappa)\,, \tag{III.5.7}$$

$$\langle a_\mu^{-\kappa}(-K)a_\nu^\kappa(K)\rangle = P_{\mu\nu}^\perp(K^\kappa)G_{m_0}(K^\kappa)\,, \tag{III.5.8}$$

where $P_{\mu\nu}^\perp(K) = \delta_{\mu\nu} - K_\mu K_\nu/K^2$ was defined in Eq. (III.1.6) and

$$G_{m_0}(K) \equiv \frac{1}{K^2 + m_0^2}\,. \tag{III.5.9}$$

The gluon propagator in each color mode is transverse with respect to the corresponding generalized momentum. Notice also that, thanks to the identity

$$(-K_\mu)^{-\kappa} = -K_\mu^\kappa\,, \tag{III.5.10}$$

the orientation of the generalized momentum in the diagrams of Fig. III.8 is arbitrary.

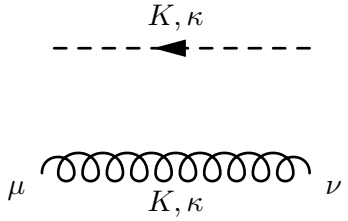

Figure III.8: Diagrammatic representation of the ghost (dashed) and gluon (wiggly) propagators for momentum K and color charge κ. The common orientation of the flow of momentum and color charge is arbitrary.

The interaction vertices are displayed in Figs. III.9 and III.10 and are the standard YM ones, that is, the ghost-antighost-gluon vertex, as well as the three- and four-gluon vertices. The conservation of the color charge is encoded in the fact that $f^{\kappa\lambda\tau}$ is zero unless $\kappa + \lambda + \tau = 0$. The expression of the ghost-anthighost-gluon vertex is

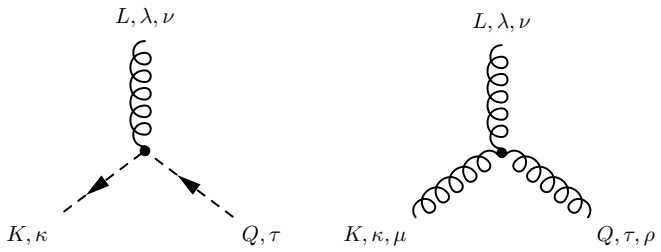

Figure III.9: Diagrammatic representation of the cubic vertices. All momenta and color charges are either outgoing or ingoing.

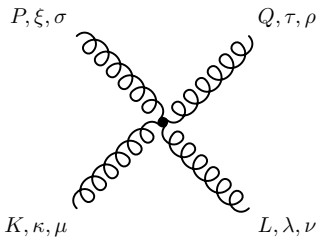

Figure III.10: Diagrammatic representation of the four-gluon vertex. All momenta and color charges are either outgoing or ingoing.

$$g_0 f_{\kappa\lambda\tau} K^{\kappa}_{\mu}\,, \tag{III.5.11}$$

where we use as convention that momenta and color charges are all either outgoing or ingoing. With similar conventions, the three gluon vertex reads

$$\frac{g_0}{6} f_{\kappa\lambda\tau}\Big[\delta_{\mu\rho}(K^{\kappa}_{\nu} - Q^{\tau}_{\nu}) + \delta_{\mu\nu}\Big(L^{\lambda}_{\rho} - K^{\kappa}_{\rho}\Big) + \delta_{\rho\nu}\Big(Q^{\tau}_{\mu} - L^{\lambda}_{\mu}\Big)\Big]. \tag{III.5.12}$$

The structure constants ensure that the color charges are conserved at both cubic vertices, which, together with the usual conservation of momenta, leads to the conservation rule for the generalized momenta: $K^{\kappa} + Q^{\tau} + L^{\lambda} = 0$. Finally, the four-gluon vertex, represented in Fig. III.10 with all momenta and charges outgoing/ingoing, is given by

$$\begin{aligned}\frac{g_0^2}{24}\sum_{\eta}\Big[&f_{\kappa\lambda\eta} f_{\tau\xi(-\eta)}\left(\delta_{\mu\rho}\delta_{\nu\sigma} - \delta_{\mu\sigma}\delta_{\nu\rho}\right) + f_{\kappa\tau\eta} f_{\lambda\xi(-\eta)}\left(\delta_{\mu\nu}\delta_{\rho\sigma} - \delta_{\mu\sigma}\delta_{\nu\rho}\right)\\ &+ f_{\kappa\xi\eta} f_{\tau\lambda(-\eta)}\left(\delta_{\mu\rho}\delta_{\nu\sigma} - \delta_{\mu\nu}\delta_{\sigma\rho}\right)\Big].\end{aligned} \tag{III.5.13}$$

[10] We reserve the set of greek letters (μ, ν, ρ, σ) to denote Euclidean space indices and the other set $(\kappa, \lambda, \eta, \xi, \tau)$ to denote color states. With this convention, K_{μ} denotes the μ component of the four-vector K, whereas K^{κ} refers to the shifted momentum $K + \kappa g_0 \bar{A} n$ with $n = (1, \mathbf{0})$.

Again, color charge and momentum conservation lead to $K^\kappa + Q^\tau + L^\lambda + P^\xi = 0$. We now apply these Feynman rules to the computation of the two-point correlators of the theory at one-loop order.

We follow the same definitions for the propagators and self-energies as those presented in Sec. III.1, but here we take care of the nontrivial color structure. The residual global SO(2) symmetry, corresponding to the color rotations that leave the background invariant, guarantees that these are "diagonal" in color space [94], in the sense

$$\mathcal{G}^{\kappa\lambda}(K) = \delta^{-\kappa,\lambda}\mathcal{G}^\lambda(K)\ , \quad \mathcal{G}^{\kappa\lambda}_{\mu\nu}(K) = \delta^{-\kappa,\lambda}\mathcal{G}^\lambda_{\mu\nu}(K) \tag{III.5.14}$$

and (note the different choice of label for the diagonal components)

$$\Sigma^{\kappa\lambda}(K) = \delta^{-\kappa,\lambda}\Sigma^\kappa(K)\ , \quad \Pi^{\kappa\lambda}_{\mu\nu}(K) = \delta^{-\kappa,\lambda}\Pi^\kappa_{\mu\nu}(K). \tag{III.5.15}$$

With these conventions, we have for the ghost propagator

$$\mathcal{G}^\lambda(K) = \frac{1}{(K^\lambda)^2 + g_0^2\Sigma^\lambda(K)} \tag{III.5.16}$$

and for the ghost dressing function at vanishing Matsubara frequency (no sum over λ)

$$F^\lambda(\omega = 0, k) = \left[K_\lambda^2\,\mathcal{G}^\lambda(K)\right]\Big|_{\omega=0}\ , \tag{III.5.17}$$

where we noted $K_\lambda^2 = (K^\lambda)^2 = K_\mu^\lambda K_\mu^\lambda$ (no sum over λ) and where we have extracted a factor g_0^2 for later convenience. As for the Landau gauge gluon propagator, the LDW gauge condition (III.4.1) implies that $\mathcal{G}^\lambda_{\mu\nu}(K)$ is transverse with respect to the generalized momentum (no sum over λ): $K_\mu^\lambda\,\mathcal{G}^\lambda_{\mu\nu}(K) = \mathcal{G}^\lambda_{\mu\nu}(K)\,K_\nu^\lambda = 0$. It thus admits the following tensorial decomposition

$$\mathcal{G}^\lambda_{\mu\nu}(K) = \mathcal{G}^\lambda_T(K)P^T_{\mu\nu}(K^\lambda) + \mathcal{G}^\lambda_L(K)P^L_{\mu\nu}(K^\lambda)\,, \tag{III.5.18}$$

where $P^T_{\mu\nu}(K)$ and $P^L_{\mu\nu}(K)$ are the transverse and longitudinal projectors (III.1.5), (III.1.6). It follows, in particular, that $\mathcal{G}^\lambda_{\mu\nu}(K) = \mathcal{G}^\lambda_{\nu\mu}(K)$. In terms of the projected self-energies

$$\Pi^\lambda_T(K) \;=\; \frac{P^T_{\mu\nu}(K^\lambda)\Pi^\lambda_{\mu\nu}(K)}{d-2}\,, \tag{III.5.19}$$

$$\Pi^\lambda_L(K) \;=\; P^L_{\mu\nu}(K^\lambda)\Pi^\lambda_{\mu\nu}(K)\,, \tag{III.5.20}$$

the scalar components of the gluon propagator read

$$\mathcal{G}^\lambda_{T/L}(K) = \frac{1}{(K^\lambda)^2 + m_0^2 + g_0^2\Pi^\lambda_{T/L}(K)}. \tag{III.5.21}$$

Finally, from Eq. (III.5.14), the propagators are real and have the property

$$\mathcal{G}^\lambda(K) = \mathcal{G}^{-\lambda}(-K)\,, \tag{III.5.22}$$

$$\mathcal{G}^\lambda_{T/L}(K) = \mathcal{G}^{-\lambda}_{T/L}(-K)\,, \tag{III.5.23}$$

and similarly for the self-energies.[11]

[11] According to the definition of the group generators in the canonical basis, (III.5.2), one has that

III.5.2 One-loop calculations

In this section, we compute the one-loop contribution to the ghost and gluon self-energies. The corresponding Feynman diagrams are depicted in Fig. III.11 and Fig. III.12. The diagrams are identical to those of the usual Landau gauge, but the rules are those of the LDW gauge. We detail here the computation of the diagram depicted in Fig. III.11 that contributes to the ghost self-energy. The calculation for the gluon sector goes along the same lines and is detailed in Appendix. I. Remarkably, the expressions of the various one-loop self-energies can be written into a readable form by means of simple scalar sum-integrals, see Eqs. (III.5.32), (III.5.36). The calculation of the relevant sum-integrals are detailed in Appendix J.

III.5.2.1 One-loop Feynman diagrams

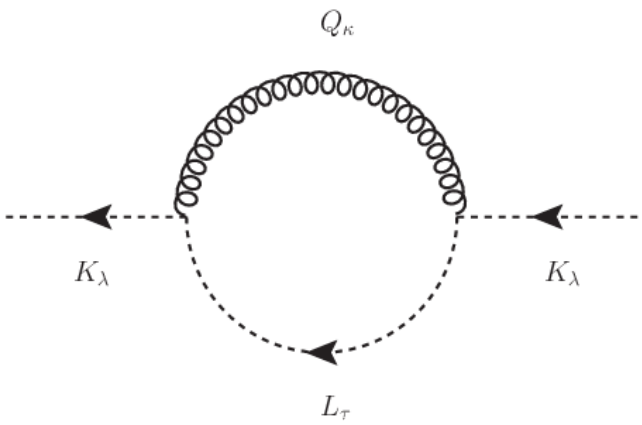

Figure III.11: One-loop contribution to the ghost self-energy. We take the convention that all momenta and color charges flow from the right vertex to the left vertex.

We note $K = (\omega, \mathbf{k})$ and λ the external momentum and color charge, and $K^\lambda = (\omega^\lambda, \mathbf{k})$ the corresponding shifted/generalized momentum. The internal loop momentum is denoted $Q \equiv (\omega_n, \mathbf{q})$ and the shifted/generalized one $Q^\kappa = (\omega_n^\kappa, \mathbf{q})$, with the Matsubara frequency $\omega_n \equiv 2\pi n T$, $n \in \mathbb{Z}$. Finally we use the notation

$$\int_Q f(Q) \equiv \mu^{2\epsilon} T \sum_{n\in\mathbb{Z}} \int \frac{d^{d-1}q}{(2\pi)^{d-1}} f(\omega_n, \mathbf{q}) \,, \tag{III.5.24}$$

where μ is the arbitrary scale associated with dimensional regularization ($d = 4 - 2\epsilon$).

A direct application of the Feynman rules of Sec. III.5.1 to the diagram of Fig. III.11

$t_\kappa^\dagger = t_{-\kappa}$. We thus have $\varphi_\kappa^* = \varphi_{-\kappa}$ for the Hermitian matrix fields $\varphi = (a_\mu, c, \bar{c}, h)$ or, in momentum space, $\varphi_\kappa^*(Q) = \varphi_{-\kappa}(-Q)$. Using the ghost conjugaison symmetry $(c, \bar{c}) \to (\bar{c}, -c)$, one concludes that $\mathcal{G}^{\kappa\lambda}(K) = \mathcal{G}^{\lambda\kappa}(-K) = \left[\mathcal{G}^{(-\lambda)(-\kappa)}(K)\right]^*$ and $\mathcal{G}^{\kappa\lambda}_{\mu\nu}(K) = \mathcal{G}^{\lambda\kappa}_{\nu\mu}(-K) = \left[\mathcal{G}^{(-\lambda)(-\kappa)}_{\nu\mu}(K)\right]^*$. Eqs. (III.5.22) and (III.5.23) then follow from the properties (III.5.10) and (III.5.14) and the decomposition (III.5.18).

yields[12]

$$\Sigma^\lambda(K) = -\sum_{\kappa,\tau} f^{\lambda\kappa\tau} f^{(-\tau)(-\kappa)(-\lambda)} \int_Q P^\perp_{\mu\nu}(Q^\kappa)(-L)^{-\tau}_\mu K^\lambda_\nu G_m(Q^\kappa) G_0(L^\tau)\,, \quad \text{(III.5.25)}$$

where $K+Q+L=0$ and where the sum runs over all color states. Using the anti-symmetry of the structure constant tensor as well as the identities (III.5.4) and (III.5.10), we arrive at

$$\Sigma^\lambda(K) = -\sum_{\kappa,\tau} \mathcal{C}_{\kappa\lambda\tau} \int_Q P^\perp_{\mu\nu}(Q^\kappa) L^\tau_\mu K^\lambda_\nu G_m(Q^\kappa) G_0(L^\tau)\,, \quad \text{(III.5.26)}$$

with the totally symmetric tensor $\mathcal{C}_{\kappa\lambda\tau} = |f_{\kappa\lambda\tau}|^2$. As discussed previously, $f_{\kappa\lambda\tau}$ vanishes if $\kappa+\lambda+\tau \neq 0$, so does $\mathcal{C}_{\kappa\lambda\tau}$, which implies the conservation of the generalized momentum at the vertices: $Q^\kappa + K^\lambda + L^\tau = 0$. We note the close ressemblance of the above expression with the corresponding one-loop expression in the Landau gauge, see Eq. (15) of [83]. For instance, one checks that Eq. (III.5.26) reduces to the Landau gauge expression in the case of a vanishing background field. Using the conservation of the generalized momentum and the definition of $P^\perp_{\mu\nu}$, Eq. (III.1.6), the expression of the ghost self-energy reads

$$\Sigma^\lambda(K) = \sum_{\kappa,\tau} \mathcal{C}_{\kappa\lambda\tau} \int_Q \left(K^2_\lambda - \frac{(Q^\kappa \cdot K\lambda)^2}{Q^2_\kappa} \right) G_m(Q^\kappa) G_0(L^\tau)\,, \quad \text{(III.5.27)}$$

where $Q^\kappa \cdot K^\lambda = Q^\kappa_\mu K^\lambda_\mu$ and where, for simplicity, we noted $K^2_\lambda = (K^\lambda)^2 = K^\lambda_\mu K^\lambda_\mu$ (no sum over λ) and similarly for Q^2_κ. The denominator $1/Q^2_\kappa$ can be eliminated by using that (for $m_1 \neq m_2$)

$$G_{m_1}(Q^\kappa) G_{m_2}(Q^\kappa) = \frac{1}{m_2^2 - m_1^2} \left[G_{m_1}(Q^\kappa) - G_{m_2}(Q^\kappa) \right]. \quad \text{(III.5.28)}$$

Furthermore, writing

$$2Q^\kappa \cdot K^\lambda = L^2_\tau - K^2_\lambda - (Q^2_\kappa + m^2) + m^2, \quad \text{(III.5.29)}$$

we obtain

$$2Q^\kappa \cdot K^\lambda\, G_m(Q^\kappa) G_0(L^\tau) = G_m(Q^\kappa) - G_0(L^\tau) - (K^2_\lambda - m^2) G_m(Q^\kappa) G_0(L^\tau) \quad \text{(III.5.30)}$$

and, applying the same trick twice,

$$\begin{aligned} 4(Q^\kappa \cdot K^\lambda)^2 G_m(Q^\kappa) G_0(L^\tau) = &\left(K^2_\lambda - m^2 + 2Q_\kappa \cdot K_\lambda \right) \left(G_m(Q^\kappa) - G_0(L^\tau) \right) \\ &+ (K^2_\lambda - m^2)^2 G_m(Q^\kappa) G_0(L^\tau)\,. \end{aligned} \quad \text{(III.5.31)}$$

Finally, according to (III.5.28) and (III.5.31), the ghost self-energy rewrites as

$$\begin{aligned} \Sigma^\lambda(K) = \sum_{\kappa,\tau} \mathcal{C}_{\kappa\lambda\tau} \Bigg[&\frac{K^2_\lambda - m^2}{4m^2} \left(J^\kappa_m - J^\kappa_0 \right) - \frac{\omega^\lambda}{2m^2} \left(\tilde{J}^\kappa_m - \tilde{J}^\kappa_0 \right) \\ &+ \frac{K^4_\lambda}{4m^2} I^{\kappa\tau}_{00}(K) - \frac{\left(K^2_\lambda + m^2 \right)^2}{4m^2} I^{\kappa\tau}_{m0}(K) \Bigg], \end{aligned} \quad \text{(III.5.32)}$$

[12] Remark that, all quantities appearing here are bare quantities. Nevertheless, for the sake of clarity we anticipate the renormalization and note m instead of m_0 as previously.

where $K_\lambda^4 = (K_\lambda^2)^2$ and where we introduced the following scalar tadpole sum-integrals

$$J_m^\kappa = \int_Q G_m(Q^\kappa), \tag{III.5.33}$$

$$\tilde{J}_m^\kappa = \int_Q \omega^\kappa G_m(Q^\kappa), \tag{III.5.34}$$

as well as the scalar bubble sum-integral ($K+Q+L=0$)

$$I_{m_1m_2}^{\kappa\tau}(K) = \int_Q G_{m_1}(Q^\kappa) G_{m_2}(L^\tau). \tag{III.5.35}$$

Clearly, $I_{m_1m_2}^{\kappa\tau}(K) = I_{m_2m_1}^{\tau\kappa}(K)$. Moreover, it follows from the identity (III.5.10) and from $G_m(Q) = G_m(-Q)$ that $I_{m_1m_2}^{\kappa\tau}(-K) = I_{m_1m_2}^{(-\kappa)(-\tau)}(K)$. Similarly, one shows that $J_m^\kappa = J_m^{-\kappa}$ and $\tilde{J}_m^\kappa = -\tilde{J}_m^{-\kappa}$. Expression (III.5.32) resembles formally to its Landau gauge counterpart which is recovered for $r=0$ (see Eq. (22) of [83]). Apart from the expected presence of the background in the sum-integrals and external momentum, there is a specific contribution of the LDW gauge, namely the second term between brackets proportional to the shifted frequency[13] ω^λ.

More generally, the relationship between loop calculations in the Landau and in the LDW gauges has been discussed in [94]. In particular, the manipulations Eqs. (III.5.28)-(III.5.31), rely only on the conservation of the (here, generalized) momentum. The only difference concerns the fact that the integral $\int_Q (K\cdot Q)[G_0(Q) - G_m(Q)] = 0$, which appeared in the Landau gauge calculation, generalizes to $\int_Q (K^\lambda \cdot Q^\kappa)[G_0(Q^\kappa) - G_m(Q^\kappa)] \neq 0$ in the LDW gauge, from which arises in Eq. (III.5.32) the term proportional to the external shifted frequency ω^λ.

The one-loop Feynman diagrams contributing to the gluon self-energy are shown in Fig. III.12. The calculation of each diagram proceeds along the same lines as for the one appearing in the ghost self-energy. As before, the obtained expressions are similar to the corresponding ones in the Landau gauge, with the various momenta in the internal lines replaced by appropriate generalized momenta. The reduction to simple tadpole and bubble loop integrals is detailed in Appendix. I. Although the complete tensorial expression of the self-energy is shown there, it follows from Eqs. (III.5.19)–(III.5.21) that it is sufficient to retain only those contributions that are transverse with respect to the external generalized momentum K^λ. These read, using the same notational conventions as before,

$$\begin{aligned}\Pi_{T/L}^\lambda(K) = \sum_{\kappa,\tau} \mathcal{C}_{\lambda\kappa\tau} \Bigg\{ & \left(1 - \frac{K_\lambda^4}{2m^4}\right) \{I_{T/L}^\lambda\}_{00}^{\kappa\tau}(K) + \left(1 + \frac{K_\lambda^2}{m^2}\right)^2 \{I_{T/L}^\lambda\}_{m0}^{\kappa\tau}(K) + \frac{(K_\lambda^2+m^2)^2}{m^2} I_{m0}^{\kappa\tau}(K) \\ & - 2\left[d - 2 + \left(1 + \frac{K_\lambda^2}{2m^2}\right)^2\right] \{I_{T/L}^\lambda\}_{mm}^{\kappa\tau}(K) - K_\lambda^2 \left(4 + \frac{K_\lambda^2}{m^2}\right) I_{mm}^{\kappa\tau}(K) \\ & + (d-2) J_m^\kappa + \frac{K_\lambda^2 + m^2}{m^2}(J_m^\kappa - J_0^\kappa) - \frac{2\omega^\lambda}{m^2}(\tilde{J}_m^\kappa - \tilde{J}_0^\kappa) \Bigg\},\end{aligned} \tag{III.5.36}$$

[13] This term vanishes in the Landau gauge since $\tilde{J}_m^\kappa = 0$ for $r=0$, see (III.5.34).

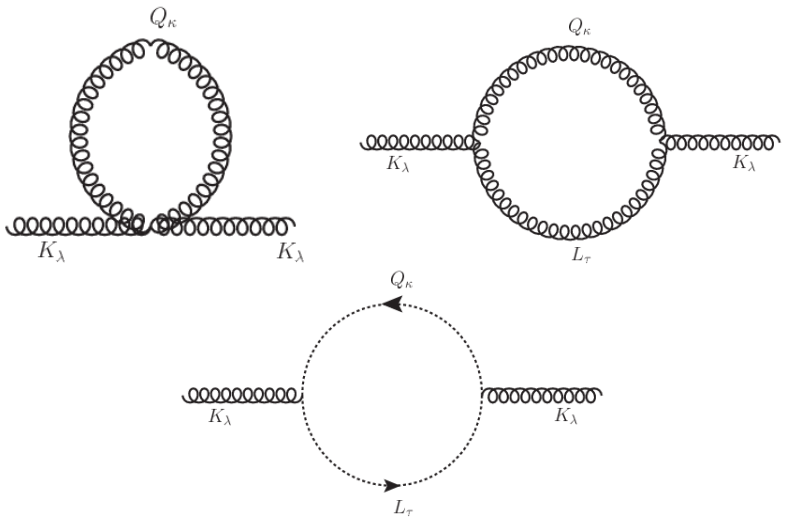

Figure III.12: One-loop diagrams for the gluon self-energy. For the last two diagrams, we take the convention that all momenta and color charges flow from the right vertex to the left vertex.

where we have introduced the following integrals

$$\{I_T^\lambda\}^{\kappa\tau}_{m_1m_2}(K) = \frac{P_{\mu\nu}^T(K^\lambda)\{I_{\mu\nu}\}^{\kappa\tau}_{m_1m_2}(K)}{d-2}\,, \tag{III.5.37}$$

$$\{I_L^\lambda\}^{\kappa\tau}_{m_1m_2}(K) = P_{\mu\nu}^L(K^\lambda)\{I_{\mu\nu}\}^{\kappa\tau}_{m_1m_2}(K)\,, \tag{III.5.38}$$

where

$$\{I_{\mu\nu}\}^{\kappa\tau}_{m_1m_2}(K) \equiv \int_Q Q_\mu^\kappa Q_\nu^\kappa G_{m_1}(Q^\kappa)G_{m_2}(L^\tau), \tag{III.5.39}$$

with $K+Q+L=0$. Using similar arguments as before, one easily shows that $\{I^\lambda_{T/L}\}^{\kappa\tau}_{m_1m_2}(K) = \{I^\lambda_{T/L}\}^{\tau\kappa}_{m_2m_1}(K) = \{I^\lambda_{T/L}\}^{(-\kappa)(-\tau)}_{m_1m_2}(-K)$. As for the ghost self-energy, only the third contribution on the second line, proportional to the external shifted frequency ω^λ is structurally new in the LDW gauge, see also Eq. (28) of [83].

III.5.2.2 Calculation of the sum-integrals

It remains to evaluate the scalar sum-integrals (III.5.33)–(III.5.35), and (III.5.37)–(III.5.38). This is detailed in Appendix. J. As an illustration, we explicitly compute here the simple tadpole integral Eq. (III.5.33). The Matsubara sum can be calculated analytically by means of standard integration contour technique [238, 83]: if $f(z)$ is a complex function with poles away from the Matsubara frequencies and that decreases fast enough as $|z|\to\infty$, we have

$$T\sum_n f(i\omega_n) = -\sum_{\omega\in\{\text{poles of f}\}} n(\omega)\,\text{Res}\, f|_\omega\,, \tag{III.5.40}$$

where $n_x = 1/(\exp(\beta x) - 1)$ is the Bose-Einstein distribution function. In this way we obtain for J_m^κ

$$J_m^\kappa = \int_{\mathbf{q}} \frac{n_{\varepsilon_{m,q} - i\kappa r T} - n_{-\varepsilon_{m,q} - i\kappa r T}}{2\varepsilon_{m,q}}\,, \tag{III.5.41}$$

where $\varepsilon_{m,q} \equiv \sqrt{q^2 + m^2}$ and $\int_{\mathbf{q}} = \int \frac{d^{d-1}q}{(2\pi)^{d-1}}$. Using that $n_{-x} = -1 - n_x$, Eq. (III.5.41) rewrites

$$J_m^\kappa = \int_{\mathbf{q}} \frac{1 + 2n_{\varepsilon_{m,q}}}{2\varepsilon_{m,q}}\,, \tag{III.5.42}$$

where the term 1 in the numerator of (III.5.42) corresponds to the vacuum contribution. The thermal contribution reads

$$J_m^\kappa \hat{=} \int_{\mathbf{q}} \mathrm{Re}\, \frac{n_{\varepsilon_{m,q} - i\kappa r T}}{\varepsilon_{m,q}} = \frac{1}{2\pi^2} \int_0^\infty dq\, q^2 \mathrm{Re}\, \frac{n_{\varepsilon_{m,q} - i\kappa r T}}{\varepsilon_{m,q}}\,. \tag{III.5.43}$$

where the symbol $\hat{=}$ means that we disregard vacuum contributions.[14] Vacuum contributions can be computed in a standard way by replacing Matsubara sums by frequency integrals $\int_Q \to \int \frac{d^d q}{(2\pi)^d}$. The previous tadpole integral reads in dimensional regularization ($d = 4 - 2\epsilon$)

$$J_m^{\mathrm{vac}} = \frac{\mu^{2\epsilon}\Gamma\left(1 - \frac{d}{2}\right)}{(4\pi)^{\frac{d}{2}}} (m^2)^{\frac{d}{2}-1} = -\frac{m^2}{16\pi^2}\left(\frac{1}{\epsilon} + \ln\frac{\bar{\mu}^2}{m^2} + 1\right) + \mathcal{O}(\epsilon)\,, \tag{III.5.44}$$

where we defined $\bar{\mu}^2 \equiv 4\pi\mu^2 e^{-\gamma}$ with γ the Euler constant. The vacuum part of the other sum-integrals (III.5.33)–(III.5.35), and (III.5.37)–(III.5.39) have been computed in [83]. Nevertheless, as emphasized below, in practice one does not need them explicitly. Indeed, at zero temperature the LDW reduces to the usual Landau gauge. For the present case, one can thus take them from the existing literature, see e.g. [79].

III.5.2.3 Background effects

A first nontrivial effect of the background can be directly read-off the loop contributions. As we have just presented, these can be recast under the form of sum-integrals that involve the Bose-Einstein distribution n_x. More precisely, the background appears as an imaginary chemical potential into the Bose-Einstein distribution: $n_{x - i\kappa r T}$, see Eq. (III.5.42) and Appendix J. In particular, in the low temperature phase where $r = \pi$, this leads to

$$n_{x - i\kappa\pi T} = -\frac{1}{\exp(\beta x) + 1}\,, \tag{III.5.45}$$

and one recognizes a Fermi-Dirac (with a wrong sign) distribution. Hereby, in the low temperature phase, the background changes the colorly charged bosonic degrees of freedom that run inside the loop into fermion-like fields[15]. Note that this feature holds true as long as the temperature is nonvanishing. Hence, although the Landau and LDW gauges are the same at zero temperature, they display a fundamental difference even at infinitely small temperatures.

[14] These are defined as the limit of the above expression as $T \to 0$ for fixed $\bar{A}$.

[15] Remark that, although ghosts are Grassmann fields, their thermal statistic follows the Bose-Einstein distribution [239].

III.5.3 Renormalization

We introduce renormalized parameters and fields, related to the corresponding bare quantities in the usual way:

$$m_0^2 = Z_{m^2} m^2 \,, \quad g_0 = Z_g g \,, \tag{III.5.46}$$

and

$$\begin{aligned} \bar{A} &= \sqrt{Z_{\bar{A}}}\, \bar{A}_R \quad , \qquad a = \sqrt{Z_a}\, a_R \,, \\ c &= \sqrt{Z_c}\, c_R \quad , \qquad \bar{c} = \sqrt{Z_c}\, \bar{c}_R \,, \end{aligned} \tag{III.5.47}$$

Notice that the background field $\bar{A}$ and the fluctuating field a receive independent renormalizations [240]. The background field gauge symmetry (III.4.11) implies that the product $g_0 \bar{A}$ is finite [118]. Imposing the renormalization condition

$$Z_g \sqrt{Z_{\bar{A}}} = 1 \tag{III.5.48}$$

for the finite parts as well, we have $g_0 \bar{A} = g \bar{A}_R$.

We define the renormalized self-energies $\Sigma_R^\lambda(K)$ and $\Pi_{R,T/L}^\lambda(K)$ from the renormalized propagators

$$\mathcal{G}_R^\lambda(K) = Z_c^{-1} \mathcal{G}^\lambda(K) \tag{III.5.49}$$

$$\mathcal{G}_{R,T/L}^\lambda(K) = Z_A^{-1} \mathcal{G}_{T/L}^\lambda(K) \tag{III.5.50}$$

as in Eqs. (III.5.16) and (III.5.21) by simply replacing $m_0^2 \to m^2$ and $g_0 \to g$ (we already anticipated this replacement in the loop expressions evaluated above). Following the structure of the sum-integrals defined in the previous section, [see Appendix J], one can separate a thermal and a vacuum contribution as

$$\Sigma_R^\lambda(K) = \Sigma_R^{\lambda,\mathrm{th}}(K) + \Sigma_R^{\mathrm{vac}}(K_\lambda^2), \tag{III.5.51}$$

and similarly for $\Pi_{R,T/L}^\lambda(K)$, with $\Pi_{R,T/L}^{\mathrm{vac}}(K^2) = \Pi_R^{\mathrm{vac}}(K^2)$ by Euclidean symmetry. The vacuum parts are defined as the $T = 0$ contributions at *fixed* background field $\bar{A}_R$. The background-field gauge symmetry (III.4.11) guarantees that these only depend on $\bar{A}_R$ through the shifted momentum, as emphasized in the notation of Eq. (III.5.51). The functions $\Sigma_R^{\mathrm{vac}}(K^2)$ and $\Pi_R^{\mathrm{vac}}(K^2)$ are thus nothing but the renormalized self-energies in the (massive) Landau gauge and one can write

$$\mathcal{G}_R^\lambda(K) = \frac{1}{K_\lambda^2 F_{R,\mathrm{vac}}^{-1}(K_\lambda^2) + g^2 \Sigma_R^{\lambda,\mathrm{th}}(K)} \tag{III.5.52}$$

$$\mathcal{G}_{R,T/L}^\lambda(K) = \frac{1}{\mathcal{G}_{R,\mathrm{vac}}^{-1}(K_\lambda^2) + g^2 \Pi_{R,T/L}^{\lambda,\mathrm{th}}(K)} \tag{III.5.53}$$

where $F_{R,\mathrm{vac}}(K^2)$ and $\mathcal{G}_{R,\mathrm{vac}}(K^2)$ are, respectively, the zero-temperature renormalized ghost dressing function and gluon propagator in the Landau gauge. For later convenience, we also define the renormalized ghost dressing function at vanishing Matsubara frequency (no sum over λ)

$$F_R^\lambda(\omega = 0, k) = \left[K_\lambda^2 \, \mathcal{G}_R^\lambda(K) \right] \Big|_{\omega = 0} \,. \tag{III.5.54}$$

The zero-temperature Landau gauge $F_{R,\mathrm{vac}}(K^2)$ and $\mathcal{G}_{R,\mathrm{vac}}(K^2)$ have been computed at one-loop order in the CF model (i.e., the Landau gauge limit of the present model) for the groups SU(N) in [79] using the set of renormalization conditions

$$\Sigma_R^{\mathrm{vac}}(K^2=\mu^2) = \Pi_R^{\mathrm{vac}}(K^2=0) = \Pi_R^{\mathrm{vac}}(K^2=\mu^2) = 0, \tag{III.5.55}$$

where μ is the renormalization scale. In principle one could implement temperature and/or background-field dependent renormalization conditions. For instance we have investigated a renormalization scheme defined as $\Sigma_R^{\lambda=0}(K^2=\mu^2) = \Pi_{R,L}^{\lambda=0}(K^2=0) = \Pi_{R,L}^{\lambda=0}(K^2=\mu^2) = 0 \ \forall T$ but no qualitative changes were observed. Remark however that there is a large number of choices of such renormalization schemes owing to the number of nondegenerate color modes λ and the thermal asymmetry T/L of the gluon self-energy. For simplicity we use the set of renormalization conditions (III.5.55). The one-loop vacuum ghost dressing function and gluon propagator in Eqs. (III.5.52) and (III.5.53) can thus be taken from Eqs. (17) of [79], which we recall here for completeness:

$$F^{-1}_{R,\mathrm{vac}}(p) = 1 + \frac{g^2 N}{64\pi^2}\Big[f(p^2/m^2) - f(\mu^2/m^2)\Big] \tag{III.5.56}$$

$$G^{-1}_{R,\mathrm{vac}}(p) = p^2 + m^2 + \frac{g^2 N p^2}{384\pi^2}\Big[g(p^2/m^2) - g(\mu^2/m^2)\Big], \tag{III.5.57}$$

where

$$f(s) = -s\log s + (s+1)^3 s^{-2}\log(s+1) - s^{-1} \tag{III.5.58}$$

and

$$\begin{aligned} g(s) = {} & 111 s^{-1} - 2s^{-2} + (2-s^2)\log s + 2(s^{-1}+1)^3\Big(s^2 - 10s + 1\Big)\log(1+s) \\ & + (4s^{-1}+1)^{3/2}\Big(s^2 - 20s + 12\Big)\log\left(\frac{\sqrt{4+s}-\sqrt{s}}{\sqrt{4+s}+\sqrt{s}}\right). \end{aligned} \tag{III.5.59}$$

In general, a fifth prescription is needed for the coupling renormalization factor Z_g. One could, for instance, use a background field generalization of the Taylor scheme [116] often used in the Landau gauge and its massive extension [79], see also Sec. II.5.4 of Chapter. II. However, this is not needed at the order of approximation considered here. In the following, we simply set $Z_g \to 1$ in the one-loop expressions.

III.5.4 Results for the SU(2) theory

At the order of approximation considered here, we minimize the two-loop background field potential of the SU(2) theory computed in [94]. As already discussed above, the parameters used in this article, namely $g = 7.5$, $m = 0.68$ GeV, and $\mu = 1$ GeV, were taken from fits of the lattice ghost and gluon propagators in the Landau gauge at zero temperature [79]. This choice was motivated by the fact that, since the background $\bar{A} \propto T$, the LDW gauge reduces to the Landau gauge at $T = 0$, see also [83]. However, in the present case, this set of parameters leads to unphysical features for temperatures around T_c: the susceptibility of neutral color modes, defined below, turns negative, which yields a pole at nonvanishing momentum in the Euclidean

propagator at zero Matsubara frequency. This is a consequence of the too large value of the coupling [96].

Here, it is worth emphasizing that, although it makes sense to fit the zero temperature propagators of the LDW gauge against the lattice data in the Landau gauge, there is *a priori* no reason to expect the parameters not to vary with temperature. This could arise, for example, from renormalization group effects or from our assumption that the present massive model effectively accounts for Gribov ambiguities, which do depend on the Euclidean spacetime volume and thus on the temperature. As a matter of fact, fitting the one-loop propagators against lattice data in the Landau gauge at finite temperature [83] indeed reveals that the best value for the coupling decreases from $g \approx 7$ at $T = 0$ to about $g \approx 5$ close to T_c. At present, we have no way to predict the possible temperature dependence of our parameters and there exists no lattice data in the present LDW gauge. As a rough guide, we shall use the value $g(\mu) = 5$ at $\mu = 1$ GeV obtained for temperatures in the vicinity of T_c in [83] in the Landau gauge. We adjust the mass parameter accordingly to the value $m(\mu) = 0.75$ GeV such that the transition temperature remains fixed to $T_c^{\text{2loop}} = 0.285$ GeV, obtained from the minimization of the background effective potential at two-loop order [94], which agrees with the lattice results.

The background field $r = r_{\min}(T)$ that minimizes the two-loop potential of [94] is shown in Fig. III.7 as a function of temperature. It presents the characteristic cusp at the second order transition of the SU(2) theory. We also show the behavior of the dimensionful background rT, that is, the effective frequency shift for charged color modes, which contributes a term $(rT)^2$ to the tree-level square mass of the corresponding propagators at zero frequency, see Eqs. (III.5.16) and (III.5.21).

III.5.4.1 Gluon susceptibilities across the phase transition

Before discussing the complete momentum dependence of the various propagators, we consider the electric and magnetic gluon inverse square masses (susceptibilities) of the neutral gluon mode, which have simple expressions and which already exhibit the most salient features of the influence of the background field on the correlation functions. They are defined as

$$\chi^0_{T/L} = \mathcal{G}^0_{T/L}(\omega = 0, \mathbf{k} \to 0) = \frac{1}{m^2 + g^2 \Pi^{0,\text{th}}_{T/L}(0, \mathbf{k} \to 0)} \,. \tag{III.5.60}$$

In contrast, the thermal dependence of the zero momentum value of the (zero Matsubara frequency) charged gluon propagators does not come only from thermal loops but also receive a contribution from the vacuum part due to the frequency shift $\omega \pm rT$. Indeed, as emphasized above, the vacuum part of the self-energies is defined as their $T = 0$ contributions evaluated at *fixed* background $\bar{A}$, such that

$$\mathcal{G}^{\pm}_{T/L}(\omega = 0, \mathbf{k} \to 0) = \frac{1}{\mathcal{G}^{-1}_{\text{vac}}\left((rT)^2\right) + g^2 \Pi^{\pm,\text{th}}_{T/L}(0, \mathbf{k} \to 0)} \,. \tag{III.5.61}$$

In order to get rid of the thermal dependence coming from the nonvanishing shifted external frequency we also define, by analogy with Eq. (III.5.60), the inverse charged

gluon square masses from the corresponding propagators at vanishing shifted frequency:

$$\chi^{\lambda}_{T/L} = \mathcal{G}^{\lambda}_{T/L}(\omega = -\lambda r T, \mathbf{k} \to 0), \tag{III.5.62}$$

where the right-hand side is to be understood as the renormalized propagators (III.5.53) analytically continued to arbitrary (i.e., non Matsubara) Euclidean frequencies.[16] By abuse of language, we shall call these susceptibilities as well. By definition, their temperature dependence entirely comes from thermal loop effects since, just as for the neutral mode, their one-loop expressions involve diagrams with vanishing external frequency and momentum. In what follows, we shall use a more standard terminology and refer to the Debye and magnetic square masses,[17] respectively defined as $M^2_{\mathrm{D},\lambda} \equiv 1/\chi^{\lambda}_L$ and $M^2_{\mathrm{mag},\lambda} \equiv 1/\chi^{\lambda}_T$. We thus have

$$M^2_{\mathrm{D},\lambda}(T) = m^2 + g^2 \Pi^{\lambda,\mathrm{th}}_L(\omega = -\lambda r T, \mathbf{k} \to 0), \tag{III.5.63}$$

$$M^2_{\mathrm{mag},\lambda}(T) = m^2 + g^2 \Pi^{\lambda,\mathrm{th}}_T(\omega = -\lambda r T, \mathbf{k} \to 0). \tag{III.5.64}$$

In particular, Eq. (III.5.23) guarantees that $M^2_{\mathrm{D},+} = M^2_{\mathrm{D},-}$ and $M^2_{\mathrm{mag},+} = M^2_{\mathrm{mag},-}$. All these quantities involve loop integrals with vanishing external frequency/momentum, which at one-loop order, admit relatively simple expressions. These are derived in Appendix. K. Here, we give the results:

$$M^2_{\mathrm{D},0}(T) = m^2 - \frac{g^2 T^2}{8}\left\{ \left(1 - \frac{r}{\pi}\right)^2 - \frac{1}{3} - \frac{\pi^2 T^2}{m^2}\left[\left(1 - \frac{r}{\pi}\right)^4 - 2\left(1 - \frac{r}{\pi}\right)^2 + \frac{7}{15}\right]\right\} + \frac{g^2 m^2}{\pi^2}\int_0^\infty dq\, \frac{\mathrm{Re}\, n_{\varepsilon_{m,q} - irT}}{\varepsilon_{m,q}}\left(3 + 6\frac{q^2}{m^2} + \frac{q^4}{m^4}\right) \tag{III.5.65}$$

and

$$M^2_{\mathrm{mag},0}(T) = m^2 + \frac{g^2 T^2}{8}\left\{ \left(1 - \frac{r}{\pi}\right)^2 - \frac{1}{3} - \frac{\pi^2 T^2}{3m^2}\left[\left(1 - \frac{r}{\pi}\right)^4 - 2\left(1 - \frac{r}{\pi}\right)^2 + \frac{7}{15}\right]\right\} - \frac{g^2 m^2}{\pi^2}\int_0^\infty dq\, \frac{\mathrm{Re}\, n_{\varepsilon_{m,q} - irT}}{\varepsilon_{m,q}}\left(\frac{q^2}{m^2} + \frac{q^4}{3m^4}\right) \tag{III.5.66}$$

for the neutral sector, and

$$M^2_{\mathrm{D},\pm}(T) = m^2 - \frac{g^2 T^2}{16}\left\{ \left(1 - \frac{r}{\pi}\right)^2 + \frac{1}{3} - \frac{\pi^2 T^2}{m^2}\left[\left(1 - \frac{r}{\pi}\right)^4 - 2\left(1 - \frac{r}{\pi}\right)^2 - \frac{1}{15}\right]\right\} + \frac{g^2 m^2}{2\pi^2}\int_0^\infty dq\, \frac{n_{\varepsilon_{m,q}} + \mathrm{Re}\, n_{\varepsilon_{m,q} - irT}}{\varepsilon_{m,q}}\left(3 + 6\frac{q^2}{m^2} + \frac{q^4}{m^4}\right), \tag{III.5.67}$$

[16] The analytical continuation has to be understood after the Matsubara sums have been performed and the external Matsubara frequency has been removed from the thermal factors by means the identity $n_{\varepsilon + i\omega_n} = n_\varepsilon$.

[17] Strictly speaking the Debye and magnetic masses are the pole masses of the corresponding electric and magnetic propagators. Nevertheless, it is common to use this terminology for the zero momentum masses/susceptibilities [45].

$$M^2_{\mathrm{mag},\pm}(T) = m^2 + \frac{g^2T^2}{16}\left\{\left(1-\frac{r}{\pi}\right)^2 + \frac{1}{3} - \frac{\pi^2T^2}{3m^2}\left[\left(1-\frac{r}{\pi}\right)^4 - 2\left(1-\frac{r}{\pi}\right)^2 - \frac{1}{15}\right]\right\}$$
$$- \frac{g^2m^2}{2\pi^2}\int_0^\infty dq\, \frac{n_{\varepsilon_{m,q}} + \mathrm{Re}\, n_{\varepsilon_{m,q}-irT}}{\varepsilon_{m,q}}\left(\frac{q^2}{m^2} + \frac{q^4}{3m^4}\right), \tag{III.5.68}$$

for the charged ones.

We shall also consider the charged gluon at vanishing frequency in the limit of zero momentum Eq. (III.5.61). From the property (III.5.23), and using spatial isotropy, we conclude that the charged propagators at vanishing frequency are degenerate:

$$\mathcal{G}^+_{T/L}(0,\mathbf{k}) = \mathcal{G}^-_{T/L}(0,\mathbf{k}). \tag{III.5.69}$$

Moreover, the general tensorial decomposition Eq. (III.1.4) is trivially generalized to the present case. In particular, according to (III.1.4), and using the definitions of the transverse and longitudinal projections Eqs. (III.1.5) and (III.1.6), we have

$$T^\lambda_T(K) = T^\lambda_\delta(K), \tag{III.5.70}$$
$$T^\lambda_L(K) = T^\lambda_\delta(K) + \frac{k^2}{(\omega+\lambda rT)^2+k^2}T^\lambda_{\mathrm{n}}(K). \tag{III.5.71}$$

For the charged modes, $\lambda \neq 0$, this implies

$$T^\pm_L(0,\mathbf{k}\to 0) = T^\pm_T(0,\mathbf{k}\to 0). \tag{III.5.72}$$

Hereby, at zero Matsubara frequency and for vanishing momentum, the gluon propagator in the charged sector satisfies

$$\mathcal{G}^\pm_L(0,\mathbf{k}\to 0) = \mathcal{G}^\pm_T(0,\mathbf{k}\to 0). \tag{III.5.73}$$

Accordingly, we define $\mathcal{G}^\pm_{T/L}(0,\mathbf{k}\to 0) = 1/M^2_{\mathrm{ch}}$, that is,

$$M^2_{\mathrm{ch}}(T) = \mathcal{G}^{-1}_{\mathrm{vac}}\left((rT)^2\right) + g^2\Pi^{\pm,\mathrm{th}}_{T/L}(0,\mathbf{k}\to 0). \tag{III.5.74}$$

One checks from Eq. (III.5.36) that M^2_{ch} reduces to the (Landau gauge) magnetic square mass at vanishing background, as expected from Eq. (III.5.70).

We now present our results for the various square masses and susceptibilities defined above. We use the previous definitions Eqs. (III.5.65)–(III.5.68) and (III.5.74) where, it is understood that r is to be taken at the minimum $r_{\mathrm{min}}(T)$ of the background field potential. In order to quantify the effects of the nontrivial background, it is interesting to compare these results with those obtained in the Landau gauge (see Eqs. (31) and (35) of [83] with $N = 2$, which we recover for $r = 0$).

The temperature dependence of the neutral gluon inverse square masses (susceptibilities) across the phase transition is shown in Fig. III.13. We observe that the magnetic susceptibility is monotonously increasing with the temperature below T_c, whereas the electric one first slightly decreases at low temperatures and then increases

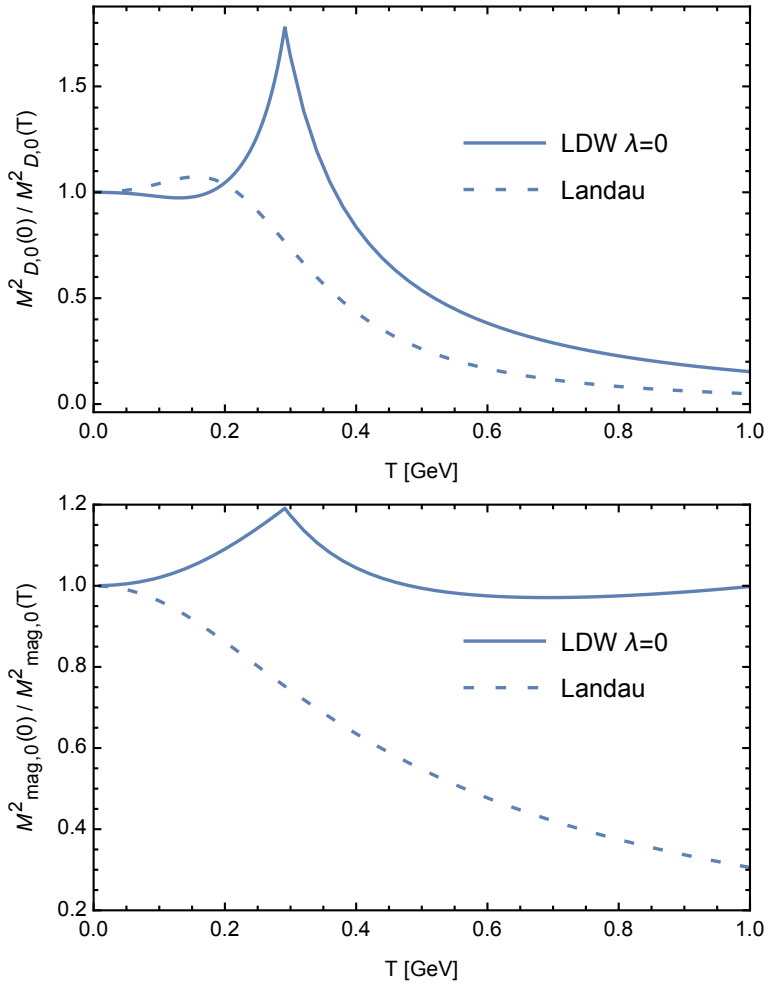

Figure III.13: Temperature dependence of the electric and magnetic inverse square masses in the neutral mode normalized to their common zero temperature value. To emphasize the effect of the Polyakov loop, we compare with the corresponding results at vanishing background field ($r = 0$), which corresponds to the Landau gauge.

to its maximum value at $T = T_c$. Both present a cusp at the transition. The electric square mass rapidly approaches a quadratic behavior $M^2_{\mathrm{D},0} \propto T^2$, whereas the magnetic mass remains essentially bounded in the range of temperature considered here.

The cusp reflects the nonanalytic behavior of the order parameter $r_{\min}(T)$ across the transition and is in sharp contrast with the corresponding perturbative results in the Landau gauge. The electric susceptibility in the Landau gauge showed a slight nonmonotonous behavior below T_c, but no cusp, in qualitative agreement with lattice results [90], see also Sec. III.3. As for the magnetic susceptibility, both the (massive) perturbative approach and the gauge-fixed lattice simulations show a smooth monotonous behavior in the Landau gauge, with a rapid decrease above T_c. This contrasts with the present results, where the magnetic susceptibility is essentially constant

in this range of temperature, see the bottom panel of Fig. III.13. More precisely, in the high temperature regime, the magnetic square mass was shown to increase as $g^2 mT$ in the Landau gauge [83]. This unbounded linear increasing eventually leads to a pole in the ghost dressing function as emphasized above, see also [83]. In the present case, the magnetic neutral mass remains bounded from above [96], thus avoiding the pole in the ghost sector, see below. Its high temperature behavior is given, by

$$M^2_{\mathrm{mag},0}(T) = m^2 \left\{ 1 + \frac{g^2 T(4M_+ + 5rT)}{12\pi(M_+ + rT)^2} - \frac{3g^2}{32\pi^2} \left[\ln\left(\frac{4\pi T}{m}\right)^2 + \Psi\left(\frac{r}{2\pi}\right) + \frac{5}{6} \right] + \mathcal{O}\left(\frac{m^2}{T^2}\right) \right\} , \tag{III.5.75}$$

where $M_+ = \sqrt{m^2 + (rT)^2}$ and $\Psi(z) = \psi(1+z) + \psi(1-z)$ with $\psi(z) = \Gamma'(z)/\Gamma(z)$, see Appendix E of [96]. Hereby, for $r \neq 0$, the leading term in Eq. (III.5.75) is the negative logarithm.[18] Eventually this leads at very high temperatures ($T \geq 10m \simeq 25T_c$) to a negative square mass, see Fig. III.14. Remark that it is expected in perturbation theory to encounter troubles at very high energies/temperatures if we do not add higher order terms or implement resummation techniques or RG effects. As a proof of principle, we employ the standard one-loop result for the running coupling constant in SU(2) and put by hand a temperature-dependent running

$$g(T) = \frac{g}{\sqrt{1 + \frac{11}{12\pi^2} g^2 \ln\left(\frac{T^2+m^2}{\mu}\right)}} , \tag{III.5.76}$$

with $\mu = 1$ GeV. As shown in Fig. III.14, with RG improvement, the magnetic square mass then remains positive.

The behavior of the charged square masses (III.5.67)and (III.5.68) can be readily understood from the various features of the curves shown in Fig. III.13, since, at one-loop order, from Eqs. (III.5.65)–(III.5.68), one has that [see Appendix. K]

$$M^2_{\mathrm{D},\pm} = \frac{M^2_{\mathrm{D},0} + M^2_{\mathrm{D},0}\big|_{r=0}}{2} , \tag{III.5.77}$$

and similarly for the magnetic mass. For completeness, these are plotted in Fig. III.15 together with the corresponding values in the absence of background.

[18] Remark that for $r = 0$, the first term becomes $g^2 T(4M_+ + 5rT)/12\pi(M_+ + rT)^2 \underset{r\to 0}{\to} g^2 T/3\pi m$ which overwhelms the logarithmic term and one recovers the linear increased found in the Landau gauge.

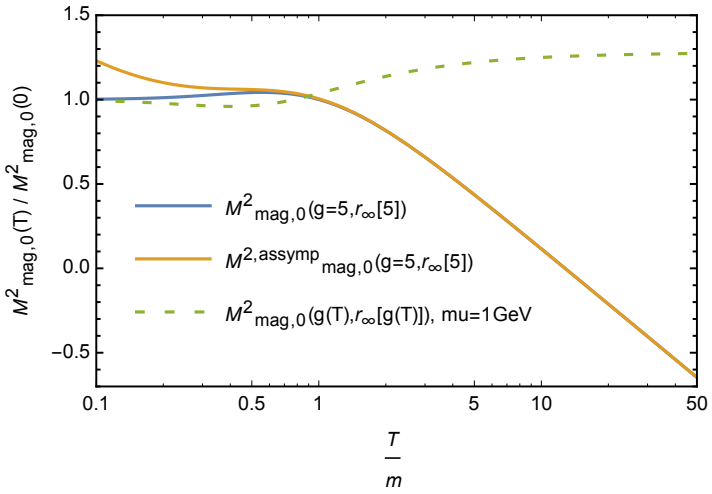

Figure III.14: The neutral magnetic gluon square mass as a function of T/m in the high temperature regime. We used $r = r_\infty(g)$, see Eq. (III.4.23). The magnetic square mass Eq. (III.5.66) (blue plain curve) is compared to its high temperature behavior Eq. (III.5.75) (yellow plain curve) both computed for $g = 5$. One sees that the leading logarithm eventually leads to negative values for sufficiently high temperatures. This artifact is cured by RG effects. To illustrate this, we put by hand a temperature dependent running coupling constant (dashed green curve) according to Eq. (III.5.76).

Finally we present in Fig. III.16 the temperature dependence of the charged square masse $M^2_{\mathrm{ch}}(T)$. Again here, the presence of a cusp at the critical temperature is inherited from that of the background. Note that, in contrast with what happens with the susceptibilities Figs. III.13, III.15, the cusp in the inverse zero-momentum square charged mass is oriented downwards. This can be understood from the fact that, M^2_{ch} possesses a background dependent tree-level part, namely $m^2 + (rT)^2$, which gives the dominant contribution, see Fig. III.7. We observe a rapid increase of $1/M^2_{\mathrm{ch}}$ above $2T_c$ and a pole at about $T \approx 0.9$ GeV. This results from the competition between the (positive) vacuum contribution and the (negative) thermal contribution in Eq. (III.5.74): M^2_{ch} turns negative in a finite range of temperature, before the positive vacuum contribution dominates again at asymptotically large temperatures. For the parameters used here, this range is $m \lesssim T \lesssim 10m$. This unphysical behavior may simply be an artifact of the present perturbative calculation which could be resolved at higher orders (which become relevant anyway at high temperatures) and/or by taking into account a possible temperature dependence of the parameters, as already mentioned. However, we cannot exclude that this behavior be a sign of a deeper problem. A study of these questions is certainly needed but it is beyond the scope of the present work. Here, we have simply checked that the temperature where the square mass turns negative is pushed to higher values when the coupling is decreased.

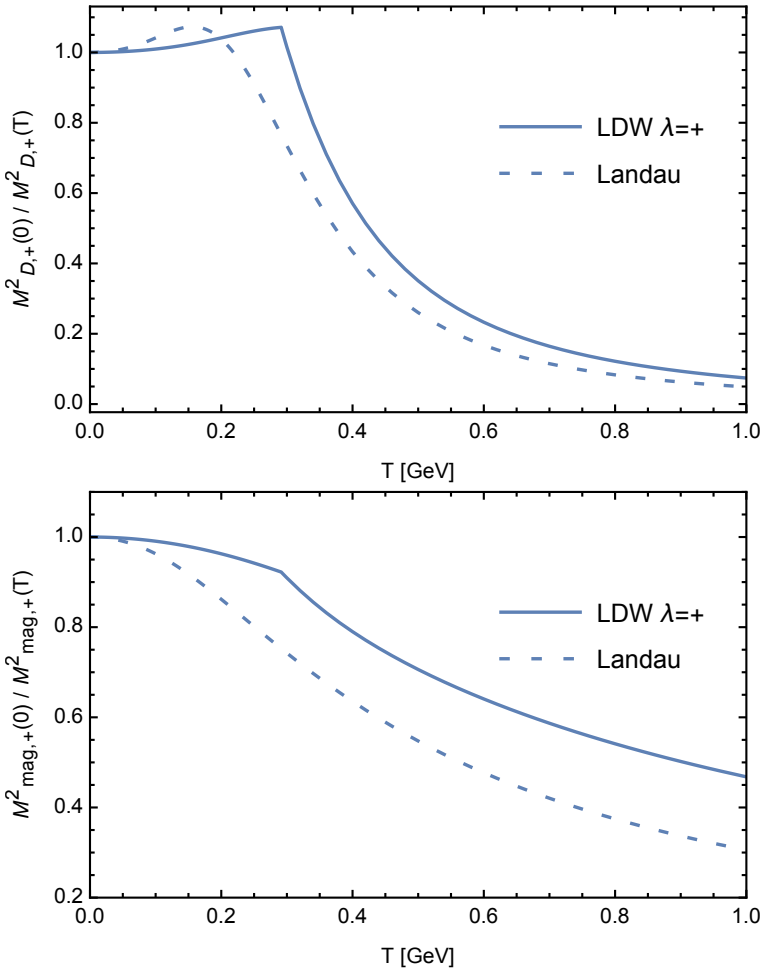

Figure III.15: Same as Fig. III.13 for the charged gluon modes, where the corresponding square masses are defined in Eqs. (III.5.63) and (III.5.64).

III.5.4.2 Gluon propagators

We now study the momentum-dependence of the gluon propagators at zero Matsubara frequency. We first consider the neutral sector. We plot the electric and magnetic propagators of the neutral color mode $\mathcal{G}^0_{T/L}(0,\mathbf{k})$ as functions of $k = |\mathbf{k}|$ for various temperatures on Fig. III.17. Both are smooth, monotonously decreasing functions of k. This is to be contrasted with the corresponding results in the Landau gauge, where both propagators exhibited a nonmonotonous behavior, more pronounced for higher temperatures, eventually resulting in an effective $3d$ behavior in the magnetic sector at high temperatures. In the present case, the main effect of the temperature can be read off the value of the propagators at vanishing momentum, respectively given by the susceptibilities $M^{-2}_{\mathrm{D},0}$ and $M^{-2}_{\mathrm{mag},0}$ and discussed in detail in the previous section.

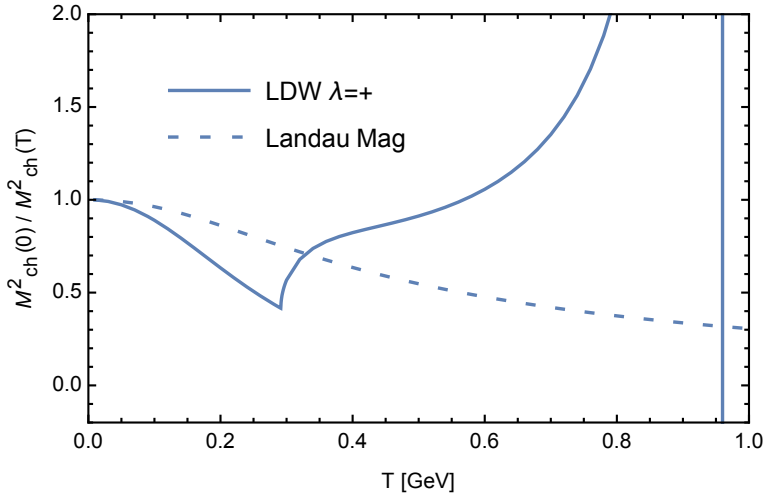

Figure III.16: Normalised inverse of the zero-momentum gluon square mass in any of the charged modes (this differs from the charged susceptibilities defined above).

We now come to the charged sector. As emphasized earlier, the charged propagators at vanishing frequency are degenerate, see (III.5.23). The electric and magnetic propagators of the charged color modes are plotted for various temperatures in Fig. III.18. They display very small differences, which is expected since both coincide for $k = 0$.

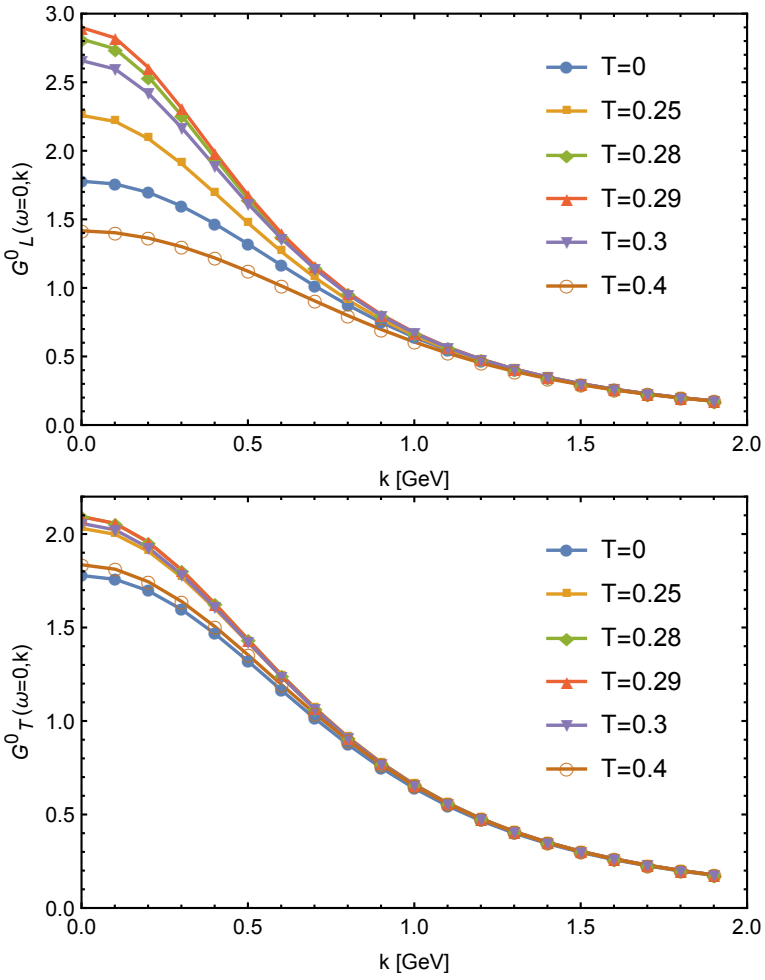

Figure III.17: The one-loop electric and magnetic propagators in the neutral sector at vanishing frequency as functions of the spatial momentum k for various temperatures.

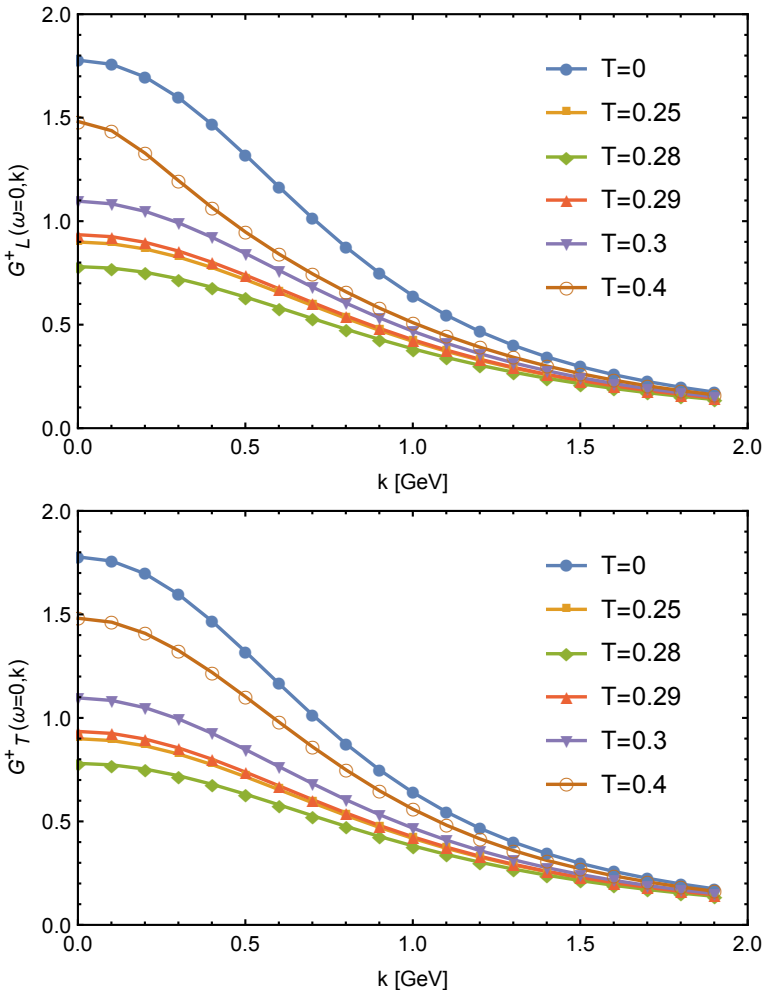

Figure III.18: The one-loop electric and magnetic propagators of the charged gluons at vanishing frequency as functions of the spatial momentum k for various temperatures.

III.5.4.3 Ghost sector

We now turn to the ghost sector. Despite the presence of a nonvanishing background, there remains an antighost shift symmetry for the neutral mode $\bar{c}^0 \to \bar{c}^0 + \text{const}$ which, together with spatial isotropy, implies

$$\Sigma^0(0,\mathbf{k}) = k^2\sigma(k), \tag{III.5.78}$$

where $\sigma(0) < \infty$. We define the ghost dressing function at vanishing frequency as $F(k) = k^2\mathcal{G}^0(0,\mathbf{k})$, that is,

$$F^{-1}(k) = 1 + g^2\sigma(k) = F_{\text{vac}}^{-1}(k^2) + g^2\sigma^{\text{th}}(k). \tag{III.5.79}$$

One striking result in the case of vanishing background [83] is the fact that the ghost dressing function develops a pole for sufficiently high temperatures, see Fig. III.5. As emphasized in Sec. III.3.2 (see Eqs. (III.3.1), (III.3.2)), this is a direct consequence of the Slavnov-Taylor identities of the present model in the Landau gauge and of the fact that the magnetic mass grows unboundedly with the temperature [83]. In the LDW gauge with a nontrivial background field, the situation is very different and we do not observe any pole, neither in the dressing function of the neutral ghost mode, shown in Fig. III.19 nor in the charged sector, discussed below. For the neutral mode, this

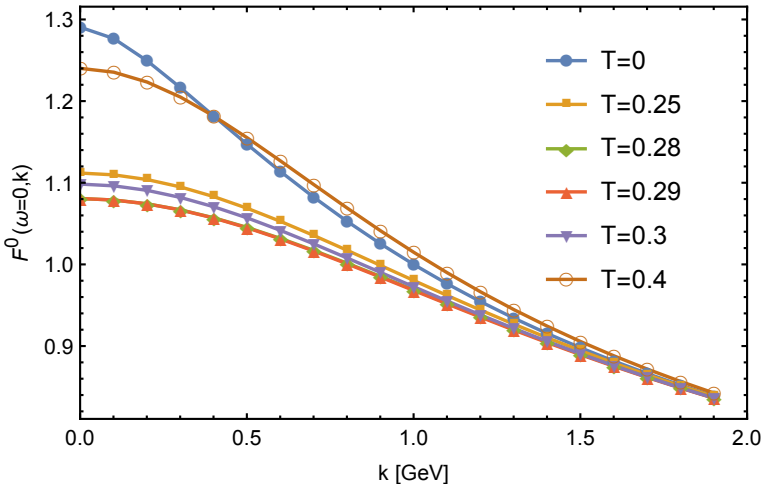

Figure III.19: The dressing function (III.5.79) of the neutral ghost color mode as a function of the momentum k for various temperatures. The pole of the vanishing-background case is absent.

can again be understood from the Slavnov-Taylor identities and the behavior of the magnetic susceptibility of the color-neutral gluon mode discussed above. Indeed, the discussion of [83] at vanishing background can be easily generalized to the present case in the neutral color sector, see Appendix F. The LDW generalization of Eq. (40) of [83] yields

$$\mathcal{G}^0_{T,B}(K)F^0_B(K)\Big|_{\omega=0,\mathbf{k}\to 0} = 1/m_0^2, \tag{III.5.80}$$

where the index B denotes bare correlators[19] and it is understood that the limit $k \to 0$ has to be taken after that $\omega = 0$. In the renormalization scheme considered here, this identity becomes, at one-loop order,

$$m^2 \sigma^{\rm th}(0) = -\Pi_T^{0,{\rm th}}(0, \mathbf{k} \to 0). \tag{III.5.81}$$

Finally, we have

$$F^{-1}(0) = F^{-1}_{R,{\rm vac}}(0) + 1 - \frac{M^2_{{\rm mag},0}}{m^2}, \tag{III.5.82}$$

see Eq. (III.5.56).

As mentioned above, at vanishing background, the magnetic mass grows linearly with the temperature, which, eventually, leads to a pole in the ghost dressing function, with $F^{-1}(0) = 0$. As discussed in Sec. III.5.4.1, the situation is different in the presence of a nontrivial background, where $M^2_{{\rm mag},0}$ remains bounded from above, thus preventing the appearance of a pole in the neutral ghost dressing function. Finally, we see from Eq. (III.5.82) that the value of the neutral ghost dressing function at vanishing momentum is controlled by that of the neutral gluon magnetic mass. In particular, the nonmonotonic behavior of the latter at T_c (see Fig. III.13) is directly visible in Fig. III.19.

As for the gluon case, the charged ghost modes at zero Matsubara frequency are degenerate,

$$\mathcal{G}^+(0, \mathbf{k}) = \mathcal{G}^-(0, \mathbf{k}), \tag{III.5.83}$$

as follows from Eq. (III.5.22) and spatial isotropy. At nonvanishing background field, there is no antighost shift symmetry in the charged sector and we shall thus directly study the propagators in this case. The charged ghost propagator at zero frequency is shown as a function of k for various temperatures in Fig. III.20. As for the neutral mode, it presents a nonmonotonic behavior in temperature with two changes of monotony at T_c and around $T = 0.4$ GeV, see also Fig. III.21. This corresponds to the change of monotony of its effective tree-level mass rT. In the limit $T \to 0$, the background field $\bar{A} \propto rT \to 0$ and we recover the original antighost shift symmetry at vanishing background, which implies that the ghost propagator diverges at zero momentum.

[19] Remark that, here, we changed our notations. Indeed, in Eq. (III.3.1) we noted bare quantities with a 0 index in order to be consistent thourhgout the present manuscript. However, in the present case, we prefer to use the B index in order to not confuse with the neutral color mode.

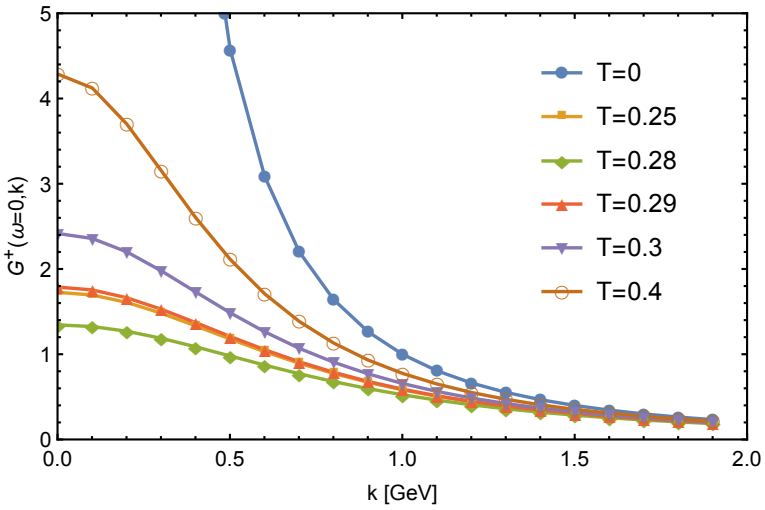

Figure III.20: The ghost propagator at vanishing frequency in the charged color sector as a function of momentum k for various temperatures.

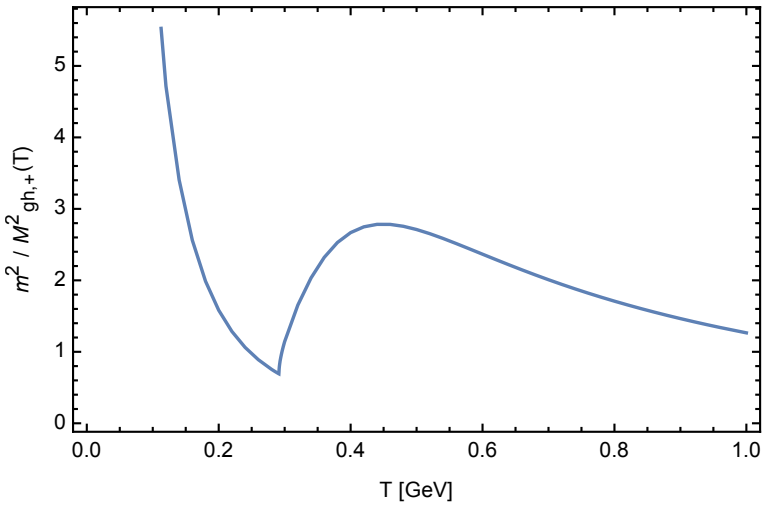

Figure III.21: The (normalized) ghost propagator for charged color modes at vanishing frequency and zero momentum as a function of temperature.

III.6 RG improvement

In this section we open some leads for further studies, namely the implementation of temperature-dependent RG effects. As we saw in the case of the neutral magnetic mass (see Fig. III.14), these are of great importance to extend the present results to higher temperatures, and would require a dedicated study. Here, as an illustration, we define the beta functions of the parameters $\alpha = m, g$ as[20]

$$\beta_\alpha^\mu = \left.\frac{d\,\alpha}{d\ln\mu}\right|_0 = -\alpha \left.\frac{d\ln Z_\alpha}{d\ln\mu}\right|_0 , \tag{III.6.1}$$

where we explicitly note by the exponent μ that these correspond to the beta functions along the renormalization scale μ axis. Nevertheless, at finite temperature, we also need to take into account the RG flows of the parameters along the temperature axis. Henceforth, we define

$$\beta_\alpha^T = \left.\frac{d\,\alpha}{dT}\right|_0 = -\alpha \left.\frac{d\ln Z_\alpha}{dT}\right|_0 . \tag{III.6.2}$$

It remains to define the beta functions for $r_{\min}$. To do so, we first use the independence of the (renormalized) effective action Γ with respect to the renormalization scale μ, that is

$$d_\mu\Gamma = 0 = \left(\partial_\mu + \beta_{m^2}^\mu\partial_{m^2} + \beta_g^\mu\partial_g + \beta_r^\mu\partial_r\right)\Gamma. \tag{III.6.3}$$

Differentiating this last equality with respect to r leads to

$$\begin{aligned} 0 = &\left(\partial_\mu + \beta_{m^2}^\mu\partial_{m^2} + \beta_g^\mu\partial_g + \beta_r^\mu\partial_r\right)\Gamma' \\ &+ \left(\partial_\mu + \beta_{m^2}^{\mu'}\partial_{m^2} + \beta_g^{\mu'}\partial_g + \beta_r^{\mu'}\partial_r\right)\Gamma, \end{aligned} \tag{III.6.4}$$

where $f' = \partial f/\partial_r$. Evaluating this last expression for $r = r_{\min}$ yields

$$\beta_{r_{\min}}^\mu = -\left.\frac{\left(\partial_\mu + \beta_{m^2}^\mu\partial_{m^2} + \beta_g^\mu\partial_g\right)\Gamma' + \left(\partial_\mu + \beta_{m^2}^{\mu,\prime}\partial_{m^2} + \beta_g^{\mu,\prime}\partial_g + \beta_r^{\mu,\prime}\partial_r\right)\Gamma}{\Gamma''}\right|_{r=r_{\min}} \tag{III.6.5}$$

where $f'' = \partial_r^2 f$ and where we used the fact that $0 = \Gamma'\big|_{r=r_{\min}}$. This last equation defines explicitly $\beta_{r_{\min}}^\mu$ since all the terms of the right-hand side are known and the (two-loop order) expression of Γ can be taken from [94]. However, since the temperature is a physical scale, Γ has no reason to be independent of the temperature and one cannot derive the temperature counterpart of Eq. (III.6.3). Nevertheless, we can use the fact that $\forall\, T, 0 = \Gamma'\big|_{r=r_{\min}}$. Accordingly, one has

$$\left[\left(\partial_T + \beta_{m^2}^T\partial_{m^2} + \beta_g^T\right)\Gamma' + \beta_r^T\Gamma''\right]\Big|_{r=r_{\min}} = 0\,, \tag{III.6.6}$$

which defines $\beta_{r_{\min}}^T$. In the case we considered here, where we adopted a temperature-independent renormalization scheme (see (III.5.55)), Eq. (III.6.6) reduces to

$$\beta_{r_{\min}}^T = \left.\frac{-\partial_T\Gamma'}{\Gamma''}\right|_{r=r_{\min}} , \tag{III.6.7}$$

[20] At the present level of approximation we did not need to explicitly renormalize the coupling constant. Nevertheless, this can be done by e.g. following the Taylor scheme presented in Sec. II.5.4.

and we explicitly checked that, using this RG equation, we reproduce the values of the background obtained by minimization of the background field potential that are depicted in Fig. III.7. The implementation of RG improvement in temperature-dependent renormalization schemes is beyond the scope of the present thesis. Nevertheless, owing to the numerous independent sectors (e.g. Π_L^0, Π_L^+, $\Pi_T^-, \dots$) a large variety of temperature-dependent renormalization prescriptions can be investigated. Moreover, we note that, for having a fully consistent picture, in order to recover the IR safe RG trajectories of [79] at zero temperature, one should use the infrared-safe renormalization scheme (see Sec. II.5.2 of Chapter. II) instead of the zero-momentum one used here to renormalize the vacuum parts.

III.7 Summary and discussion

In this chapter, we investigated YM theories at finite temperature close to the phase transition. We worked in the LDW gauge, which is a background field extension of the usual Landau one. In particular, the LDW gauge can be formulated as the extrema of an external functional, see (III.4.5), which allows us to implement this gauge according to the ST gauge-fixing procedure. For what concerns the gluon and ghost sectors studied here, it results effectively in a simple massive extension of the LDW FP gauge-fixed action. In particular, the massive gauge-fixed action (III.4.6) preserves the center symmetry and the background field stands as an equivalent order parameter for the confinement-deconfinement phase transition. The latter has been investigated perturbatively at next-to-leading order in thist context in [94] for SU(2) and in [95] for SU(3) and other groups. In the present case, we studied the SU(2) theory and computed the gluon and ghost propagators at one-loop order (i.e. next-to-leading order) in perturbation theory. In particular, due to the presence of the background field that singles out a particular color direction (the one of the Cartan subalgebra), the various color modes are not degenerate as in the usual Landau gauge. Our most stringent result concerns the neutral mode of the electric gluon propagator which presents a clear signal of the phase transition at the critical temperature, see Fig. III.13. More generally, the nonanalityc behavior of the order parameter of the phase transition (see Fig. III.7) is imprinted in the temperature dependence of all corelators, see e.g. Figs. III.13, III.21.

Moreover, the presence of the background circumvent some of the issues related to the perturbative approach that one encounters in the Landau gauge. In the latter case, one finds at one-loop order a pole in the ghost dressing function due to the unbounded increase of the magnetic mass [83], see also Fig. III.5. Although in the LDW gauge, for the neutral mode, the ghost dressing function remains related to the magnetic gluon sector, see Eq. (III.5.80), the presence of a nontrivial background dramatically changes the high temperature behavior of the latter. Indeed, the magnetic mass remains bounded from above and the (neutral) ghost dressing function does not develop a pole, see Fig. III.19. However, as observed in Fig. III.14, for sufficiently large temperatures the magnetic mass turns negative. This feature could be a consequence of the fact that RG effects were not taken into account. This hypothesis can be substantiated by introducing by hand a temperature-dependent running coupling

constant (III.5.76), which actually leads to a positive magnetic mass for the range of temperatures investigated, see Fig. III.14. This suggests that, as expected, the present perturbative approach requires to take into account higher loop contributions/RG effects to be extended at higher temperatures. This can be done for instance, by including RG effects in a temperature-dependent renormalization scheme as described in Sec. III.6. Nevertheless, the fact that, at high temperatures in the charged sector, $M^2_{\rm ch}$ turns negative (see Fig. III.16) could be a deeper problem. Indeed, as emphasized in the main text, our attempts by putting by hand a running coupling constant did not cure completely this issue. It should be mentioned again that we have checked that as the coupling is reduced, the temperature at which this mass turns negative is increased. This may signals that other effects than RG are needed to circumvent this problem and which are missed in the strict one-loop calculations presented here.

Another possibility may lie in the possible background dependence of the mass. Indeed, in the present context, the mass term appears due to the treatment of Gribov copies in the ST gauge-fixing procedure, and hence, should, in principle, depend on the background. As emphasized earlier, so far, we have not derived a kind of gap equation that would allow to fix the value of the mass in an *ab initio* way. Instead, for the time being, we are left with an additional free parameter. In the case where lattice data are available, one can fix the value of the mass by performing fits against the lattice results. This strategy has been used in the case of the Landau gauge in [83], where it leads to temperature-dependent mass and coupling that have eventually cured the presence of a pole in the ghost dressing function. One may think that, following the same strategy, a background dependence of the mass would be revealed and, in turn, would cure the appearance of the pole in $M^2_{\rm ch}$. Such a scenario, however, requires to have lattice data at our disposal. Lattice simulations can be performed in the LDW gauge [237] by minimizing the functional (III.4.5). The formal resemblance of the latter with the functional used to implement the Landau gauge, see (I.4.1) of Chapter. I, allows one to use the minimization algorithms routinely employed in the case of the Landau gauge. The situation is even more simple in the low temperature phase where, we know that, $r_{\rm min} = \pi$. Hereby, one can use the already existing numerical codes that compute the propagators in Landau gauge at finite temperature, and simply performs the shift $A_\mu \to A_\mu + \delta_{\mu 0} t^3 \pi T/g_0$ to get those of the LDW gauge in the low temperature regime.

Conclusion and perspectives

In this thesis, in a first part, we extended the Serreau-Tissier (ST) gauge-fixing proposal of [74] to a one-parameter family of nonlinear covariant gauges. The central idea of this procedure consists in defining expectation values of gauge-invariant quantities by a two-step averaging procedure that includes a pseudo average over the Gribov copies along each gauge orbit in order to lift their degeneracy. The resulting gauge-fixed theory is free of Gribov ambiguities and can be cast under the form of a local field theory at the cost of introducing the replicas [75]. In the present case, the replica sector consists in $n-1$ copies of supersymmetric nonlinear sigma models. Eventually, the resulting local gauge-fixed action corresponds to a massive extension of the Curci-Ferrari-Delbourgo-Jarvis gauges [77, 100] coupled to the replica sector, while average values of gauge-invariant quantities are obtained in the limit of vanishing replica number $n \to 0$. In particular, we have proved that the local gauge-fixed action is renormalizable in $d = 4$ for any value of n and we provided explicit expression of the relevant counter-terms at one-loop order. In particular, renormalizability is insured by the presence of a modified non-nilpotent BRST symmetry that allows to control the UV divergences, though it is not known up to now how to construct the physical space of the theory.

In the case of the Landau gauge, the gluon and ghost sectors effectively reduce to those of the Curci-Ferrari (CF) model [76, 77], which consists in a simple massive extension of the Landau gauge Faddeev-Popov gauge-fixed Yang-Mills action. On the contrary, away from the Landau limit, clear differences appear between the present gauge-fixed theory and the CF model. These differences can conveniently be investigated in the gluon and ghost sectors by studying them either in the limit $n \to 0$, or for $n = 1$, which correspond respectively to the ST and the CF cases. For instance, in the former case, the gluon propagator remains transverse even away of the Landau gauge and the renormalization group (RG) flows never freeze in the infrared because of the presence of massless modes in the replica sector. These behaviors are to be put in regard with the case $n = 1$ where the gluon propagator develops a longitudinal part and all the modes are massive, which lead to the freezing of the RG flows below the mass scale of the problem. In practice, we computed, with and without RG improvement, the various propagators of the ST and the CF actions at one-loop order in perturbation theory. In particular, we have shown, for the gauges investigated and for the infrared-safe renormalization scheme considered here, that both the ST and the CF cases admit infrared safe RG trajectories and the perturbative RG flows can be integrated down to zero momentum.

The massive and perturbative approach is mainly supported by the fact that, in the

Landau gauge, one-loop calculations of various correlation functions in the CF model reproduce accurately the lattice results, see [79, 80, 81, 82, 203]. However, a definite rigorous proof that the effective CF mass actually comes from a treatment of the Gribov copies *à la* ST is still missing. Indeed, as mentioned earlier, one of the possible loophole of the ST procedure lies in the assumption that one can freely interchange the $n \to 0$ limit and the path-integral over the gauge field A. Although a rigorous proof would require a detailed mathematical treatment of the path-integral, we believe that a strong argument in favor of the ST approach would be to have an *ab initio* way to fix the renormalized mass. One lead is to construct, in the Landau gauge for instance, a multiplicatively renormalizable effective potential for the local composite operator A^2, following the lines of e.g. [241, 242]. In the present framework, investigation of such an effective potential can be done in perturbation theory. A possible scenario would be that, since the gauge parameter $\beta_0 > 0$, introduced to lift the degeneracy of the Gribov copies, softly breaks the initial nilpotent BRST symmetry (though a modified non-nilpotent one remains), some operators can now develop nonvanishing expectation values, while these were prevented in the presence of the initial nilpotent BRST symmetry. Hereby, one may expect that, due to such a soft-breaking of the BRST symmetry, nontrivial minima of the effective potential for A^2 now exist. The latter corresponding to nonvanishing renormalized gluon mass, this would further enforce the choice of considering n-dependent renormalization schemes as considered in Sec. II.5.2. We find worth mentioning that, in the context of the FRG, recently a bare gluon mass was introduced to the bare action in order to account for the soft breaking of the initial nilpotent BRST symmetry due to the presence of the regulator [243].

In the second part of this thesis, we extended to the finite temperature case the massive approach (or equivalently the ST proposal under the assumption mentioned above) to a background field extension of the Landau gauge, namely the Landau-DeWitt (LDW) gauge. This consists in working in presence of a nontrivial background value $\bar{A}$ for the gauge field, which (when evaluated at the value that minimizes a certain potential) stands as an order parameter for the confinement-deconfinement phase transition. In particular, the LDW gauge allows to work in an approach where the $\mathbb{Z}_N$-center symmetry is preserved, which is probably a crucial property for approximate methods since the spontaneous breaking of the former is associated to the phase transition. We considered the SU(2) theory whose deconfinement phase transition was accurately described in perturbation theory [93, 94]. More precisely, in the present background field approach, physical observables must be evaluated at the value of the background that minimizes the background field potential (III.4.18), and the value of the former signals whether the center symmetry is realized or spontaneously broken. In practice, the background field potential was computed up to two-loop order in [94] for the SU(2) theory, and a second order phase transition was observed, in agreement with the lattice. The presence of a nontrivial background field defines preferred color directions (those of the Cartan subalgebra of the color symmetry group), and the various color modes couple differently with the background, which, in turn, lifts their degeneracy. Regarding practical aspects, the standard Cartesian color basis becomes not the best suited for actual calculations and, instead, we used the Feynman rules derived in the canonical basis. In this basis, for the SU(2) theory, the three color modes of the

adjoint representation correspond to one neutral mode (the color direction singled by the background) and two charged ones. In the present manuscript, we computed at one-loop order the gluon and ghost propagators for the various color modes. At the difference of the Landau gauge, we observed characteristic signals of the phase transition directly at the level of the correlators. This is particularly clear for the neutral electric gluon susceptibility (electric gluon propagator evaluated at zero Matsubara frequency and vanishing momentum) which displays a peak at the critical temperature. More generally, although less impressive, all the temperature dependences of the zero Matsubara/momentum value of the correlators present a cusp at the phase transition. This is because, at the difference of the Landau gauge, in the LDW gauge the non-analyticity of the order parameter at the phase transition is directly imprinted into the correlators.

The first natural extension of this work is to investigate the correlators in the SU(3) case, where we expect to observe, instead of a cusp, a discontinuity owing to the first order character of the phase transition in the SU(3) theory. Also, as emphasized earlier, one should consider temperature-dependent renormalization schemes, and then, the study of temperature-dependent RG flows in order to investigate possible infrared safe (i.e. without a Landau pole) RG trajectories along the temperature axis. We believe that, these are necessary studies in order to confirm the consistency of the present perturbative approach.

Another case of interest is the investigation of the QCD phase diagram. The present approach has already been extended at finite chemical potential for static quarks of infinitely heavy masses (quenched approximation) in [97]. In this case, although much less severe than on the lattice, there exists a sign problem for real chemical potential. Indeed, the generating functional becomes, in general, not real and so does the average value of A. Hence, for having self-consistent background fields (as our approach requires, see Sec. III.4) that satisfy $\langle A \rangle = \bar{A}$ one thus needs to consider complex background fields. The fact that, in this case, the action is complex is not an obstacle to perform actual perturbative calculations (at the difference of lattice simulations). However, the background field potential is now a complex function of complex variables, and, in turn, it is not clear which of its extrema actually identify the physical values of the background (in the case of zero chemical potential these are identified by the absolute minima of the background field potential). In [97], the extrema were chosen such that the limit of vanishing chemical potential is smooth, and such that in this limit one recovers the results of the pure temperature case. Although this (arbitrary) criterion seems quite fair for small values of the chemical potential, its extension to the high chemical potential region should deserved dedicated study.

The next stage would be to consider dynamical light quarks. In a first step, one could for instance study the effects of the nontrivial background on the quark propagator as well as on the quark-antiquark-gluon vertex. Nevertheless, the study of the QCD phase diagram in the light quark region requires the treatment of the chiral symmetry breaking that is currently not accounted for in the present approach, and requires some refinement. A possible way would be to construct an effective potential for an order parameter associated to the chiral phase transition, as for instance in [244]. The possible implementation of such an order parameter at the level of the microscopic action should be, in principle, possible by using again background field methods [118].

This would result in an effective action where the pure gauge sector corresponds to the massive LDW action presented in this thesis (that contains the relevant order parameter for the deconfinement phase transition), supplemented by the action for the matter fields that depends on a background field value associated to order parameter of the chiral phase transition.

Appendix A

Dyson-Schwinger equation for the ghost propagator

Here we derive explicitly the DSE for the ghost propagator in the Landau gauge. The starting point is the DSE Eq. (I.3.8). We introduce a set of sources for the different fields: two scalar ones J^a_μ for the gauge field and M^a for ih^a, as well as a couple of Grassmann sources $\bar{\eta}^a$ and η^a for the FP ghost c^a and anthighost $\bar{c}^a$ fields. We thus have for generating functional

$$Z[J,M,\bar{\eta},\eta] = \int \mathcal{D}A\mathcal{D}h\mathcal{D}\bar{c}\mathcal{D}c \exp\left\{-S_{\rm gf} + \int_x J^a_\mu A^a_\mu + M^a i h^a + \bar{c}^a\eta^a + \bar{\eta}^a c^a\right\}, \tag{A.0.1}$$

with $S_{\rm gf}$ the Landau gauge FP action that was defined in Eq. (I.2.9)

$$S_{\rm gf} = \int_x \left\{\frac{1}{4}F^a_{\mu\nu}F^a_{\mu\nu} + \partial_\mu\bar{c}^a D_\mu c^a + ih^a\partial_\mu A^a_\mu\right\}. \tag{A.0.2}$$

Using Eq. (I.3.8) with $\varphi(x) = \bar{c}^a(x)$ yields

$$\langle \partial_\mu D_\mu c^a(x) + \eta^a(x)\rangle_{J_\mu,M,\eta,\bar{\eta}} = 0, \tag{A.0.3}$$

with the convention of left derivatives for fermionic quantities and we have identified $\delta S/\delta\bar{c}^a = -\partial_\mu D_\mu c^a$ in Eq. (A.0.3). In the following we use a short-hand notation where space-time coordinates are put as indices, such that $A^a_\mu(x) \equiv A^a_{\mu,x}$. Accordingly Eq. (A.0.3) writes

$$\begin{aligned} 0 &= \left\langle \partial^2_x c^a_x + g_0 f^{acd}\partial_{\mu,x}\left(A^c_{\mu,x}c^d_x\right) + \eta^a_x\right\rangle_{J_\mu,M,\eta,\bar{\eta}} \\ &= \partial^2_x \frac{\delta W}{\delta\bar{\eta}^a_x} + g_0 f^{acd}\partial_{\mu,x}\frac{\delta^2 W}{\delta J^c_{\mu,x}\delta\bar{\eta}^d_x} + \eta^a_x\,, \end{aligned} \tag{A.0.4}$$

where the generating functional $W[J_\mu,M,\eta,\bar{\eta}]$ has been defined in (I.3.1). Differentiating further this last equality with respect to the source η^b_y one gets

$$0 = -\partial^2_x \frac{\delta^2 W}{\delta\bar{\eta}^a_x\delta\eta^b_y} - g_0 f^{acd}\partial_{\mu,x}\frac{\delta^3 W}{\delta J^c_{\mu,x}\delta\bar{\eta}^d_x\delta\eta^b_y} + \delta^{ab}\delta_{x,y}\,. \tag{A.0.5}$$

Finally, performing the Legendre transformation with respect to the sources J_μ, M, η, $\bar{\eta}$ and ultimately taking the limit of vanishing sources leads to the following relations

$$\begin{aligned} \frac{\delta\varphi}{\delta J_\phi} &= \frac{\delta^2 W}{\delta J_\phi \delta J_\varphi} \quad \text{for } \phi,\varphi = (A_\mu, ih, c, \bar{c}) \,, \\ \frac{\delta^2 W}{\delta\bar{\eta}^a_x \delta\eta^b_y} &= -\left(\frac{\delta^2\Gamma}{\delta c^a_x \delta\bar{c}^b_y}\right)^{-1} , \\ \frac{\delta^2 W}{\delta J^a_{\mu,x}\delta J^e_{\nu,z}} &= \left(\frac{\delta^2\Gamma}{\delta A^a_{\mu,x}\delta A^e_{\nu,z}}\right)^{-1} . \end{aligned} \tag{A.0.6}$$

Using these relations one gets

$$\frac{\delta}{\delta J^a_{\mu,x}} = \sum_{\phi=A_\mu,ih,c,\bar{c}} \int_z \frac{\delta\phi^e_z}{\delta J^a_{\mu,x}} \frac{\delta}{\delta\phi^e_z} = \int_z \left(\frac{\delta^2\Gamma}{\delta A^a_{\mu,x}\delta A^e_{\nu,z}}\right)^{-1} \frac{\delta}{\delta A^e_{\nu,z}} \,, \tag{A.0.7}$$

which, along with the relations (A.0.6) yields

$$\begin{aligned} \frac{\delta}{\delta J^c_{\mu,x}}\left(\frac{\delta^2 W}{\delta\bar{\eta}^d_x\delta\eta^b_y}\right) &= -\int_z \left(\frac{\delta^2\Gamma}{\delta A^c_{\mu,x}\delta A^e_{\nu,z}}\right)^{-1} \frac{\delta}{\delta A^e_{\nu,z}}\left(\frac{\delta^2\Gamma}{\delta c^d_x\delta\bar{c}^b_y}\right)^{-1} \\ &= -\int_{z,t,u} \left(\frac{\delta^2\Gamma}{\delta A^c_{\mu,x}\delta A^e_{\nu,z}}\right)^{-1} \left(\frac{\delta^2\Gamma}{\delta c^d_x\delta\bar{c}^n_t}\right)^{-1} \frac{\delta^3\Gamma}{\delta c^n_t\delta\bar{c}^m_u\delta A^e_{\nu,z}} \left(\frac{\delta^2\Gamma}{\delta c^m_u\delta\bar{c}^b_y}\right)^{-1} . \end{aligned} \tag{A.0.8}$$

Applying a Fourier transformation with the convention that $\partial_\mu \to -ip_\mu$ and plugging this identity into the DSE Eq. (A.0.5) eventually leads to

$$-p^2 G^{ab}_{\rm gh}(p) + \delta^{ab} + ig_0 p_\mu f^{acd} \int_k G^{ce}_{\mu\nu}(k) G^{dn}_{\rm gh}(k) \Gamma^{nme}_{c\bar{c}A_\nu}(p,-k,k) G^{mb}_{\rm gh}(p) = 0 \,, \tag{A.0.9}$$

where $G_{\rm gh}$ and $G_{\mu\nu}$ are respectively the fully dressed ghost and gluon propagators, and $\Gamma_{c\bar{c}A_\nu}$ is the fully dressed ghost-antighost-gluon vertex. This equation is more conveniently written under the following form

$$\delta^{ab} = \left[p^2\delta^{as} - ig_0 p_\mu f^{acd} \int_k G^{ce}_{\mu\nu}(k) G^{dn}_{\rm gh}(k) \Gamma^{nse}_{c\bar{c}A_\nu}(p,-k,k)\right] G^{sb}_{\rm gh}(p) \,, \tag{A.0.10}$$

which eventually leads to

$$\left(G^{-1}_{\rm gh}\right)^{ab}(p) = p^2\delta^{as} - ig_0 p_\mu f^{acd} \int_k G^{ce}_{\mu\nu}(k) G^{dn}_{\rm gh}(k) \Gamma^{nse}_{c\bar{c}A_\nu}(p,-k,k) \,, \tag{A.0.11}$$

that displays explicitly the one loop structure of Fig. I.2.

Appendix B

Miscellaneous identities

In this appendix, we present various identities used throughout the main text of Chapter. II. We preferred to report them in a separated appendix in order to not encumber the main discussion.

B.1 Identities among renormalization constants

First of all, we consider the renormalization constants appearing in the proof of renormalizability, see Sec. II.3.2. There is an obvious permutation symmetry among the replicas $k > 2$. The latter guarantees for instance that Z_2 and Z_3 do not depend on k, see Eq. (II.3.53). There is also a less obvious permutation symmetry between the replicas $k > 2$ and $k = 1$, which has been (arbitrarily) singled out to factor out the volume of the gauge group. To exploit this symmetry we employ a parametrization of $\tilde{\mathcal{V}}_k$ similar to (II.3.6)

$$\tilde{\mathcal{V}}_k = \sqrt{Z} \exp\left\{ i\tilde{g}\Big(\bar{C}_k\theta + \bar{\theta}C_k + \bar{\theta}\theta\hat{H}_k \Big) \right\} \tilde{U}_k. \tag{B.1.1}$$

with $\hat{H}^a_k = iH^a_k + \frac{\tilde{g}}{2} f^{abc}\bar{C}^b_k C^c_k$ and $\tilde{U}^\dagger_k \tilde{U}_k = \mathbb{1}$. Here, we introduced the fields $C_k, \bar{C}_k, H_k$ and $\tilde{U}_k$ in order to take into account a possible renormalization between the bare fields introduced in (II.3.6) and the variables of the effective action Γ. Using this parametrization in Eq. (II.3.51) leads to

$$\begin{aligned}
\int_{\underline{\theta}} \mathcal{L}_2 = \frac{Z_2 Z^2}{\kappa_1} \Big\{ & \frac{\beta_0}{2\kappa_1} (A^a_\mu)^2 - iA^a_\mu \partial_\mu H^a_k \\
& + \partial_\mu \bar{C}^a_k \left(\kappa_1 \partial_\mu C^a_k + \tilde{g} f^{abc} A^b_\mu C^c_k \right) \Big\}_{A = A^{\tilde{U}_k}} \\
& + Z_3 Z^2 \Big\{ \beta_0 \bar{C}^a_k C^a_k + \frac{(H^a_k)^2}{2} \\
& - \frac{\tilde{g}}{2} f^{abc} i H^a_k \bar{C}^b_k C^c_k - \frac{\tilde{g}^2}{4} (f^{abc} \bar{C}^b_k C^c_k)^2 \Big\}.
\end{aligned} \tag{B.1.2}$$

To make contact with the original fields $(c_k, \bar{c}_k, h_k)$ to which the replica symmetry applies, we introduce possible renormalization factors as

$$\begin{aligned} C_k^a &= \hat{Z}_c c_k^a + \dots \\ \bar{C}_k^a &= \hat{Z}_c \bar{c}_k^a + \dots \\ iH_k^a &= \hat{Z}_h i h_k^a + \hat{Z}_A \partial_\mu A_\mu^a + g_0 \hat{Z}_{c\bar{c}} f^{abc} \bar{c}_k^b c_k^c + \dots \end{aligned} \tag{B.1.3}$$

where the dots stand for terms involving λ_k and nonlocal contributions. Here we included all possible local terms having the correct dimension, ghost number, and symmetry properties. The replica symmetry guarantees that the factors $\hat{Z}_{c,h,A,c\bar{c}}$ above do not depend on k. Inserting (B.1.3) in the equation above, setting $\tilde{U}_k = \mathbb{1}$, and identifying terms involving $(c_k, \bar{c}_k, h_k)$ with the corresponding ones involving $(c, \bar{c}, h)$ in (II.3.46), we obtain, after some algebra,

$$\hat{Z}_c = \hat{Z}_h = 1 \quad \text{and} \quad \hat{Z}_{c\bar{c}} = \hat{Z}_A = 0, \tag{B.1.4}$$

as well as the two relations

$$Z_2 Z^2 = \kappa_1 \kappa_2 \quad \text{and} \quad Z_3 Z^2 = \kappa_3, \tag{B.1.5}$$

which reduce the number of independent renormalization constants to six. Note that $Z_A = 0$ guarantees that there is no term $(\partial_\mu A_\mu^a)^2$. The relation $Z_2 Z^2 = \kappa_1 \kappa_2$ guarantees that all replicas contribute the same to the gluon mass squared, which thus scales as n.

The definitions of the renormalized constants $\kappa_{1,2,3}$, $Z_{1,2,3}$, Z, and $\tilde{g}$ used above and in the proof of renormalizability, see Sec. II.3.2 differ from those used in perturbative calculations, namely Z_A, Z_c, Z_h, Z_Λ, Z_β, Z_ξ and Z_g, see (II.4.24), (II.4.25) and (II.4.29). The dictionary between the two sets is given in (II.4.32), (II.4.33). In particular, the renormalization constants of the second set [Eqs.(II.4.24), (II.4.25) and (II.4.29)] satisfy the constraint

$$Z_h = Z_\beta Z_c \,, \tag{B.1.6}$$

which leads to six independent renormalization constants among the seven defined. This number of independent renormalization constants is further reduced in the Landau gauge ($\xi_0 = 0$). Indeed, the case $\xi_0 = 0$ studied in [74] exhibits various simplifications as compared to the general class of gauges studied here. The first obvious one is the fact that the h sector does not receive any loop corrections, i.e.,

$$\frac{\delta \Gamma}{\delta i h^a} = \frac{\delta S}{\delta i h^a} = \partial_\mu A_\mu^a. \tag{B.1.7}$$

This can be seen, e.g., by applying a infinitesimal shift $ih \to ih + f$ under the defining path integral for Γ (see also Appendix. F). In terms of the divergent constants introduced in Sec. II.3.2.2, this implies that $\kappa_2 = 1$ or, equivalently [232, 202],

$$Z_A Z_\beta Z_c = 1, \tag{B.1.8}$$

where we used the relation (B.1.6).

The next simplification comes from the fact that for $\xi_0 = 0$, the superfield correlator (II.4.14) is ultralocal in Grassmann space, i.e., it is proportional to $\delta(\underline{\theta}, \underline{\theta}')$ and the mixed correlator (II.4.16) vanishes. As pointed out in [74] and emphasized in the main text, since all vertices of the theory are also local in Grassmann space (for $\xi_0 = 0$ there are no term involving Grassmann derivatives) it follows that closed loops involving superfields are proportional to $\delta(\underline{\theta}, \underline{\theta}) = 0$, see Eq. (II.4.18). An important consequence is that the Λ_k sector effectively decouples in the (perturbative) calculation of correlators in the sector $(A, c, \bar{c}, h)$ at all orders. The only effect of the superfields Λ_k is the mass term $n\beta_0$ for the gauge field.

A first consequence of this dramatic simplification for the renormalizability of the theory is that the usual nonrenormalization theorems of the CF model with $\xi_0 = 0$ are valid. One of them is the relation (B.1.8) above. The second one comes from the Taylor theorem, which states that the ghost-antighost-gluon vertex in a particular momentum configuration does not receive loop corrections [116]. It follows that

$$Z_g \sqrt{Z_A} Z_c = 1. \tag{B.1.9}$$

We observe that Eqs. (B.1.8) and (B.1.9) together with the last relation in Eq. (II.4.33) imply that $Z = Z_\Lambda / Z_c$. Another consequence of the absence of loops of the superfield is the fact that there can be no loop diagram with only one external Λ_k leg. This is easy to show by direct inspection. It follows that those vertices are tree-level exact, i.e.,

$$\left.\frac{\delta_\theta \Gamma}{\delta \Lambda_k^a}\right|_{\Lambda_k = 0} = \left.\frac{\delta_\theta S}{\delta \Lambda_k^a}\right|_{\Lambda_k = 0} = -\partial_\mu A_\mu^a. \tag{B.1.10}$$

Taking into account the rescaling (II.4.26) of Grassmann variables, which implies, together with (II.4.29), that

$$\delta \mathcal{F}[\Lambda] = \int_{x,\underline{\theta}} \frac{\delta_\theta \mathcal{F}}{\delta \Lambda} \delta\Lambda = \sqrt{Z_\beta Z_\Lambda} \int_{x,\underline{\theta_r}} \frac{\delta_\theta \mathcal{F}}{\delta \Lambda} \delta\Lambda_r, \tag{B.1.11}$$

for any given functional $\mathcal{F}[\Lambda]$, we conclude that $Z_A Z_\Lambda Z_\beta = 1$. When combined with Eq. (B.1.8), this gives

$$Z_\Lambda = Z_c, \tag{B.1.12}$$

or, equivalently, $Z = 1$. Equations (II.3.41), (II.3.46), (II.3.51), together with the relations (II.3.53), (II.4.33), (B.1.8), (B.1.9), and (B.1.12), the results of [74]. In the Landau gauge, the number of independent renormalization factors is reduced from 6 to 3. The relations (B.1.8), (B.1.9), and (B.1.12) are readily checked from the one-loop results of Sec. II.4.3.2 for $\xi = 0$.

In order to summarize, in the case of the Landau gauge ($\xi_0 = 0$), the number of independent renormalization constants in reduced from 6 down to 3 due to the three additional constraints $Z_A Z_c Z_\beta = Z_g \sqrt{Z_A} Z_c = Z_\Lambda / Z_c = 1$.

B.2 Slavnov-Taylor identities in the CF model

As already discussed, the CF model can be obtained from the theory considered here by setting the number of replicas $n = 1$. Its action is given by

$$S[A, c, \bar{c}, h] = S_{\rm YM}[A] + S_{\rm CF}[A, c, \bar{c}, h] \tag{B.2.1}$$

where $S_{\rm YM}$ is the YM action and $S_{\rm CF}$ is given in Eq. (II.2.10). This model possesses a (non-nilpotent) BRST symmetry, whose action on the fields is

$$sA^a_\mu = D_\mu c^a\,, \quad sc^a = -\frac{g}{2} f^{abc} c^b c^c \tag{B.2.2}$$

and

$$s\bar{c}^a = ih^a\,, \quad sih^a = \beta_0 c^a. \tag{B.2.3}$$

The Zinn-Justin equation corresponding to this symmetry is obtained as usual, i.e., by introducing external sources for the fields and for all the independent BRST variations, $S \to S - S_1$ with

$$S_1 = \int_x \Big\{ J^a_\mu A^a_\mu + \bar{\eta}^a c^a + \bar{c}^a \eta^a + M^a ih^a + \bar{K}^a_\mu sA^a_\mu + \bar{L}^a sc^a \Big\}, \tag{B.2.4}$$

and by performing a Legendre transform with respect to the sources J^a_μ, η^a, $\bar{\eta}^a$, and M^a. It reads

$$\int_x \left\{ \frac{\delta\Gamma}{\delta \bar{K}^a_\mu}\frac{\delta\Gamma}{\delta A^a_\mu} + \frac{\delta\Gamma}{\delta \bar{L}^a}\frac{\delta\Gamma}{\delta c^a} - ih^a \frac{\delta\Gamma}{\delta \bar{c}^a} - \beta_0 c^a \frac{\delta\Gamma}{\delta ih^a} \right\} = 0. \tag{B.2.5}$$

Taking two derivatives of this equation with respect either to ih^a and c^a or to A^a_μ and c^a and setting the sources to zero, one obtains the following symmetry identities for the two-point vertex functions in momentum space:

$$\Gamma_{c\bar{K}_\mu}(p)\Gamma_{A_\mu ih}(p) - \Gamma_{c\bar{c}}(p) - \beta_0 \Gamma_{ihih}(p) = 0 \tag{B.2.6}$$

and

$$\Gamma_{c\bar{K}_\mu}(p)\Gamma_{A_\mu A_\nu}(p) - \beta_0 \Gamma_{ihA_\nu}(p) = 0. \tag{B.2.7}$$

Eliminating $\Gamma_{c\bar{K}_\mu}(p)$, we obtain, finally,

$$p^2 \left[\Gamma_{ihA}(p)\right]^2 - \Gamma_L(p)\Gamma_{ihih}(p) = \frac{\Gamma_L(p)\Gamma_{c\bar{c}}(p)}{\beta_0}. \tag{B.2.8}$$

Taking $n = 1$ in Eq. (II.5.3), and further using the above identity leads to

$$G^{\rm CF}_L(p) = -\left.\frac{m^2 \Gamma_{ihih}(p)}{\Gamma_L(p)\Gamma_{c\bar{c}}(p)}\right|_{n=1}. \tag{B.2.9}$$

Appendix C

One-loop expressions of the Feynman diagrams

Here, we present the Feynman rules associated to the non-standard vertices, namely $c\bar{c}c\bar{c}$, $ihc\bar{c}$ and the supersymmetric ones $A\Lambda^3$ and Λ^4. Then, we report the one-loop expressions of the Feynman diagrams of Figs. II.1 – II.5 once the Grassmann variables internal to the loops (if any) have been integrated out. The resulting expressions are standard one-loop momentum integral that we treat by means of the introduction Feynman parameters. In practice, only one parameter is needed. However, the full expression of the finite parts is too cumbersome and was treated using Mathematica. These, are reported into a Mathematica file corresponding to the supplemental material, Ref. [51], of [99]. Nevertheless, the divergent parts of the diagrams can be straightforwardly extracted from their one-loop expressions displayed below and are explicitly reported. In the following, we use the notation $\int_k = \mu^\epsilon \int \frac{d^dk}{(2\pi)^d}$, with $d = 4-\epsilon$ in dimensional regularization, $\kappa = g_0^2 N/8\pi^2\varepsilon$ and $k \cdot p = k_\mu p_\mu$.

C.1 Feynman rules

The four ghost vertex and the $ihc\bar{c}$ interaction reads respectively

$$\begin{aligned}\frac{\delta}{\delta c^d(p_4)}\frac{\delta}{\delta \bar{c}^c(p_3)}\frac{\delta}{\delta c^b(p_2)}\frac{\delta}{\delta \bar{c}^a(p_1)}S &= \frac{g_0^2\xi_0}{2}(f^{eab}f^{ecd} - f^{ead}f^{ecb})(2\pi)^d\delta^{(d)}(p_1+p_2+p_3+p_4)\,,\\ \frac{\delta}{\delta c^c(p_3)}\frac{\delta}{\delta \bar{c}^b(p_2)}\frac{\delta}{\delta ih^a(p_1)}S &= \frac{g_0\xi_0}{2}f^{abc}(2\pi)^d\delta^{(d)}(p_1+p_2+p_3)\,.\end{aligned} \tag{C.1.1}$$

We also recall the $A\Lambda_k\Lambda_k$ vertex

$$\frac{\delta_\theta}{\delta\Lambda_k^a(p_1,\underline{\theta})}\frac{\delta_{\theta'}}{\delta\Lambda_l^b(p_2,\underline{\theta}')}\frac{\delta}{\delta A_\mu^c(p_3)}S = i\frac{g_0}{4}f^{abc}\delta_{kl}(2\pi)^d\delta^{(d)}(p_1+p_2+p_3)\delta(\underline{\theta},\underline{\theta}')(p_1-p_2)_\mu\,. \tag{C.1.2}$$

Finally, the two quartic vertices $A\Lambda_k^3$ and Λ_k^4 reads respectively

$$\begin{aligned}
&\frac{\delta_{\theta_3}}{\delta\Lambda_j^c(p_3,\underline{\theta}_3)}\frac{\delta_{\theta_2}}{\delta\Lambda_l^b(p_2,\underline{\theta}_2)}\frac{\delta_{\theta_1}}{\delta\Lambda_k^a(p_1,\underline{\theta}_1)}\frac{\delta}{\delta A_\mu^d(p_4)}S = -i\frac{g_0^2}{6}\delta_{kl}\delta_{kj}(2\pi)^d\delta^{(d)}(p_1+p_2+p_3+p_4)\\
&\times\delta(\underline{\theta}_1,\underline{\theta}_2)\delta(\underline{\theta}_1,\underline{\theta}_3)\Big\{f^{eab}f^{ecd}\,(p_1-p_2)_\mu + f^{eca}f^{ebd}(p_3-p_1)_\mu\\
&\qquad\qquad + f^{ead}f^{ebc}(p_2-p_3)_\mu + f^{ead}f^{ebc}(p_2-p_3)_\mu\Big\},
\end{aligned} \tag{C.1.3}$$

and

$$\begin{aligned}
&\frac{\delta_{\theta_4}}{\delta\Lambda_m^d(p_4,\underline{\theta}_4)}\frac{\delta_{\theta_3}}{\delta\Lambda_j^c(p_3,\underline{\theta}_3)}\frac{\delta_{\theta_2}}{\delta\Lambda_l^b(p_2,\underline{\theta}_2)}\frac{\delta_{\theta_1}}{\delta\Lambda_k^a(p_1,\underline{\theta})}S\\
&= -\frac{g_0^2}{12}\delta_{kl}\delta_{kj}\delta_{km}(2\pi)^d\delta^{(d)}(p_1+p_2+p_3+p_4)\Big\{\delta(\underline{\theta}_1,\underline{\theta}_2)\delta(\underline{\theta}_1,\underline{\theta}_3)\delta(\underline{\theta}_1,\underline{\theta}_4)\Big[\\
&\qquad f^{ead}f^{ecb}(p_1\cdot p_2-p_1\cdot p_3-p_2\cdot p_4+p_3\cdot p_4)\\
&\qquad +f^{eac}f^{ebd}(-p_1\cdot p_2+p_1\cdot p_4+p_2\cdot p_3-p_3\cdot p_4)\\
&\qquad +f^{eab}f^{edc}(p_1\cdot p_3-p_1\cdot p_4-p_2\cdot p_3+p_2\cdot p_4)\Big]\\
&+\xi_0 g^{MN}\int_{\underline{\theta}}\Big[(f^{ead}f^{ecb}-f^{eac}f^{ebd})(\delta(\underline{\theta},\underline{\theta}_3)\delta(\underline{\theta},\underline{\theta}_4)\partial_N\delta(\underline{\theta},\underline{\theta}_1)\partial_M\delta(\underline{\theta},\underline{\theta}_2)\\
&\qquad +\delta(\underline{\theta},\underline{\theta}_1)\delta(\underline{\theta},\underline{\theta}_2)\partial_N\delta(\underline{\theta},\underline{\theta}_3)\partial_M\delta(\underline{\theta},\underline{\theta}_4))\\
&\qquad +(f^{eab}f^{edc}-f^{ead}f^{ecb})(\delta(\underline{\theta},\underline{\theta}_4)\delta(\underline{\theta},\underline{\theta}_2)\partial_N\delta(\underline{\theta},\underline{\theta}_1)\partial_M\delta(\underline{\theta},\underline{\theta}_3)\\
&\qquad +\delta(\underline{\theta},\underline{\theta}_3)\delta(\underline{\theta},\underline{\theta}_1)\partial_N\delta(\underline{\theta},\underline{\theta}_2)\partial_M\delta(\underline{\theta},\underline{\theta}_4))\\
&\qquad +(f^{eab}f^{ecd}-f^{eac}f^{edb})(\delta(\underline{\theta},\underline{\theta}_2)\delta(\underline{\theta},\underline{\theta}_3)\partial_N\delta(\underline{\theta},\underline{\theta}_1)\partial_M\delta(\underline{\theta},\underline{\theta}_4)\\
&\qquad +\delta(\underline{\theta},\underline{\theta}_1)\delta(\underline{\theta},\underline{\theta}_4)\partial_N\delta(\underline{\theta},\underline{\theta}_2)\partial_M\delta(\underline{\theta},\underline{\theta}_3))\Big]\Big\}.
\end{aligned} \tag{C.1.4}$$

C.2 Expression of the one-loop Feynman diagrams

C.2.1 Gluon sector

Expression of the first diagram of Fig. II.1 is, for external legs carrying momentum p, color indices $a,\ b$, and Lorentz indices $\mu,\ \nu$

$$\frac{g_0^2 N}{2}\delta^{ab}\int_k (2\delta_{\mu\nu}\delta_{\rho\sigma}-\delta_{\mu\rho}\delta_{\nu\sigma}-\delta_{\mu\sigma}\delta_{\rho\nu})\left(\frac{P^T_{\rho\sigma}(k)}{k^2+n\beta_0}+\xi_0\frac{P^L_{\rho\sigma}(k)}{k^2+\beta_0\xi_0}\right), \tag{C.2.1}$$

it yields the divergent part

$$-\frac{3\kappa}{4}\delta_{\mu\nu}(3n\beta_0+\beta_0\xi_0^2)\,. \tag{C.2.2}$$

Expression of the second diagram of Fig. II.1 is, for external legs carrying momentum p, color indices $a,\ b$, and Lorentz indices $\mu,\ \nu$

$$\begin{aligned}\frac{g_0^2 N}{2}\delta^{ab}\ \int_k\ &(p_\tau\delta_{\mu\sigma}-p_\sigma\delta_{\mu\tau}-k_\mu\delta_{\tau\sigma}+k_\tau\delta_{\mu\sigma}+(k-p)_\sigma\delta_{\mu\tau}-(k-p)_\mu\delta_{\sigma\tau})\\ &\times(-p_\lambda\delta_{\nu\rho}+p_\rho\delta_{\nu\lambda}+k_\nu\delta_{\lambda\rho}-k_\lambda\delta_{\nu\rho}-(k-p)_\rho\delta_{\nu\lambda}+(k-p)_\nu\delta_{\rho\lambda})\\ &\times\left(\frac{P^T_{\sigma\rho}(k)}{k^2+n\beta_0}+\xi_0\frac{P^L_{\sigma\rho}(k)}{k^2+\beta_0\xi_0}\right)\left(\frac{P^T_{\tau\lambda}(k-p)}{(k-p)^2+n\beta_0}+\xi_0\frac{P^L_{\tau\lambda}(k-p)}{(k-p)^2+\beta_0\xi_0}\right)\end{aligned} \tag{C.2.3}$$

it yields the divergent part

$$\frac{\kappa}{12}\left(\delta_{\mu\nu}(9\beta_0\xi_0^2+9n\beta_0(4+\xi_0)+p^2(6\xi_0-25))-2p_\mu p_\nu(3\xi_0-14)\right)\,. \tag{C.2.4}$$

Expression of the third diagram of Fig. II.1 is, for external legs carrying momentum p, color indices $a,\ b$, and Lorentz indices $\mu,\ \nu$

$$g_0^2 N\delta^{ab}\int_k\frac{k_\mu}{k^2+\beta_0\xi_0}\frac{(k-p)_\nu}{(k-p)^2+\beta_0\xi_)}\,, \tag{C.2.5}$$

it yields the divergent part

$$-\frac{\kappa}{12}\left[\delta_{\mu\nu}(6\beta_0\xi_0+p^2)+2p_\mu p_\nu\right]\,. \tag{C.2.6}$$

Expression of the fourth diagram of Fig. II.1 is, for external legs carrying momentum p, color indices $a,\ b$, and Lorentz indices $\mu,\ \nu$

$$-\delta^{ad}(n-1)\frac{g_0^2 N\beta_0\xi_0}{8}\int_k\frac{(k_\mu+(k-p)_\mu)\,(k_\nu+(k-p)_\nu)}{(k^2+\beta_0\xi_0)\,((k-p)^2+\beta_0\xi_0)}\left(\frac{2}{k^2}+\frac{2}{(k-p)^2}+\frac{(n+2)\beta_0\xi_0}{k^2(k-p)^2}\right), \tag{C.2.7}$$

it yields the divergent part

$$-\frac{\kappa}{2}(n-1)\beta_0\xi_0\delta_{\mu\nu}\,. \tag{C.2.8}$$

Expression of the fifth diagram of Fig. II.1 is, for external legs carrying momentum p, color indices $a,\ b$, and Lorentz indices $\mu,\ \nu$

$$-\delta^{ad}(n-1)\frac{g_0^2 N\beta_0\xi_0^2}{d-1}P^T_{\mu\nu}(p)\times\int_k\frac{k^2p^2-(k\cdot p)^2}{k^2(k-p)^2\,(k^2+\beta_0\xi_0)\,((k-p)^2+\beta_0\xi_0)}\,, \tag{C.2.9}$$

it is finite in $d=4$ dimensions.

C.2.2 Ghost sector

Expression of the first diagram of Fig. II.2 is, for external legs carrying momentum p, color indices $a,\ b$

$$g_0^2 N\delta^{ab}\int_k\frac{(k-p)_\mu p_\nu}{(k-p)^2+\beta_0\xi_0}\left(\frac{P^T_{\mu\nu}(k)}{k^2+n\beta_0}+\xi_0\frac{P^L_{\mu\nu}}{k^2+\beta_0\xi_0}\right)\,, \tag{C.2.10}$$

it yields the divergent part

$$\frac{\kappa}{4}p^2(\xi_0 - 3)\,. \tag{C.2.11}$$

Expression of the second diagram of Fig. II.2 is, for external legs carrying momentum p, color indices $a,\ b$

$$\frac{g_0^2 N}{2}\delta^{ab}\xi_0 \int_k \frac{1}{k^2 + \beta_0\xi_0}\,, \tag{C.2.12}$$

it yields the divergent part

$$-\frac{\kappa}{2}\xi_0^2\beta_0\,. \tag{C.2.13}$$

Expression of the third diagram of Fig. II.2 is, for external legs carrying momentum p, color indices $a,\ b$

$$-\frac{g_0^2 N}{4}\delta^{ab}\xi_0^2\beta_0 \int_k \frac{1}{k^2 + \beta_0\xi_0}\frac{1}{(k-p)^2 + \beta_0\xi_0}\,, \tag{C.2.14}$$

it yields the divergent part

$$-\frac{\kappa}{4}\xi_0^2\beta_0\,. \tag{C.2.15}$$

Expression of the sum of the fourth and fifth diagrams of Fig. II.2 is, for external legs carrying momentum p, color indices $a,\ b$

$$-\frac{g_0^2 N}{2}\delta^{ab}\xi_0 \int_k \frac{k^2}{k^2 + \beta_0\xi_0}\frac{1}{(k-p)^2 + \beta_0\xi_0}\,, \tag{C.2.16}$$

it yields the divergent part

$$\kappa\xi_0^2\beta_0\,. \tag{C.2.17}$$

C.2.3 $ih - ih$ and $A - ih$ sectors

Expression of the first diagram of Fig. II.3 is, for external legs carrying momentum p, color indices $a,\ b$

$$-\frac{g_0^2 N}{4}\delta^{ab}\xi_0^2 \int_k \frac{1}{k^2 + \beta_0\xi_0}\frac{1}{(k-p)^2 + \beta_0\xi_0}\,, \tag{C.2.18}$$

it yields the divergent part

$$-\frac{\kappa}{4}\xi_0^2\,. \tag{C.2.19}$$

Expression of the first diagram of Fig. II.5 is, for external legs carrying momentum p, color indices $a,\ b$ and for the gluon leg carrying the Lorentz index μ

$$\frac{g_0^2 N}{2}\delta^{ab}\xi_0 i \int_k \frac{k_\mu}{k^2 + \beta_0\xi_0}\frac{1}{(k-p)^2 + \beta_0\xi_0}\,, \tag{C.2.20}$$

it yields the divergent part

$$\frac{\kappa}{4}\xi_0 i p_\mu\,. \tag{C.2.21}$$

C.2.4 $\Lambda - \Lambda$ sector

Expression of the first diagram of Fig. II.4 is, for external legs carrying momentum p, color indices $a,\ b$ and replica indices $i,\ j$

$$-\frac{g_0^2 N}{6}\delta^{ab}\delta_{ij}\int_k \left(\delta(\underline{\theta}_i,\underline{\theta}_j)\frac{p^2+\frac{k^2}{2}}{k^2(k^2+\beta_0\xi_0)}+\frac{\xi_0}{2}\frac{\Box_{\underline{\theta}_i}\delta(\underline{\theta}_i,\underline{\theta}_j)}{k^2(k^2+\beta_0\xi_0)}\right), \tag{C.2.22}$$

it yields the divergent part

$$-\frac{\kappa}{12}\delta_{ij}\xi_0\left(\delta(\underline{\theta}_i,\underline{\theta}_j)(2p^2-\beta_0\xi_0)+\xi_0\Box_{\underline{\theta}_i}\delta(\underline{\theta}_i,\underline{\theta}_j\right). \tag{C.2.23}$$

Expression of the second diagram of Fig. II.4 is, for external legs carrying momentum p, color indices $a,\ b$ and replica indices $i,\ j$

$$\frac{g_0^2 N}{3}\delta^{ab}\delta_{ij}\int_k \xi_0\delta(\underline{\theta}_i,\underline{\theta}_j)\frac{1}{(k^2+\beta_0\xi_0)}, \tag{C.2.24}$$

it yields the divergent part

$$-\frac{\kappa}{3}\delta_{ij}\beta_0\xi_0^2\delta(\underline{\theta}_i,\underline{\theta}_j). \tag{C.2.25}$$

Expression of the third diagram of Fig. II.4 is, for external legs carrying momentum p, color indices $a,\ b$ and replica indices $i,\ j$

$$\begin{aligned}-\frac{g_0^2 N}{4}\delta^{ab}\int_k &\left(4\frac{p^2-\frac{(k\cdot p)^2}{k^2}}{k^2+n\beta_0}+\xi_0\frac{(k^2+4(-k\cdot p+\frac{(k\cdot p)^2}{k^2}}{k^2+\beta_0\xi_0}\right)\\ &\times\left(\frac{\delta_{ij}\delta(\underline{\theta}_i,\underline{\theta}_j)}{(k-p)^2+\beta_0\xi_0}+\xi_0\frac{1+\delta_{ij}}{(k-p)^2((k-p)^2+\beta_0\xi_0)}\right),\end{aligned} \tag{C.2.26}$$

it yields the divergent part

$$\delta_{ij}\delta(\underline{\theta}_i,\underline{\theta}_j)\left(\frac{\kappa}{4}(p^2(\xi_0-3)+2\beta_0\xi_0^2)\right)-(1+\delta_{ij})\frac{\kappa}{4}\xi_0^2. \tag{C.2.27}$$

Expression of the fourth diagram of Fig. II.4 is, for external legs carrying momentum p, color indices $a,\ b$ and replica indices $i,\ j$

$$-(1+\delta_{ij})\frac{g_0^2 N}{4}\xi_0^2\delta^{ab}\int_k\left(\frac{2k\cdot p-k^2}{k^2(k^2+\xi_0\beta_0)}\frac{k^2-p^2}{(k-p)^2((k-p)^2+\beta_0\xi_0)}\right), \tag{C.2.28}$$

it yields the divergent part

$$(1+\delta_{ij})\frac{\kappa}{4}\xi_0^2. \tag{C.2.29}$$

C.2.5 $A - \Lambda$ sector

Expression of the first diagram of Fig. II.5 is, for external legs carrying momentum p, color indices $a,\ b$ and for the gluon leg carrying the Lorentz indiex μ

$$\frac{g_0^2 N}{3}\delta^{ab}\xi_0\int_k\frac{ip_\mu}{k^2(k^2+\beta_0\xi_0)}, \tag{C.2.30}$$

it yields the divergent part

$$\frac{\kappa}{3}\xi_0 i p_\mu \,. \tag{C.2.31}$$

Expression of the first diagram of Fig. II.5 is, for external legs carrying momentum p, color indices $a,\ b$ and for the gluon leg carrying the Lorentz index μ

$$-\frac{g_0^2 N}{4}\delta^{ab}\xi_0 \int_k \frac{i(2k_\mu - p_\mu)(p^2-k^2)}{(k-p)^2((k-p)^2+\beta_0\xi_0)}\left(\frac{1}{k^2+\beta_0\xi_0}+\frac{n\beta_0\xi_0}{k^2(k^2+\beta_0\xi_0)}\right), \tag{C.2.32}$$

it yields the divergent part

$$\frac{\kappa}{4}\xi_0 i p_\mu \,. \tag{C.2.33}$$

Expression of the third diagram of Fig. II.5 is, for external legs carrying momentum p, color indices $a,\ b$ and for the gluon leg carrying the Lorentz index μ

$$\begin{aligned} i\frac{g_0^2 N}{2}\xi_0\delta^{ab} \int_k & (p_\rho\delta_{\mu\nu} - p_\nu\delta_{\mu\rho} - k_\mu\delta_{\rho\nu} + k_\rho\delta_{\mu\nu} + (k-p)_\nu\delta_{\rho\mu} - (k-p)_\mu\delta_{\rho\nu}) \\ & \times\left(\frac{P^T_{\nu\sigma}(k)}{k^2+n\beta_0} + \xi_0\frac{P^L_{\nu\sigma}(k)}{k^2+\beta_0\xi_0}\right)\frac{(k-2p)_\sigma(k-p)_\rho}{(k-p)^2((k-p)^2+\beta_0\xi_0)}\,, \end{aligned} \tag{C.2.34}$$

it yields the divergent part

$$-3\frac{\kappa}{4}\xi_0 i p_\mu \,. \tag{C.2.35}$$

Appendix D

Complete propagators

We detail the inversion of the one-loop two-point vertex function matrix Eq. (II.4.9) that reads

$$\Gamma^{(2)} = \begin{pmatrix} \Gamma_T P^T_{\mu\nu} + \Gamma_L P^L_{\mu\nu} & -ip_\mu \Gamma_{ihA} & ip_\mu \Gamma_4 \\ ip_\nu \Gamma_{ihA} & \Gamma_{ihih} & 0 \\ -ip_\nu \Gamma_4 & 0 & \delta_{kl}\Big[\Gamma_1 \delta(\underline{\theta}_k, \underline{\theta}'_l) + \Gamma_2 \Box_{\underline{\theta}_k} \delta(\underline{\theta}_k, \underline{\theta}'_l)\Big] + (\delta_{kl} - 1)\Gamma_3 \end{pmatrix}, \tag{D.0.1}$$

where the scalar functions Γ_T, Γ_L, Γ_{ihA} and $\Gamma_{1,\dots,4}$ only depend on p^2 and where $\Box_{\underline{\theta}}$ is the Laplace operator on the curved Grassmann space, defined as [202, 98]

$$\Box_{\underline{\theta}} = \frac{1}{\sqrt{g(\underline{\theta})}} \partial_M \sqrt{g(\underline{\theta})} g^{MN} \partial_N = 2\beta_0(\theta\partial_\theta + \bar{\theta}\partial_{\bar{\theta}}) + 2(1 - \beta_0 \bar{\theta}\theta)\partial_\theta \partial_{\bar{\theta}}, \tag{D.0.2}$$

and which satisfies $\Box_{\underline{\theta}} \delta(\underline{\theta}, \underline{\theta}') = -2 + 2\beta_0 \delta(\underline{\theta}, \underline{\theta}')$. In particular, in (D.0.1), we used the fact that, at one-loop order, there is no contribution to $\Gamma_{ih\Lambda_k}$. Note that, since there are $n-1$ replicas, the matrix representation (II.4.9) only makes sense for $n > 0$ and the limit $n \to 0$ must be done after the inversion. Using the symmetries of the problem , the most general form of the inverse matrix $(\Gamma^{(2)})^{-1}$ reads

$$(\Gamma^{(2)})^{-1} = \begin{pmatrix} \Delta_T P^T_{\rho\nu} + \Delta_L P^L_{\rho\nu} & ip_\rho \Delta_{ihA} & -ip_\rho \Delta_4 \\ -ip_\nu \Delta_{ihA} & \Delta_{ihih} & \Delta_5 \\ ip_\nu \Delta_4 & \Delta_5 & \delta_{lm}\left[\Delta_1 \delta(\underline{\theta}_l, \underline{\theta}_m) + \Delta_2 \Box_{\underline{\theta}_l} \delta(\underline{\theta}_l, \underline{\theta}_m)\right] + (1 - \delta_{lm})\Delta_3 \end{pmatrix}, \tag{D.0.3}$$

where the unknown scalar functions Δ_T, Δ_L, Δ_{ihA}, and $\Delta_{1,\dots,5}$ only depend on p^2. The inversion is defined by

$$\Gamma^{(2)} \times \left(\Gamma^{(2)}\right)^{-1} = \begin{pmatrix} \delta_{\mu\rho} & 0 & 0 \\ 0 & 1 & 0 \\ 0 & 0 & \delta_{km}\delta(\underline{\theta}_k, \underline{\theta}_m) \end{pmatrix}, \tag{D.0.4}$$

where the product $\times$ involves a sum over Lorentz and replica indices and an integral over the Grassmann variable $\underline{\theta}_l$. The calculation is straightforward. We get, for the gluon sector,

$$\Delta_T = \frac{1}{\Gamma_T} \quad \text{and} \quad \Delta_L = \frac{\Gamma_{ihih}\left(\Gamma_1 + (n-2)\beta_0\Gamma_3\right)}{\left(\Gamma_L\Gamma_{ihih} - p^2\Gamma^2_{ihA}\right)\left(\Gamma_1 + (n-2)\beta_0\Gamma_3\right) - (n-1)\beta_0 p^2 \Gamma_{ihih}\Gamma_4^2}. \tag{D.0.5}$$

The other components in the (A, ih) sector are obtained from these as

$$\Delta_{ihA} = \frac{\Gamma_{ihA}}{\Gamma_{ihih}}\Delta_L \quad \text{and} \quad \Delta_{ihih} = \frac{1 + p^2\Gamma_{ihA}\Delta_{ihA}}{\Gamma_{ihih}}. \tag{D.0.6}$$

Finally, the components in the superfield sector read

$$\Delta_4 = -\frac{1}{(n-1)\beta_0 p^2\Gamma_4}\left\{1 - \frac{\Delta_{ihA}(\Gamma_L\Gamma_{ihih} - p^2\Gamma_{ihA}^2)}{\Gamma_{ihA}}\right\} \tag{D.0.7}$$

$$\Delta_5 = -p^2\frac{\Gamma_{ihA}}{\Gamma_{ihih}}\Delta_4 \tag{D.0.8}$$

$$\Delta_3 = \frac{1}{\Gamma_1 + (n-2)\beta_0\Gamma_3}\left\{p^2\Gamma_4\Delta_4 - \frac{\Gamma_3}{(\Gamma_1 - \beta_0\Gamma_3)}\right\} \tag{D.0.9}$$

$$\Delta_1 = \frac{1}{\Gamma_1 - \Gamma_3\beta_0} + \beta_0\Delta_3 \tag{D.0.10}$$

$$\Delta_2 = \frac{1}{2\beta_0(\Gamma_1 + 2\beta_0\Gamma_2)} - \frac{\Delta_1}{2\beta_0}. \tag{D.0.11}$$

The propagators are obtained by taking the limit $n \to 0$. For instance, the longitudinal gluon propagator is given by

$$G_L(p) = \lim_{n\to 0}\Delta_L(p), \tag{D.0.12}$$

which is Eq. (II.5.3).

Appendix E

Superfield and ih sectors

In this Appendix, we consider the propagators of the superfield and ih sectors. We recall the decomposition of the superfireld Eq. (II.4.57), namely

$$\Lambda_k = \lambda_k + \bar{\theta} c'_k + \bar{c}'_k \theta + \bar{\theta}\theta \hat{h}'_k, \tag{E.0.1}$$

where the primes are to be distinguished from the basic fields c_k, $\bar{c}_k$, $\hat{h}_k$ appearing in the non supersymmetric version of the ST action, Eqs. (II.4.48) and (II.4.49). One easily extracts the correlators of the fields λ_k, c'_k, $\bar{c}'_k$, $\hat{h}'_k$ from the $\Lambda - \Lambda$ correlator. For instance we have that $[\lambda_k \lambda_l]_0$ is given by the $\underline{\theta}_k$, $\underline{\theta}_l$ independent part of $[\Lambda_k \Lambda_l]_0$. According to the definition of the previous section we have

$$[\lambda_k(-p)\lambda_l(p)]_0 = -2\delta_{kl}\Delta_2(p) + (1-\delta_{kl})\Delta_3(p). \tag{E.0.2}$$

In the $n \to 0$ limit one finds[1]

$$[\lambda_k(-p)\lambda_l(p)]_0 \;\to\; 0 \tag{E.0.3}$$
$$\left[\hat{h}'_k(-p)\hat{h}'_l(p)\right]_0 \;\to\; \infty \tag{E.0.4}$$
$$[ih(-p)ih(p)]_0 \;\to\; \infty \tag{E.0.5}$$
$$[c_k(-p)\,\bar{c}_l(p)]_0 \;\to\; \delta_{kl} G^{(k)}_{gh}, \tag{E.0.6}$$

where $G^{(k)}_{gh}$ is the propagator of the replica ghost, as well as for the mixed correlators

$$[\lambda_k(-p)A_\mu(p)]_0 \;\to\; 0 \tag{E.0.7}$$
$$[ih(-p)A_\mu(p)]_0 \;\to\; 0 \tag{E.0.8}$$
$$[ih(-p)\,\lambda_l(p)]_0 \;\to\; G_{ih\lambda}. \tag{E.0.9}$$

Note in particular the indefinite limits Eqs. (E.0.4), (E.0.5) and the trivial one Eq. (E.0.3). These are consequences of the renormalization definitions for the (bare) gauge parameters β_0 and ξ_0 Eq. (II.5.4) and can be related to the non-canonical mass dimension

[1] For simplicity we extracted everywhere a trivial unit color matrix δ^{ab} and do not write explicitly the color indices.

of the λ_k and $\hat{h}'_k$, ih fields which are respectively 0, 2 and 2. For instance, if we consider Γ_{ihih} at tree-level, we have $\Gamma_{ihih} = \xi n$ which trivially vanishes for $n \to 0$. On the other hand, remark that the (renormalized) Grassmann measure gets an explicit n dependence as it reads, in terms of renormalized quantities, $\bar{\theta}\theta m^2/n - 1$. One can cope with this issue by rescaling the fields with non-canonical dimensions as well as the Grassmann variables. For simplicity we note $\beta = m^2/n$ and denote with a tilda the rescaled (renormalized) quantities. We define the rescaled Grassmannian parameters $\tilde{\theta}_k = \sqrt{\beta}\theta$, $\tilde{\bar{\theta}}_k = \sqrt{\beta}\bar{\theta}$ such that the Grassmann integration reads, in terms of rescaled parameters,

$$\int_{\underline{\theta}} = \int d\theta\, d\bar{\theta}(\beta\bar{\theta}\theta - 1) = \beta \int d\tilde{\theta}\, d\tilde{\bar{\theta}}(\tilde{\bar{\theta}}\tilde{\theta} - 1) = \beta \int_{\underline{\tilde{\theta}}}, \tag{E.0.10}$$

along with the following identities

$$\delta\left(\underline{\theta}_k, \underline{\theta}_l\right) = \frac{1}{\beta}\delta\left(\underline{\tilde{\theta}}_k, \underline{\tilde{\theta}}_l\right), \quad \Box_{\underline{\theta}_k}\delta\left(\underline{\theta}_k, \underline{\theta}_l\right) = \Box_{\underline{\tilde{\theta}}_k}\delta\left(\underline{\tilde{\theta}}_k, \underline{\tilde{\theta}}_l\right). \tag{E.0.11}$$

Accordingly we define

$$\tilde{\Lambda}_k = \tilde{\lambda}_k + \tilde{\bar{\theta}}\tilde{c}'_k + \tilde{\bar{c}}'_k\tilde{\theta} + \tilde{\bar{\theta}}\tilde{\theta}\,\hat{\tilde{h}}'_k, \tag{E.0.12}$$

with $\tilde{\Lambda}_k = \sqrt{\beta}\Lambda_k$. A direct comparison with Eq. (E.0.1) shows that

$$\begin{aligned} \tilde{\lambda}_k = \sqrt{\beta}\lambda_k\ , \quad \hat{\tilde{h}}'_k = \frac{\hat{h}'_k}{\sqrt{\beta}}\,, \\ \tilde{c}'_k = c'_k\ , \quad \tilde{\bar{c}}'_k = \bar{c}'_k\,. \end{aligned} \tag{E.0.13}$$

Remark that, in doing so, we do nothing more than absorbing the n dependence that arises when performing the renormalization Eq. (II.5.4) directly into the Feynman rules of the rescaled fields. Equivalently, this amounts to reabsorb part of the n dependence into the bare fields. For instance the $\Lambda - \Lambda$ sector of the effective action reads

$$\int_{p,\underline{\theta}_k,\underline{\theta}_l} \Lambda_k\left(-p, \underline{\theta}_k\right)\Gamma_{\Lambda_k\Lambda_l}\left(p, \underline{\theta}_k, \underline{\theta}_l\right)\Lambda_l\left(p, \underline{\theta}_l\right) = \int_{p,\underline{\tilde{\theta}}_k,\underline{\tilde{\theta}}_l} \tilde{\Lambda}_k\left(-p, \underline{\tilde{\theta}}_k\right)\beta\,\Gamma_{\tilde{\Lambda}_k\tilde{\Lambda}_l}\left(p, \underline{\theta}_k, \underline{\theta}_l\right)\tilde{\Lambda}_l\left(p, \underline{\tilde{\theta}}_l\right), \tag{E.0.14}$$

which yields

$$\Gamma_{\tilde{\Lambda}_k\tilde{\Lambda}_l}\left(p, \underline{\tilde{\theta}}_k, \underline{\tilde{\theta}}_l\right) = \beta\,\Gamma_{\Lambda_k\Lambda_l}\left(p, \underline{\theta}_k, \underline{\theta}_l\right). \tag{E.0.15}$$

Using the identities (E.0.11) along with the decomposition of $\Gamma_{\Lambda_k\Lambda_l}$ from (D.0.1) we finally obtain

$$\begin{aligned} \tilde{\Gamma}_1(p) &= \Gamma_1(p)\,, \\ \tilde{\Gamma}_2(p) &= \beta\Gamma_2(p)\,, \\ \tilde{\Gamma}_3(p) &= \beta\Gamma_3(p)\,. \end{aligned} \tag{E.0.16}$$

Along the same lines we define $i\tilde{h} = ih/\sqrt{\beta}$. Eventually the remaining one-loop rescaled scalar functions appearing into the various two-point vertex functions Eq. (D.0.1) read

$$\begin{aligned}\tilde{\Gamma}_{i\tilde{h}A}(p) &= \sqrt{\beta}\Gamma_{ihA}(p)\,,\\ \tilde{\Gamma}_4(p) &= \frac{1}{\sqrt{\beta}}\Gamma_4(p)\,,\\ \tilde{\Gamma}_{i\tilde{h}i\tilde{h}}(p) &= \beta\Gamma_{ihih}(p)\,.\end{aligned} \tag{E.0.17}$$

Note for instance that, at tree-level, $\tilde{\Gamma}_{i\tilde{h}i\tilde{h}}(p) = m^2\xi$. Accordingly, we obtain the various $\tilde{\Delta}_\chi$ functions for the rescaled fields appearing in (D.0.3) and perform the $n \to 0$ limit to get the various rescaled propagators. We note the propagators as $\tilde{G}_\chi = \lim_{n\to 0}\tilde{\Delta}_\chi$. In particular we have that

$$\tilde{G}_L(p) = \tilde{G}_{ihA}(p) = \tilde{G}_4(p) = 0, \tag{E.0.18}$$

while none is divergent anymore.

Appendix F

Nonrenormalization theorem for the mass

Here we derive the nonrenormalization theorem (III.5.80) for the neutral color mode by adapting the proof provided in [78] to the LDW gauge. As in Eq. (I.5.3) of Sec. I.5.1, we introduce sources (with periodic boundary conditions) for the various fields and their independent (modified) BRST transformations and we work in the canonical basis (III.5.3)

$$S_1 = \int_x \sum_\kappa \left\{ J_\mu^{-\kappa} a_\mu^\kappa + \bar\eta^{-\kappa} c^\kappa + \bar c^\kappa \eta^{-\kappa} + i h^\kappa M^{-\kappa} + \bar K_\mu^{-\kappa} s a_\mu^\kappa + \bar L^{-\kappa} s c^\kappa \right\}, \tag{F.0.1}$$

where, for clarity, we explicitly write the sums over color modes, and where the modified BRST symmetry is given by[95]

$$s a_\mu^\kappa = D_\mu c^\kappa \,, \quad s c^\kappa = -\frac{g_0}{2} f^{\kappa\lambda\tau} c^\lambda c^\tau \,, \tag{F.0.2}$$

and

$$s \bar c^\kappa = i h^\kappa \,, \quad s i h^\kappa = m_0^2 c^\kappa . \tag{F.0.3}$$

We define the effective action Γ as the Legendre transform, with respect to the sources J_μ, η, $\bar\eta$, M, of the functional $W = \ln \int \mathcal{D}(a, c, \bar c, h)\, e^{-S_{\bar A} + S_1}$, where $S_{\bar A}$ has been defined in Eq. (III.4.6), keeping the sources $\bar K$ and $\bar L$ fixed. It is implicitly assumed here that we a use self-consistent background, which, at vanishing sources, is given by the minimum of the background potential (III.4.18). In the following all quantities are bare ones.

First of all, one performs the shift of the antighost field $\bar c^\kappa(x) \to \bar c^\kappa(x) + \bar\theta^\kappa(x)$. Since it is merely a change of variable the partition function is not changed and one gets

$$\begin{aligned} 0 &= \int \mathcal{D}(a, c, \bar c, h)\, e^{-S_{\bar A} + S_1} \left[\left(\bar D_\mu D_\mu c \right)^{-\kappa}(x) + \eta^{-\kappa}(x) \right] \\ &= -\partial_\mu^{-\kappa} \frac{\delta \Gamma}{\delta \bar K_\mu^\kappa(x)} + \frac{\delta \Gamma}{\bar c^\kappa(x)} \,, \end{aligned} \tag{F.0.4}$$

where there is no sum over κ and in the second line we took the limit of vanishing sources. The short-hand notation ∂_μ^λ has been defined in Eq. (III.5.6). Differentiating this equation with respect to $c^\lambda(y)$ and taking the Fourier transform, with the convention of Eq. (III.5.5), namely $\partial_\mu^\kappa \to -iP_\mu^\kappa$, leads to

$$\Gamma_{\bar{c}^\kappa c^\lambda}(\omega,\mathbf{p}) = -iP_\mu^{-\kappa}\Gamma_{\bar{K}_\mu^\kappa c^\lambda}(\omega,\mathbf{p})\,, \tag{F.0.5}$$

where $P=(\omega,\mathbf{p})$.

Secondly, performing the shift $ih^\kappa \to ih^\kappa + \xi^\kappa$ yields (no sum over κ)

$$\frac{\delta\Gamma}{\delta ih^\kappa(x)} = \partial_\mu^{-\kappa} a_\mu^{-\kappa}(x)\,, \tag{F.0.6}$$

which guarantees that the h sector is not renormalized, just as in the Landau gauge. Taking, in the last equality, one derivative with respect to $a_\nu^\lambda(y)$ leads, in Fourier space, to

$$\frac{\delta\Gamma}{\delta a_\nu^\lambda \delta ih^\kappa}(\omega,\mathbf{p}) = -iP_\nu^{-\kappa}\delta^{-\kappa,\lambda}\,. \tag{F.0.7}$$

Moreover, the Slavnov-Taylor identity (I.5.6) of Sec. I.5.1 is accordingly adapted to the LDW gauge in a straightforward manner

$$\int_x \sum_\kappa \left\{ -\frac{\delta\Gamma}{\delta a_\mu^\kappa}\frac{\delta\Gamma}{\delta \bar{K}_\mu^{-\kappa}} - \frac{\delta\Gamma}{\delta c^\kappa}\frac{\delta\Gamma}{\delta \bar{L}^{-\kappa}} + ih^\kappa \frac{\delta\Gamma}{\delta \bar{c}^{-\kappa}} + m_0^2 \frac{\delta\Gamma}{\delta ih^\kappa} c^\kappa = 0 \right\}, \tag{F.0.8}$$

which, after differentiation with respect to $a_\nu^\lambda(y)$ and $c^\tau(z)$, yields, at vanishing sources and in Fourier space,

$$\sum_\kappa \left\{ \frac{\delta^2\Gamma}{\delta a_\nu^\lambda \delta a_\mu^\kappa}(\omega,\mathbf{p}) \frac{\delta^2\Gamma}{\delta \bar{K}_\mu^{-\kappa}\delta c^\tau}(\omega,\mathbf{p}) + m_0^2\delta^{\kappa,\tau}\frac{\delta^2\Gamma}{\delta a_\nu^\lambda \delta ih^\kappa}(\omega,\mathbf{p}) \right\} = 0\,. \tag{F.0.9}$$

Using Eq. (F.0.7) and contracting with P_ν^λ, we have

$$\sum_\kappa P_\nu^\lambda \frac{\delta^2\Gamma}{\delta a_\nu^\lambda \delta a_\mu^\kappa}(\omega,\mathbf{p}) \frac{\delta^2\Gamma}{\delta \bar{K}_\mu^{-\kappa}\delta c^\tau}(\omega,\mathbf{p}) = im_0^2 P_\lambda^2 \delta^{\lambda,-\tau}\,. \tag{F.0.10}$$

Following our conventions for the self-energies, Eq. (III.5.15), we have that $\delta^2\Gamma/\delta a_\nu^\lambda \delta a_\mu^\kappa = \delta^{-\lambda\kappa}\Gamma_{\nu\mu}^\lambda$. Furthemore, the general tensorial decomposition Eq. (III.1.4) yields for $P_\nu^\lambda \Gamma_{\nu\mu}^\lambda$

$$\begin{aligned} P_\nu^\lambda \Gamma_{\nu\mu}^\lambda =& \delta_{\mu\nu}\Gamma_\delta^\lambda + n_\mu \omega^\lambda \Gamma_{\rm n}^\lambda + P_\mu^\lambda P_\lambda^2 \Gamma_{\rm P}^\lambda + (n_\mu P_\lambda^2 + P_\mu^\lambda \omega^\lambda)\Gamma_{\rm nP}^\lambda \\ \underset{\omega=0}{=}& \delta_{\mu\nu}\Gamma_\delta^\lambda(0,p) + n_\mu \lambda r T \Gamma_{\rm n}^\lambda(0,p) + P_\mu^\lambda \left((\lambda r T)^2 + p^2\right)\Gamma_{\rm P}^\lambda(0,p) \\ &+ (n_\mu \left((\lambda r T)^2 + p^2\right) + P_\mu^\lambda \lambda r T)\Gamma_{\rm nP}^\lambda(0,p)\,, \end{aligned} \tag{F.0.11}$$

where the second line is evaluated at zero Matsubara frequency, $p=|\mathbf{p}|$, and it is understood that $r = r_{\min}$. The discussion cannot be pushed much further for the

charged modes. On the contrary, for $\lambda = 0$, the analiticity of $\Gamma^0_{\nu\mu}(0,\mathbf{p})$ as $p \to 0$ requires that $\lim_{p\to 0}\Gamma^\lambda_{\rm P}(0,p) = \lim_{p\to 0}\Gamma^\lambda_{\rm nP}(0,p) = 0$. Hereby,

$$\begin{aligned}\sum_\kappa P^0_\nu \frac{\delta^2\Gamma}{\delta a^0_\nu \delta a^\kappa_\nu}(\omega,\mathbf{p})\frac{\delta^2\Gamma}{\delta \bar{K}^{-\kappa}_\mu \delta c^\tau}(\omega,\mathbf{p}) &\underset{\substack{\omega=0,\\ p\to 0}}{=} \lim_{p\to 0}\Gamma^0_\delta(0,p)\, P^0_\nu \frac{\delta^2\Gamma}{\delta \bar{K}^0_\mu \delta c^\tau}(0,\mathbf{p}) \\ &\underset{\substack{\omega=0,\\ p\to 0}}{=} i\lim_{p\to 0}\Gamma^0_\delta(0,p)\,\Gamma_{\bar{c}^0 c^\tau}(0,p)\,,\end{aligned} \tag{F.0.12}$$

where we used Eq. (F.0.5) in the second line and it is understood that the limit $p \to 0$ is performed after that $\omega = 0$. Noting that $\left(\mathcal{G}^0_T\right)^{-1} = \Gamma^0_\delta$, one finally gets, by using the last line of Eq. (F.0.12) in Eq. (F.0.10), that

$$\left(\mathcal{G}^0_T\right)^{-1}\left(F^0\right)^{-1}\Big|_{\omega=0,\ p\to 0} = m_0^2\,. \tag{F.0.13}$$

Appendix G

Background field (in)dependence of the partition function

It is worth mentioning here the discussion put forward in [95], that investigates the background (in)dependence of the partition function. In particular, it was shown that, at vanishing sources,

$$\frac{\delta \ln Z[\bar{A}]}{\delta \bar{A}^a_\mu} = m_0^2 \left\langle a^a_\mu \right\rangle_{\min} = m_0^2 \, a^a_{\min,\mu}[\bar{A}] \,, \tag{G.0.1}$$

where $Z[\bar{A}]$ is the partition function in presence of an arbitrary background $\bar{A}$. Hereby, the presence of the mass term softly breaks the exact background field independence of the partition function which is recovered locally for self-consistent backgrounds. We interpret this as an argument to consider self-consistent backgrounds.

On the other hand, the relationship between self-consistent background and the absolute minima of $\tilde{\Gamma}[\bar{A}]$ is unclear as the arguments developed in Sec. III.4 relied upon the background independence of the partition function. In fact, the statement that self-consistent backgrounds are absolute minima of $\tilde{\Gamma}[\bar{A}]$ has to be milded as follows: we introduce a source J^a_μ for the fluctuating field $\bar{a}$ and define the partition function in presence of the source

$$Z[J, \bar{A}] = \int \mathcal{D}\,(a, c, \bar{c}, h)\, e^{-S_{\bar{A}} + \int_x J^a_\mu a^a_\mu} \,, \tag{G.0.2}$$

where $S_{\bar{A}}$ has been defined in Eq. (III.4.6). Accordingly, we define the usual Legendre transform $\Gamma[a, \bar{A}]$ (here for the sake of clarity we change our notations from those of the main text and put $\bar{A}$ as an argument of Γ)

$$\Gamma[a, \bar{A}] = -\ln Z[J, \bar{A}] + \int_x J^a_\mu[a, \bar{A}] a^a_\mu \,. \tag{G.0.3}$$

Owing to the definition of $\tilde{\Gamma}[\bar{A}] = \Gamma[0, \bar{A}]$, one has, for a self-consistent background and at vanishing sources, that

$$\left.\frac{\delta \tilde{\Gamma}[\bar{A}]}{\delta \bar{A}^a_\mu}\right|_{\bar{A}=\bar{A}_s} = - \left.\frac{\delta \ln Z[0, \bar{A}]}{\delta \bar{A}^a_\mu}\right|_{\bar{A}=\bar{A}_s} \,, \tag{G.0.4}$$

such that, according to Eq. (G.0.1),

$$\left.\frac{\delta\tilde{\Gamma}[\bar{A}]}{\delta\bar{A}^a_\mu}\right|_{\bar{A}=\bar{A}_s} = 0\,. \tag{G.0.5}$$

Hereby, self-consistent backgrounds are always extrema of $\tilde{\Gamma}[\bar{A}]$.

We find it worth mentioning that the bare mass m_0 comes from the ST gauge-fixing proposal. In particular, we recall that $m_0^2 = n\beta_0$, where n is the number of replicas and should be ultimately taken to 0. Moreover, in this proposal, the parameter m_0 accounts for the presence of Gribov copies and thus may in principle depend on $\bar{A}$ which would lead to additional terms in Eq. (G.0.1). Following these two remarks, one may thus recover the exact background independence of the partition function. This requires further investigation.

Appendix H

Generalization to SU(3) and other groups

The calculations of the one-loop correlators in the LDW gauge for the SU(2) theory can be generalized to the SU(3) case and other groups. Details on the generalization of the present procedure to general groups is given in [95], while, here, we shall focus on the aspects concerning the calculation of the propagators. The main difference with the SU(2) case rises from the fact that, in general, the Cartan subalgebra is of dimension d_C. Hence, in the canonical basis, there are d_C neutral modes that we note $\kappa = 0^{(j)}\,,\ j = 1, \ldots, d_C$, and accordingly we note $t^{0^{(j)}}$ the generators of the Cartan subalgebra. In the canonical basis, we note t^α the remaining generators that do not belong to the Cartan subalgebra. One defines the root α by the equation of the root system

$$\left[t^{0^{(j)}}, t^\alpha\right] = i\alpha^j t^\alpha\,,\ \ \forall j \tag{H.0.1}$$

with $\alpha = (\alpha^1, \ldots, \alpha^j)$. Accordingly, a field φ in the adjoint representation decomposes in the canonical basis as

$$\varphi = \varphi^\kappa t^\kappa\,, \tag{H.0.2}$$

with $\kappa = 0^{(j)}$ or $\kappa = \alpha$. Furthermore, the action of the covariant background derivative is

$$\bar{D}_\mu \varphi = \left(\partial_\mu + \delta_{\mu 0} g_0 \bar{A}\cdot\kappa\right)\varphi^\kappa t^\kappa\,, \tag{H.0.3}$$

where $\bar{A}\cdot\kappa = \bar{A}_j\kappa_j\,,\ \ j = 1, \ldots, d_C$ and a sum over repeated indices is understood.

To be more specific, let us take the example of SU(3) whose Cartan subalgebra is of dimension two. The standard Cartan subalgebra directions correspond to the Cartesian directions $a = 3, 8$ and, accordingly, the two generators of the Cartan subalgebra are chosen as $t_3 = 1/2\,\mathrm{diag}(1, -1, 0)$ and $t_8 = 1/(2\sqrt{3})\,\mathrm{diag}(1, 1, -2)$. The six roots corresponds to the six vectors $\pm\alpha_{(1)} = \pm(1/2, -\sqrt{3}/2)\,,\ \pm\alpha_{(2)} = \pm(1/2, \sqrt{3}/2)\,,\ \pm\alpha_{(3)} =$

$\pm(-1,0)$. For instance, we have for $\kappa = +\alpha_{(1)}$

$$\begin{aligned}\left(\bar{D}_\mu\varphi\right)^{\alpha_{(1)}} &= \left(\partial_\mu + g_0\frac{\bar{A}^{0(1)}}{2} - g_0\frac{\sqrt{3}\bar{A}^{0(2)}}{2}\right)\varphi^{\alpha_{(1)}} \\ \left(\bar{D}_\mu\varphi\right)^{\alpha_{(1)}} &= \left(\partial_\mu + g_0\frac{\bar{A}^{3}}{2} - g_0\frac{\sqrt{3}\bar{A}^{8}}{2}\right)\varphi^{\alpha_{(1)}}\,.\end{aligned} \tag{H.0.4}$$

The Feynman rules are formally the same as those of the SU(2) theory presented in Sec. III.5.1, but, now, the generalized momentum is defined as

$$K_\mu^\kappa \equiv K_\mu + \delta_{\mu 0} g_0 \bar{A}\cdot\kappa\,. \tag{H.0.5}$$

Thus, the calculations of the Feynman diagrams are similar to those performed in Sec. III.5.2, where the main difference lies in the expression of the group coefficient $\mathcal{C}_{\kappa\lambda\tau} = |f_{\kappa\lambda\tau}|^2$. The self-energies assume the same expressions in terms of the sum-integrals, see Eqs. (III.5.32), (III.5.36), but now, instead of the usual product κr in the SU(2) case, the latters depend on the scalar product $\kappa\cdot r = \kappa_j r_j$ with $r_j = \beta g_0 \bar{A}_j$. Finally, the self-energies are to be evaluated for $r_j = r_{j,\min}$ that minimizes the background field potential of the appropriate group.

We mention that, following this procedure the phase transition was studied for SU(3) [93] and was found to be of first order. In the present case, we did not extended the calculation of the propagators to this group. Nevertheless, akin for the SU(2) case, we expect to observe strong signals of the phase transition at the level of the susceptibilities and in particular we expect to observe a discontinuity at the transition temperature since it is a first order phase transition.

Appendix I

Details on the evaluation of the gluon self-energy

The gluon self-energy has three one-loop contributions, $\Pi^{\mathrm{tad},\lambda}_{\mu\nu}$, $\Pi^{\mathrm{gh},\lambda}_{\mu\nu}$ and $\Pi^{\mathrm{gl},\lambda}_{\mu\nu}$, which stand respectively for the tadpole diagram, the ghost bubble diagram and the gluon bubble diagram. A direct application of the Feynman rules given in the main text leads to

$$\begin{aligned}\Pi^{\mathrm{gl},\lambda}_{\mu\nu}(K)= \sum_{\kappa,\tau}\mathcal{C}_{\kappa\lambda\tau}\frac{1}{2}\Bigg\{\Bigg[-\frac{1}{2}\int_Q (Q^\kappa-L^\tau)_\mu(Q^\kappa-L^\tau)_\nu \mathrm{Tr}\left[P_\perp(Q^\kappa)\cdot P_\perp(L^\tau)\right] \\ \times G_m(Q^\kappa)G_m(L^\tau) \\ -4\int_Q\Big[Q^\kappa\cdot P_\perp(L^\tau)\cdot Q^\kappa\Big]P^\perp_{\mu\nu}(Q^\kappa)\,G_m(Q^\kappa)G_m(L^\tau) \\ +2\int_Q\Big\{(Q^\kappa-L^\tau)_\mu\Big[Q^\kappa\cdot P_\perp(L^\tau)\cdot P_\perp(Q^\kappa)\Big]_\nu+(\mu\leftrightarrow\nu)\Big\}G_m(Q^\kappa)G_m(L^\tau) \\ +4\int_Q\Big[L^\tau\cdot P_\perp(Q^\kappa)\Big]_\mu\Big[Q^\kappa\cdot P_\perp(L^\tau)\Big]_\nu G_m(Q^\kappa)G_m(L^\tau)\Big]+(\kappa\leftrightarrow\tau)\Big\},\end{aligned} \tag{I.0.1}$$

where, for convenience, we have symmetrized the summand in $\kappa\leftrightarrow\tau$ by using that $\mathcal{C}_{\kappa\lambda\tau}$ is totally symmetric. Evaluating the trace and using $(Q^\kappa-L^\tau)_\mu(Q^\kappa-L^\tau)_\nu = 2L^\tau_\mu L^\tau_\nu+2Q^\kappa_\mu Q^\kappa_\nu-K^\lambda_\mu K^\lambda_\nu$, the factor multiplying $G_m(Q^\kappa)G_m(L^\tau)$ in the first integral becomes (for this integral symmetrization in $\kappa\leftrightarrow\tau$ does not change anything)

$$-\frac{1}{2}(2Q^\kappa_\mu Q^\kappa_\nu+2L^\tau_\mu L^\tau_\nu-K^\lambda_\mu K^\lambda_\nu)\left(d-2+\frac{(Q^\kappa\cdot L^\tau)^2}{Q^2_\kappa L^2_\tau}\right). \tag{I.0.2}$$

The similar factor in the second integral becomes, after symmetrization,

$$-2\delta_{\mu\nu}\left(Q^2_\kappa+L^2_\tau-\frac{(Q^\kappa\cdot L^\tau)^2}{L^2_\tau}-\frac{(Q^\kappa\cdot L^\tau)^2}{Q^2_\kappa}\right)+2\left(Q^\kappa_\mu Q^\kappa_\nu+L^\tau_\mu L^\tau_\nu\right)\left(1-\frac{(Q^\kappa\cdot L^\tau)^2}{Q^2_\kappa L^2_\tau}\right). \tag{I.0.3}$$

For the third integral, we obtain

$$\left(Q_\mu^\kappa Q_\nu^\kappa + 3L_\mu^\tau L_\nu^\tau - K_\mu^\lambda K_\nu^\lambda\right)\frac{Q^\kappa\cdot L^\tau}{L_\tau^2} + \left(3Q_\mu^\kappa Q_\nu^\kappa + L_\mu^\tau L_\nu^\tau - K_\mu^\lambda K_\nu^\lambda\right)\frac{Q^\kappa\cdot L^\tau}{Q_\kappa^2} + \left(4Q_\mu^\kappa Q_\nu^\kappa + 4L_\mu^\tau L_\nu^\tau - 2K_\mu^\lambda K_\nu^\lambda\right)\frac{(Q^\kappa\cdot L^\tau)^2}{Q_\kappa^2 L_\tau^2} \tag{I.0.4}$$

and for the fourth

$$2\left(K_\mu^\lambda K_\nu^\lambda - Q_\mu^\kappa Q_\nu^\kappa - L_\mu^\tau L_\nu^\tau\right)\left(1+\frac{(Q^\kappa\cdot L^\tau)^2}{Q_\kappa^2 L_\tau^2}\right) - 4Q_\mu^\kappa Q_\nu^\kappa\frac{Q^\kappa\cdot L^\tau}{Q_\kappa^2} - 4L_\mu^\tau L_\nu^\tau\frac{Q^\kappa\cdot L^\tau}{L_\tau^2}\,. \tag{I.0.5}$$

Putting all these pieces together, we arrive at

$$\begin{aligned}\Pi_{\mu\nu}^{\mathrm{gl},\lambda}(K) = \sum_{\kappa,\tau}\mathcal{C}_{\kappa\lambda\tau}\Bigg\{ &-4\delta_{\mu\nu}\int_Q\left(L_\tau^2 - \frac{(Q^\kappa\cdot L^\tau)^2}{Q_\kappa^2}\right)G_m(Q^\kappa)G_m(L^\tau)\\ &+2\int_Q(-Q_\mu^\kappa Q_\nu^\kappa + L_\mu^\tau L_\nu^\tau - K_\mu^\lambda K_\nu^\lambda)\frac{Q^\kappa\cdot L^\tau}{Q_\kappa^2}\,G_m(Q^\kappa)G_m(L^\tau)\\ &+\int_Q\left(\frac{1}{2}K_\mu^\lambda K_\nu^\lambda - Q_\mu^\kappa Q_\nu^\kappa - L_\mu^\tau L_\nu^\tau\right)\frac{(Q^\kappa\cdot L^\tau)^2}{Q_\kappa^2 L_\tau^2}\,G_m(Q^\kappa)G_m(L^\tau)\\ &+\int_Q\left[\left(\frac{d-2}{2}+2\right)K_\mu^\lambda K_\nu^\lambda - (d-2)(Q_\mu^\kappa Q_\nu^\kappa + L_\mu^\tau L_\nu^\tau)\right]G_m(Q^\kappa)G_m(L^\tau)\Bigg\}.\end{aligned} \tag{I.0.6}$$

The next step uses the identity

$$\frac{Q^\kappa\cdot L^\tau}{Q_\kappa^2}G_m(Q^\kappa)G_m(L^\tau) = \frac{K_\lambda^2+m^2}{2m^2}G_0(Q^\kappa)G_m(L^\tau) - \frac{K_\lambda^2+2m^2}{2m^2}G_m(Q^\kappa)G_m(L^\tau) - \frac{1}{2m^2}\left[G_0(Q^\kappa) - G_m(Q^\kappa)\right], \tag{I.0.7}$$

as well as

$$\begin{aligned}\frac{(Q^\kappa\cdot L^\tau)^2}{Q_\kappa^2 L_\tau^2}G_m(Q^\kappa)G_m(L^\tau) = &\frac{(K_\lambda^2+2m^2)^2}{4m^4}G_m(Q^\kappa)G_m(L^\tau) + \frac{K_\lambda^4}{4m^4}G_0(Q^\kappa)G_0(L^\tau)\\ &-\frac{(K_\lambda^2+m^2)^2}{4m^4}\Big[G_m(Q^\kappa)G_0(L^\tau) + G_0(Q^\kappa)G_m(L^\tau)\Big]\\ &+\frac{1}{4m^2}\Big[G_0(Q^\kappa) + G_0(L^\tau) - G_m(Q^\kappa) - G_m(L^\tau)\Big],\end{aligned} \tag{I.0.8}$$

and

$$\left(L_\tau^2-\frac{(Q^\kappa\cdot L^\tau)^2}{Q_\kappa^2}\right)G_m(Q^\tau)G_m(L^\tau)=\frac{K_\lambda^2(K_\lambda^2+4m^2)}{4m^2}G_m(Q^\kappa)G_m(L^\tau)-\frac{1}{4}G_m(L^\tau)$$
$$-\frac{(K_\lambda^2+m^2)^2}{4m^2}G_0(Q^\kappa)G_m(L^\tau)$$
$$-\frac{K_\lambda^2}{4m^2}G_m(Q^\kappa)+\frac{K_\lambda^2+m^2}{4m^2}G_0(Q^\kappa)$$
$$-\frac{(K^\lambda\cdot Q^\kappa)}{2m^2}[G_0(Q^\kappa)-G_m(Q^\kappa)]. \qquad \text{(I.0.9)}$$

These identities allow us to express Eq. (I.0.6) in terms of the sum-integrals (III.5.33), (III.5.35), and (III.5.39). Using the symmetry properties of the latter and of the tensor $\mathcal{C}_{\kappa\lambda\tau}$, we obtain

$$\Pi_{\mu\nu}^{\mathrm{gl},\lambda}(K)=\sum_{\kappa,\tau}\mathcal{C}_{\kappa\lambda\tau}\Bigg\{\delta_{\mu\nu}\left[\frac{(K_\lambda^2+m^2)^2}{m^2}I_{m0}^{\kappa\tau}(K)-\frac{K_\lambda^2(K_\lambda^2+4m^2)}{m^2}I_{mm}^{\kappa\tau}(K)\right.$$
$$\left.+\frac{K_\lambda^2+m^2}{m^2}(J_m^\kappa-J_0^\kappa)+2\frac{\omega^\lambda}{m^2}(\tilde{J}_0^\kappa-\tilde{J}_m^\kappa)\right]$$
$$+K_\mu^\lambda K_\nu^\lambda\left[\left(\frac{d-2}{2}+\frac{(K_\lambda^2+6m^2)^2}{8m^4}\right)I_{mm}^{\kappa\tau}(K)+\frac{K_\lambda^4}{8m^4}I_{00}^{\kappa\tau}(K)\right.$$
$$\left.-\frac{(K_\lambda^2+m^2)(K_\lambda^2+5m^2)}{4m^4}I_{m0}^{\kappa\tau}(K)+\frac{5}{4m^2}(J_0^\kappa-J_m^\kappa)\right]$$
$$+\left(4-2d-\frac{(K_\lambda^2+2m^2)^2}{2m^4}\right)\{I_{\mu\nu}\}_{mm}^{\kappa\tau}(K)-\frac{K_\lambda^4}{2m^4}\{I_{\mu\nu}\}_{00}^{\kappa\tau}(K)$$
$$+\frac{(K_\lambda^2+m^2)(K_\lambda^2+3m^2)}{2m^4}\{I_{\mu\nu}\}_{m0}^{\kappa\tau}(K)+\frac{(K_\lambda^4-m^4)}{2m^4}\{I_{\mu\nu}\}_{0m}^{\kappa\tau}(K)$$
$$+\frac{1}{2m^2}\int_Q(Q_\mu^\kappa Q_\nu^\kappa-3L_\mu^\tau L_\nu^\tau)[G_0(Q^\kappa)-G_m(Q^\kappa)]\Bigg\}. \qquad \text{(I.0.10)}$$

To treat the last integral, we use $Q^\kappa_\mu Q^\kappa_\nu - 3L^\tau_\mu L^\tau_\nu = -2Q^\kappa_\mu Q^\kappa_\nu - 3K^\lambda_\mu K^\lambda_\nu - 3(K^\lambda_\mu Q^\kappa_\nu + K^\lambda_\nu Q^\kappa_\mu)$ to get

$$\begin{aligned}\Pi^{\mathrm{gl},\lambda}_{\mu\nu}(K) = \sum_{\kappa,\tau}\mathcal{C}_{\kappa\lambda\tau}\Bigg\{&\delta_{\mu\nu}\left[\frac{(K^2_\lambda+m^2)^2}{m^2}I^{\kappa\tau}_{m0}(K) - \frac{K^2_\lambda(K^2_\lambda+4m^2)}{m^2}I^{\kappa\tau}_{mm}(K)\right.\\ &\left.+\frac{K^2_\lambda+m^2}{m^2}(J^\kappa_m - J^\kappa_0) + 2\frac{\omega^\lambda}{m^2}(\tilde{J}^\kappa_0 - \tilde{J}^\kappa_m)\right]\\ &+K^\lambda_\mu K^\lambda_\nu\left[\left(\frac{d-2}{2}+\frac{(K^2_\lambda+6m^2)^2}{8m^4}\right)I^{\kappa\tau}_{mm}(K) + \frac{K^4_\lambda}{8m^4}I^{\kappa\tau}_{00}(K)\right.\\ &\left.-\frac{(K^2_\lambda+m^2)(K^2_\lambda+5m^2)}{4m^4}I^{\kappa\tau}_{m0}(K) - \frac{J^\kappa_0 - J^\kappa_m}{4m^2}\right]\\ &+\left(4-2d-\frac{(K^2_\lambda+2m^2)^2}{2m^4}\right)\{I_{\mu\nu}\}^{\kappa\tau}_{mm}(K) - \frac{K^4_\lambda}{2m^4}\{I_{\mu\nu}\}^{\kappa\tau}_{00}(K)\\ &+\frac{(K^2_\lambda+m^2)(K^2_\lambda+3m^2)}{2m^4}\{I_{\mu\nu}\}^{\kappa\tau}_{m0}(K) + \frac{(K^4_\lambda-m^4)}{2m^4}\{I_{\mu\nu}\}^{\kappa\tau}_{0m}(K)\\ &-\frac{3}{2}\Big(K^\lambda_\mu n_\nu + K^\lambda_\nu n_\mu\Big)\frac{\tilde{J}^\kappa_0 - \tilde{J}^\kappa_m}{m^2} - \frac{\{J_{\mu\nu}\}^\kappa_0 - \{J_{\mu\nu}\}^\kappa_m}{m^2}\Bigg\},\end{aligned} \tag{I.0.11}$$

where we defined

$$\{J_{\mu\nu}\}^\kappa_m = \int_Q Q^\kappa_\mu Q^\kappa_\nu G_m(Q^\kappa). \tag{I.0.12}$$

Similarly, we obtain

$$\Pi^{\mathrm{tad},\lambda}_{\mu\nu} = \sum_{\kappa,\tau}\mathcal{C}_{\kappa\lambda\tau}\left[(d-2)\delta^{\mu\nu}J^\kappa_m + \frac{\{J_{\mu\nu}\}^\kappa_0 - \{J_{\mu\nu}\}^\kappa_m}{m^2}\right], \tag{I.0.13}$$

and

$$\Pi^{\mathrm{gh},\lambda}_{\mu\nu}(K) = \sum_{\kappa,\tau}\mathcal{C}_{\kappa\lambda\tau}\left[\{I_{\mu\nu}\}^{\kappa\tau}_{00}(K) - \frac{K^\lambda_\mu K^\lambda_\nu}{2}I^{\kappa\tau}_{00}(K)\right]. \tag{I.0.14}$$

The total gluon self-energy is then

$$\begin{aligned}\Pi^{\lambda}_{\mu\nu}(K) = \sum_{\kappa,\tau}\mathcal{C}_{\kappa\lambda\tau}\Bigg\{&\delta_{\mu\nu}\left[\frac{(K^2_\lambda+m^2)^2}{m^2}I^{\kappa\tau}_{m0}(K) - \frac{K^2_\lambda(K^2_\lambda+4m^2)}{m^2}I^{\kappa\tau}_{mm}(K)\right.\\ &\left.+(d-2)J^{\kappa}_m + \frac{K^2_\lambda+m^2}{m^2}(J^{\kappa}_m - J^{\kappa}_0) + 2\frac{\omega^\lambda}{m^2}(\tilde{J}^{\kappa}_0 - \tilde{J}^{\kappa}_m)\right]\\ &+\left(4-2d-\frac{(K^2_\lambda+2m^2)^2}{2m^4}\right)\{I_{\mu\nu}\}^{\kappa\tau}_{mm}(K) - \left(\frac{K^4_\lambda}{2m^4}-1\right)\{I_{\mu\nu}\}^{\kappa\tau}_{00}(K)\\ &+\frac{(K^2_\lambda+m^2)}{2m^4}\Big[(K^2_\lambda+3m^2)\{I_{\mu\nu}\}^{\kappa\tau}_{m0}(K) + (K^2_\lambda-m^2)\{I_{\mu\nu}\}^{\kappa\tau}_{0m}(K)\Big]\\ &+K^\lambda_\mu K^\lambda_\nu\left[\left(\frac{d-2}{2}+\frac{(K^2_\lambda+6m^2)^2}{8m^4}\right)I^{\kappa\tau}_{mm}(K) - \frac{J^{\kappa}_0-J^{\kappa}_m}{4m^2}\right.\\ &\left.-\frac{(K^2_\lambda+m^2)(K^2_\lambda+5m^2)}{4m^4}I^{\kappa\tau}_{m0}(K)\left(\frac{K^4_\lambda}{8m^4}-\frac{1}{2}\right)I^{\kappa\tau}_{00}(K)\right]\\ &-\frac{3}{2}\Big(K^\lambda_\mu n_\nu + K^\lambda_\nu n_\mu\Big)\frac{\tilde{J}^{\kappa}_0-\tilde{J}^{\kappa}_m}{m^2}\Bigg\}. \end{aligned} \tag{I.0.15}$$

The transverse and longitudinal projections of this formula leads to Eq. (III.5.36) after using $\{I^\lambda_{T/L}\}^{\kappa\tau}_{m0}(K) = \{I^\lambda_{T/L}\}^{\tau\kappa}_{0m}(K)$ and the fact that $\mathcal{C}_{\kappa\lambda\tau}$ is totally symmetric. Note, in particular, that the last two lines are not transverse (with respect to the generalized momentum K^λ) and, hence, do not contribute to $\Pi^\lambda_{T/L}(K)$.

Appendix J

Sum-integrals

In what follows, we define $\kappa r T \equiv \kappa r T$. The Matsubara sums of all the elementary integrals defined in the main text can be performed using standard integration contour techniques, see for instance [83, 238]. For the tadpole-like sum-integrals, this yields

$$J_m^\kappa \hat{=} \int_{\mathbf{q}} \mathrm{Re}\, \frac{n_{\varepsilon_{m,q}-i\kappa r T}}{\varepsilon_{m,q}} = \frac{1}{2\pi^2}\int_0^\infty dq\, q^2 \mathrm{Re}\, \frac{n_{\varepsilon_{m,q}-i\kappa r T}}{\varepsilon_{m,q}} \tag{J.0.1}$$

and

$$\tilde{J}_m^\kappa = \int_{\mathbf{q}} \mathrm{Im}\, n_{\varepsilon_{m,q}-i\kappa r T} = \frac{1}{2\pi^2}\int_0^\infty dq\, q^2 \mathrm{Im}\, n_{\varepsilon_{m,q}-i\kappa r T}\,, \tag{J.0.2}$$

where $\int_{\mathbf{q}} = \int \frac{d^3q}{(2\pi)^3}$, $\varepsilon_{m,q} = \sqrt{q^2+m^2}$, and $n_z = (\exp \beta z - 1)^{-1}$ is the Bose-Einstein distribution function, which satisfies $n_{-z} = -1 - n_z$. The symbol $\hat{=}$ means that we disregard vacuum contributions defined as the limit of the above expressions as $T \to 0$ for fixed r. The reason why we can do so is that, as explained in the main text, the vacuum contributions to the self-energies can be very easily obtained from the results of [79].

For the bubble-like sum-integrals, we similarly obtain

$$I^{\kappa\tau}_{m_1 m_2}(K) \hat{=} \int_{\mathbf{q}} \mathrm{Re}\left[\frac{n_{\varepsilon_{m_1,q}+i\kappa r T}}{\varepsilon_{m_1,q}} G_{m_2}(\omega^\lambda + i\varepsilon_{m_1,q}, l) + (m_1,\kappa \leftrightarrow m_2,\tau)\right], \tag{J.0.3}$$

$$2\{I_T^\lambda\}^{\kappa\tau}_{m_1 m_2}(K) \hat{=} \int_{\mathbf{q}} \left(q^2 - \frac{(\mathbf{k}\cdot\mathbf{q})^2}{k^2}\right) \mathrm{Re}\left[\frac{n_{\varepsilon_{m_1,q}+i\kappa r T}}{\varepsilon_{m_1,q}} G_{m_2}(\omega^\lambda + i\varepsilon_{m_1,q}, l)\right. , + (m_1,\kappa \leftrightarrow m_2,\tau)\Big] \tag{J.0.4}$$

$$k^2 K_\lambda^2 \{I_L^\lambda\}^{\kappa\tau}_{m_1 m_2}(K) \hat{=} \int_{\mathbf{q}} \mathrm{Re}\left[\frac{n_{\varepsilon_{m_1,q}+i\kappa r T}}{\varepsilon_{m_1,q}} \left(-ik^2\varepsilon_{m_1,q} + \omega^\lambda(\mathbf{k}\cdot\mathbf{q})\right)^2 G_{m_2}(\omega^\lambda + i\varepsilon_{m_1,q}, l) + (m_1,\kappa \leftrightarrow m_2,\tau)\right] \tag{J.0.5}$$

where we have introduced $\lambda = \tau - \kappa$ and $\omega^\lambda = \omega + \lambda r T$. An angular integration leads then to

$$I^{\kappa\tau}_{m_1 m_2}(K) \;\hat{=}\; -\frac{1}{8\pi^2 k}\int_0^\infty dq\, q\,\mathrm{Re}\Big[\frac{n_{\varepsilon_{m_1,q}+i\kappa r T}}{\varepsilon_{m_1,q}} g_{m_2}(\omega^\lambda + i\varepsilon_{m_1,q}; q, K_\lambda) + (m_1, \kappa \leftrightarrow m_2, \tau)\Big], \quad \text{(J.0.6)}$$

$$\{I^\lambda_T\}^{\kappa\tau}_{m_1 m_2}(K) \;\hat{=}\; \frac{1}{64\pi^2 k^3}\int_0^\infty dq\, q\,\mathrm{Re}\Big[\frac{n_{\varepsilon_{m_1,q}+i\kappa r T}}{\varepsilon_{m_1,q}}\Big\{4kq\left(K_\lambda^2 + 2i\omega^\lambda\varepsilon_{m_1,q} + m_2^2 - m_1^2\right) + \ell_T^{m_2}(\omega^\lambda + i\varepsilon_{m_1,q}; q, K_\lambda)\Big\} + (m_1, \kappa \leftrightarrow m_2, \tau)\Big], \quad \text{(J.0.7)}$$

$$\{I^\lambda_L\}^{\kappa\tau}_{m_1 m_2}(K) \;\hat{=}\; -\frac{\omega_\lambda^2}{32\pi^2 K_\lambda^2 k^3}\int_0^\infty dq\, q\,\mathrm{Re}\Big[\frac{n_{\varepsilon_{m_1,q}+i\kappa r T}}{\varepsilon_{m_1,q}}\Big\{\ell_L^{m_2}(\omega^\lambda + i\varepsilon_{m_1,q}; q, K_\lambda) + 4kq\left(K_\lambda^2 + m_2^2 - m_1^2 + 2i\omega^\lambda\varepsilon_{m_1,q}\left(1 - \frac{2kq}{\omega_\lambda^2}\right)\right)\Big\} + (m_1, \kappa \leftrightarrow m_2, \tau)\Big], \quad \text{(J.0.8)}$$

where we introduced the functions

$$g_\beta(z; q, K) = \ln\frac{z^2 + \varepsilon^2_{\beta,k-q}}{z^2 + \varepsilon^2_{\beta,k+q}}, \quad \text{(J.0.9)}$$

$$\ell_T^\beta(z; q, K) = \left(\varepsilon^2_{\beta,k+q} + z^2\right)\left(\varepsilon^2_{\beta,k-q} + z^2\right) g_\beta(z; q, K) \quad \text{(J.0.10)}$$

and

$$\ell_L^\beta(z; q, K) = \left[\varepsilon^2_{\beta,q} + z^2 + k^2\left(\frac{2z}{\omega} - 1\right)\right]^2 g_\beta(z; q, K). \quad \text{(J.0.11)}$$

Appendix K

Gluon susceptibilities

In this section, we derive the expressions of the gluon susceptibilities (III.5.63) and (III.5.64) in terms of simple one-dimensional integrals. We consider the neutral and charged color sectors separately.

K.0.6 Neutral sector

From Eq. (III.5.36), we obtain

$$\begin{aligned}\Pi^0_{T/L}(0,\mathbf{0}) &= 2(d-1)J^+_m - 2J^+_0 + 2m^2 I^{+-}_{m0}(0,\mathbf{0}) \\ &\quad + 2\{I^0_{T/L}\}^{+-}_{00}(0,\mathbf{0}) + 2\{I^0_{T/L}\}^{+-}_{m0}(0,\mathbf{0}) \\ &\quad - 4(d-1)\{I^0_{T/L}\}^{+-}_{mm}(0,\mathbf{0}),\end{aligned} \tag{K.0.1}$$

where we used the symmetry properties of the integrals (III.5.33)–(III.5.35) and (III.5.37)–(III.5.39). Here and in the following, we write $\mathbf{0}$ for $\mathbf{k} \to \mathbf{0}$ for simplicity but we warn the reader that it is sometimes important to take this limit after setting $\omega = 0$; see below.

This can be simplified as follows. First, using the identity (III.5.10) as well as $G_m(Q) = G_m(-Q)$, we have

$$I^{+-}_{m_1m_2}(0,\mathbf{0}) = \int_Q G_{m_1}(Q^+)G_{m_2}(Q^+), \tag{K.0.2}$$

$$\left\{I^0_T\right\}^{+-}_{m_1m_2}(0,\mathbf{0}) = \frac{1}{d-1}\int_Q q^2 G_{m_1}(Q^+)G_{m_2}(Q^+), \tag{K.0.3}$$

and

$$\begin{aligned}\left\{I^0_L\right\}^{+-}_{m_1m_2}(0,\mathbf{0}) &= \int_Q \left(Q_+^2 - q^2\right) G_{m_1}(Q^+)G_{m_2}(Q^+) \\ &= J^+_{m_1} - m_2^2 I^{+-}_{m_1m_2}(0,\mathbf{0}) - (d-1)\left\{I^0_T\right\}^{+-}_{m_1m_2}(0,\mathbf{0}).\end{aligned} \tag{K.0.4}$$

Note that

$$\left\{I^0_{T/L}\right\}^{+-}_{m_1m_2}(0,\mathbf{0}) = \left\{I^0_{T/L}\right\}^{+-}_{m_2m_1}(0,\mathbf{0}). \tag{K.0.5}$$

For $m_1 \neq m_2$, we use the identity

$$G_{m_1}(Q)G_{m_2}(Q) = -\frac{G_{m_1}(Q) - G_{m_2}(Q)}{m_1^2 - m_2^2} \tag{K.0.6}$$

which leads to

$$I^{+-}_{m0}(0, \mathbf{k} \to 0) = \frac{J_0^+ - J_m^+}{m^2}\,, \tag{K.0.7}$$

$$\left\{I_T^0\right\}^{+-}_{m0}(0, \mathbf{0}) = \frac{1}{d-1}\frac{N_0^+ - N_m^+}{m^2}\,, \tag{K.0.8}$$

$$\left\{I_L^0\right\}^{+-}_{m0}(0, \mathbf{0}) = J_m^+ + \frac{N_m^+ - N_0^+}{m^2}\,, \tag{K.0.9}$$

and allows us to rewrite the above integrals in terms of

$$J_m^+ \equiv \int_Q G_m(Q^+) \,\hat{=}\, \frac{1}{2\pi^2}\int_0^\infty dq \frac{q^2}{\varepsilon_{m,q}} \mathrm{Re}\, n_{\varepsilon_{m,q} - irT} \tag{K.0.10}$$

and

$$N_m^+ \equiv \int_Q q^2 G_m(Q^+) \,\hat{=}\, \frac{1}{2\pi^2}\int_0^\infty dq \frac{q^4}{\varepsilon_{m,q}} \mathrm{Re}\, n_{\varepsilon_{m,q} - irT}\,, \tag{K.0.11}$$

where the symbol $\hat{=}$ means that we only keep the thermal contributions, since our renormalization scheme is anyway such that the vacuum corrections to the gluon masses of the neutral mode, are zero. When $m_1 = m_2 = m$, we can use

$$\begin{aligned}\int_Q q^{2n} G_m^2(Q^+) &= -\int_Q q^{2n}\frac{dG_m(Q_+)}{dq^2} \\ &\,\hat{=}\, \frac{2n+1}{2}\int_Q q^{2n-2} G_m(Q^+) \\ &\,\hat{=}\, \frac{2n+1}{4\pi^2}\int_0^\infty dq \frac{q^{2n}}{\varepsilon_{m,q}} \mathrm{Re}\, n_{\varepsilon_{m,q} - irT}\,.\end{aligned} \tag{K.0.12}$$

In particular, in addition to J_m^+ and N_m^+, we are lead to consider

$$S_m^+ \equiv \int_Q G_m^2(Q^+) \,\hat{=}\, \frac{1}{4\pi^2}\int_0^\infty dq \frac{1}{\varepsilon_{m,q}} \mathrm{Re}\, n_{\varepsilon_{m,q} - irT}\,. \tag{K.0.13}$$

We have then

$$\left\{I_T^0\right\}^{+-}_{mm}(0, \mathbf{0}) \,\hat{=}\, \frac{1}{2} J_m^+\,, \tag{K.0.14}$$

$$\left\{I_L^0\right\}^{+-}_{mm}(0, \mathbf{0}) \,\hat{=}\, -\frac{1}{2} J_m^+ - m^2 S_m^+\,, \tag{K.0.15}$$

which, together with Eqs. (K.0.7)–(K.0.9) allow us to rewrite Eq. (K.0.1) as

$$\Pi_L^{0,\mathrm{th}}(0, \mathbf{k} \to 0) \,\hat{=}\, 12m^2 S_m^+ + 12 J_m^+ - J_0^+ + 2\frac{N_m^+ - N_0^+}{m^2} \tag{K.0.16}$$

and

$$\Pi_T^{0,\mathrm{th}}(0, \mathbf{k} \to 0) \,\hat{=}\, J_0^+ - 2J_m^+ + \frac{2}{3}\frac{N_0^+ - N_m^+}{m^2}\,, \tag{K.0.17}$$

We have, explicitly, for $\varepsilon, r \in \mathrm{R}$,

$$\mathrm{Re}\, n_{\varepsilon - irT} = \frac{e^{\beta\varepsilon}\cos r - 1}{e^{2\beta\varepsilon} - 2e^{\beta\varepsilon}\cos r + 1}. \tag{K.0.18}$$

The massless integrals J_0^+ and N_0^+ can be determined analytically. For $r \in [0, 2\pi]$, we get[1]

$$\frac{J_0^\lambda}{T^2} = \frac{1}{8}\left[\left(1 - \frac{\lambda r}{\pi}\right)^2 - \frac{1}{3}\right], \tag{K.0.19}$$

$$\frac{N_0^\lambda}{T^4} = -\frac{\pi^2}{16}\left[\left(1 - \frac{\lambda r}{\pi}\right)^4 - 2\left(1 - \frac{\lambda r}{\pi}\right)^2 + \frac{7}{15}\right]. \tag{K.0.20}$$

We mention that the same results can be obtained from the formulae derived in Appendix J after performing the Matsubara sums but it is then important to take the limit $\mathbf{k} \to 0$ only after setting $\omega = 0$.

K.0.7 Charged sector

Similarly, we obtain

$$\begin{aligned}\Pi^+_{T/L}(-rT, \mathbf{0}) = {} & 2\{I^+_{T/L}\}^{0-}_{00}(-rT, \mathbf{0}) + \{I^+_{T/L}\}^{0-}_{m0}(-rT, \mathbf{0}) + \{I^+_{T/L}\}^{0-}_{0m}(-rT, \mathbf{0}) \\ & - 4(d-1)[\{I^+_{T/L}\}^{0-}_{mm}(-rT, \mathbf{0}) + m^2\left[I^{0-}_{m0}(-rT, \mathbf{0}) + I^{0-}_{0m}(-rT, \mathbf{0})\right] \\ & + (d-1)\left(J^+_m + J^0_m\right) - J^+_0 - J^0_0\,,\end{aligned} \tag{K.0.21}$$

where all quantities are appropriate analytical continuations (after the Matsubara sums have been performed and the external Matsubara frequency has been removed from the thermal factors using $n_{\varepsilon + i\omega_n} = n_\varepsilon$) evaluated at $\omega = -rT$ and $\mathbf{k} \to 0$. As before, we write $\mathbf{0}$ for $\mathbf{k} \to 0$ for simplicity but it is important to perform the continuation and set $\omega = -rT$ before taking the limit $\mathbf{k} \to 0$. For $m_1 \neq m_2$, we obtain

$$I^{0-}_{m_1 m_2}(-rT, \mathbf{0}) \mathrel{\hat{=}} \frac{J^+_{m_2} - J^0_{m_1}}{m_1^2 - m_2^2}\,, \tag{K.0.22}$$

$$\left\{I^+_T\right\}^{0-}_{m_1 m_2}(-rT, \mathbf{0}) \mathrel{\hat{=}} \frac{1}{d-1}\frac{N^+_{m_2} - N^0_{m_1}}{m_1^2 - m_2^2}\,, \tag{K.0.23}$$

$$\left\{I^+_L\right\}^{0-}_{m_1 m_2}(-rT, \mathbf{0}) \mathrel{\hat{=}} \frac{N^+_{m_2} - N^0_{m_1} + m_2^2 J^+_{m_2} - m_1^2 J^0_{m_1}}{m_2^2 - m_1^2}, \tag{K.0.24}$$

where we have used[2]

$$\left\{I^+_L\right\}^{0-}_{m_1 m_2}(-rT, \mathbf{0}) = \int_Q \omega_n^2\, G_{m_1}(Q) G_{m_2}(Q + K^+)\Big|_{\omega = -rT, \mathbf{k} \to 0} \tag{K.0.25}$$

[1] We have $J_0^\lambda/T^2 = P_2(\lambda r)/(2\pi^2)$ and $N_0^\lambda/T^4 = P_4(\lambda r)/(2\pi^2)$, where $P_{2n+2}(z) = \mathrm{Re}\int_0^\infty dx/[\exp(x - iz) - 1]$. In the interval $z \in [0, 2\pi]$, these integral can be expressed as simple polynoms; see, e.g. [94].

[2] We exploit the fact that the replacement $\omega \to -rT$ can be done before the Matsubara sum for any occurence of ω, except that in the denominators.

For $m_1 = m_2 = m$, we obtain (note that these are not the limits $m_1 \to m_2$ of the formulae given above)

$$\left\{I_T^+\right\}_{mm}^{0-}(-rT,\mathbf{0}) \hat{=} \frac{J_m^+ + J_m^0}{4}\,, \tag{K.0.26}$$

$$\left\{I_L^+\right\}_{mm}^{0-}(-rT,\mathbf{0}) \hat{=} -\frac{J_m^+ + J_m^0 + 2m^2(S_m^+ + S_m^0)}{4}\,, \tag{K.0.27}$$

We finally obtain

$$\begin{aligned}\Pi_L^+(-rT,\mathbf{0}) \hat{=}\; & 6m^2\left(S_m^0 + S_m^+\right) \\ & + 6(J_m^0 + J_m^+) - \frac{1}{2}(J_0^0 + J_0^+) + \frac{N_m^0 + N_m^+ - N_0^0 - N_0^+}{m^2}\end{aligned} \tag{K.0.28}$$

and

$$\begin{aligned}\Pi_T^+(-rT,\mathbf{0}) \hat{=}\; & \frac{1}{2}\left(J_0^0 + J_0^+\right) - \left(J_m^0 + J_m^+\right) \\ & + \frac{1}{3}\left(N_0^0 + N_0^+ - N_m^0 - N_m^+\right).\end{aligned} \tag{K.0.29}$$

which are nothing but the average between the respective neutral components and the corresponding expressions at $r = 0$. We thus obtain

$$M_{\mathrm{D},\pm}^2 = \frac{M_{\mathrm{D},0}^2 + M_{\mathrm{D},0}^2\big|_{r=0}}{2}\,. \tag{K.0.30}$$

List of Figures

Bibliography

[1] M. Gell-Mann, "A Schematic Model of Baryons and Mesons," Phys. Lett. **8**, 214–215 (1964).

[2] G. Zweig, "An SU(3) model for strong interaction symmetry and its breaking. Version 2," in "DEVELOPMENTS IN THE QUARK THEORY OF HADRONS. VOL. 1. 1964 - 1978," , D. Lichtenberg and S. P. Rosen, eds. (1964), pp. 22–101.

[3] H. Fritzsch, M. Gell-Mann, and H. Leutwyler, "Advantages of the Color Octet Gluon Picture," Phys. Lett. **B47**, 365–368 (1973).

[4] W. A. Bardeen, H. Fritzsch, and M. Gell-Mann, "Light cone current algebra, pi0 decay, and e+ e- annihilation," in "Topical Meeting on the Outlook for Broken Conformal Symmetry in Elementary Particle Physics Frascati, Italy, May 4-5, 1972," (1972).

[5] H. D. Politzer, "Reliable Perturbative Results for Strong Interactions?" Phys. Rev. Lett. **30**, 1346–1349 (1973).

[6] D. J. Gross and F. Wilczek, "Ultraviolet Behavior of Nonabelian Gauge Theories," Phys. Rev. Lett. **30**, 1343–1346 (1973).

[7] C.-N. Yang and R. L. Mills, "Conservation of Isotopic Spin and Isotopic Gauge Invariance," Phys. Rev. **96**, 191–195 (1954).

[8] K. G. Wilson, "Confinement of Quarks," Phys. Rev. **D10**, 2445–2459 (1974). [,45(1974)].

[9] M. Creutz, "Monte Carlo Study of Quantized SU(2) Gauge Theory," Phys. Rev. **D21**, 2308–2315 (1980).

[10] I. Montvay and G. Munster, Quantum fields on a lattice (Cambridge University Press, 1997).

[11] J. Greensite, "The Confinement problem in lattice gauge theory," Prog. Part. Nucl. Phys. **51**, 1 (2003).

[12] J. Greensite, "An introduction to the confinement problem," Lect. Notes Phys. **821**, 1–211 (2011).

[13] E. Braaten and R. D. Pisarski, "Deducing Hard Thermal Loops From Ward Identities," Nucl. Phys. **B339**, 310–324 (1990).

[14] E. Braaten and R. D. Pisarski, "Soft Amplitudes in Hot Gauge Theories: A General Analysis," Nucl. Phys. **B337**, 569–634 (1990).

[15] E. Braaten and R. D. Pisarski, "Simple effective Lagrangian for hard thermal loops," Phys. Rev. **D45**, 1827–1830 (1992).

[16] J. P. Blaizot, E. Iancu, and A. Rebhan, "The Entropy of the QCD plasma," Phys. Rev. Lett. **83**, 2906–2909 (1999).

[17] J. P. Blaizot, E. Iancu, and A. Rebhan, "Quark number susceptibilities from HTL resummed thermodynamics," Phys. Lett. **B523**, 143–150 (2001).

[18] J. P. Blaizot, E. Iancu, and A. Rebhan, "Approximately selfconsistent resummations for the thermodynamics of the quark gluon plasma. 1. Entropy and density," Phys. Rev. **D63**, 065003 (2001).

[19] J. Engels, F. Karsch, H. Satz, and I. Montvay, "High Temperature SU(2) Gluon Matter on the Lattice," Phys. Lett. **B101**, 89 (1981). [,293(1980)].

[20] L. D. McLerran and B. Svetitsky, "A Monte Carlo Study of SU(2) Yang-Mills Theory at Finite Temperature," Phys. Lett. **B98**, 195 (1981). [,283(1980)].

[21] J. Kuti, J. Polonyi, and K. Szlachanyi, "Monte Carlo Study of SU(2) Gauge Theory at Finite Temperature," Phys. Lett. **B98**, 199 (1981). [,287(1980)].

[22] J. Fingberg, U. M. Heller, and F. Karsch, "Scaling and asymptotic scaling in the SU(2) gauge theory," Nucl. Phys. **B392**, 493–517 (1993).

[23] A. Bazavov et al., "Equation of state in (2+1)-flavor QCD," Phys. Rev. **D90**, 094503 (2014).

[24] S. Borsanyi, Z. Fodor, C. Hoelbling, S. D. Katz, S. Krieg, and K. K. Szabo, "Full result for the QCD equation of state with 2+1 flavors," Phys. Lett. **B730**, 99–104 (2014).

[25] P. de Forcrand, "Simulating QCD at finite density," PoS **LAT2009**, 010 (2009).

[26] O. Philipsen, "Lattice QCD at non-zero temperature and baryon density," in "Modern perspectives in lattice QCD: Quantum field theory and high performance computing. Proceedings, International School, 93rd Session, Les Houches, France, August 3-28, 2009," (2010), pp. 273–330.

[27] D. Sexty, "Progress in complex Langevin simulations of full QCD at non-zero density," Nucl. Phys. **A931**, 856–860 (2014).

[28] Y. Tanizaki, H. Nishimura, and K. Kashiwa, "Evading the sign problem in the mean-field approximation through Lefschetz-thimble path integral," Phys. Rev. **D91**, 101701 (2015).

[29] R. Alkofer and L. von Smekal, "The Infrared behavior of QCD Green's functions: Confinement dynamical symmetry breaking, and hadrons as relativistic bound states," Phys. Rept. **353**, 281 (2001).

[30] L. von Smekal, R. Alkofer, and A. Hauck, "The Infrared behavior of gluon and ghost propagators in Landau gauge QCD," Phys. Rev. Lett. **79**, 3591–3594 (1997).

[31] U. Ellwanger, M. Hirsch, and A. Weber, "The Heavy quark potential from Wilson's exact renormalization group," Eur. Phys. J. **C1**, 563–578 (1998).

[32] F. Marhauser and J. M. Pawlowski, "Confinement in Polyakov Gauge," (2008).

[33] J. Braun, H. Gies, and J. M. Pawlowski, "Quark Confinement from Color Confinement," Phys. Lett. **B684**, 262–267 (2010).

[34] J. Braun, A. Eichhorn, H. Gies, and J. M. Pawlowski, "On the Nature of the Phase Transition in SU(N), Sp(2) and E(7) Yang-Mills theory," Eur. Phys. J. **C70**, 689–702 (2010).

[35] L. Fister and J. M. Pawlowski, "Confinement from Correlation Functions," Phys. Rev. **D88**, 045010 (2013).

[36] D. Epple, H. Reinhardt, and W. Schleifenbaum, "Confining Solution of the Dyson-Schwinger Equations in Coulomb Gauge," Phys. Rev. **D75**, 045011 (2007).

[37] R. Alkofer, C. S. Fischer, and F. J. Llanes-Estrada, "Dynamically induced scalar quark confinement," Mod. Phys. Lett. **A23**, 1105–1113 (2008).

[38] C. S. Fischer, "Deconfinement phase transition and the quark condensate," Phys. Rev. Lett. **103**, 052003 (2009).

[39] C. S. Fischer and J. A. Mueller, "Chiral and deconfinement transition from Dyson-Schwinger equations," Phys. Rev. **D80**, 074029 (2009).

[40] L. D. Faddeev and V. N. Popov, "Feynman Diagrams for the Yang-Mills Field," Phys. Lett. **B25**, 29–30 (1967).

[41] P. Boucaud, J. P. Leroy, A. L. Yaouanc, J. Micheli, O. Pene, and J. Rodriguez-Quintero, "The Infrared Behaviour of the Pure Yang-Mills Green Functions," Few Body Syst. **53**, 387–436 (2012).

[42] I. L. Bogolubsky, E. M. Ilgenfritz, M. Muller-Preussker, and A. Sternbeck, "Lattice gluodynamics computation of Landau gauge Green's functions in the deep infrared," Phys. Lett. **B676**, 69–73 (2009).

[43] P. Boucaud, J. P. Leroy, A. Le Yaouanc, J. Micheli, O. Pene, and J. Rodriguez-Quintero, "On the IR behaviour of the Landau-gauge ghost propagator," JHEP **06**, 099 (2008).

[44] A. Cucchieri and T. Mendes, "Landau-gauge propagators in Yang-Mills theories at beta = 0: Massive solution versus conformal scaling," Phys. Rev. **D81**, 016005 (2010).

[45] A. Maas, "Describing gauge bosons at zero and finite temperature," Phys. Rept. **524**, 203–300 (2013).

[46] A. Maas, J. M. Pawlowski, L. von Smekal, and D. Spielmann, "The Gluon propagator close to criticality," Phys. Rev. **D85**, 034037 (2012).

[47] H. Neuberger, "NONPERTURBATIVE BRS INVARIANCE," Phys. Lett. **B175**, 69 (1986).

[48] H. Neuberger, "Nonperturbative BRS Invariance and the Gribov Problem," Phys. Lett. **B183**, 337 (1987).

[49] J. E. Mandula and M. Ogilvie, "Efficient gauge fixing via overrelaxation," Phys. Lett. **B248**, 156–158 (1990).

[50] C. T. H. Davies, G. G. Batrouni, G. R. Katz, A. S. Kronfeld, G. P. Lepage, K. G. Wilson, P. Rossi, and B. Svetitsky, "Fourier Acceleration in Lattice Gauge Theories. 1. Landau Gauge Fixing," Phys. Rev. **D37**, 1581 (1988).

[51] R. Gupta, G. Guralnik, G. Kilcup, A. Patel, S. R. Sharpe, and T. Warnock, "The Hadron Spectrum on a 18**3 X 42 Lattice," Phys. Rev. **D36**, 2813 (1987).

[52] A. Cucchieri and T. Mendes, "Critical slowing down in SU(2) Landau gauge fixing algorithms," Nucl. Phys. **B471**, 263–292 (1996).

[53] T. Kugo and I. Ojima, "Local Covariant Operator Formalism of Nonabelian Gauge Theories and Quark Confinement Problem," Prog. Theor. Phys. Suppl. **66**, 1–130 (1979).

[54] P. O. Bowman, U. M. Heller, D. B. Leinweber, M. B. Parappilly, A. Sternbeck, L. von Smekal, A. G. Williams, and J.-b. Zhang, "Scaling behavior and positivity violation of the gluon propagator in full QCD," Phys. Rev. **D76**, 094505 (2007).

[55] A. Cucchieri, T. Mendes, and A. R. Taurines, "Positivity violation for the lattice Landau gluon propagator," Phys. Rev. **D71**, 051902 (2005).

[56] A. C. Aguilar, D. Binosi, and J. Papavassiliou, "Gluon and ghost propagators in the Landau gauge: Deriving lattice results from Schwinger-Dyson equations," Phys. Rev. **D78**, 025010 (2008).

[57] A. C. Aguilar and J. Papavassiliou, "Power-law running of the effective gluon mass," Eur. Phys. J. **A35**, 189–205 (2008).

[58] P. Boucaud, T. Bruntjen, J. P. Leroy, A. Le Yaouanc, A. Y. Lokhov, J. Micheli, O. Pene, and J. Rodriguez-Quintero, "Is the QCD ghost dressing function finite at zero momentum?" JHEP **06**, 001 (2006).

[59] A. C. Aguilar and A. A. Natale, "A Dynamical gluon mass solution in a coupled system of the Schwinger-Dyson equations," JHEP **08**, 057 (2004).

[60] J. C. R. Bloch, "Two loop improved truncation of the ghost gluon Dyson-Schwinger equations: Multiplicatively renormalizable propagators and nonperturbative running coupling," Few Body Syst. **33**, 111–152 (2003).

[61] M. Q. Huber and L. von Smekal, "On the influence of three-point functions on the propagators of Landau gauge Yang-Mills theory," JHEP **04**, 149 (2013).

[62] J. Rodriguez-Quintero, "On the massive gluon propagator, the PT-BFM scheme and the low-momentum behaviour of decoupling and scaling DSE solutions," JHEP **01**, 105 (2011).

[63] V. N. Gribov, "Quantization of Nonabelian Gauge Theories," Nucl. Phys. **B139**, 1 (1978).

[64] I. M. Singer, "Some Remarks on the Gribov Ambiguity," Commun. Math. Phys. **60**, 7–12 (1978).

[65] D. Zwanziger, "Local and Renormalizable Action From the Gribov Horizon," Nucl. Phys. **B323**, 513–544 (1989).

[66] D. Dudal, J. A. Gracey, S. P. Sorella, N. Vandersickel, and H. Verschelde, "A Refinement of the Gribov-Zwanziger approach in the Landau gauge: Infrared propagators in harmony with the lattice results," Phys. Rev. **D78**, 065047 (2008).

[67] A. Cucchieri, T. Mendes, and E. M. S. Santos, "Covariant gauge on the lattice: A New implementation," Phys. Rev. Lett. **103**, 141602 (2009).

[68] A. Cucchieri, T. Mendes, and E. M. d. S. Santos, "Simulating linear covariant gauges on the lattice: A New approach," PoS **QCD-TNT09**, 009 (2009).

[69] A. Cucchieri, T. Mendes, G. M. Nakamura, and E. M. S. Santos, "Gluon Propagators in Linear Covariant Gauge," PoS **FACESQCD**, 026 (2010).

[70] A. Cucchieri, T. Mendes, G. M. Nakamura, and E. M. S. Santos, "Feynman gauge on the lattice: New results and perspectives," AIP Conf. Proc. **1354**, 45–50 (2011).

[71] P. Bicudo, D. Binosi, N. Cardoso, O. Oliveira, and P. J. Silva, "Lattice gluon propagator in renormalizable ξ gauges," Phys. Rev. **D92**, 114514 (2015).

[72] M. A. L. Capri, D. Fiorentini, M. S. Guimaraes, B. W. Mintz, L. F. Palhares, S. P. Sorella, D. Dudal, I. F. Justo, A. D. Pereira, and R. F. Sobreiro, "More on the nonperturbative Gribov-Zwanziger quantization of linear covariant gauges," Phys. Rev. **D93**, 065019 (2016).

[73] A. D. Pereira, R. F. Sobreiro, and S. P. Sorella, "Non-perturbative BRST quantization of Euclidean Yang-Mills theories in Curci-Ferrari gauges," (2016).

[74] J. Serreau and M. Tissier, "Lifting the Gribov ambiguity in Yang-Mills theories," Phys. Lett. **B712**, 97–103 (2012).

[75] A. P. Young, Spin glasses and random fields, vol. 12 (World Scientific, 1997).

[76] G. Curci and R. Ferrari, "A Theory of Massive Yang-Mills Field," (1975).

[77] G. Curci and R. Ferrari, "On a Class of Lagrangian Models for Massive and Massless Yang-Mills Fields," Nuovo Cim. **A32**, 151–168 (1976).

[78] M. Tissier and N. Wschebor, "An Infrared Safe perturbative approach to Yang-Mills correlators," Phys. Rev. **D84**, 045018 (2011).

[79] M. Tissier and N. Wschebor, "Infrared propagators of Yang-Mills theory from perturbation theory," Phys. Rev. **D82**, 101701 (2010).

[80] M. Pelaez, M. Tissier, and N. Wschebor, "Three-point correlation functions in Yang-Mills theory," Phys. Rev. **D88**, 125003 (2013).

[81] M. Peláez, M. Tissier, and N. Wschebor, "Two-point correlation functions of QCD in the Landau gauge," Phys. Rev. **D90**, 065031 (2014).

[82] M. Peláez, M. Tissier, and N. Wschebor, "Quark-gluon vertex from the Landau gauge Curci-Ferrari model," Phys. Rev. **D92**, 045012 (2015).

[83] U. Reinosa, J. Serreau, M. Tissier, and N. Wschebor, "Yang-Mills correlators at finite temperature: A perturbative perspective," Phys. Rev. **D89**, 105016 (2014).

[84] U. M. Heller, F. Karsch, and J. Rank, "The Gluon propagator at high temperature," Phys. Lett. **B355**, 511–517 (1995).

[85] U. M. Heller, F. Karsch, and J. Rank, "The Gluon propagator at high temperature: Screening, improvement and nonzero momenta," Phys. Rev. **D57**, 1438–1448 (1998).

[86] A. Cucchieri, F. Karsch, and P. Petreczky, "Magnetic screening in hot non-Abelian gauge theory," Phys. Lett. **B497**, 80–84 (2001).

[87] A. Cucchieri, F. Karsch, and P. Petreczky, "Propagators and dimensional reduction of hot SU(2) gauge theory," Phys. Rev. **D64**, 036001 (2001).

[88] A. Cucchieri, A. Maas, and T. Mendes, "Infrared properties of propagators in Landau-gauge pure Yang-Mills theory at finite temperature," Phys. Rev. **D75**, 076003 (2007).

[89] C. S. Fischer, A. Maas, and J. A. Muller, "Chiral and deconfinement transition from correlation functions: SU(2) vs. SU(3)," Eur. Phys. J. **C68**, 165–181 (2010).

[90] A. Cucchieri and T. Mendes, "Electric and Magnetic Screening Masses around the Deconfinement Transition," PoS **LATTICE2011**, 206 (2011).

[91] R. Aouane, V. G. Bornyakov, E. M. Ilgenfritz, V. K. Mitrjushkin, M. Muller-Preussker, and A. Sternbeck, "Landau gauge gluon and ghost propagators at finite temperature from quenched lattice QCD," Phys. Rev. **D85**, 034501 (2012).

[92] P. J. Silva, O. Oliveira, P. Bicudo, and N. Cardoso, "Gluon screening mass at finite temperature from the Landau gauge gluon propagator in lattice QCD," Phys. Rev. **D89**, 074503 (2014).

[93] U. Reinosa, J. Serreau, M. Tissier, and N. Wschebor, "Deconfinement transition in SU(N) theories from perturbation theory," Phys. Lett. **B742**, 61–68 (2015).

[94] U. Reinosa, J. Serreau, M. Tissier, and N. Wschebor, "Deconfinement transition in SU(2) Yang-Mills theory: A two-loop study," Phys. Rev. **D91**, 045035 (2015).

[95] U. Reinosa, J. Serreau, M. Tissier, and N. Wschebor, "Two-loop study of the deconfinement transition in Yang-Mills theories: SU(3) and beyond," Phys. Rev. **D93**, 105002 (2016).

[96] U. Reinosa, J. Serreau, M. Tissier, and A. Tresmontant, "Yang-Mills correlators across the deconfinement phase transition," (2016).

[97] U. Reinosa, J. Serreau, and M. Tissier, "Perturbative study of the QCD phase diagram for heavy quarks at nonzero chemical potential," Phys. Rev. **D92**, 025021 (2015).

[98] J. Serreau, M. Tissier, and A. Tresmontant, "Covariant gauges without Gribov ambiguities in Yang-Mills theories," Phys. Rev. **D89**, 125019 (2014).

[99] J. Serreau, M. Tissier, and A. Tresmontant, "Influence of Gribov ambiguities in a class of nonlinear covariant gauges," Phys. Rev. **D92**, 105003 (2015).

[100] R. Delbourgo and P. D. Jarvis, "Extended BRS Invariance and Osp(4/2) Supersymmetry," J. Phys. **A15**, 611 (1982).

[101] A. Cucchieri and T. Mendes, "Electric and magnetic Landau-gauge gluon propagators in finite-temperature SU(2) gauge theory," PoS **FACESQCD**, 007 (2010).

[102] N. Nakanishi and I. Ojima, "Covariant operator formalism of gauge theories and quantum gravity," World Sci. Lect. Notes Phys. **27**, 1–434 (1990).

[103] I. V. Tyutin, "Gauge Invariance in Field Theory and Statistical Physics in Operator Formalism," (1975).

[104] C. Becchi, A. Rouet, and R. Stora, "Renormalization of the Abelian Higgs-Kibble Model," Commun. Math. Phys. **42**, 127–162 (1975).

[105] C. Becchi, A. Rouet, and R. Stora, "Renormalization of Gauge Theories," Annals Phys. **98**, 287–321 (1976).

[106] C. Wetterich, "Exact evolution equation for the effective potential," Phys. Lett. **B301**, 90–94 (1993).

[107] F. J. Dyson, "The S matrix in quantum electrodynamics," Phys. Rev. **75**, 1736–1755 (1949).

[108] J. S. Schwinger, "On the Green's functions of quantized fields. 1." Proc. Nat. Acad. Sci. **37**, 452–455 (1951).

[109] D. Zwanziger, "Vanishing of zero momentum lattice gluon propagator and color confinement," Nucl. Phys. **B364**, 127–161 (1991).

[110] D. Zwanziger, "Renormalizability of the critical limit of lattice gauge theory by BRS invariance," Nucl. Phys. **B399**, 477–513 (1993).

[111] D. Zwanziger, "Fundamental modular region, Boltzmann factor and area law in lattice gauge theory," Nucl. Phys. **B412**, 657–730 (1994).

[112] I. F. Justo, M. A. L. Capri, D. Dudal, A. J. Gómez, M. S. Guimaraes, S. P. Sorella, and D. Vercauteren, "Confinement interpretation in a Yang-Mills + Higgs theory when considering Gribov's ambiguity," in "4th Winter Workshop on Non-Perturbative Quantum Field Theory (WWNPQFT) Sophia-Antipolis, France, February 2-5, 2015," (2015).

[113] S. R. Coleman and D. J. Gross, "Price of asymptotic freedom," Phys. Rev. Lett. **31**, 851–854 (1973).

[114] D. P. Landau and K. Binder, A guide to Monte Carlo simulations in statistical physics (Cambridge university press, 2014).

[115] S. Aoki et al., "Quenched light hadron spectrum," Phys. Rev. Lett. **84**, 238–241 (2000).

[116] J. C. Taylor, "Ward Identities and Charge Renormalization of the Yang-Mills Field," Nucl. Phys. **B33**, 436–444 (1971).

[117] W. J. Marciano and H. Pagels, "Quantum Chromodynamics: A Review," Phys. Rept. **36**, 137 (1978).

[118] S. Weinberg, The quantum theory of fields. Vol. 2: Modern applications (Cambridge University Press, 2013).

[119] N. Nakanishi, "Indefinite metric quantum field theory," Prog. Theor. Phys. Suppl. **51**, 1–95 (1972).

[120] B. Lautrup, "CANONICAL QUANTUM ELECTRODYNAMICS IN COVARIANT GAUGES," Kong. Dan. Vid. Sel. Mat. Fys. Med. **35** (1967).

[121] G. 't Hooft, "Renormalizable Lagrangians for Massive Yang-Mills Fields," Nucl. Phys. **B35**, 167–188 (1971).

[122] G. 't Hooft, "Renormalization of Massless Yang-Mills Fields," Nucl. Phys. **B33**, 173–199 (1971).

[123] S. Mandelstam, "Approximation Scheme for QCD," Phys. Rev. **D20**, 3223 (1979).

[124] N. Brown and M. R. Pennington, "Studies of Confinement: How the Gluon Propagates," Phys. Rev. **D39**, 2723 (1989).

[125] A. Hauck, L. von Smekal, and R. Alkofer, "Solving the gluon Dyson-Schwinger equations in the Mandelstam approximation," Comput. Phys. Commun. **112**, 149 (1998).

[126] R. Alkofer, M. Q. Huber, and K. Schwenzer, "Infrared singularities in Landau gauge Yang-Mills theory," Phys. Rev. **D81**, 105010 (2010).

[127] L. von Smekal, A. Hauck, and R. Alkofer, "A Solution to Coupled Dyson–Schwinger Equations for Gluons and Ghosts in Landau Gauge," Annals Phys. **267**, 1–60 (1998). [Erratum: Annals Phys.269,182(1998)].

[128] R. Alkofer, C. S. Fischer, and F. J. Llanes-Estrada, "Vertex functions and infrared fixed point in Landau gauge SU(N) Yang-Mills theory," Phys. Lett. **B611**, 279–288 (2005). [Erratum: Phys. Lett.670,460(2009)].

[129] C. S. Fischer and J. M. Pawlowski, "Uniqueness of infrared asymptotics in Landau gauge Yang-Mills theory II," Phys. Rev. **D80**, 025023 (2009).

[130] M. Q. Huber, "On gauge fixing aspects of the infrared behavior of Yang-Mills Green functions," Ph.D. thesis, Graz U. (2010).

[131] A. Blum, M. Q. Huber, M. Mitter, and L. von Smekal, "Gluonic three-point correlations in pure Landau gauge QCD," Phys. Rev. **D89**, 061703 (2014).

[132] A. K. Cyrol, M. Q. Huber, and L. von Smekal, "A Dyson–Schwinger study of the four-gluon vertex," Eur. Phys. J. **C75**, 102 (2015).

[133] M. Q. Huber, A. K. Cyrol, and L. von Smekal, "On Dyson-Schwinger studies of Yang-Mills theory and the four-gluon vertex," Acta Phys. Polon. Supp. **8**, 497 (2015).

[134] E. M. Ilgenfritz, M. Muller-Preussker, A. Sternbeck, A. Schiller, and I. L. Bogolubsky, "Landau gauge gluon and ghost propagators from lattice QCD," Braz. J. Phys. **37**, 193–200 (2007).

[135] A. Cucchieri, A. Maas, and T. Mendes, "Exploratory study of three-point Green's functions in Landau-gauge Yang-Mills theory," Phys. Rev. **D74**, 014503 (2006).

[136] A. Cucchieri, A. Maas, and T. Mendes, "Three-point vertices in Landau-gauge Yang-Mills theory," Phys. Rev. **D77**, 094510 (2008).

[137] J. C. R. Bloch, A. Cucchieri, K. Langfeld, and T. Mendes, "Propagators and running coupling from SU(2) lattice gauge theory," Nucl. Phys. **B687**, 76–100 (2004).

[138] A. Cucchieri and T. Mendes, "Infrared behavior of gluon and ghost propagators from asymmetric lattices," Phys. Rev. **D73**, 071502 (2006).

[139] A. Cucchieri and T. Mendes, "Constraints on the IR behavior of the gluon propagator in Yang-Mills theories," Phys. Rev. Lett. **100**, 241601 (2008).

[140] A. Cucchieri and T. Mendes, "Constraints on the IR behavior of the ghost propagator in Yang-Mills theories," Phys. Rev. **D78**, 094503 (2008).

[141] S. Furui and H. Nakajima, "Infrared features of the Landau gauge QCD," Phys. Rev. **D69**, 074505 (2004).

[142] D. B. Leinweber, J. I. Skullerud, A. G. Williams, and C. Parrinello, "Gluon propagator in the infrared region," Phys. Rev. **D58**, 031501 (1998).

[143] F. D. R. Bonnet, P. O. Bowman, D. B. Leinweber, and A. G. Williams, "Infrared behavior of the gluon propagator on a large volume lattice," Phys. Rev. **D62**, 051501 (2000).

[144] P. Boucaud, J. P. Leroy, A. Le Yaouanc, A. Y. Lokhov, J. Micheli, O. Pene, J. Rodriguez-Quintero, and C. Roiesnel, "The Infrared behaviour of the pure Yang-Mills green functions," (2005).

[145] A. Sternbeck, L. von Smekal, D. B. Leinweber, and A. G. Williams, "Comparing SU(2) to SU(3) gluodynamics on large lattices," PoS **LAT2007**, 340 (2007).

[146] A. Sternbeck and M. Müller-Preussker, "Another look at the Landau-gauge gluon and ghost propagators at low momentum," PoS **ConfinementX**, 074 (2012).

[147] V. G. Bornyakov, V. K. Mitrjushkin, and M. Muller-Preussker, "Infrared behavior and Gribov ambiguity in SU(2) lattice gauge theory," Phys. Rev. **D79**, 074504 (2009).

[148] V. G. Bornyakov, V. K. Mitrjushkin, and M. Muller-Preussker, "SU(2) lattice gluon propagator: Continuum limit, finite-volume effects and infrared mass scale m(IR)," Phys. Rev. **D81**, 054503 (2010).

[149] D. Dudal, O. Oliveira, and N. Vandersickel, "Indirect lattice evidence for the Refined Gribov-Zwanziger formalism and the gluon condensate $\langle A^2 \rangle$ in the Landau gauge," Phys. Rev. **D81**, 074505 (2010).

[150] C. S. Fischer and R. Alkofer, "Nonperturbative propagators, running coupling and dynamical quark mass of Landau gauge QCD," Phys. Rev. **D67**, 094020 (2003).

[151] C. S. Fischer, A. Maas, and J. M. Pawlowski, "On the infrared behavior of Landau gauge Yang-Mills theory," Annals Phys. **324**, 2408–2437 (2009).

[152] D. Zwanziger, "Nonperturbative Landau gauge and infrared critical exponents in QCD," Phys. Rev. **D65**, 094039 (2002).

[153] D. Dudal, S. P. Sorella, N. Vandersickel, and H. Verschelde, "Gribov no-pole condition, Zwanziger horizon function, Kugo-Ojima confinement criterion, boundary conditions, BRST breaking and all that," Phys. Rev. **D79**, 121701 (2009).

[154] N. Vandersickel, "A Study of the Gribov-Zwanziger action: from propagators to glueballs," Ph.D. thesis, Gent U. (2011).

[155] N. Vandersickel and D. Zwanziger, "The Gribov problem and QCD dynamics," Phys. Rept. **520**, 175–251 (2012).

[156] M. A. L. Capri, D. Dudal, D. Fiorentini, M. S. Guimaraes, I. F. Justo, A. D. Pereira, B. W. Mintz, L. F. Palhares, R. F. Sobreiro, and S. P. Sorella, "A local and BRST-invariant Yang-Mills theory within the Gribov horizon," (2016).

[157] C. Itzykson and J. B. Zuber, Quantum Field Theory, International Series In Pure and Applied Physics (McGraw-Hill, New York, 1980).

[158] S. Weinberg, The Quantum theory of fields. Vol. 1: Foundations (Cambridge University Press, 2005).

[159] T. Kugo, "The Universal renormalization factors Z(1) / Z(3) and color confinement condition in nonAbelian gauge theory," in "BRS symmetry. Proceedings, International Symposium on the Occasion of its 20th Anniversary, Kyoto, Japan, September 18-22, 1995," (1995), pp. 107–119.

[160] H. Aiso, J. Fromm, M. Fukuda, T. Iwamiya, A. Nakamura, M. Stingl, and M. Yoshida, "Towards understanding of confinement of gluons," Nucl. Phys. Proc. Suppl. **53**, 570–573 (1997).

[161] A. C. Aguilar, D. Ibáñez, and J. Papavassiliou, "Ghost propagator and ghost-gluon vertex from Schwinger-Dyson equations," Phys. Rev. **D87**, 114020 (2013).

[162] J. M. Pawlowski, "Aspects of the functional renormalisation group," Annals Phys. **322**, 2831–2915 (2007).

[163] H. Gies, "Introduction to the functional RG and applications to gauge theories," Lect. Notes Phys. **852**, 287–348 (2012).

[164] U. Ellwanger, "Flow equations and BRS invariance for Yang-Mills theories," Phys. Lett. **B335**, 364–370 (1994).

[165] M. Bonini, M. D'Attanasio, and G. Marchesini, "BRS symmetry for Yang-Mills theory with exact renormalization group," Nucl. Phys. **B437**, 163–186 (1995).

[166] U. Ellwanger, M. Hirsch, and A. Weber, "Flow equations for the relevant part of the pure Yang-Mills action," Z. Phys. **C69**, 687–698 (1996).

[167] A. Sternbeck, E. M. Ilgenfritz, M. Muller-Preussker, A. Schiller, and I. L. Bogolubsky, "Lattice study of the infrared behavior of QCD Green's functions in Landau gauge," PoS **LAT2006**, 076 (2006).

[168] H. Reinhardt and J. Heffner, "The effective potential of the confinement order parameter in the Hamilton approach," Phys. Lett. **B718**, 672–677 (2012).

[169] H. Reinhardt and J. Heffner, "Effective potential of the confinement order parameter in the Hamiltonian approach," Phys. Rev. **D88**, 045024 (2013).

[170] K. Fukushima and K. Kashiwa, "Polyakov loop and QCD thermodynamics from the gluon and ghost propagators," Phys. Lett. **B723**, 360–364 (2013).

[171] P. van Baal, "More (thoughts on) Gribov copies," Nucl. Phys. **B369**, 259–275 (1992).

[172] P. van Baal, "Gribov ambiguities and the fundamental domain," in "Confinement, duality, and nonperturbative aspects of QCD. Proceedings, NATO Advanced Study Institute, Newton Institute Workshop, Cambridge, UK, June 23-July 4, 1997," (1997).

[173] G. Dell'Antonio and D. Zwanziger, "All gauge orbits and some gribov copies encompassed by the gribov horizon," (1989).

[174] C. Hughes, D. Mehta, and J.-I. Skullerud, "Enumerating Gribov copies on the lattice," Annals Phys. **331**, 188–215 (2013).

[175] G. Dell'Antonio and D. Zwanziger, "Every gauge orbit passes inside the gribov horizon," Commun. Math. Phys. **138**, 291–299 (1991).

[176] D. Zwanziger, "Nonperturbative Faddeev-Popov formula and infrared limit of QCD," Phys. Rev. **D69**, 016002 (2004).

[177] D. Zwanziger, "Fundamental modular region, Boltzmann factor, and area law in lattice theory," Nucl. Phys. Proc. Suppl. **34**, 198–200 (1994).

[178] D. Zwanziger, "Renormalizability of the critical limit of lattice gauge theory by BRS invariance," Nucl. Phys. Proc. Suppl. **30**, 221–223 (1993).

[179] D. Dudal, S. P. Sorella, and N. Vandersickel, "More on the renormalization of the horizon function of the Gribov-Zwanziger action and the Kugo-Ojima Green function(s)," Eur. Phys. J. **C68**, 283–298 (2010).

[180] A. J. Gomez, M. S. Guimaraes, R. F. Sobreiro, and S. P. Sorella, "Equivalence between Zwanziger's horizon function and Gribov's no-pole ghost form factor," Phys. Lett. **B683**, 217–221 (2010).

[181] D. Zwanziger, "Some exact infrared properties of gluon and ghost propagators and long-range force in QCD," (2009).

[182] N. Maggiore and M. Schaden, "Landau gauge within the Gribov horizon," Phys. Rev. **D50**, 6616–6625 (1994).

[183] D. Dudal, R. F. Sobreiro, S. P. Sorella, and H. Verschelde, "The Gribov parameter and the dimension two gluon condensate in Euclidean Yang-Mills theories in the Landau gauge," Phys. Rev. **D72**, 014016 (2005).

[184] M. A. L. Capri, D. Dudal, D. Fiorentini, M. S. Guimaraes, I. F. Justo, A. D. Pereira, B. W. Mintz, L. F. Palhares, R. F. Sobreiro, and S. P. Sorella, "Exact nilpotent nonperturbative BRST symmetry for the Gribov-Zwanziger action in the linear covariant gauge," Phys. Rev. **D92**, 045039 (2015).

[185] J. A. Gracey, "Two loop correction to the Gribov mass gap equation in Landau gauge QCD," Phys. Lett. **B632**, 282–286 (2006). [Erratum: Phys. Lett.686,319(2010)].

[186] R. F. Sobreiro and S. P. Sorella, "A Study of the Gribov copies in linear covariant gauges in Euclidean Yang-Mills theories," JHEP **06**, 054 (2005).

[187] A. Cucchieri and D. Zwanziger, "Static color - Coulomb force," Phys. Rev. Lett. **78**, 3814–3817 (1997).

[188] D. Zwanziger, "No confinement without Coulomb confinement," Phys. Rev. Lett. **90**, 102001 (2003).

[189] J. Greensite, S. Olejnik, and D. Zwanziger, "Coulomb energy, remnant symmetry, and the phases of nonAbelian gauge theories," Phys. Rev. **D69**, 074506 (2004).

[190] C. Feuchter and H. Reinhardt, "Variational solution of the Yang-Mills Schrodinger equation in Coulomb gauge," Phys. Rev. **D70**, 105021 (2004).

[191] H. Reinhardt and C. Feuchter, "On the Yang-Mills wave functional in Coulomb gauge," Phys. Rev. **D71**, 105002 (2005).

[192] M. A. L. Capri, A. J. Gomez, M. S. Guimaraes, V. E. R. Lemes, and S. P. Sorella, "Study of the properties of the Gribov region in SU(N) Euclidean Yang-Mills theories in the maximal Abelian gauge," J. Phys. **A43**, 245402 (2010).

[193] M. A. L. Capri, V. E. R. Lemes, R. F. Sobreiro, S. P. Sorella, and R. Thibes, "The Gluon and ghost propagators in Euclidean Yang-Mills theory in the maximal Abelian gauge: Taking into account the effects of the Gribov copies and of the dimension two condensates," Phys. Rev. **D77**, 105023 (2008).

[194] M. A. L. Capri, V. E. R. Lemes, R. F. Sobreiro, S. P. Sorella, and R. Thibes, "The Influence of the Gribov copies on the gluon and ghost propagators in Euclidean Yang-Mills theory in the maximal Abelian gauge," Phys. Rev. **D72**, 085021 (2005).

[195] M. A. L. Capri, V. E. R. Lemes, R. F. Sobreiro, S. P. Sorella, and R. Thibes, "A Study of the maximal Abelian gauge in SU(2) Euclidean Yang-Mills theory in the presence of the Gribov horizon," Phys. Rev. **D74**, 105007 (2006).

[196] A. Cucchieri and T. Mendes, "Numerical test of the Gribov-Zwanziger scenario in Landau gauge," PoS **QCD-TNT09**, 026 (2009).

[197] D. Dudal, J. A. Gracey, S. P. Sorella, N. Vandersickel, and H. Verschelde, "The Landau gauge gluon and ghost propagator in the refined Gribov-Zwanziger framework in 3 dimensions," Phys. Rev. **D78**, 125012 (2008).

[198] D. Dudal, S. P. Sorella, and N. Vandersickel, "The dynamical origin of the refinement of the Gribov-Zwanziger theory," Phys. Rev. **D84**, 065039 (2011).

[199] J. A. Gracey, "Three loop MS-bar renormalization of the Curci-Ferrari model and the dimension two BRST invariant composite operator in QCD," Phys. Lett. **B552**, 101–110 (2003).

[200] A. A. Slavnov, "Ward Identities in Gauge Theories," Theor. Math. Phys. **10**, 99–107 (1972). [Teor. Mat. Fiz.10,153(1972)].

[201] N. Wschebor, "Some non-renormalization theorems in Curci-Ferrari model," Int. J. Mod. Phys. **A23**, 2961–2973 (2008).

[202] M. Tissier and N. Wschebor, "Gauged supersymmetries in Yang-Mills theory," Phys. Rev. **D79**, 065008 (2009).

[203] M. Peláez, "Infrared correlation functions in Quantum Chromodynamics," Ph.D. thesis, Paris U., VI, LPTL (2015).

[204] C. Parrinello and G. Jona-Lasinio, "A Modified Faddeev-Popov formula and the Gribov ambiguity," Phys. Lett. **B251**, 175–180 (1990).

[205] D. Zwanziger, "Quantization of Gauge Fields, Classical Gauge Invariance and Gluon Confinement," Nucl. Phys. **B345**, 461–471 (1990).

[206] S. Fachin and C. Parrinello, "Global gauge fixing in lattice gauge theories," Phys. Rev. **D44**, 2558–2564 (1991).

[207] D. S. Henty, O. Oliveira, C. Parrinello, and S. Ryan, "Soft covariant gauges on the lattice," Phys. Rev. **D54**, 6923–6927 (1996).

[208] S. P. Fachin, "Quantization of Yang-Mills theory without Gribov copies: Perturbative renormalization," Phys. Rev. **D47**, 3487–3495 (1993).

[209] J. Serreau, "A class of nonperturbative nonlinear covariant gauges in Yang-Mills theories," PoS **QCD-TNT-III**, 038 (2013).

[210] J. de Boer, K. Skenderis, P. van Nieuwenhuizen, and A. Waldron, "On the renormalizability and unitarity of the Curci-Ferrari model for massive vector bosons," Phys. Lett. **B367**, 175–182 (1996).

[211] M. Tissier and N. Wschebor, "A linear realization of the BRST symmetry," (2009).

[212] P. de Forcrand, "Multigrid Techniques for Quark Propagator," Nucl. Phys. Proc. Suppl. **9**, 516–520 (1989).

[213] P. Nath and R. L. Arnowitt, "Generalized Supergauge Symmetry as a New Framework for Unified Gauge Theories," Phys. Lett. **B56**, 177–180 (1975).

[214] R. E. Browne, D. Dudal, J. A. Gracey, V. E. R. Lemes, M. S. Sarandy, R. F. Sobreiro, S. P. Sorella, and H. Verschelde, "Renormalization group aspects of the local composite operator method," J. Phys. **A39**, 7889–7900 (2006).

[215] G. Boyd, J. Engels, F. Karsch, E. Laermann, C. Legeland, M. Lutgemeier, and B. Petersson, "Equation of state for the SU(3) gauge theory," Phys. Rev. Lett. **75**, 4169–4172 (1995).

[216] B. Svetitsky, "Symmetry Aspects of Finite Temperature Confinement Transitions," Phys. Rept. **132**, 1–53 (1986).

[217] F. E. Canfora, D. Dudal, I. F. Justo, P. Pais, L. Rosa, and D. Vercauteren, "Effect of the Gribov horizon on the Polyakov loop and vice versa," Eur. Phys. J. **C75**, 326 (2015).

[218] K. Fukushima and N. Su, "Stabilizing perturbative Yang-Mills thermodynamics with Gribov quantization," Phys. Rev. **D88**, 076008 (2013).

[219] L. Fister and J. M. Pawlowski, "Yang-Mills correlation functions at finite temperature," (2011).

[220] M. Q. Huber and L. von Smekal, "On two- and three-point functions of Landau gauge Yang-Mills theory," PoS **LATTICE2013**, 364 (2014).

[221] C. S. Fischer and J. Luecker, "Propagators and phase structure of Nf=2 and Nf=2+1 QCD," Phys. Lett. **B718**, 1036–1043 (2013).

[222] M. Quandt, H. Reinhardt, and J. Heffner, "Covariant variational approach to Yang-Mills theory," Phys. Rev. **D89**, 065037 (2014).

[223] M. Quandt and H. Reinhardt, "A covariant variational approach to Yang-Mills Theory at finite temperatures," Phys. Rev. **D92**, 025051 (2015).

[224] T. Mendes and A. Cucchieri, "Systematic Effects at Criticality for the SU(2)-Landau-Gauge Gluon Propagator," PoS **LATTICE2013**, 456 (2014).

[225] P. J. Silva and O. Oliveira, "Gluon Dynamics, Center Symmetry and the Deconfinement Phase Transition in SU(3) Pure Yang-Mills Theory," Phys. Rev. **D93**, 114509 (2016).

[226] T. K. Herbst, J. Luecker, and J. M. Pawlowski, "Confinement order parameters and fluctuations," (2015).

[227] M. Laine, "Basics of thermal field theory," unpublished, http://www.laine.itp.unibe.ch .

[228] A. M. Polyakov, "Thermal Properties of Gauge Fields and Quark Liberation," Phys. Lett. **B72**, 477–480 (1978).

[229] R. D. Pisarski, "Notes on the deconfining phase transition," in "QCD perspectives on hot and dense matter. Proceedings, NATO Advanced Study Institute, Summer School, Cargese, France, August 6-18, 2001," (2002), pp. 353–384.

[230] G. 't Hooft, "A Property of Electric and Magnetic Flux in Nonabelian Gauge Theories," Nucl. Phys. **B153**, 141–160 (1979).

[231] J. Engels, F. Karsch, H. Satz, and I. Montvay, "Gauge Field Thermodynamics for the SU(2) Yang-Mills System," Nucl. Phys. **B205**, 545–577 (1982).

[232] D. Dudal, H. Verschelde, and S. P. Sorella, "The Anomalous dimension of the composite operator A**2 in the Landau gauge," Phys. Lett. **B555**, 126–131 (2003).

[233] A. Cucchieri and T. Mendes, "To be buplished," .

[234] B. S. DeWitt, "Quantum Theory of Gravity. 2. The Manifestly Covariant Theory," Phys. Rev. **162**, 1195–1239 (1967).

[235] L. F. Abbott, "The Background Field Method Beyond One Loop," Nucl. Phys. **B185**, 189–203 (1981).

[236] L. F. Abbott, "Introduction to the Background Field Method," Acta Phys. Polon. **B13**, 33 (1982).

[237] A. Cucchieri and T. Mendes, "The Minimal Landau Background Gauge on the Lattice," Phys. Rev. **D86**, 071503 (2012).

[238] M. L. Bellac, Thermal Field Theory (Cambridge University Press, 2011).

[239] M. Laine, "Finite temperature field theory - with applications to cosmology," in "Astroparticle physics and cosmology. Proceedings: Summer School, Trieste, Italy, Jun 17-Jul 5 2002," (2002), pp. 189–254.

[240] D. Binosi and A. Quadri, "Anti-BRST symmetry and background field method," Phys. Rev. **D88**, 085036 (2013).

[241] H. Verschelde, K. Knecht, K. Van Acoleyen, and M. Vanderkelen, "The Non-perturbative groundstate of QCD and the local composite operator A(mu)**2," Phys. Lett. **B516**, 307–313 (2001).

[242] D. Dudal, M. A. L. Capri, J. A. Gracey, V. E. R. Lemes, R. F. Sobreiro, S. P. Sorella, and H. Verschelde, "Dimension two gluon condensates in a variety of gauges and a gauge invariant Yang-Mills action with a mass," Nucl. Phys. Proc. Suppl. **174**, 201–204 (2007).

[243] A. K. Cyrol, L. Fister, M. Mitter, J. M. Pawlowski, and N. Strodthoff, "On Landau gauge Yang-Mills correlation functions," (2016).

[244] R. D. Pisarski and F. Wilczek, "Remarks on the Chiral Phase Transition in Chromodynamics," Phys. Rev. **D29**, 338–341 (1984).

[245] M. Tarzia and A. Coniglio, "Pattern formation and glassy phase in the phi(4) theory with a screened electrostatic repulsion," Phys. Rev. Lett. **96**, 075702 (2006).

[246] T. Mendes, "Private communication," (2016).

[247] M. Laine and O. Philipsen, "The Nonperturbative QCD Debye mass from a Wilson line operator," Phys. Lett. **B459**, 259–264 (1999).

[248] K. Kajantie, M. Laine, J. Peisa, A. Rajantie, K. Rummukainen, and M. E. Shaposhnikov, "Nonperturbative Debye mass in finite temperature QCD," Phys. Rev. Lett. **79**, 3130–3133 (1997).

[249] S. Necco and R. Sommer, "The N(f) = 0 heavy quark potential from short to intermediate distances," Nucl. Phys. **B622**, 328–346 (2002).

[250] S. Necco and R. Sommer, "Testing perturbation theory on the N(f) = 0 static quark potential," Phys. Lett. **B523**, 135–142 (2001).

[251] S. Kratochvila and P. de Forcrand, "Observing string breaking with Wilson loops," Nucl. Phys. **B671**, 103–132 (2003).

[252] S. L. Adler, "Algorithms for Pure Gauge Theory," Nucl. Phys. Proc. Suppl. **9**, 437–446 (1989).

[253] A. Sternbeck and M. Müller-Preussker, "Lattice evidence for the family of decoupling solutions of Landau gauge Yang-Mills theory," Phys. Lett. **B726**, 396–403 (2013).

[254] A. Maas, "More on Gribov copies and propagators in Landau-gauge Yang-Mills theory," Phys. Rev. **D79**, 014505 (2009).

[255] O. Oliveira, D. Dudal, and P. J. Silva, "Glueball spectral densities from the lattice," PoS **LATTICE2012**, 214 (2012).

[256] J. Zinn-Justin, "From Slavnov-Taylor identities to the ZJ equation," Proc. Steklov Inst. Math. **272**, 288–292 (2011).

[257] A. Cucchieri, T. Mendes, O. Oliveira, and P. J. Silva, "Just how different are SU(2) and SU(3) Landau propagators in the IR regime?" Phys. Rev. **D76**, 114507 (2007).

[258] M. Q. Huber, K. Schwenzer, and R. Alkofer, "On the infrared scaling solution of SU(N) Yang-Mills theories in the maximally Abelian gauge," Eur. Phys. J. **C68**, 581–600 (2010).

[259] M. Q. Huber, R. Alkofer, and K. Schwenzer, "Infrared Behavior of three-Point Functions in Landau Gauge Yang-Mills Theory," PoS **CONFINEMENT8**, 174 (2008).

[260] C. Kellermann and C. S. Fischer, "The Running coupling from the four-gluon vertex in Landau gauge Yang-Mills theory," Phys. Rev. **D78**, 025015 (2008).

[261] C. S. Fischer and J. M. Pawlowski, "Uniqueness of infrared asymptotics in Landau gauge Yang-Mills theory," Phys. Rev. **D75**, 025012 (2007).

[262] J. Berges, N. Tetradis, and C. Wetterich, "Nonperturbative renormalization flow in quantum field theory and statistical physics," Phys. Rept. **363**, 223–386 (2002).

Aspects du confinement dans les théories de Yang-Mills

Résumé long : L'interaction forte est l'une des quatres interactions fondamentales de la Nature (avec les interactions électromagnétiques, faibles et gravitationnelles). Les interactions fortes sont responsables de la cohésion des noyaux d'atomes malgré la présence d'interactions électromagnétiques répulsives entre les protons du noyau. Les particules soumises à l'interaction forte se nomment hadrons, parmi lesquelles, en plus des protons, on trouve par exemple les neutrons et les pions. La physique des hadrons a été étudiée pendant des années, aussi bien expérimentalement que théoriquement, ce qui amena Gell-Mann et Zweig à proposer en 1964 le modèle des quarks [1, 2]. Ce dernier postule que les hadrons ne sont pas des particules élémentaires mais sont formés de particules de spin 1/2 nommées quarks. Différents types, ou saveures, de quarks existent, et aujourd'hui il en a été observé six différentes expérimentalement. Plus tard, Gell-Mann et Fritszch [3, 4] proposèrent que la théorie décrivant les interactions fortes admette un groupe de symétrie SU(3), appelé groupe de couleur. Ce dernier induit l'existence de nouveaux nombres quantiques, la couleur, portés par les quarks. Finalement, le groupe de symétrie de couleur a été pris comme groupe de jauge ce qui donna lieu à la chromodynamique quantique (QCD). De nos jours, la QCD est largement admise comme étant la théorie décrivant les interactions fortes au niveau microscopique. Les bosons de jauges associés, appelés gluons, sont les médiateurs de l'interaction forte, d'une manière analogue aux photons en électrodynamique quantique. Cependant, bien qu'à haute énergie les quarks et les gluons (les deux portant des nombres quantiques de couleur) soient les degrés de liberté pertinents pour la description de l'interaction forte, ils ne font pas partie du spectre physique de QCD qui est, quant à lui, uniquement composé d'hadrons incolores. Ce phénomène est appelé phénomène de confinement (ou simplement confinement). En particulier, c'est un phénomène concernant le domaine de basse énergie de la théorie. Cependant, un obstacle de taille est le fait que le domaine infrarouge de QCD est couramment considéré comme étant non perturbatif, du fait que l'utilisation de la théorie de perturbation (l'outil habituel en théorie quantique des champs (TQC)) n'est pas possible.

Cet aspect est une conséquence du secteur de "pure jauge" de QCD. En effet, QCD est une théorie de jauge non-Abélienne ce qui, à la différence de l'électrodynamique quantique, induit des auto-couplages entre les gluons. Ces derniers changent drastiquement la dynamique des degrés de liberté fondamentaux (les quarks et les gluons) qui, par exemple, deviennent de plus en plus faiblement couplés à hautes energies. C'est la propriété de liberté asymptotique découverte par Politzer, Gross et Wilzeck [5, 6]. En revanche, en allant dans l'infrarouge, on trouve que la constante de couplage diverge à une énergie finie (pôle de Landau) Λ_{QCD} (qui est typiquement de l'ordre de la masse du proton). Cette divergence de la constante de couplage est en général considérée comme un artéfact de la théorie de perturbation, cette dernière ne pouvant déjà plus être fiable à couplage fini mais grand. Ainsi, le domaine infrarouge de QCD est couramment considéré comme non-perturbatif. Cet aspect est généralement considéré comme étant intimement relié à la propriété de liberté asymptotique, et qu'ils sont tous les deux une des conséquences du secteur de pure jauge de QCD. Ceci constitue une des raisons pour lesquelles on pense qu'une grande partie des caractéristiques de QCD, et en particulier le phénomène de confinement, sont génériques aux théories de jauge non-Abélienne. Ainsi, dans un premier temps, il est naturel d'étudier leur archétype correspondant aux théories de Yang-Mills (YM) qui constituent le secteur de pure jauge de QCD.

Les simulations numériques ("sur le réseau") Monte-Carlo, proposées par Wilson [8] et

initiées par Creutz [9], constituent une méthode de calcul non-perturbatif et invariant de jauge et ont été intensément utilisées pour l'investigation du domaine infrarouge de QCD. Ce dernier est de nos jours raisonnablement bien décrit par les simulations réseaux qui ont, par exemple, permis de déterminer le spectre des particules de la théorie, ainsi que de calculer certains éléments de matrices entrant dans les calculs d'amplitudes de diffusions, voir par exemple [10]. Bien que ces simulations aient clairement établi que le confinement a lieu (en utilisant uniquement la théorie microscopique comme point de départ), elles n'ont pour l'instant pas permis d'en expliquer les mécanismes fondamentaux malgré le grand nombre de scénarios possibles avancés, voir par exemple [11, 12] pour des revues.

Une autre piste peut consister à étudier la théorie à température finie. On pense que QCD admet un diagramme de phase particulièrement riche dont l'étude est un défi théorique avec de nombreuses applications phénoménologiques pour l'astrophysique, la cosmologie primordiale, ou les expériences de collisions d'ions lourds utrarelativistes. En particulier, selon l'axe de température, la théorie admet une transition de phase confinement-déconfinement, où, à hautes températures, les hadrons se transforment en un plasma de quarks et de gluons. Grâce à la propriété de liberté asymptotique, le régime de hautes températures peut être étudié perturbativement (à la condition d'utiliser des techniques de resommation, les bien connues dites "hard thermal loops" [13, 14, 15]). Ainsi, on peut accéder aux propriétés thermodynamiques du plasma déconfiné, tandis que la présence du pôle de Landau empêche l'utilisation de la théorie de perturbation à basses températures et dans le voisinage de la transition, qui sont généralement considérées comme étant non-perturbatifs. Au vu de ses succès pour l'étude du cas à température nulle, il est naturel d'avoir de nouveau recours aux simulations réseau, qui ont aujourd'hui clairement établi l'existence d'une transition de phase confiement-déconfinement dans le cas des théories de YM SU(N). Cette dernière est reliée à la valeur moyenne de la boucle de Polyakov (qui constitue le paramètre d'ordre de la transition de phase [22]) qui devient non nulle dans la phase de hautes températures, ce qui est associé à la brisure spontanée de la symétrie du centre (Z_N) du groupe de jauge. Finalement, l'étude a pu être étendue au cas de QCD où, dans ce cas, il a été trouvée un crossover [23, 24]. En plus de son intérêt propre, la transition confinement-déconfinement peut être considérée comme une opportunité pour la recherche des mécanismes à l'origine du confinement. En effet, le passage de la phase confinée à la déconfinée devrait mettre en lumière certaines propriétés clés de la dynamique responsable du confinement.

Néanmoins, le diagramme de phase est beaucoup moins bien compris dans le cas d'un potentiel chimique fini car les simulations réseaux souffrent d'un problème de signe [25, 26]. Ainsi, dans ce cas, les approches analytiques semblent plus appropriées car, bien qu'elles aussi soient soumises à un problème de signe, ce dernier est moins sévère. Plus généralement, un des inconvénients des simulations numériques est leur caractère "boite noire". En effet, bien que ces simulations fournissent des résultats exacts à partir de la théorie microscopique, elles ne permettent pas toujours de saisir les aspects essentiels/dominants de la dynamique qui amènent à ces résultats. En revanche, les approches analytiques, bien qu'approximatives en général, sont bien plus appropriées pour développer un raisonnement explicatif des phénomènes observés. Parmi les plus utilisées pour l'étude du domaine infrarouge des theories de YM, on compte, entre autres, les approches fonctionnelles (non-perturbatives) telles que les équations de Dyson-Schwinger (DS), ou le groupe de renormalisation fonctionnel (FRG) [29, 30, 31, 32, 33, 34, 35, 36, 37, 38, 39]. En particulier, le FRG a montré qu'il reproduisait le diagramme de phase des théories de YM avec des valeurs pour les températures de transition en accord avec les simulations réseaux [33, 35].

Cependant, de telles approches analytiques (de même que la plupart des approches continues) ne sont pas basées directement sur le calcul d'observables physiques, mais, à la place, se reposent sur les fonctions de Green (fonctions de corrélations) des champs élémentaires.

Ces quantités ne sont pas invariantes de jauge et il faut "fixer la jauge" pour pouvoir y accéder. La procédure de fixation de jauge standard pour les approches continues est donnée par celle de Faddeev-Popov [40]. Néanmoins, travailler directement avec/sur les fonctions de Green amène des difficultés additionnelles car, la théorie étant fixée de jauge, le problème devient spécifique à la jauge considérée. En particulier, comparer les résultats obtenus par deux méthodes différentes devient plus compliqué car il faut s'assurer que chacune a bien été menée dans la même jauge (ce qui peut être particulièrement délicat lorsque des approximations sont réalisées ou pour comparer des méthodes numériques et analytiques). Il est particulièrement important de réaliser de telles comparaisons (en particulier avec des résultats du réseau) dans le cas des approches continues. En effet, ces dernières, pour pouvoir être menées à bien, demandent en pratique d'avoir recours à des approximations dont il est nécessaire de savoir en quantifier les effets. Par exemple, les équations (non-perturbatives) du FRG ou de DS ne peuvent pas être résolues exactement et, en pratique, doivent être tronquées pour pouvoir obtenir une solution approchée. En particulier, une critique généralement portée à l'encontre de telles approches non-perturbatives est qu'elles n'offrent pas de schémas d'approximation dont les effets peuvent être quantifiés d'une manière systématique et, donc, il n'est pas clair comment calculer les corrections aux résultats approchés obtenus. Ainsi, il est désirable de pouvoir tester ces résultats directement contre ceux de méthodes *ab initio*. Ces dernières sont données par les simulations réseaux réalisées à jauge fixée et qui, en particulier, produisent des résultats exacts pour les fonctions de corrélations. Dans ce contexte, ces simulations sont considérées comme étant "l'expérience", et apportent un support important pour guider les approches continues. Cependant, fixer la jauge sur le réseau n'est pas simple. C'est particulièrement vrai pour les jauges covariantes (les mieux adaptées pour les approches analytiques) car imposer leur condition de jauge revient à résoudre un système comportant de nombreuses équations différentielles non-linéaires couplées entre elles. Pire, la théorie fixée de jauge à la Faddeev-Popov ne peut pas être directement implémentée dans les simulations réseau car les valeurs moyennes d'observables invariantes de jauge sont données par la forme indéfinie $0/0$. Ceci est connu en tant que problème de Neuberger [47, 48]. Concernant ces points, la jauge de Landau est un cas particulier car elle est covariante et elle peut être définie comme correspondant aux extrema d'une certaine fonctionnelle. Par conséquent, elle peut être implémentée sur le réseau (via une extremisation numérique d'une certaine fonctionnelle) par une procédure de fixation de jauge alternative à celle de Faddev-Popov ce qui permet ainsi d'éviter le problème de Neuberger [49, 50, 51, 52].

Plus généralement, au-delà du fait que les fonctions de corrélation soient à la base des approches continues, elles constituent les quantités élémentaires de toute théorie des champs et, par conséquent, contiennent toutes les informations de la théorie. Cela suggère notamment que, d'une manière ou d'une autre, elles contiennent toute l'information relative au phénomène de confinement. Elles ont été particulièrement étudiées dans la jauge de Landau après les travaux de Kugo et Ojima [53]. En effet, ces derniers ont dérivé dans la jauge de Landau un scénario cohérent expliquant le confinement qui se base sur le comportement des fonctions de corrélations dans l'infrarouge profond. Ce comportement est dit de *scaling* et, dans l'Euclidien, est caractérisé par une "fonction de dressing" du ghost dans l'espace des impulsions (propagateur normalisé par sa valeur dans la théorie sans intéraction) qui diverge à impulsion nulle. Ces travaux amènent donc à étudier le comportement des fonctions de corrélation dans l'infrarouge profond pour voir si le système réalise la solution de scaling. Bien que cette dernière soit une solution des équations de DS et du FRG, les simulations réseau (à jauge fixée) ont montré qu'en pratique, la solution de scaling n'est pas réalisée. Au contraire, les fonctions de corrélation suivent la solution dite de *decoupling* où la fonction de dressing du ghost ainsi que le propagateur des gluons restent tous deux finis à moment nul. Dans l'Euclidien, un propagateur fini à moment

nul est en général associé à des champs massifs. Cependant, il a été clairement établi que la fonction spectrale associée au propagateur des gluons n'est pas définie positive et, par conséquent, ces derniers ne peuvent pas être interprétés comme des états asymptotiques [54, 55]. Ceci est en accord avec le confinement. Il a été montré que la solution de decoupling est une solution des équations de DS et du FRG, cependant, dans ces approches, rien ne permet de déterminer laquelle, entre les solutions de decoupling ou de scaling, est réalisée par le système [56, 57, 58, 59, 60, 43, 61, 62].

Finalement, mis ensemble, ces résultats suggèrent que nous sommes loin de complètement comprendre le comportement infrarouge des fonctions de Green, bien que ces dernières soient les quantités élémentaires de la théorie. Un ingrédient manquant pourrait provenir de certains effets non triviaux de la procédure de fixation de jauge elle-même qui sont ignorés dans la construction de Faddeev-Popov. En effet, dans ses travaux, Gribov a montré que, dans le cas de théories de jauge non-Abélienne, la solution de la condition de jauge n'est pas unique [63]. Au contraire, il existe un ensemble infini et discret de solutions qui sont reliées les unes aux autres par des transformations de jauge. Ces ambiguités, appelées copies de Gribov, ne sont pas prises en compte dans la procédure de Faddeev-Popov. Dans ce cas, elles donnent à la fonction de partition des contributions dégénérées qui consistent en une somme infinie de signes alternés qui finalement se compensent et conduisent au problème de Neuberger. Les copies de Gribov sont négligeables dans le domaine ultraviolet, mais leur présence pourrait changer drastiquement le comportement infrarouge des fonctions de corrélations. Dans le cas des simulations réseau à jauge fixée, les algorithmes de minimisation utilisés permettent de sélectionner une unique copie et donc d'éviter le problème de l'ambiguité de Gribov mentionné ci-dessus. En revanche, il n'est pas possible analytiquement de construire une action locale (qui est à la base de toute approche continue) qui ne contienne pas de copie de Gribov [64]. Gribov et Zwanziger se sont confrontés à ce problème et proposèrent de restreindre à un sous espace de configurations l'intégrale de chemin utilisée dans le calcul des fonctions de corrélations [63, 65]. Ainsi, la restriction à un tel sous espace permet de réduire grandement le nombre de copies de Gribov bien que certaines soient encore présentes dans la théorie fixée de jauge. Cette construction est appelée scénario de Gribov-Zwanziger et prédit que les fonctions de corrélations suivent la solution de scaling. Cette construction a été par la suite étendue à ce qui est connu comme le scénario de Gribov-Zwanziger "raffiné" [66], où les effets de condensats de dimension deux due à la présence des copies sont pris en compte. En particulier, ce raffinement prédit la réalisation de la solution de decoupling, ce qui est en accord avec le réseau. Tout ceci suggère que, au moins dans la jauge de Landau, la présence des copies de Gribov est un ingrédient clé du comportement infrarouge des fonctions de corrélations. Néanmoins, la jauge de Landau est une seule représentante des jauges covariantes et présente un certain nombre de symétries qui lui sont propres. Ainsi, pour mieux comprendre l'importance générale de prendre en compte les copies de Gribov, il serait intéréssant d'étudier leurs effets sur les fonctions de corrélations dans d'autres jauges. Seulement récemment les jauges linéaires covariantes ont pu être implémentées sur le réseau [67, 68, 69, 70, 71], et dans la construction de Gribov-Zwanziger (raffinée) [72, 73]. Un premier point important de la thèse présentée ici concerne l'implémentation des jauges covariantes non-linéaires dans une approche alternative qui vise à prendre en compte la présence des copies de Gribov (voir ci-dessous).

Récemment, une nouvelle procédure de fixation de jauge prenant en compte les copies de Gribov a été proposée par Serreau et Tissier dans le cas de la jauge de Landau [74]. L'idée centrale consiste à lever la dégénérescence des contributions des copies en réalisant une moyenne sur ces dernières avec un (pseudo) poids statistique non-uniforme. Ce faisant, l'ambiguité de Gribov est levée et il n'y a pas de problème de Neuberger. Pour ce faire, on définit les valeurs moyennes des observables invariantes de jauge par une procédure en deux

temps. Dans une première étape, on réalise une (pseudo) moyenne avec un poids statistique non-uniforme sur les copies appartenant à une même orbite de jauge et où ainsi leur dégénérescence est levée. Puis, dans un second temps, la moyenne sur les configurations du champs de jauge est réalisée avec l'action de YM. Cette construction définit une authentique fixation de jauge qui peut être formulée sous la forme d'une théorie quantique des champs locale. Pour ce faire, on a recours à la méthode dite des répliques [75] qui est utilisée dans l'étude des systèmes désordonnés en théorie statistique des champs. En particulier, la théorie locale fixée de jauge que l'on obtient est renormalisable en $d = 4$. En ce qui concerne les secteurs des ghosts et des gluons, dans le cas de la jauge de Landau, la procédure se réduit de manière effective à la seule introduction d'un terme de masse pour les gluons. Ainsi la théorie effective est (perturbativement) équivalente au modèle de Curci et Ferrari (CF) [76, 77] pris dans la limite de Landau, qui correspond à une simple extension massive de l'action de YM en jauge de Landau obtenue par la procédure de Faddeev-Popov. Le modèle de CF a l'avantage de présenter, dans l'infrarouge, des trajectoires du groupe de renormalisation (RG) sans pôle de Landau dites "saines" ou "infrarouge saines". De ce fait, le régime infrarouge du modèle peut être étudié perturbativement jusqu'à moment nul. En particulier, dans ce modèle, les calculs à une boucle des fonctions de vertex à deux et trois points reproduisent avec une bonne précision les résultats du réseau [79, 80, 81, 82]. Ceci montre que (dans le vide et dans la jauge de Landau) la majeure partie de la dynamique non-perturbative est précisément saisie par la présence d'une masse effective pour les gluons. Cette série de travaux constitue la base des études réalisées dans la thèse ici présente.

L'étude des fonctions de corrélations en jauge de Landau a naturellement été étendue à températures finies, aussi bien dans les cadre des approches continues [83, 36, 37, 38, 33, 32, 35, 34] que dans celui des simulations réseau [84, 85, 86, 87, 88, 89, 90, 91, 46, 92]. Comme nous l'avons mentionné avant, les fonctions de corrélations sont à la base des approches analytiques, et leur étude est donc une étape nécessaire pour pouvoir ensuite étudier par exemple le diagramme de phase de QCD. Les premiers résultats réseau en jauge de Landau étaient très controversés dû au fait que les erreurs systématiques associées à la discrétisation sont grandes. Finalement, les récentes simulations réalisées à grands volumes ont montré que les fonctions de corrélation en jauge de Landau sont essentiellement insensibles à la transition de phase [90], ce qui est problématique pour les méthodes approchées qui tentent de décrire cette transition. Il est possible que cette faible sensibilité soit due au fait que, dans la jauge de Landau, le paramètre d'ordre de la transition de phase (la boucle de Polyakov) n'entre pas directement ni dans les définitions ni dans les calculs des fonctions de corrélation. Récemment, il a été proposé que le paramètre d'ordre de la transition peut être efficacement pris en compte dans les calculs analytiques grâce à l'introduction d'un champs "de fond" dans la théorie microscopique fixée de jauge [33, 35, 34]. Ceci revient à travailler dans une extension de la jauge de Landau en présence d'un champ de fond, communément appelée jauge de Landau-DeWitt (LDW). En particulier, il a été montré que le FRG reproduit correctement la transition de phase dans cette jauge [33, 35, 34]. Cette approche en présence d'un champ de fond a naturellement été étendue au cas massif et perturbatif présenté ci-dessus [93, 94, 95, 96] où la transition de phase a été décrite en théorie de perturbation, ainsi qu'à potentiel chimique non-nul en présence de quarks lourds [97].

Dans cette thèse, nous concentrons notre étude sur les théories de YM fixées de jauge par la méthode de Serreau et Tissier. Dans un premier temps, en Chapitre I, nous passons en revue certains aspects pertinents pour l'étude du confinement et décrire comment il peuvent être reliés au comportement des fonctions de corrélations. Pour ce faire, nous prenons comme exemple la jauge de Landau où nous présentons brièvement les travaux de Kugo et Ojima [53]. Comme mentionné ci-dessus, ces derniers conduisent naturellement à

l'étude des propriétés infrarouge des fonctions de corrélation. Ainsi nous revoyons certains aspects des approches fonctionnelles, en particulier de DS et du FRG. Ces deux approches combinées ne permettant pas de discriminer la solution de decoupling ou de scaling, nous sommes amenés à considérer les simulations réseau à jauge fixée. Cependant, comme nous le présentons, ces dernières ne sont pas directement réalisables à partir de la théorie fixée de jauge à la Faddeev-Popov à cause du problème de Neuberger. Ce dernier est dû à la présence des copies de Gribov. Nous présentons les généralités concernant ces dernières dans le cas de la jauge de Landau ainsi que le scénario de Gribov-Zwanziger (raffiné). Ensuite, nous montrons comment, par une procédure d'extrémisation (qui revient à sélectionner une unique copie de Gribov), la jauge de Landau peut être implémentée sur le réseau et échappe au problème de Neuberger. Nous présentons le modèle de CF qui correspond à une extension massive de l'action fixée de jauge à la Faddeev-Popov. En particulier nous discutons les résultats perturbatifs obtenus dans ce modèle et mettons en avant leurs accords avec les résultats réseau. Finalement, nous présentons brièvement la procédure de Serreau et Tissier qui consiste à lever la dégénérescence des contributions des copies de Gribov par une pseudo moyenne réalisée sur ces dernières le long de l'orbite de jauge. Appliquée à la jauge de Landau, la procédure se réduit d'une manière effective à inclure un terme de masse pour les gluons, et l'action fixée de jauge est effectivement équivalente (pour les secteurs des ghosts et des gluons) au modèle de CF.

Dans le Chapitre II, nous généralisons la procédure de Serreau-Tissier à une famille de jauge covariantes non-linéaires. Pour cela, nous proposons de considérer une certaine fonctionnelle covariante (qui est une généralisation simple de celle utilisée pour la jauge de Landau lors de la fixation de jauge sur le réseau) et nous définissons la condition de jauge comme correspondant à ses extrema. Les différents extrema de cette fonctionnelle sont, par construction, tous des solutions de la condition de jauge et correspondent donc aux copies de Gribov. Lorsqu'on néglige la présence des copies (ce qui est au mieux valide à hautes énergies) et qu'on implémente la condition de jauge via Faddeev-Popov, on obtient les jauges (covariantes et non-linéaires) de Curci-Ferrari-Delbourgo-Jarvis (CFDJ) [77, 100]. Ces dernières ont été étudiées dans la littérature [77, 100, 210, 201, 211]. En particulier elles sont renormalisables (en $d = 4$) et unitaires mais présentent des ambiguités de Gribov. Du fait que ces jauges peuvent être formulées comme les extrema d'une fonctionnelle, leur implémentation réseau via une généralisation des techniques utilisées dans Landau est envisageable. Ceci demanderait de réaliser une généralisation détaillée des différents algorithmes de minimisations (locaux et globaux) qui sont utilisés dans le cas de la jauge de Landau. Une telle discussion ne rentre pas dans les objectifs de la thèse ci-présente, et nous discutons seulement d'une généralisation possible d'un algorithme de minimisation locale utilisé dans Landau. Ensuite, nous appliquons la procédure de Serreau-Tissier aux jauges sus-mentionnées. La procédure se décompose en deux temps. Une première étape est une pseudo moyenne le long des orbites de jauges réalisée sur les copies de Gribov où elles sont pourvues d'un poids statistique non-uniforme de sorte à lever leur dégénérescence. La seconde étape est une moyenne sur les configurations du champ jauge avec l'action de YM. Mises ensembles, ces deux étapes constituent une authentique fixation de jauge dans le sens que les valeurs moyennes d'observables invariantes de jauges sont insensibles à la moyenne sur les copies de Gribov. Cependant cette procédure ne correspond pas directement à une TQC locale. Pour pallier à ce problème, on a recours à la technique des répliques [75]. Finalement, la procédure peut être mise sous forme d'une action locale qui correspond à une extension massive des jauges CFDJ (ce qui correspond au modèle de CF dans les jauges ξ) augmenter d'un nombre $n - 1$ (avec n arbitraire) de répliques de modèle sigma non-linéaire supersymmetrique. En particulier, l'évaluation des quantités dans la construction de Serreau-Tissier correspond à faire $n \to 0$ tandis que pour $n = 1$ le secteur des répliques découple et on retrouve le modèle de CF. Ceci nous permet d'étudier simplement l'effet de

notre traitement des copies de Gribov en réalisant des comparaisons entre les cas $n \to 0$ et $n = 1$. Une fois cette construction présentée nous prouvons que la théorie fixée de jauge est renormalisable en $d = 4$ pour toutes valeurs de n et nous calculons explicitement à l'ordre d'une boucle les contre-termes. Nous poursuivons le calcul perturbatif pour calculer à une boucle les différents propagateurs de la théorie. Plus précisément, nous considérons des schémas de renormalisation où une part de la dépendance en n est absorbée dans les paramètres "nus" de la théorie. Nous montrons que dans ce cas, la théorie admet des trajectoires de RG qui sont saines dans l'infrarouge. Nous comparons nos résultats pour les propagateurs, avec et sans implémentation du RG, entre la théorie fixée de jauge et le modèle de CF. En particulier nous observons de nettes différences dues à notre traitement des copies de Gribov. Par exemple, dans le cas Serreau-Tissier, le propagateur du gluon est toujours transverse même loin de la jauge de Landau alors que, pour le modèle de CF, il présente une composante longitudinale à part dans le cas particulier de Landau. Nous observons aussi de nettes différences entre les deux cas dans les flots de RG où, pour le modèle de CF, ces derniers se gèlent sous l'échelle de masse de la théorie tandis que, dans le cas Serreau-Tissier, le secteur des répliques contient des modes sans masses et les flots de RG ne se gèlent jamais. Dans les deux cas nous pouvons intégrer les flots jusqu'à moment nul.

Finalement, au Chapitre III, nous nous intéressons au cas à température finie. Dans un premier temps nous revoyons les généralités concernant la transition de phase confinement-déconfinement et en particulier son lien avec la boucle de Polyakov et la brisure spontanée de la symétrie du centre. Nous présentons ensuite les résultats obtenus dans le cas de la jauge de Landau où, comme mentionné précédament, les simulations réseau et les approches continues trouvent des propagateurs essentiellement insensibles à la transition de phase. Nous introduisons ensuite les méthodes de jauge de champ de fond ("background gauge fields methods") où une valeur de fond du champ de jauge est introduite. Cela correspond à travailler dans une généralisation de la jauge de Landau connue comme la jauge de Landau-DeWitt (LDW). En particulier, cette valeur du champ de fond constitue un paramètre d'ordre pour la transition de phase. Nous présentons aussi le fait que dans le cas LDW la symétrie du centre est explicitement préservée au niveau de l'action nue alors qu'elle est explicitement brisée dans le cas de Landau. Nous revoyons comment dans l'extension massive de la jauge de LDW (ce qui d'un point de vue effectif correspond à l'implémenter selon la procédure de Serreau-Tissier) la transition de phase peut être étudiée en théorie de perturbation. En particulier dans la théorie SU(2) on trouve que la transition de phase est du second ordre [94] en accord avec les résultats réseau. Une des conséquences importantes de la présence du champ de fond est que des directions de couleur sont privilégiées (celles dans lesquelles le champ de fond pointe). Ainsi, les différents modes de couleurs des différents champs, par exemple des ghosts et des gluons, ne se couplent pas de la même manière avec le champ de fond et leur habituelle dégénérescence est levée. Nous calculons dans la théorie SU(2), à l'ordre d'une boucle en théorie de perturbation, les propagateurs des gluons et des ghosts pour les différents modes de couleurs et nous nous concentrons sur leur comportement dans la région de température autour de la transition de phase. Pour SU(2), la transition de phase est second ordre, et donc le paramètre d'ordre, bien que continu, présente une non-analitycité à la température critique. On observe cette non-analyticité dans tous les propagateurs et susceptibilités (valeur du propagateur à fréquence de Matsubara nulle et à impulsion nulel). Ceci est particulièrement marqué dans le secteur électrique du gluon du mode de couleur neutre (mode de couleur dans lequel le champ de fond pointe), où sa susceptibilité présente un pic très marqué à la température critique.

Mots clés : Théories de Yang-Mills, fixation de jauge, fonctions de corrélation infrarouge, ambiguités de Gribov, TQC à températures finies, transition de phase confinement-déconfinement